

Electrochemical Generation of Alkyl Radicals for Carbon-Carbon Bond Forming Reactions

Jonathan Charles Churchill

Doctor of Philosophy

Department of Chemistry

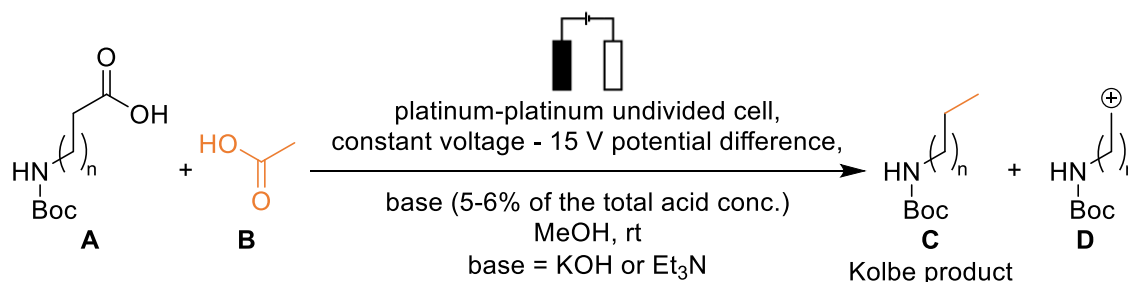
University of York

March 2022

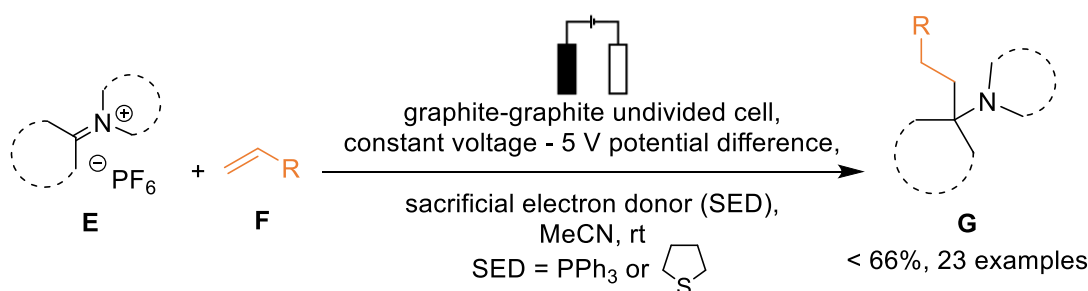
Abstract

Synthetic electroorganic radical chemistry provides an attractive method for creating complex molecules. This thesis describes the development of two electrochemical approaches for the construction of carbon-carbon bonds. Oxidative and reductive electrochemical reactions were used to generate alkyl radicals which underwent either radical-radical couplings or underwent addition to alkenes.

In Chapter 2, the factors that determine the selectivity of Kolbe electrolysis were explored. Alkyl radicals derived from the oxidation of protected amino acids **A**, were coupled with methyl radicals (from acetic acid **B**) to yield cross-coupled products **C**. α -Amino radicals underwent a second electron oxidation, forming stabilised carbocations (such as **D**) which reacted with solvent to give non-Kolbe products. Radicals which formed further from nitrogen gave higher yields of Kolbe products **C**. The yield of the Kolbe product couldn't be improved from that achieved with "standard Kolbe conditions", as the Kolbe:non-Kolbe product ratio was highly substrate dependent.



Next, a reductive approach to sterically hindered tertiary amine synthesis is detailed in Chapter 3. Iminium ions **E** were electrochemically reduced, forming nucleophilic α -amino radicals that underwent addition to alkenes **F**. Sacrificial electron donors were oxidised at the anode whilst the reduction occurred at the cathode, generating a range of α -substituted tertiary amines **G**. Under optimised conditions, yields of up to 66% were achieved using pure iminium ions and electron-deficient alkenes. Using crude iminium ions, up to 53% yields over two steps from a variety of cyclic amines and ketones were achieved.



Acknowledgments

Firstly, I would like to thank my supervisors; Victor Chechik, Peter O'Brien and Alison Parkin for all their help, guidance and support throughout my PhD, and the opportunity to do this project. I have learnt so much from all of them and they are the reason I am the researcher I am today.

I would also like to thank Nigel Willetts at Syngenta for his input to the project, and Will Unsworth for his guidance as my independent panel member. I would like to thank the technical staff at York including Heather, Scott and Karl for their work running the NMR, chromatography, and mass spectrometry services.

I would like to thank the past and present members of the VC, POB and AP groups over the years who have contributed to many helpful discussions, provided technical insight, and loan of chemicals. I would particularly like to thank Sophie Berrell, who laid the foundations of the electrosynthesis project at York, and who was always willing to help me and provide emotional support (and for some reason still is!). Many thanks to all the members of the E014 lab who always made the lab an enjoyable place to work and suffered my poor taste in lab music, particularly on Fridays. Thanks to Will, Peter and Nik of the Chechik group who were always there to provide a sounding board, to develop my ideas or just have a coffee with. Thanks to the POB group members for weekly games nights and pub quizzes.

Finally, I would like to thank my friends from my undergraduate studies, Alex, Anil, Charlotte, Jenny and Stefan, for keeping me sane. I would like to thank my family, Barbara, Ian and Rebecca, who have supported me both emotionally and financially throughout my time at York, and for always being on the other end of the phone. Special thanks also to my grandparents, Ernest and Hazel Churchill and Peter and Mary Kelly, who were always proud of the achievements of their grandchildren. Finally, a massive thank you to Beth for her love, encouragement, and putting up with me for all these years.

Declaration of Authorship

I declare that this thesis is a presentation of original work, and I am the sole author unless otherwise stated. This work has not previously been presented for an award at this, or any other, University. All sources are acknowledged as References.

Table of Contents

Abstract	ii
Acknowledgments	iii
Declaration of Authorship	iv
Table of Contents	v
List of Figures	viii
List of Tables	xi
List Of Abbreviations	xiii
Chapter 1: Introduction	1
1.1 History of Radical Chemistry	1
1.1.1 Traditional Methods of Radical Generation: Homolysis and Electron Transfer	2
1.1.2 Radical Generation with Photoredox Catalysts	4
1.1.3 Radical Generation with Electrochemistry	7
1.2 Highlights of Electrochemical Alkyl Radical Generation from Recent Literature	11
1.3 Aims of Project.....	16
Chapter 2: Developing Kolbe Electrolysis for Electrochemically Generating Alkyl Radicals from Amino Acids	18
2.1 Introduction	18
2.1.1 History of Kolbe Electrolysis.....	18
2.1.2 Previous Mechanistic Proposals for Kolbe Electrolysis	19
2.1.3 Current Mechanistic Proposal for Kolbe Electrolysis.....	21
2.1.4 Experimental Conditions for Kolbe Electrolysis	28
2.1.5 Broadening the Synthetic Scope of Kolbe Electrolysis	33
2.1.6 Intramolecular Cyclisation	38
2.1.7 Non-Kolbe Oxidation Pathway	40
2.1.8 Chapter Aims	53
2.2 Results and Discussion	55

2.2.1	Electrochemical Set-Up and Reproducibility	55
2.2.2	Electrolysis of <i>N</i> -Boc Amino Acids	63
2.2.3	Monitoring Kolbe Electrolysis by ¹ H NMR Spectroscopy.....	77
2.2.4	Further Optimising Conditions for Kolbe Electrolysis.....	84
2.3	Conclusions and Future Work.....	95
Chapter 3: Synthesis of Sterically Hindered Tertiary Amines using Electrochemically Generated α-Amino Radicals		97
3.1	Introduction.....	97
3.1.1	General Methods for the Synthesis of Amines	97
3.1.2	Oxidative Approaches for α -Amino Radical Formation	101
3.1.3	Photocatalytic Reduction of Iminium Ions and Imines	109
3.1.4	Reduction of Iminium Ion and Imines with Samarium(II) Iodide.....	119
3.1.5	Electrochemical Reductions of Iminium Ions	126
3.1.6	Chapter Aims	139
3.2	Results and Discussion.....	141
3.2.1	Methods for Iminium Ion Synthesis	141
3.2.2	Iminium Ion Synthesis with 4 Å Molecular Sieves	146
3.2.3	Iminium Ion Synthesis with Azeotropic Distillation.....	148
3.2.4	Electrolysis of an Iminium Ion	152
3.2.5	Iminium Ion Reduction and Reaction with Acrylonitrile: Optimisation of Electrolysis Conditions.....	153
3.2.6	Iminium Ion Reduction and Reaction with Acrylonitrile: Study the Mechanism with Cyclic Voltammetry	166
3.2.7	Investigation of <i>In-Situ</i> Iminium Ion Formation with 4 Å Molecular Sieves and Reaction with Acrylonitrile Under Electrolysis Conditions.....	173
3.2.8	Use of Unpurified Iminium Ions and Reaction with Acrylonitrile Under Electrolysis Conditions.....	176
3.2.9	Use of Pure Iminium Ions and Reaction with Different Alkenes Under Electrolysis Conditions.....	181

3.3	Conclusions and Future Work	185
Chapter 4: Overall Conclusions and Future Work.....		187
Chapter 5: Experimental		190
5.1	General	190
5.1.1	General Methods	190
5.1.2	General Procedure for Calculating the End Point of Electrochemical Reactions	190
5.2	Experimental for Chapter 2	192
5.2.1	General Methods for Chapter 2.....	192
5.2.2	Platinised Titanium Electrodes and 9 mL Electrochemical Cell	192
5.2.3	Platinum Wire Electrodes and 2 mL Electrochemical Cell	192
5.2.4	Variations of the Platinum Wire Electrodes and 2 mL Electrochemical Cell....	193
5.2.5	General Procedures for Chapter 2	193
5.2.6	Experimental Procedures and Characterisation Data for Chapter 2.....	198
5.2.7	Overview of Changes and Yields for Section 2.2	208
5.3	Experimental for Chapter 3	209
5.3.1	General Methods for Chapter 3.....	209
5.3.2	Electrolysis Set-Up – ElectraSyn 2.0	209
5.3.3	Cleaning ElectraSyn 2.0 Graphite Electrodes	210
5.3.4	Modified ElectraSyn 2.0 Set-Up to Accommodate Reticulated Vitreous Carbon (RVC) Electrodes	211
5.3.5	General Procedures for Chapter 3	213
5.3.6	Experimental Procedures and Characterisation Data for Chapter 3.....	217
Appendix		247
References		263

List of Figures

Figure 2.1 Tafel plot for sodium acetate in acetic acid showing log(current density) vs anode potential with critical potential (ca. 2.1 V vs NHE) reproduced from Dickinson et al. 1961. ⁶⁶	23
Figure 2.2 Circuit diagram for electrochemical set-up including powerpacks, Labjack [®] , polarity inverter and electrodes	55
Figure 2.3 Labelled image (left) and photograph (right) of the platinised titanium electrodes in the 9 mL cell.....	57
Figure 2.4 Labelled image (left) and photograph (right) of the platinum wire electrodes in the 2 mL cell.....	58
Figure 2.5 Overlay of current vs time plot for General Procedure 2A and General Procedure 2B, using Table 2.10, entries 1 and 4	63
Figure 2.6 Stacked ¹ H NMR spectra showing the formation of Kolbe product 2.90 and non-Kolbe product 2.91-d₃ , recorded every 10 minutes during Kolbe electrolysis of N-Boc β-alanine 2.89 and acetic acid.....	79
Figure 2.7 Plot of Kolbe product 2.90 and non-Kolbe product 2.91-d₃ yields and starting material remaining as quantified by ¹ H NMR spectroscopy using mesitylene and an external standard. Also plotted is the equivalents of charge in F mol ⁻¹	80
Figure 2.8 Plots of reagent and product time-traces as quantified by ¹ H NMR spectroscopy using mesitylene as an external standard from reactions carried out under various electrolysis conditions, as summarised in Table 2.12. Also plotted is the equivalents of charge in F mol ⁻¹	82
Figure 2.9 Recorded potential difference and current density plotted against time for the electrolysis of N-Boc β-alanine and acetic acid with no water bath (uncontrolled temperature).....	83
Figure 3.1 Various tertiary amines used in pharmaceuticals. ¹⁵²	98
Figure 3.2 Oxidation potentials for various amines. ¹²⁰	101
Figure 3.3 Reduction potentials for various aldehydes, ketones, imines and iminium ions. ^{120,173,177,178}	110
Figure 3.4 Stacked ¹ H NMR spectra showing the formation of iminium ion 3.154 over 20 h with and without 4 Å molecular sieves.....	147

Figure 3.5 Cyclic voltammogram (CV) for iminium ion 3.154 . Recorded using platinum wire working and counter electrodes and an Ag/AgCl reference electrode. The CV was performed with an EmStat potentiostat with 10% methanol in acetonitrile as the solvent and 0.1 M iminium salt. Reduction maxima at -1.60 V vs Ag/AgCl, scan rate 50 mV s^{-1}	153
Figure 3.6 A graph showing negative absolute current vs time, for the first 35 minutes, for a series of electrochemical reductions of iminium ion 3.154 with and without a reference electrode and at 0.5 min polarity inversion intervals	157
Figure 3.7 A graph showing the actual current output for the ElectraSyn vs time, for the first 35 minutes, for a series of electrochemical reductions of iminium ion 3.154 with and without a reference electrode and at 0.5 min polarity inversion intervals	159
Figure 3.8 Cyclic voltammograms of the different sacrificial electron donors at 0.07 M, recorded at 500 mV s^{-1}	167
Figure 3.9 Overlaid current traces showing negative absolute current vs time for the different sacrificial electron donors.	168
Figure 3.10 Cyclic voltammograms of the different sacrificial electron donors at 0.03 M, recorded at 100 mV s^{-1}	169
Figure 3.11 Cyclic voltammograms of amine 3.116 (0.012 M) with and without tetrahydrothiophene (0.049 M), recorded at 500 mV s^{-1}	170
Figure 3.12 Cyclic voltammogram of iminium ion 3.154 recorded using the modified ElectraSyn set-up, at 0.026 M, 500 mV s^{-1}	171
Figure 3.13 Overlaid cyclic voltammograms of iminium ion 3.154 (0.026 M) and increased amounts of acrylonitrile, recorded at 500 mV s^{-1}	172
Figure 3.14 Cyclic voltammogram of iminium ion 3.154 (0.021 M), acrylonitrile (0.062 M) and tetrahydrothiophene (0.042 M), recorded at 500 mV s^{-1}	173
Figure 3.15 A graph showing current vs time, for the first 35 minutes, for electrolysis with vinyl pyridine and acrylonitrile.....	184
Figure 5.1 Calibration curve for quantification of N-Boc β -alanine 2.89	196
Figure 5.2 Calibration curve for quantification of Kolbe product 2.90	196
Figure 5.3 Calibration curve for quantification of non-Kolbe product 2.91	196
Figure 5.4: 1. ElectraSyn vial lid, 2. 20 mL ElectraSyn Vial, 3. 27.0 mm internal diameter O ring, 4. ElectraSyn SK-50 graphite electrodes, 5. 17 suba seal, 6. ElectraSyn stirrer bar, 7. Suba seal fitted in ElectraSyn vial lid, 8. Modified ElectraSyn vial lid (top view), 9. Modified ElectraSyn vial lid (side view).....	210

Figure 5.5: Left. Graphite electrodes after 10 reactions showing visible electrode fouling and reduction in thickness due to abrasive cleaning. Right. New graphite electrodes..... 211

Figure 5.6 Modified ElectraSyn 2.0 set-up to allow the reaction to be performed with RVC electrodes 212

List of Tables

Table 2.1 Products from coupling between cyanoalkyl radicals from different sources. ⁶⁵	.26
Table 2.2 The effect of solvent on the Kolbe:non-Kolbe product ratio. ⁹⁶	29
Table 2.3 The effect of current density on the outcome of Kolbe electrolysis and the overall Kolbe:non-Kolbe product ratio. ⁸⁴	30
Table 2.4 The effect of an supporting electrolyte (NaClO ₄) on the outcome of Kolbe electrolysis and the Faradaic efficiencies ⁹⁸	32
Table 2.5 The effect of increased amount of co-acid on the outcome of Kolbe electrolysis ⁹¹	38
Table 2.6 The effect of solvent on the outcome of the non-Kolbe pathway for α -amino acids by Linstead et al. ⁸⁵	42
Table 2.7 The effect of electrode material on the outcome of the non-Kolbe product distribution. ⁸⁷	50
Table 2.8 The effect of a co-acid on the outcome of Kolbe electrolysis. ⁸⁴	52
Table 2.9 Summary of the two sets of Kolbe electrosynthesis conditions used in this chapter, General Procedure 2A and 2B; these are based on published work by Schäfer and co-workers ¹⁰⁸ and Seebach and co-workers, respectively. ⁹⁷	59
Table 2.10 Yields of Kolbe product 2.90 and non-Kolbe product 2.91 by ¹ H NMR spectroscopy after using either General Procedure 2A and 2B and the 2 mL electrochemical cell, as detailed in Scheme 2.32	61
Table 2.11 Table showing Kolbe product yields, total non-Kolbe product yields and the ratios of Kolbe:non-Kolbe product for N-Boc amino acids	76
Table 2.12 Yields of Kolbe product 2.90 and non-Kolbe product 2.91-d₃ after 90 or 45 minutes in the electrolysis of N-Boc β -alanine and acetic acid, quantified with ¹ H NMR spectroscopy using mesitylene as an external standard	81
Table 2.13 Table showing the applied potential difference, average current densities and yield of Kolbe hetero-coupled product 2.90 determined by GC for the electrolysis of N-Boc β -alanine and acetic acid using various solvents	85
Table 2.14 Table showing the yield of Kolbe hetero-coupled product 2.90 , non-Kolbe product 2.91 and Kolbe:non-Kolbe product ratio determined by GC for the electrolysis of N-Boc β -alanine and acetic acid using methanol, dried methanol and methanol with water	87

Table 2.15 Table showing average current densities, the yield of Kolbe hetero-coupled product 2.90 , non-Kolbe product 2.01 and Kolbe:non-Kolbe product ratio determined by GC for the electrolysis of N-Boc β -alanine and acetic acid using various anode materials; platinum, gold and palladium	88
Table 2.16 Table showing the average current densities and yield of Kolbe hetero-coupled product 2.90 , non-Kolbe product 2.91 and remaining starting material 2.89 determined by GC for the electrolysis of N-Boc β -alanine and acetic acid in methanol using tetrabutylammonium hexafluorophosphate (Bu_4NPF_6) as supporting electrolyte.....	91
Table 2.17 Table showing the applied potential difference, degree of neutralisation (N), anode surface area, average current density and the yield of Kolbe hetero-coupled product 2.90 , non-Kolbe product 2.91 and Kolbe:non-Kolbe product ratio determined by GC for the electrolysis of N-Boc β -alanine and acetic acid	93
Table 3.1 The effect of polarity inversion on the outcome of the reduction of iminium ion 3.154 in the presence of acrylonitrile	158
Table 3.2 The effect of changing electrode material and equivalents of charge on the outcome of the reduction of iminium ion 3.154 in the presence of acrylonitrile	161
Table 3.3 The effect of solvent and equivalents of alkene on the outcome of the reduction of iminium ion 3.154 in the presence of acrylonitrile.....	162
Table 3.4 The effect of sacrificial electron donor on the outcome of the reduction of iminium ion 3.154 in the presence of acrylonitrile	165
Table 3.5 The outcome of in-situ formation of iminium ion 3.154 and subsequent electrolysis to form amine 3.116	175
Table 5.1 Summary of electrochemical changes for optimising Kolbe electrolysis of N-Boc β -alanine and acetic acid, including amount of charge passed, average current density, average voltage, and yields of the Kolbe product 2.90 and non-Kolbe product 2.91	208
Table 5.2 Summary of electrochemical changes for optimising Kolbe electrolysis of N-Boc β -alanine and acetic acid, including amount of charge passed, average current density, average voltage, and yields of the Kolbe product 2.90 and non-Kolbe product 2.91	208

List Of Abbreviations

μL	Microliter	GC	Gas Chromatography
A	Ampere (Amp)	h	Hour(s)
Ac	Acetyl	HAT	Hydrogen Atom Transfer
AIBN	Azobisisobutyronitrile	HOMO	Highest Occupied Molecular Orbital
Aq	Aqueous	HRMS	High Resolution Mass Spectrometry
Ar	Aryl	Hz	Hertz
ATR	Attenuated Total Reflectance	I	Current
AU	Arbitrary Units	i	iso
Bn	Benzyl	IR	Infra-red
Boc	<i>tert</i> -Butyloxycarbonyl	ISC	Intersystem Crossing
Br	Broad	<i>J</i>	Coupling Constant in Hz
Bu	Butyl	LUMO	Lowest Unoccupied Molecular Orbital
C	Coulombs	M	Molar
calcd	Calculated	m	Multiplet (in NMR)
cm	Centimetre	<i>m/z</i>	Mass to Charge Ratio
cm^{-1}	Wavenumber (in IR)	M^+	Molecular Ion
CV	Cyclic Voltammetry	mA cm^{-2}	Current Density
d	Doublet (in NMR)	Me	Methyl
d.r.	Diastereomeric Ratio	$\text{MeCN-}d_3$	Deuterated Acetonitrile
DC	Direct Current	$\text{MeOH-}d_4$	Deuterated Methanol
DCM	Dichloromethane	mg	Milligram(s)
DEPT	Distortionless Enhancement by Polarisation Transfer	MHDE	Mercury Hanging Drop Electrodes
DMF	Dimethylformamide	MHz	Megahertz
DMSO	Dimethyl Sulfoxide	min	Minute(s)
e.e.	Enantiomeric Excess	mL	Millilitre(s)
e.r.	Enatiomeric Ratio	MLCT	Metal-to-Ligand Charge Transfer
eq.	Equivalents	mm	Millimetre(s)
ESI	Electrospray Ionization	mmol	Millimole(s)
Et	Ethyl	mp	Melting Point
EWG	Electron Withdrawing Group	MS	Mass Spectrometry
FID	Flame Ionization Detector	Mw	Molecular Weight
FT	Fourier Transform		
g	Gram(s)		

N	Neutrisation
NHE	Normal Hydrogen Electrode
NMR	Nuclear Magnetic Resonance
PCET	Proton Coupled Electron Transfer
Ph	Phenyl
ppm	Parts Per Million
Pr	Propyl
q	Quartet (in NMR)
R	Resistance
R_F	Retention Factor (in TLC)
rt	Room Temperature
RVC	Reticulated Vitrous Carbon
s	Singlet (in NMR)
SCE	Saturated Calomel Electrode
SED	Sacrificial Electron Donor
SET	Single Electron Transfer
SOMO	Singly Occupied Molecular Orbital
t	Triplet (in NMR)
<i>tert</i>	Tertiary
TEMPO	2,2,6,6- Tetramethylpiperidinyloxy
THF	Tetrahydrofuran
TLC	Thin Layer Chromatography
UPLC	Ultra Performance Liquid Chromatography
V	Voltage
δ_C	^{13}C NMR Chemical Shift
δ_H	^1H NMR Chemical Shift

Chapter 1: Introduction

Using electrochemistry in organic synthesis has been well documented and recently this area of chemistry has undergone a resurgence motivated by synthetic chemists wanting to create complex molecules sustainably and with good atom economy.¹ Furthermore, the development of methods of radical initiation and radical precursors, has led to a wealth of new radical transformations to meet the growing need for methods of late-stage functionalisation, which often requires mild and tolerant reactions conditions.² Electroorganic synthesis can be employed as method of radical generation, using electrons as reagents which avoids waste material making it an attractive method for functionalisation.³ Both oxidative and reductive transformations are made possible without the need for stoichiometric amounts of, often toxic, reducing or oxidising agents.⁴

The construction of sp^3 - sp^3 hybridised carbon-carbon bonds is often challenging with classical two-electron approaches, particularly around sterically hindered centres, and is therefore of importance for organic chemists to develop new methods. Alkyl radicals can be utilised to form such bonds, with high levels of reactivity and functional group tolerance, often by either radical-radical couplings, additions to alkenes, or atom transfers.⁵

This introduction will briefly cover the importance of radical chemistry in organic synthesis, covering different methods of radical generation with emphasis on methods of alkyl radicals for carbon-carbon bond forming reactions. Finally, the advantages and disadvantages of electroorganic synthesis will be described in more detail. The two subsequent results and discussion chapters, detailing oxidative decarboxylation and the reduction of iminium ions, will provide additional literature reviews covering publications most relevant to each topic and introduce the two specific areas of chemistry studied in this project.

1.1 History of Radical Chemistry

In 1900, Moses Gomberg reported the first example of a stabilised carbon centred radical in solution, the triphenylmethyl radical, formed during the preparation of hexaphenylethane from triphenylchloromethane.⁶ This discovery led to much interest in radical chemistry, however, radical reactions were often thought to be chaotic and uncontrollable, and as such, radical reactions were not readily developed for the synthesis applications of small molecules.⁷⁻⁹ Instead, the largest application of radical chemistry was in industrial polymer

synthesis.¹⁰ It was only in the latter part of the 20th Century that radical reactions were shown to be highly effective and efficient methods of synthesising complex molecules.^{11,12} This has led numerous synthetic chemists to further develop radical transformations and thus a resurgence in the field in the 21st Century.¹³

Radicals exhibit several properties that make them advantageous for use in synthetic transformations. For example, carbon centred alkyl radicals are highly reactive, enabling mild reaction conditions, whilst also exhibiting levels of chemo-, regio- and stereoselectivity. As radicals have early transition states, they are ideal for creating complex and crowded chemical centres.¹⁴ Radicals also undergo facile, irreversible, addition to alkenes under kinetic control, which has been utilised in organic synthesis to create new bonds.¹⁵ The protection of starting materials bearing alcohols and amines is usually not required as radicals are chemically inert towards these functionalities, meaning they have high levels of functional group tolerance and can be applied to late stage functionalisation.¹⁴

Radical reactions are often limited by the method of radical generation.^{16,17} In the following sections methods of radical generation from traditional homolysis and electron transfer processes, to photocatalysts and electrolysis, will be briefly reviewed.

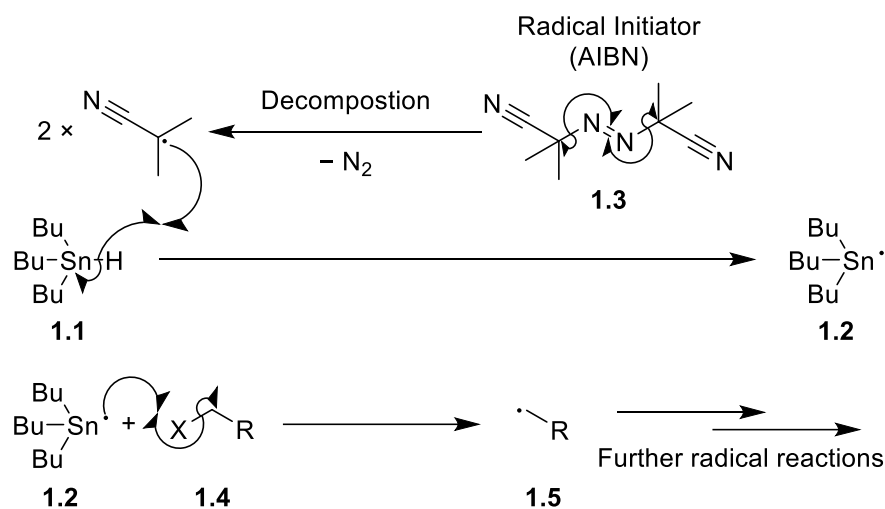
1.1.1 Traditional Methods of Radical Generation: Homolysis and Electron Transfer

One of the simplest ways to generate radicals is by homolysis. Weak covalent bonds, typically heteroatom-heteroatom, carbon-heteroatom or metal-metal bonds, can be broken with heat or light, which results in the formation of two radicals. Temperatures of up to 150 °C, are often used to break bonds with energies between 125-165 kJ mol⁻¹, such as oxygen-oxygen bonds in dialkyl and diacyl peroxides.¹⁸ Carbon-nitrogen bonds in azo compounds can also be broken by thermolysis, which is driven forward by the formation of nitrogen gas. Photolysis can also be used to cleave covalent bonds, usually by photoexcitation of an electron into an antibonding orbital, causing fragmentation and the formation of two radicals. Common functional groups that undergo photolysis are peroxides, azo compounds, organohalides, nitriles, organometallics and carbonyls.¹⁸

Neither thermolysis nor photolysis are suited for the selective formation of alkyl radicals for synthetic applications. Whilst light can be used to cleave R-X bonds in alkyl halides, a prerequisite of photolysis is for the molecule to absorb light, which can be used to improve

the selectivity of photolysis compared to thermolysis, however, this can also limit the application.¹⁸ The products of homolysis can be used as radical initiators, however, the radicals formed are often far too reactive (e.g. alkoxy radical) to be selective for the formation of alkyl radicals. Homolysis is therefore typically used alongside a radical mediator.

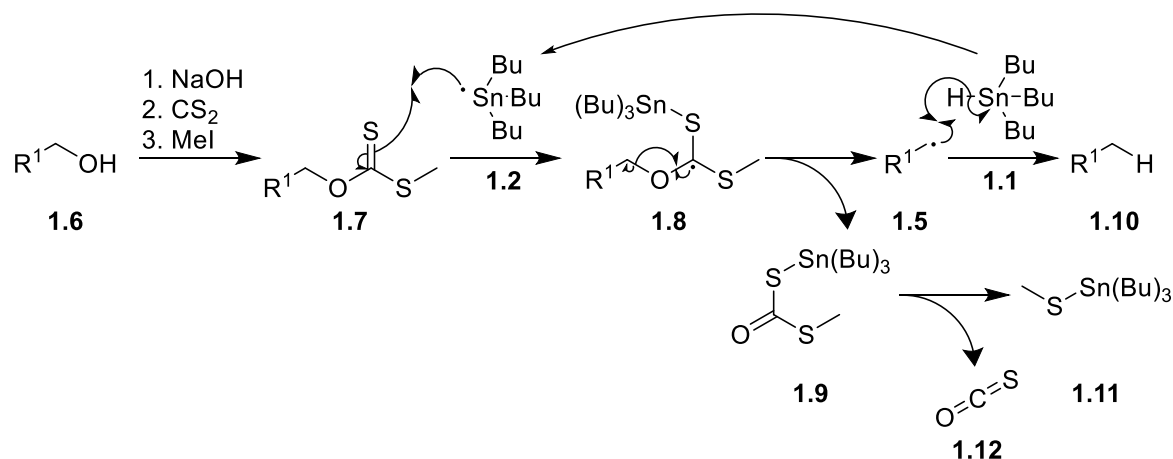
Mediators have been employed to tune the selectivity of radical generation, for example tributyltin hydride (Bu_3SnH , **1.1**) has been used as a reducing agent in many organic radical reactions to form alkyl radicals from alkyl halides (Scheme 1.1).¹⁹ The dual role of tributyltin hydride is to form the tributylstannyl radical **1.2** that is involved in the selective cleavage of the carbon-halogen bond and to provide a hydrogen atom to the resulting alkyl radical. Reactions require a radical initiator, such as azobisisobutyronitrile (AIBN, **1.3**) which can undergo homolysis, before generating the tin centred radical. The reaction of tributylstannyl radical and alkyl halides (**1.4**) is driven by the formation of strong tin-halogen and carbon-hydrogen bonds at the expense of more labile tin-hydrogen and carbon-halogen bonds.¹⁷ The alkyl radicals (**1.5**) generated in these reaction typically undergo hydrogen atom transfers or coupling with alkenes, the latter is known as Giese radical addition.¹⁵



Scheme 1.1 Mechanism for activation of tributyltin hydride by AIBN and subsequent halogen atom abstraction to generate an alkyl radical

One of the key reactions that utilised tributyltin hydride as a radical mediator was the Barton-McCombie deoxygenation, developed in 1975 (Scheme 1.2).²⁰ Alcohols (**1.6**) were first converted to the corresponding thiocarbonyl (**1.7**) prior to treatment with an excess of tributyl tin hydride, as the radical reducing agent. Mechanistically, tributylstannyl radical

(**1.2**), derived from a reaction with a radical initiator, such as AIBN, reacts with the thiocarbonyl **1.7** to give alkyl radical **1.8**. β -Scission delivers alkyl radical **1.5** and *S*-methyl-*S*-tributylthiocarbonate **1.9** which further decomposes to form carbon oxysulfide (**1.12**) and methyltributylstannylsulfide **1.11**). Tributyltin hydride (**1.1**) then acts as a hydrogen atom donor, to give alkane **1.10** and regenerate tributylstannyl radical (**1.2**).²¹



Scheme 1.2 Mechanism for the Barton-McCombie deoxygenation with tributyltin hydride

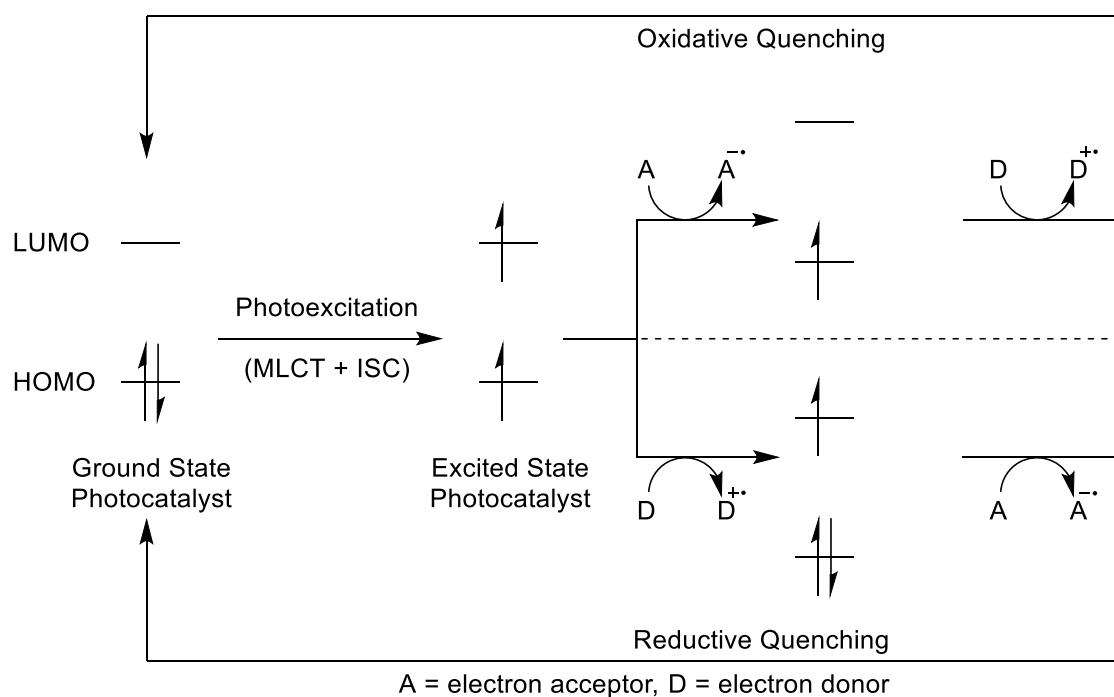
Apart from bond homolysis, organic radicals can be generated by the transfer of a single electron, either to or from a substrate, by a reducing or oxidising agent respectively.¹⁸ Common examples of electron transfer agents include metal oxidants, such as Mn(III) acetate, and metal reductants, such as Ti(III) catalysts or Sm(II) iodide, which have all been employed as methods of forming alkyl radicals.¹⁷ However, these reagents often require stoichiometric amounts, meaning a large amount of waste is generated during the reaction. More recently photoredox catalysts and electrochemistry have been popularised as more sustainable methods of forming radicals by the transfer of electrons, both of which will be discussed in more detail next.

1.1.2 Radical Generation with Photoredox Catalysts

Although the application of photochemistry as a method of radical generation has had significant applications, it was only the development of new types of selective, visible light photocatalysts, that has led to a growth in its use for synthetic organic chemistry.²² An appropriate organic or transition metal (typically ruthenium or iridium) photocatalyst is

capable of converting visible light into chemical energy under very mild conditions, which can be used for the generation of reactive intermediates such as radicals.^{23,24}

In a typical photocatalytic cycle for a transition metal photocatalyst, upon absorption of a photon, an electron in the HOMO is promoted to the LUMO (Scheme 1.3).²² In the case of commonly used Ru(II) and Ir(III) octahedral metal based photocatalyst, a metal-to-ligand charge transfer (MLCT) occurs followed by intersystem crossing (ISC) which gives rise to a long-lived triplet excited state. This photoexcited species will not readily decay back to the singlet ground state as this transition is spin-forbidden. The triplet state is both an effective oxidising and reducing agent, proceeding either *via* oxidative or reductive quenching cycles to reform the ground state of the catalyst and generate reactive intermediates. The choice of cycle is dependent on the specific reaction conditions.²²

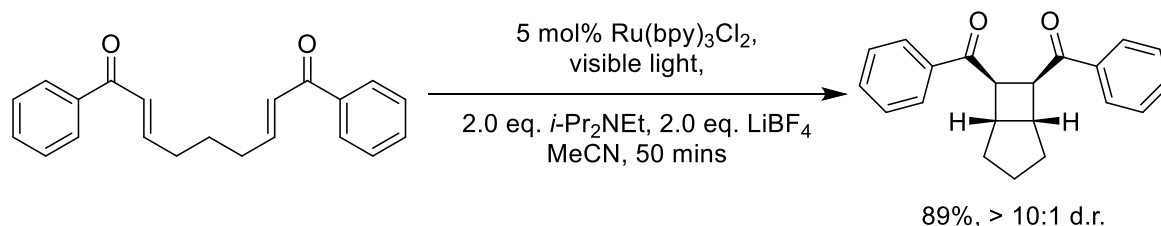


Scheme 1.3 Typical photocatalytic cycle for an octahedral Ru(II) or Ir(III) transition metal based photocatalyst

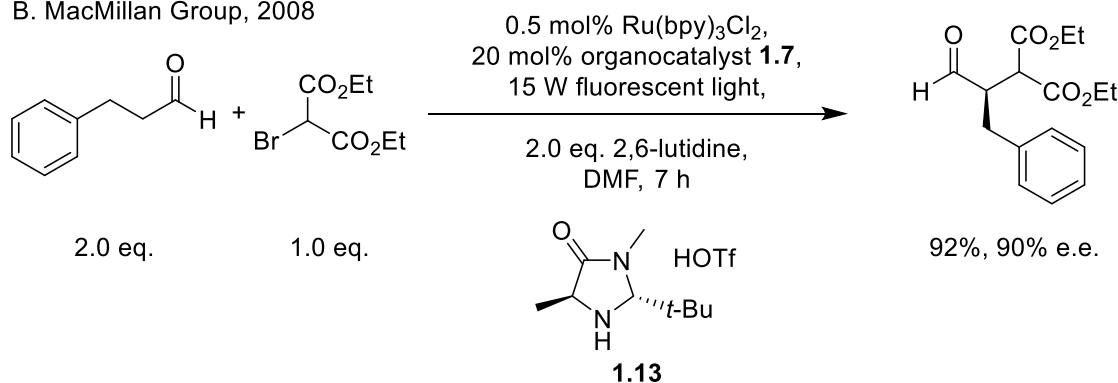
Visible light mediated photocatalysis has been shown to mediate a plethora of bond forming reactions under mild reaction conditions, without the need for stoichiometric amounts of oxidising or reducing agents. Reaction involving photocatalysts can also be redox neutral, as both oxidants and reductants are formed in the same mixture. Finally, as many organic molecules do not absorb visible light, there is less chance of side reactions from photoexcitation of the substrate, meaning high functional group tolerance.²²

Photocatalysts were rarely used in organic synthesis reactions prior to 2008, when Yoon and co-workers developed an effective [2+2] cycloaddition reaction (Scheme 1.4, A) and the MacMillan group published an asymmetric alkylation of aldehydes (Scheme 1.4, B).^{25,26} Both reactions employed ruthenium photocatalysts and light to generate alkyl radicals. MacMillan's approach had an additional imidazolidinone organocatalyst **1.13** which underwent a reversible condensation reaction with the aldehyde, forming an imine, that subsequently favoured radical addition on one face enabling the reaction to be enantioselective.²⁶ A year later, Stephenson and co-workers published the development of a reductive dehalogenation reaction, analogous to those with tributyltin hydride, but with a ruthenium photocatalyst (Scheme 1.4, C).²⁷ These reactions were pivotal in the development of synthetic organic radical transformations and the growth of photoredox catalysis as reactive alkyl radical species could be generated selectively under mild reaction conditions.²⁷

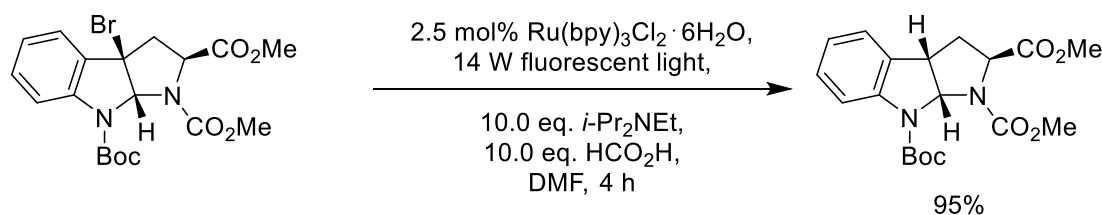
A. Yoon Group, 2008



B. MacMillan Group, 2008



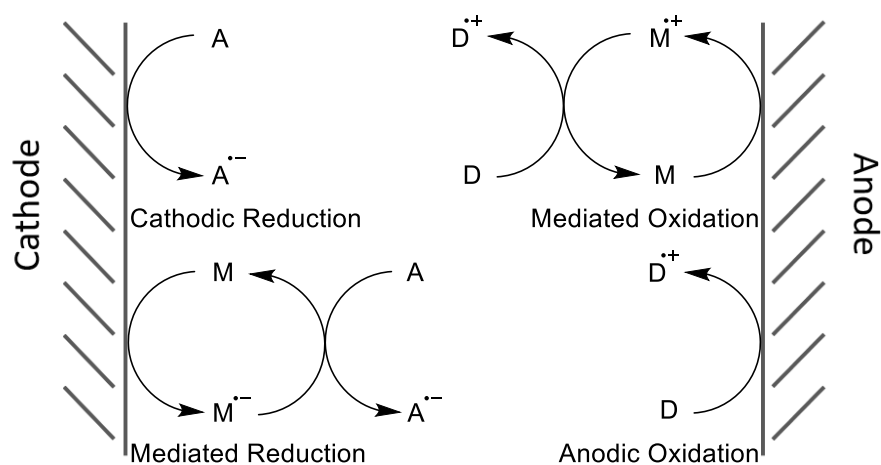
C. Stephenson Group, 2009



Scheme 1.4 Early examples of photocatalytic transformations of small molecules using ruthenium based photocatalysts, A – Yoon group 2008, B – MacMillan group 2008, C – Stephenson group 2009

1.1.3 Radical Generation with Electrochemistry

Electrochemistry offers an alternative method of generating radicals under mild reaction conditions.²⁸ Typically with a photoredox catalyst, a homogenous single electron transfer occurs, whilst in synthetic electrochemistry a heterogeneous process happens.²⁹ Single-electron transfers either occur directly by cathodic reduction or anodic oxidation or *via* mediators. Scheme 1.5 gives four possible routes for electrochemical single-electron transfers. The electrochemical generation of radicals provides an attractive method for creating complex molecules sustainably and with good atom economy by using electrons as reagents.³⁰



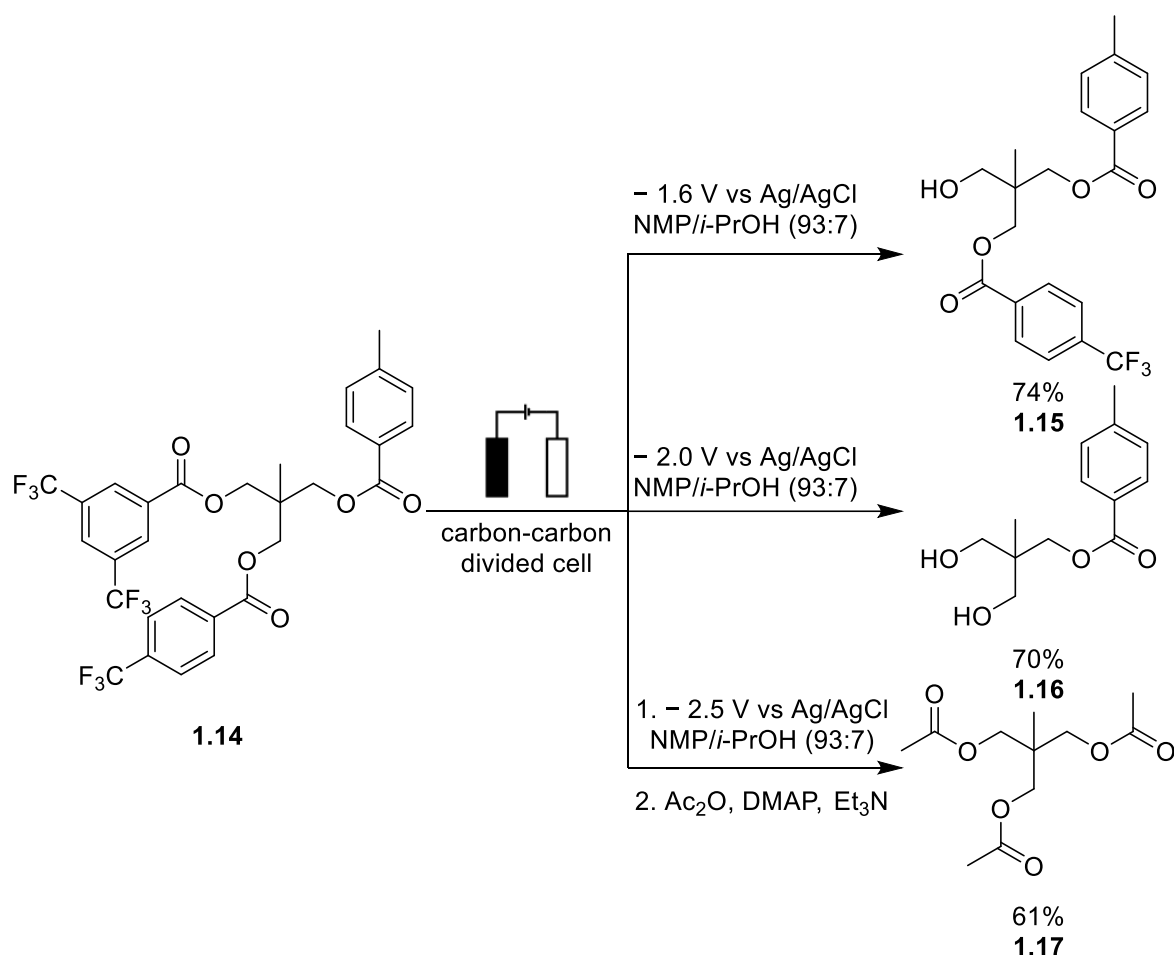
A = electron acceptor, D = electron donor, M = mediator

Arrows which touch the electrode surface indicate an electron transfer process (typically one electron)

Scheme 1.5 Electron transfer mechanisms in an electrochemical cell

Electrolysis reactions can be performed in divided or undivided cells. An undivided set-up is the simplest as only one chamber is required where both the anodic and cathodic processes occur. Whereas in a divided set-up, the anodic and cathodic reactions are separated by a porous frit to allow charge transfer, but no solution mixing.³¹ Whilst the undivided set-up is more common due to its simplicity, the divided set-up is used when one of the reagents or products is prone to an undesired oxidation or reduction. Both the current and the potential can be controlled and varied, which controls the reaction kinetics and thermodynamics respectively. A constant potential experiment is usually used to achieve a selective oxidation or reduction, as only functional groups with an oxidation or reduction potential within the

applied potential window can thermodynamically undergo electron transfer at the electrode.³² For example, Lam *et al.* showed that changing the applied electrochemical potential can selectively cleave different aromatic esters on **1.14** to reveal the desired hydroxyl group **1.15-1.17** (Scheme 1.6).³³

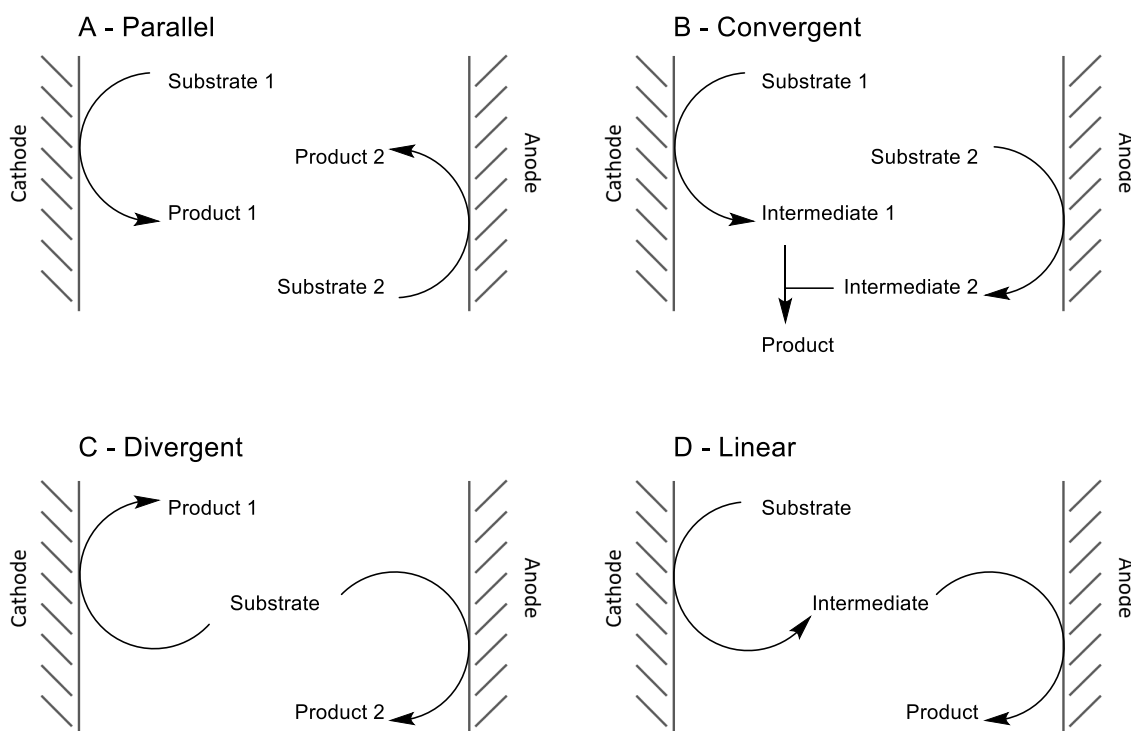


Scheme 1.6 The effect of cell potential on the outcome of cleaving various aromatic esters

One issue with adopting electrochemistry for synthetic applications is the initial development of an appropriate set-up, cell and electrode design.³⁴ However, recently commercial electrochemical set-ups, such as the ElectraSyn 2.0 developed by Baran and IKA®, have been released. Standardised electrochemical set-ups allow practising organic chemists to access electroorganic methodologies without first developing a bespoke electrochemical set-up which is said to improve the reproducibility of literature procedures.²⁸

In electrochemistry, in order for the desired reaction to occur at the working electrode (either the anode or the cathode), a simultaneous process must also take place at the counter

electrode. This paired electrolysis can be used in many ways and can be termed parallel, convergent, divergent, and linear (Scheme 1.7).³⁵ A parallel process is the most common. In a parallel process, two separate starting materials are added to the electrochemical cell, one is oxidised whilst the other is reduced and two separate products are obtained (Scheme 1.7 A), whereas in the convergent synthesis, the products of oxidation and reduction combine to form only one product (Scheme 1.7 B). A convergent synthesis requires the reaction to be performed in an undivided cell. In a divergent electrosynthesis, one starting material is added, which yields two separate products, one the product of oxidation and the other the product of reduction (Scheme 1.7 C). Finally in the linear electrosynthesis, only one starting material is added that is both oxidised and reduced to afford the final desired product (Scheme 1.7 D shows an example where reduction is followed by oxidation).³⁵



Arrows which touch the electrode surface indicate an electron transfer process (typically one electron)

Scheme 1.7 Various approaches to paired electrolysis: A – parallel, B – convergent, C – divergent, D – linear

Many of the electrosynthetic reaction parameters can be varied to achieve high yields of desired product.³¹ These include the applied cell potential, which can be used to increase the rate of the reaction as a higher voltage can lead to a higher current, however, this can also lead to unwanted side reactions that may occur above or below the potential of the desired

reaction. Increasing the current can lead to a higher radical concentration near or at the electrode surface which will favour radical-radical coupling. The degree to which the reaction is performed can be varied by changing the amount of charge passed.³⁵ Other factors that can influence the outcome of the reaction include electrode material and or spacing, the reaction solvent and the addition of a supporting electrolyte.³¹

Electrosynthesis not only avoids harmful metal-based oxidised or reducing agents but has the added advantage over photoredox catalysis in that the electrodes can be easily removed at the end of the reaction and reused (unless a sacrificial electrode was employed).⁴ An important advantage of electrochemical radical generation is electroanalytical data can be obtained for a specific substrate-electrode interaction and this data can be used selectively to achieve a desired reaction.³¹ This information can be used to set specific redox potentials more easily than with a photocatalyst.

Since reactions can be performed directly at the electrodes surface, only using electrons as reagents, negligible amounts of waste can be generated during electrolysis.³⁶ Furthermore, when combined with renewable energy source, electrosynthesis can be a carbon-neutral method of chemical manufacturing.³⁵ Electrolysis does however require a conducting (often ionic) medium and so typically a supporting electrolyte is added to aid the flow of electrons. As supporting electrolytes are often charged species and used in a large excess of the starting materials, they can sometimes be challenging to remove and contribute to the amount of waste produced during the reaction.²⁹ In some cases, charged species are used as reagents, avoiding the need for a supporting electrolyte and close electrode spacing minimises solvent resistance.³⁵

Unlike in photochemistry, during electrolysis a high localised radical concentration can be formed at the interphase of the electrode surface and solution. This results in an increase in transient radical-transient radical (short lived radicals) coupling, compared to photoredox catalysis where one of the radicals must be persistent (longer lived) to achieve coupling. However, the high local radical concentration at the electrode surface can lead to radicals undergoing a second electron transfer as they are in the vicinity of the electrode. This contrasts photochemical reactions, where the likelihood of a radical encountering an active photocatalyst again is low, due to low catalyst concentrations.²⁹ The addition of a mediator in electrochemical approaches has been shown to improve the yields of the single electron

process, over unwanted second electron transfers, by moving the electron transfer away from the electrode surface.^{29,37}

Researchers have been trying to further expand the field of electrosynthesis by developing new transformations and reviving old reactions. Established photoredox reactions can create a basis for the development of new electrochemical methodology.^{3,29} In the next section, some of the more recent developments in the field of synthetic organic electrochemistry will be highlighted, mainly focusing on the generation of alkyl radicals for carbon-carbon bond formation.

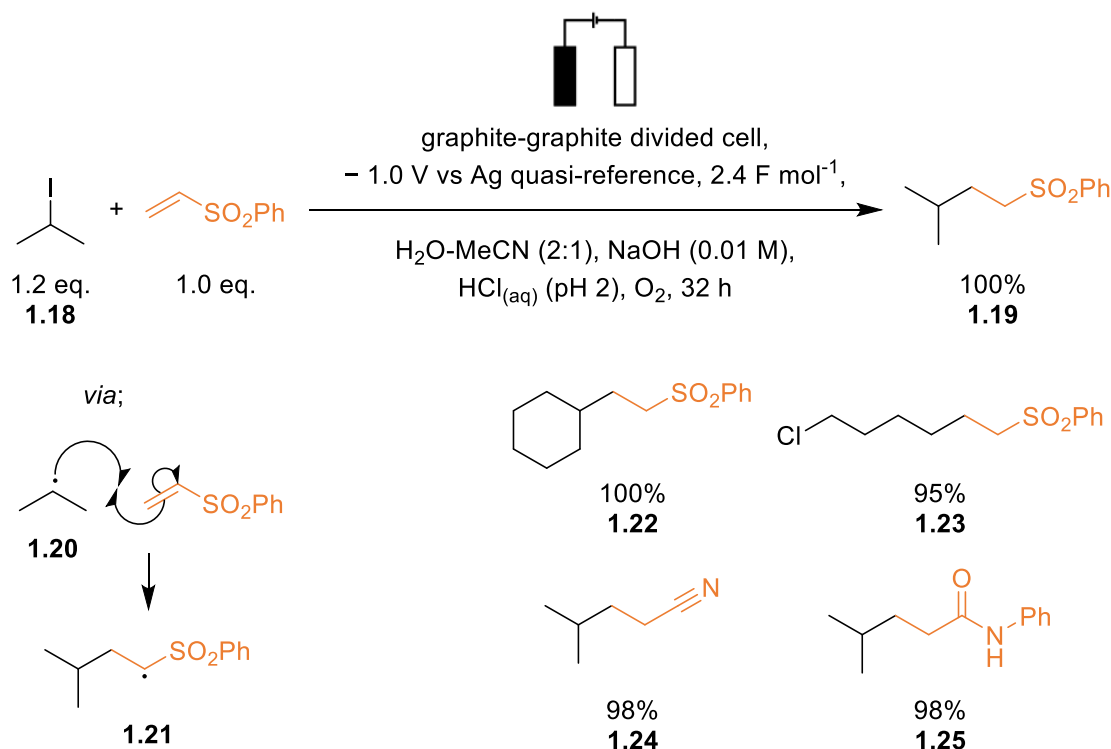
1.2 Highlights of Electrochemical Alkyl Radical Generation from Recent Literature

Recent reviews have illustrated the variety of transformations available for organic electrochemistry.^{3,4,29,38,39} Some examples of notable electrosynthetic transformation include C-N bond forming radical cascades to access imidazo-fused *N*-heteroaromatic compounds,⁴⁰ intramolecular aminooxygenation to access 1,2-aminoalcohol motifs,⁴¹ C-H activation to cross-couple phenols and thiophenes,⁴² the reduction of nitrones to amines,⁴³ the arylation of alcohols,⁴⁴ and the ring expansion of cyclobutanols.⁴⁵ Organic electrochemistry has also been used to construct natural products such as Dixiamycin B.⁴⁶ In order to illustrate the importance and value of synthetic electrochemistry in organic synthesis, this section will focus on three different methods of carbon-carbon bond formation *via* electrochemical generated alkyl radicals, which have been published since 2020.⁴⁷⁻⁴⁹ Whilst this is not a comprehensive list of reactions, these three highlight a range of different approaches to electrochemical alkyl radical generation.

The Wilden Group demonstrated that it was possible to electrochemically generate alkyl radicals from alkyl halides (Scheme 1.8).⁴⁷ A divided cell was used, meaning the reductive and oxidative processes were separated, with graphite working and counter electrodes. As the reaction required both oxygen and water, mechanistically, it was thought that initially oxygen was reduced at the cathode to superoxide radicals which reacted to form hydroxyl radicals. The hydroxyl radicals then reacted with the alkyl halide, typically iodide (**1.18**), forming an unstable I(II) species that fragmented to give an alkyl radical (**1.20**) and generate IOH. A pH of less than 2 was maintained, by adding hydrochloric acid at the start of the reaction, to avoid the formation of hydroxide, which could preferentially react with the

electron-deficient alkenes.⁴⁷ After addition to the alkene, the resulting alkyl radical **1.21** either underwent a hydrogen atom transfer or a second electron reduction to the corresponding anion which was subsequently protonated, delivering the desired coupled product **1.19**.

The tin free electrochemical reaction of alkyl halides gave high yields of the coupled products, often in higher yields than with organostannanes. A range of alkyl iodides were compatible (see **1.19** and **1.22** for representative examples) and the reaction was found to be selective for the cleavage of carbon-iodine bonds over carbon-chlorine (**1.23**). Alkyl bromides were also reactive substrates but were found to be lower yielding (**1.19** was achieved in a 21% with the corresponding alkyl bromide). Finally the reaction was compatible with a broad range of electron-deficient alkenes (see **1.24** and **1.25** for representative examples).⁴⁷

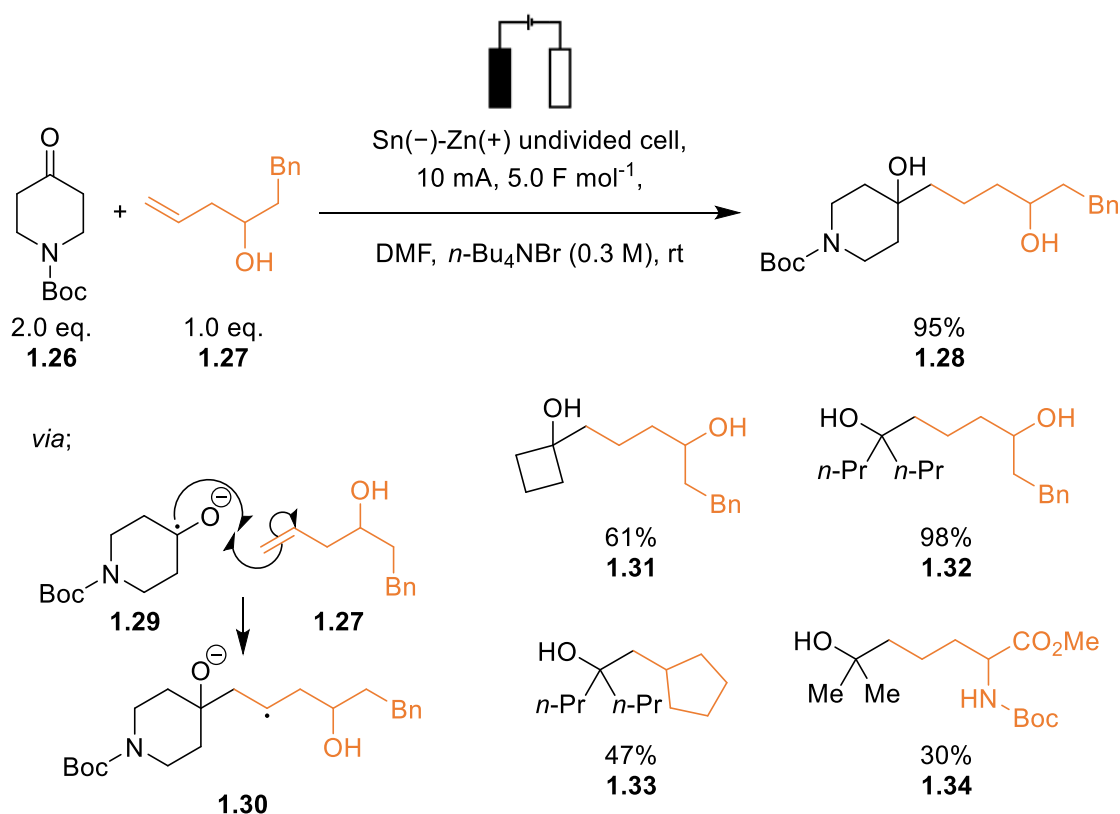


Scheme 1.8 Electrochemical generation of alkyl radicals from alkyl halides and coupling with electron-deficient alkenes by the Wilden group⁴⁷

In another approach, alkyl radicals were electrochemically generated *via* the reduction of ketones (Scheme 1.9).⁴⁸ The Baran Group used an undivided cell, constant current (10 mA) and the reaction still proceeded in air and did not require dry conditions. A tin cathode was

used to reduce the ketone and zinc was used as a sacrificial anode. Mechanistically, at the cathode, the ketone **1.26** was reduced to the corresponding carbon centred ketyl radical anion **1.29**, which was theorised to be adsorbed onto the tin electrode. This radical anion in turn underwent radical addition to alkenes (such as **1.27**) resulting in alkyl radical **1.30**. A second electron reduction gave a dianion that was subsequently protonated by a second equivalent of the ketone, and finally, the anion was protonated in the work-up step to give **1.28**.⁴⁸

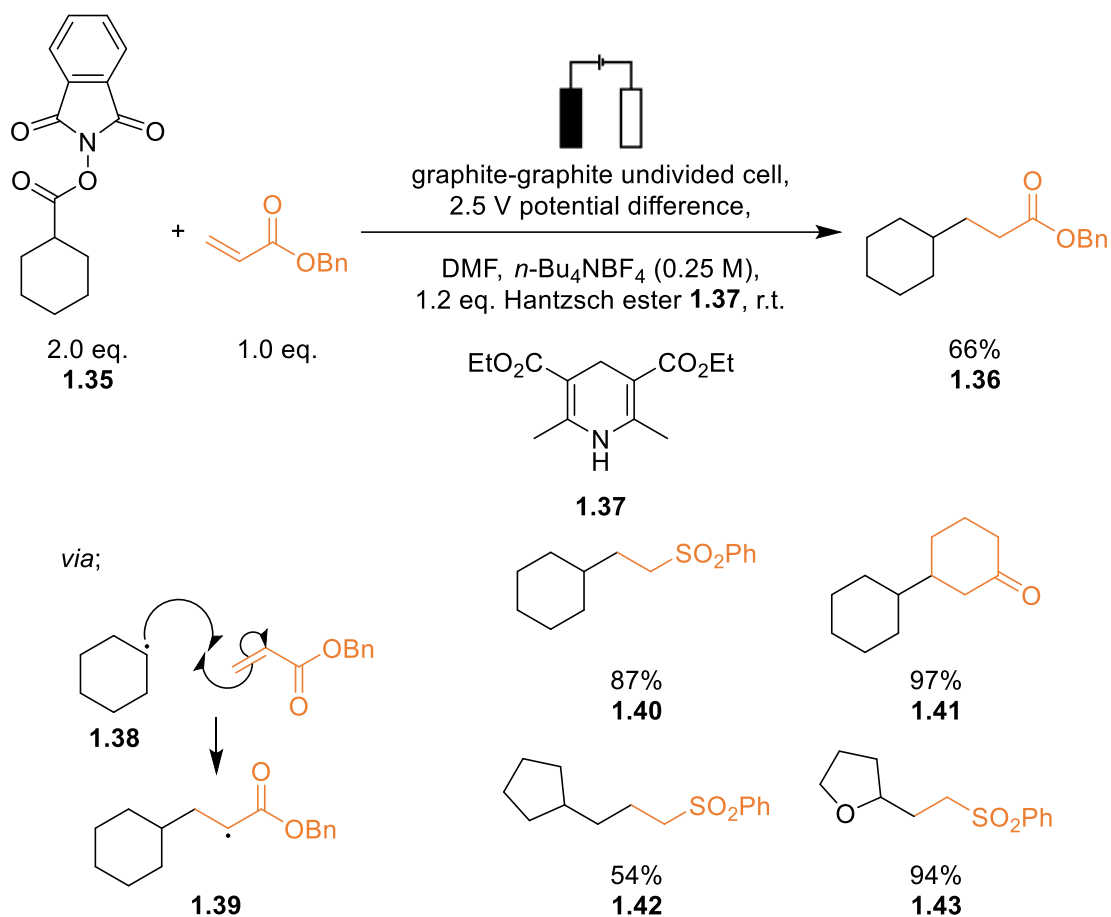
A large number of cyclic and acyclic ketones were successfully reacted under the optimised conditions (see **1.28**, **1.31** and **1.32** for representative examples), however the introduction of larger *iso*-propyl groups significantly reduced the yield of the alcohol addition product due to increased steric hinderance and α -substituents (such as esters) were unsuccessful. A variety of different alkenes were compatible (see **1.33** and **1.34** for representative examples) and using a flow system, the reaction was successfully scaled up to a 100 g synthesis.⁴⁸



Scheme 1.9 Electrochemical reduction of unactivated ketones to alkyl radicals and addition to alkenes by the Baran group⁴⁸

Even though radical decarboxylation was first studied in the 19th century (Kolbe electrolysis), it remains a very successful method of electrochemical generation of alkyl

radicals.^{50–53} Carbon centred radicals can be formed through a one electron oxidation of a carboxylic acid (this will be discussed in more detail in Chapter 2).³ Alternatively, in a reductive variant, a redox-active ester is used to accept an electron, before fragmenting and decarboxylating to form an alkyl radical.⁴⁹ Photochemistry, metal mediated electron transfers and electrochemistry have all been used to facilitate the reduction of redox-active esters.^{23,29} In the work by the Wang Group, alkyl radicals were generated at a graphite cathode by reduction of a redox-active phthalimide ester **1.35**, which fragmented, to form phthalimide, carbon dioxide and an alkyl radical **1.38**. The radical formed was then used for coupling to electron-deficient alkenes, delivering new alkyl radicals **1.39** which underwent a hydrogen atom transfer, giving the coupled product **1.36** (Scheme 1.10).⁴⁹ The electrolysis was performed in an undivided cell, and a Hantzsch ester (**1.37**) was used as a sacrificial electron donor and hydrogen atom transfer agent. A range of electron withdrawing groups were tolerated on the alkene (see **1.36**, **1.40** and **1.41** for representative examples) with a variety of redox active esters (see **1.42** and **1.43** for representative examples).⁴⁹ This approach, whilst highly selective for the reduction of the phthalimide ester, has a significant limitation in that it has a very poor atom economy as the redox-active ester is lost during the reaction.



Scheme 1.10 Electrochemical reduction of redox-active phthalimide esters to alkyl radicals and addition to electron-deficient alkenes by the Wang group⁴⁹

Electroorganic chemistry has been shown to be a versatile method of alkyl radical generation. The electron rich alkyl radicals which were formed, have typically undergone addition to electron-deficient alkenes to generate intermolecular carbon-carbon bonds without the need for harsh reducing or oxidising agents. Electrochemistry has even allowed reactions to be scaled up and reduce the number of steps required for the synthesis of complex molecules.⁴⁸ However, as the fields of both electrochemistry and radical chemistry are undergoing a renaissance, there is scope to revisit and improve old reactions and develop new.

1.3 Aims of Project

The overall aim of this work is to improve understanding and develop synthetic electrochemistry for the construction of carbon-carbon bonds *via* alkyl radicals. Synthetic electrochemistry has demonstrated a wide range of capabilities and alkyl radicals can be generated under very mild conditions, often in air and without using toxic or expensive catalysts.

Initially, this work will build on the knowledge of an existing electrochemical reaction, Kolbe electrolysis, which can be used for the coupling of two carboxylic acids, *via* oxidative decarboxylation (Chapter 2). Kolbe electrolysis is at the basis of many of recent synthetic methods for alkyl radical formation as carboxylic acids are cheap, readily available starting materials (Scheme 1.11). The aim of Chapter 2 is to further develop Kolbe electrolysis for the coupling of alkyl radicals derived from carboxylates as a method for small molecule synthesis and try and improve the selectivity of the reaction to favour the hetero-coupling of two different alkyl radicals.



Scheme 1.11 General Kolbe electrochemical hetero-coupling as proposed for Chapter 2

Next, an electrochemical variant for the photochemical construction of tertiary amines, by reduction of iminium ions, will be developed (Chapter 3). Amines are important moieties in many pharmaceuticals and agrochemicals and recent photocatalytic work has shown that complex, sterically hindered, tertiary amines can be constructed by reductively generated α -amino radicals. A complementary electrochemical variety of the photochemical reductions will avoid the need for expensive, precious metal, iridium photocatalysts that have typically been employed to generate the intermediate radicals. The aim of the work will be to develop an electrochemical approach for the generation of α -amino radicals, which will undergo radical addition to alkenes to construct a new carbon-carbon bond and create complex α -tertiary centres (Scheme 1.12).



Scheme 1.12 General iminium ion reduction and addition to alkene as proposed for Chapter 3

Chapter 2: Developing Kolbe Electrolysis for Electrochemically Generating Alkyl Radicals from Amino Acids

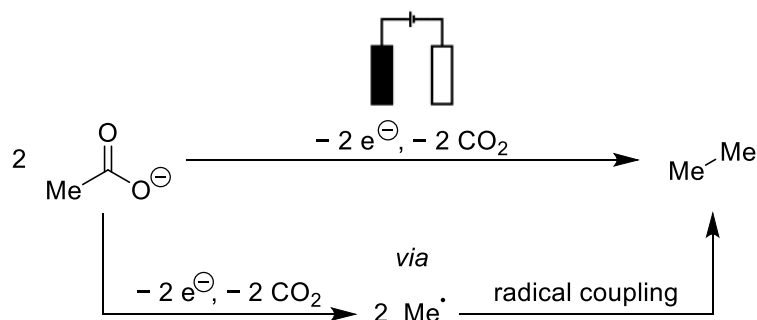
2.1 Introduction

Kolbe electrolysis is a well-known electrosynthetic reaction in which carboxylates are anodically oxidised to form CO₂ and alkyl radicals. The alkyl radicals formed typically partake in radical-radical coupling reactions, forming synthetically useful sp^3 - sp^3 hybridised carbon-carbon bonds. Carboxylic acids are widely abundant and useful precursors, for instance, six out of ten bio-based chemicals promoted by the UK biorefinery network LBNet as the most promising sustainable long term resource for chemical building blocks are carboxylic acids.⁵⁴ This means radical transformations involving carboxylic acids are very attractive. Since its discovery in 1834, a large amount of literature has been published on Kolbe electrolysis, looking at the mechanism of the reaction and some of the small scale synthetic and some industrial applications. The current understanding of the reaction mechanism will be described below. This work aims to further study and develop Kolbe electrolysis as a synthetic reaction for the hetero-coupling of alkyl radicals derived from two different carboxylic acids. This chapter begins with a review of the mechanism for Kolbe electrolysis, factors that affect the outcome, and a brief overview of the synthetic scope of the reaction limited to decarboxylative radical-radical couplings and the products of further oxidation. The second half of this chapter endeavours to improve the selectivity of the reaction in favour of radical coupling over further oxidation.

2.1.1 History of Kolbe Electrolysis

Kolbe electrolysis offers a useful way of forming C-C bonds *via* anodic decarboxylation of carboxylic acids to form carbon centred radicals (Scheme 2.1) which has been applied to industrial process, such as the synthesis of sebacic acid.⁵⁵ This reaction was discovered in 1834, when Faraday studied the effect of electrolysis on acetic acid solutions and reported the production of an unknown gas, which was later revealed to be ethane.⁵⁶ In 1849 it was Hermann Kolbe who described this reaction in more detail and concluded that ethane was generated by the homo-coupling of methyl radicals through a decarboxylative radical reaction (Scheme 2.1).⁵⁷ In 1855, Wurtz was the first to report a successful hetero-coupling

of two different carboxylic acids *via* electrolysis.⁵⁶ Both homo- and hetero-coupling of carboxylic acids *via* anodic decarboxylation are now commonly referred to as “Kolbe electrolysis”. The balancing cathodic process is generally attributed to proton reduction to generate hydrogen, as detailed later.



Scheme 2.1 Kolbe homo-coupling of methyl radicals derived from acetic acid first observed by Faraday.⁵⁶

Since the discovery of Kolbe electrolysis, a large amount of literature has been published. The latter half of the 20th Century saw many studies focusing on the reaction mechanism.^{30,55,56,58} Despite the age of the reaction, it is still relevant for synthetic organic chemists to study today. The apparent simplicity of set-up for Kolbe electrolysis, a two electrode configuration, in an undivided cell with a controlled potential or current, makes it attractive to synthetic chemists with no prior electrochemistry background.⁵⁹

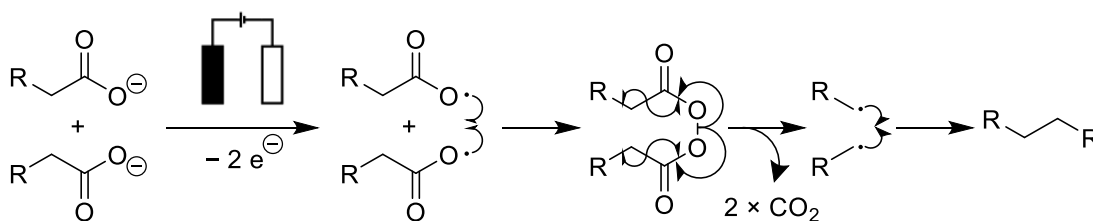
2.1.2 Previous Mechanistic Proposals for Kolbe Electrolysis

Early mechanistic proposals have been previously reviewed, however a brief overview of them will be given here.⁵⁶ The current mechanistic proposals will be discussed in more detail in a later section (Section 2.1.3).

2.1.2.1 Acyl Peroxide Theory

Schall (1896) and Fichter (1929) proposed that carboxylate anions oxidise at the electrode surface before diffusing away from the electrode as carboxyl radicals.⁶⁰ These radicals then couple to form an acyl peroxide which subsequently decomposes to form two alkyl radicals. Finally, the two alkyl radicals, free in solution, combine to form the Kolbe product and two molecules of CO₂ (Scheme 2.2). This theory was dismissed as only small amounts of acyl peroxides (at low temperatures and under flow conditions) were ever observed.⁶¹ In addition, when samples of dipropionyl peroxide were thermally decomposed (homolytic

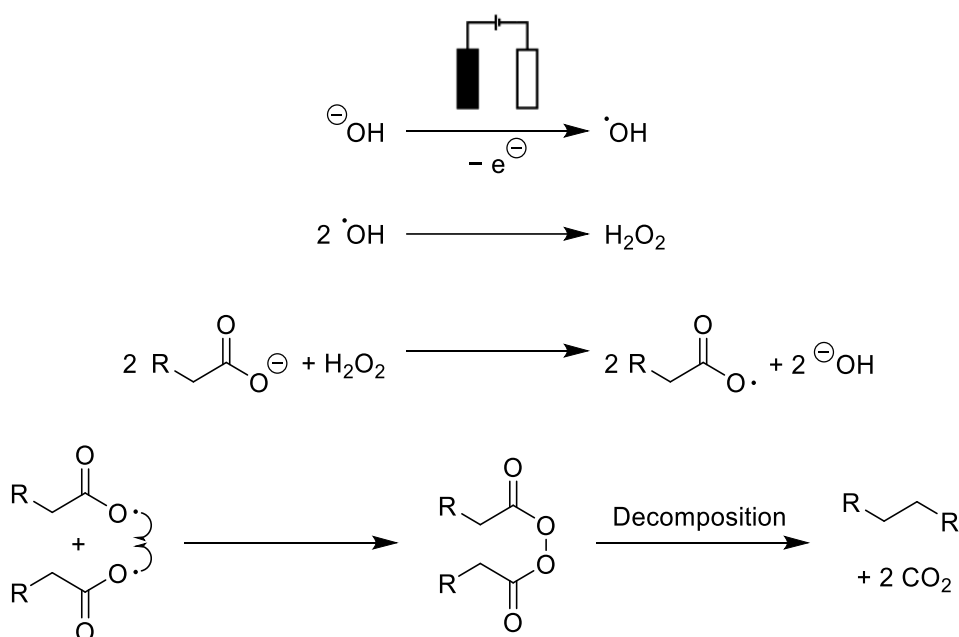
decomposition), a different ratio of radical coupling products (*n*-butane) were observed compared to electrolysis of the equivalent Kolbe starting acid, propanoic acid.⁵⁶



Scheme 2.2 Kolbe electrolysis acyl peroxide mechanism proposed by Schall and Fichter.⁶⁰

2.1.2.2 Hydrogen Peroxide Theory

Glasstone and Hickling (1930s) suggested that, in aqueous solutions, hydroxide anions are electrochemically oxidised to hydroxyl radicals which combine to form hydrogen peroxide.^{60,62} The hydrogen peroxide formed then reacts with the carboxylate ion to form carboxyl radicals which, like in the acyl peroxide theory, can combine and decompose to give the Kolbe product and CO₂ (Scheme 2.3).⁶³ However, when additional hydrogen peroxide was added to Kolbe electrolysis, only trace amounts of Kolbe products were observed. Hydrogen peroxide was never detected during Kolbe electrolysis and the best Kolbe electrolysis efficiencies are observed in non-aqueous media. Therefore, it is very unlikely that hydrogen peroxide is involved in the mechanism.⁵⁶



Scheme 2.3 Kolbe electrolysis hydrogen peroxide mechanism proposed by Glasstone and Hickling.^{62,63}

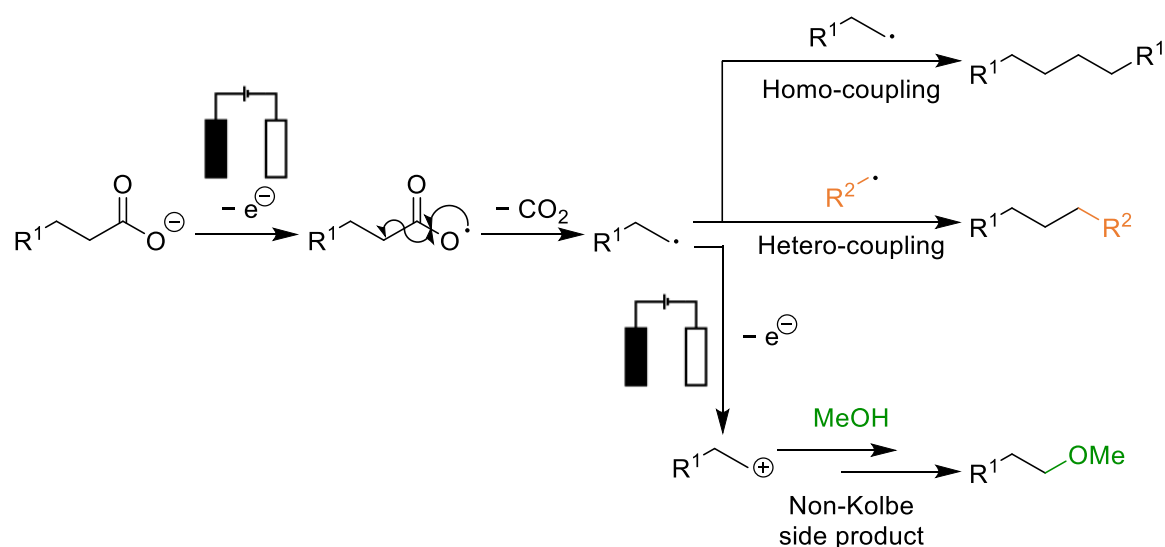
2.1.2.3 Alkyl-Radical Theory

Crum-Brown and Walker (1891 and then developed by Walker in the 1930s) originally proposed that Kolbe electrolysis proceeded *via* a direct electrochemical oxidation of carboxylate anions to carboxyl radicals which fragmented to give alkyl radicals.⁶⁰ The early mechanism lacked details about whether radicals were free in solution or adsorbed onto the electrode surface. The mechanism by Crum-Brown and Walker forms the basis of the current understanding of the mechanism of Kolbe electrolysis.⁵⁵

2.1.3 Current Mechanistic Proposal for Kolbe Electrolysis

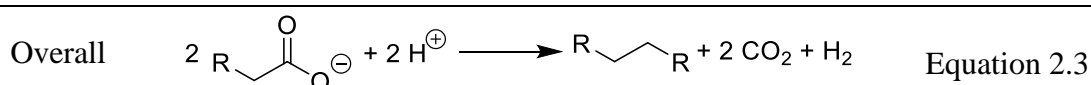
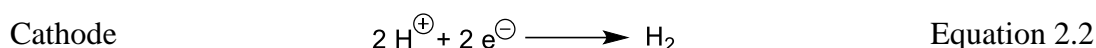
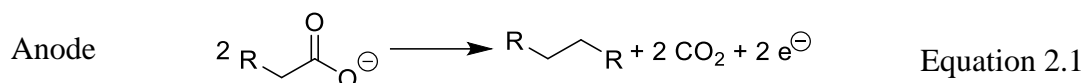
2.1.3.1 Overview of Currently-Accepted Mechanism for Kolbe Electrolysis

The widely accepted general mechanism for Kolbe electrolysis is that carboxyl radicals are formed at the anode (typically platinum) from carboxylate ions that are generated by deprotonation of the carboxylic acid starting material. The carboxyl radicals undergo decarboxylation to form a carbon-centred radical. The carbon radicals can homo-couple, where two of the same radicals combine, or in reactions where mixtures of different carboxylic acids are used, hetero-coupling between two different radicals is observed.³⁰ Alternatively, radicals can be further oxidised at the anode to form carbocations which subsequently react to yield a range of side-products conventionally termed “non-Kolbe” products. In the example below the non-Kolbe product is derived from nucleophilic attack from the solvent, methanol (Scheme 2.4).⁶⁴



Scheme 2.4 Currently accepted mechanism for Kolbe electrolysis showing homo-coupling, hetero-coupling and the non-Kolbe pathway and carbocation formation

As mentioned above, the complementary half-reaction to carboxylate oxidation at the anode (Equation 2.1) is proton reduction at the, typically a platinum, cathode to give hydrogen gas (Equation 2.2). The overall net redox reaction of Kolbe electrolysis is therefore as given in Equation 2.3.



The Kolbe reaction has been studied in great depth. Mechanistic features have been determined by analysing both electrolysis products and electrochemical characteristics of the process.^{56,65} There is still some dispute about certain steps in the mechanism, however the concepts presented below are generally considered to be an accurate depiction of the mechanism. The critical components of the mechanism are: deprotonation of carboxylic acid by base to form negatively charged carboxylate species, oxidation of the adsorbed carboxylate to a carboxyl radical followed by decarboxylation and desorption of alkyl radicals. Finally, radicals, either free in solution or weakly adsorbed, couple to form Kolbe products.

2.1.3.2 Maintaining Constant Carboxylate Concentration

The carboxylate ion is formed from the carboxylic acid starting material using a relatively small amount of base, typically 5-10% of the total acid concentration. Carboxylate anions and the corresponding protonated base-derived cations make up the electrolyte, i.e. inert salts are not added to increase the ionic conductivity of the solution. In Kolbe electrolysis, base is not consumed as protons are reduced at the cathode (Equation 2.2).⁵⁸ This means that during electrolysis, the carboxylate concentration, and subsequent pH of the solution, will remain nearly constant until the end of the reaction. When all the acid is consumed the solution becomes basic. Measuring the pH of the reaction has been used as a method of determining the end point of Kolbe electrolysis.⁵⁸

2.1.3.3 Formation of a Carboxylate Monolayer at the Electrode Surface

Kolbe electrolysis will only proceed above an applied critical anode potential. This is clearly visualised in Tafel plots that show the anode potential as a function of $\log(\text{current density})$. For example, Figure 2.1 shows a Tafel plot for Kolbe electrolysis of sodium acetate (0.5 M in acetic acid); below the critical potential of approximately 2.1 V vs normal hydrogen electrode (NHE), very little oxidative current flows. In non-aqueous solutions, e.g. methanol, this region is associated with solvent oxidation. Above the critical potential of 2.1 V the desired Kolbe product is observed.⁶⁶⁻⁶⁸

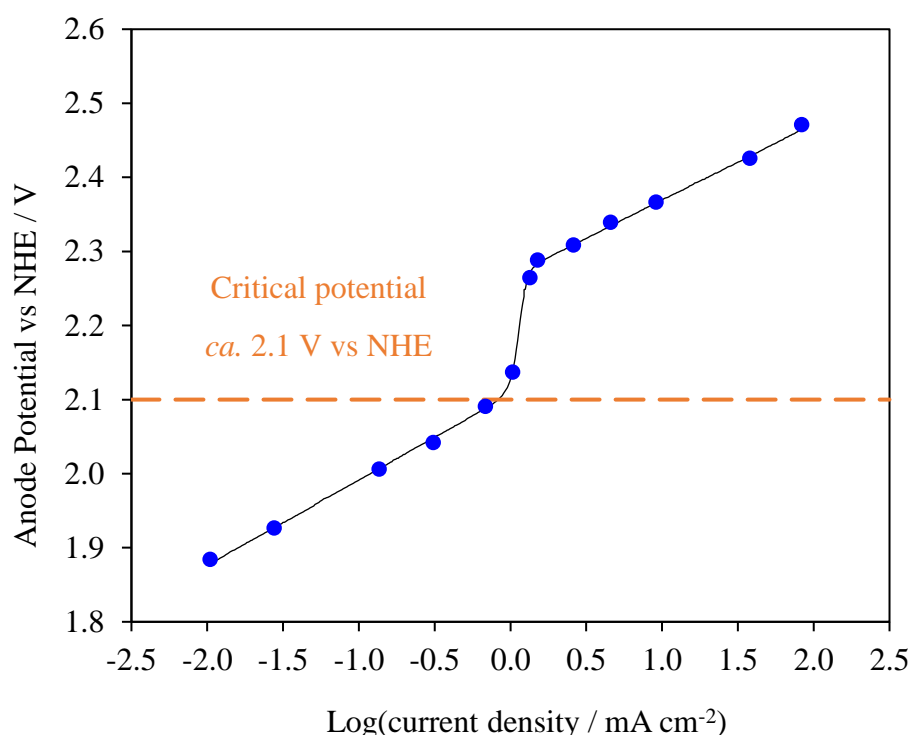


Figure 2.1 Tafel plot for sodium acetate in acetic acid showing $\log(\text{current density})$ vs anode potential with critical potential (ca. 2.1 V vs NHE) reproduced from Dickinson et al. 1961.⁶⁶

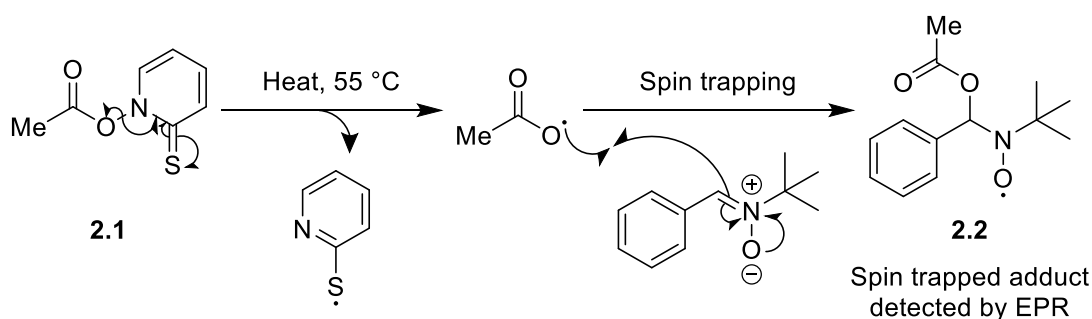
The critical potential does not map on to the thermodynamic oxidation potential of the carboxylic acid. Instead, the shape of a Kolbe electrolysis Tafel plot is ascribed to the requirement for the acid starting material to displace the solvent molecules from the electrode surface, i.e. the formation of a carboxylate layer at the anode surface occurs above the critical potential. This formation of an adsorbed layer of carboxylate ions inhibits competing solvent oxidation.⁶⁹ Formation of the adsorbed layer of carboxylate has been confirmed by using radiochemical techniques.⁷⁰ In the electrolysis of ¹⁴C labelled acetic acid,

labelled at either the methyl or carbonyl, chemisorbed species were detected by the β count at the platinum anode providing strong evidence in favour of adsorbed carboxylates.⁷¹

2.1.3.4 Concerted or Stepwise Oxidation and Decarboxylation

At the surface of the electrode, once a layer of carboxylate anions have adsorbed onto the anode, the carboxylates are oxidised *via* the loss of a single electron from the highest occupied molecular orbital.⁵⁹ Ebersson *et al.* proposed that this single electron transfer from a carboxylate to the anode occurs alongside simultaneous breaking of a C-C bond to release CO₂ and form the intermediate alkyl radical in a single, concerted step.⁶⁵ Conversely, a stepwise oxidation and subsequent decarboxylation Kolbe reaction mechanism has been proposed by Conway *et al.* who suggested the detection of carboxyl radicals in Kolbe electrolysis may be challenging because they are extremely short-lived (half-life *ca.* 10⁻⁸ s).^{58,72}

Carboxyl radical have been observed by EPR in photo-Kolbe reactions on TiO₂ powders, and as spin-trapped adducts **2.2** in the thermal decomposition of *N*-(acyloxy)pyridine-2-thione, **2.1** (Scheme 2.5).^{73,74} Based on this evidence from related reactions, Kolbe electrolysis now thought to proceed *via* a stepwise mechanism.

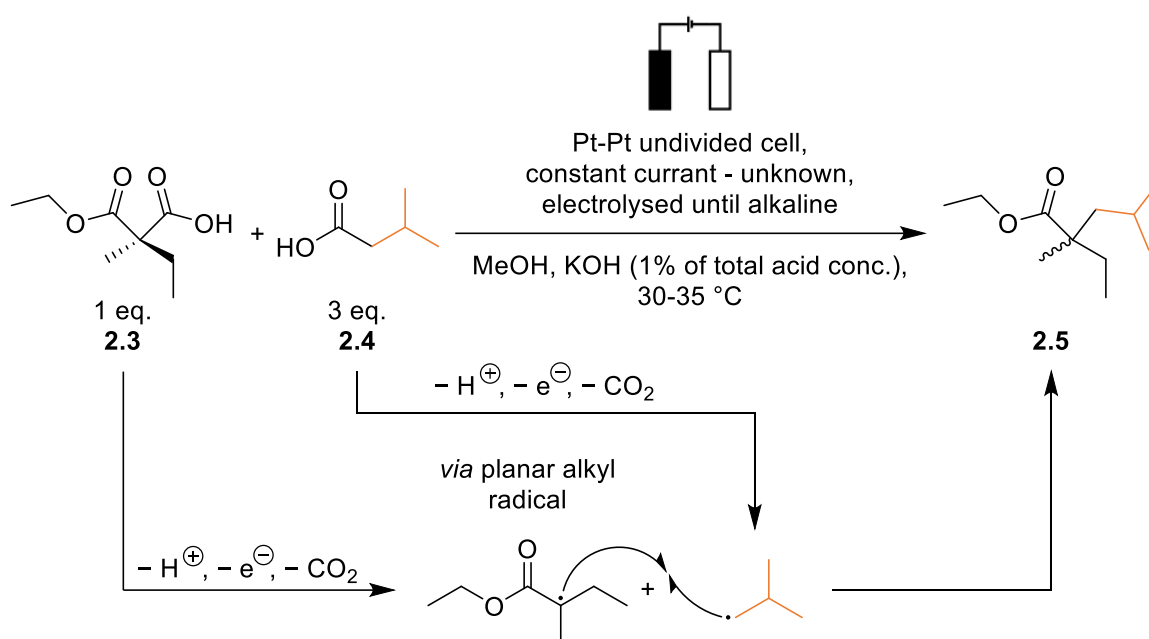


Scheme 2.5 Spin trapping of carboxyl radicals in photo-Kolbe reactions.^{73,74}

2.1.3.5 Adsorbed Alkyl Radical Intermediates

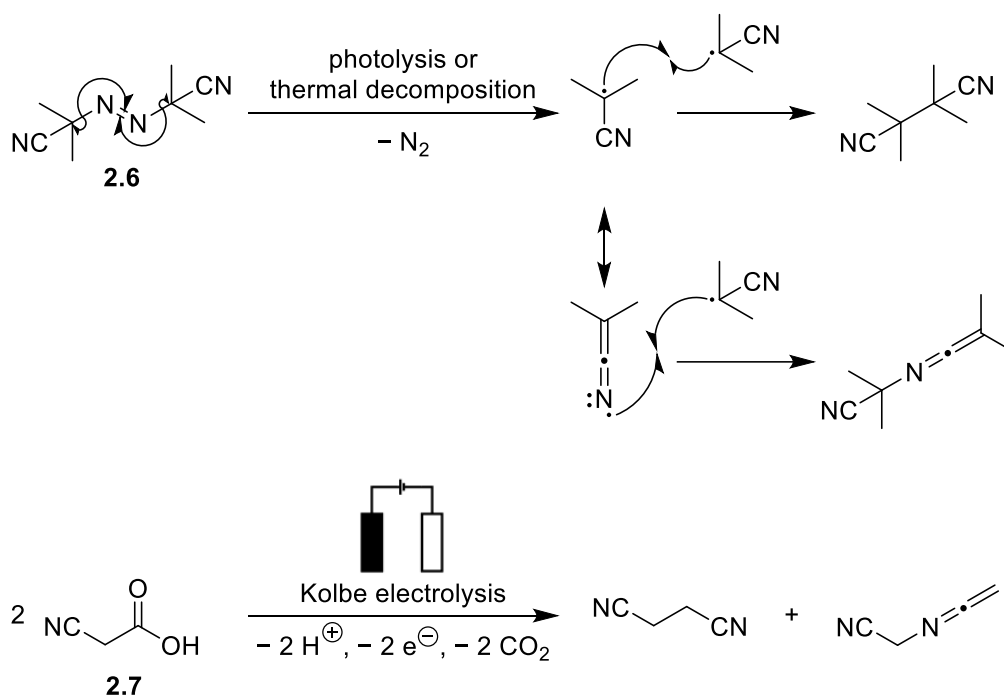
There is still debate about the fate of the alkyl radicals formed in Kolbe electrolysis. When an α -chiral carboxylate, monoethyl (+)-ethylmethylmalonate **2.3**, was electrolysed with isovaleric acid **2.4**, 99.98% racemisation was observed (**2.5**, Scheme 2.6).⁷⁵ This result is consistent with the loss of chirality observed for other related enantioenriched carboxylates.⁷⁶ This outcome favours a “free radical” mechanism, where radicals formed in Kolbe electrolysis can tumble or freely rotate in solution and are not strongly adsorbed onto

the electrode surface. Another possible explanation for the experimental results could be rapid desorption and re-adsorption of the radical onto the electrode surface, which would also result in a loss of chirality and thus suggest the radical is weakly adsorbed onto the surface.^{58,75,77} Some propose the loss of chirality can be explained by “microscopic roughness” of the anode surface (not a smooth electrode surface on a microscopic level) which would result in a loss of stereochemistry, although it would be expected that some degree of chirality would be retained.⁵⁶ Furthermore, the loss of chirality may occur after decarboxylation, prior to adsorption of the alkyl radical. Therefore, whilst these results strongly support a free or weakly adsorbed radical mechanism, further evidence is required.



Scheme 2.6 Kolbe electrolysis of monoethyl (+)-ethylmethylmalonate and isovaleric acid to give racemised product **2.5**.⁷⁵

Further experimental evidence in favour of a free radical mechanism has been given by the regioselectivity of Kolbe electrolysis with cyanoalkyl radical precursors.⁶⁵ When formed, cyanoalkyl radicals are known to homo-couple either through a radical localised on the carbon or on the nitrogen (Scheme 2.7). Similar ratios of products (C-C coupling and C-N coupling) were found after both homogeneous radical formation with AIBN **2.6** and electrolysis of α -cyanoacetic acid **2.7** (Table 2.1). This result suggests that cyanoalkyl radicals, prepared by Kolbe electrolysis, are free in solution.^{58,65}

Scheme 2.7 The fate of cyanoalkyl radicals formed from photolysis, thermolysis and Kolbe electrolysis.⁶⁵Table 2.1 Products from coupling between cyanoalkyl radicals from different sources.⁶⁵

Entry	Starting Material	Reaction	Solvent	C-C coupling / %	C-N coupling / %
1	2.6	Thermal decomposition	CCl ₄	46	54
2	2.6	Photolysis	CCl ₄	43	57
3	2.7	Electrolysis	MeOH	49	51
4	2.7	Electrolysis	MeCN	46	54
5	2.7	Electrolysis	DMF	45	55
6	2.7	Electrolysis	H ₂ O	64	36
7	2.7	Persulfate oxidation	H ₂ O	58	42

In contrast, there is reasonable indirect evidence from electrochemical studies to support adsorbed alkyl radical intermediates. Adsorbed radicals have been detected and are accepted in many electrochemical reactions.⁷⁸ Therefore, it would be surprising that Kolbe electrolysis would proceed *via* a totally different free-radical mechanism.⁷⁹ Furthermore, the adsorption of related alkyl radicals, derived from the oxidation of gaseous ethane in 1 M HClO_{4(aq)}, have been detected on solid platinum electrodes.^{80,81}

Further evidence for alkyl radical adsorption follows the electrolysis of aqueous solutions of acetate at various pulse frequencies. It was found that the carbocation derived non-Kolbe product was favoured over the radical derived Kolbe product at increased pulse frequencies.^{82,83} The non-Kolbe product arises from further oxidation of alkyl radicals to carbocations and therefore the radicals would be required to be at the surface of the electrode to undergo the second electron oxidation. If the radicals were free in solution, then the pulse frequency would not affect the outcome as once they desorb and move into the bulk solution, away from the electrode, they will not be able to undergo the second electron oxidation. Therefore as the non-Kolbe product yield increased, the radicals must be sufficiently adsorbed or close to the electrode surface.

Whilst there is evidence to support both the presence of radicals adsorbed onto the electrode surface and the coupling of “truly free radicals” in solution, it is likely that Kolbe electrolysis proceeds *via* alkyl radicals that are adsorbed onto the electrode surface. The radicals may be able to desorb and re-adsorb, which would account for the loss of stereochemistry and the regiochemical results. It should also be mentioned that different carboxylates and different conditions may favour the adsorbed pathway over the free radical one and *vice versa*. Additionally, other functional groups on the carboxylate may be able to adsorb strongly to the electrode favouring a second electron oxidation.⁸⁴

2.1.3.6 The Non-Kolbe Pathway

At the anode, alkyl radicals, typically derived from α -substituted carboxylates, may undergo a second electron oxidation to form carbocations and in some cases this reaction can completely suppress the formation of the desired Kolbe product.⁸⁵ Typically intermediate alkyl radicals with ionisation potentials less than 8 eV will further oxidise to a carbocation sufficiently quickly to outcompete Kolbe product formation.⁸⁶ Experimental conditions that promote binding of the intermediate alkyl radical to the anode or disfavour radical coupling will favour the carbocation formation.⁵⁵ Carbocations may undergo solvolysis, fragmentation, rearrangement or elimination to give non-Kolbe products. Solvolysis products from anodic decarboxylation (typically in aqueous media) are often referred to as Hofer-Moest products.⁷⁷ The non-Kolbe pathway will be discussed in more detail in Section 2.1.7.

2.1.4 Experimental Conditions for Kolbe Electrolysis

The experimental conditions for Kolbe electrolysis can be optimised to maximise the yield of radical derived Kolbe products over non-Kolbe products. The following sections describe the factors that need to be considered when choosing and optimising reaction conditions.

2.1.4.1 Choice of Electrode Material for Kolbe Electrolysis

Kolbe electrolysis is typically performed using an undivided electrochemical cell. A divided cell is generally only used when a starting material contains an easily reduced functional group.⁵⁸ By far the most common anode material for the formation of the Kolbe product is platinum, usually as a foil or mesh to maximise surface area whilst minimising cost.⁷⁷ Other anode materials which have successfully yielded desired Kolbe products have included gold and hard, non-porous carbon.^{87,88} Porous graphite almost exclusively favours the second electron oxidation to form carbocations and thus non-Kolbe products.^{30,89,90} The variation in selectivity between non-porous and porous carbon has been attributed to the difference in the surface area as the “real” surface area for porous graphite will be a lot greater. As the surface area is larger for porous graphite, the current density will be lower and therefore the concentration of radicals at the electrode surface will be lower. This means radical coupling is less likely and radicals will instead undergo a second electron oxidation to carbocations which will lead to more non-Kolbe product formation.^{58,87}

A platinum cathode is generally used for proton reduction. However, in an undivided cell, in the presence of unsaturated carboxylic acids, a steel cathode may be preferred to avoid cathodic hydrogenation.⁵⁵

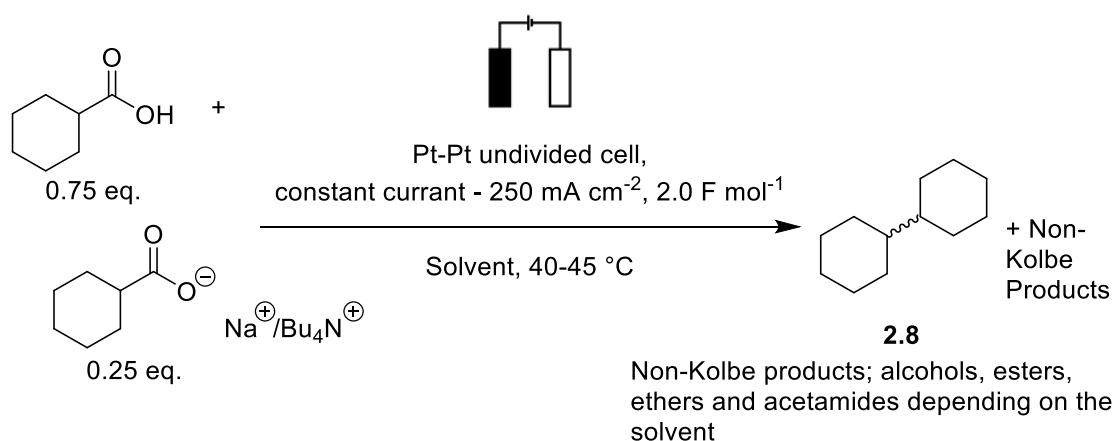
Passivation of the platinum electrodes, a build-up of insulating residue on the electrode surface, has been observed after Kolbe electrolysis.⁹¹ Polarity inversion has been used to prevent this; when electrodes are polarity inverted, the anode and cathode potentials are changed (inverted) so the anode becomes the cathode and the cathode becomes the anode.⁹² This requires both electrodes to be the same material.^{93,94}

2.1.4.2 Choice of Solvent for Kolbe Electrolysis

Kolbe electrolysis can be performed in neat carboxylic acid, however, it is most commonly performed in methanol, although some methanol water mixtures have been used to aid solubility. Methanol is a good solvent choice for Kolbe electrolysis as above the critical

potential methanol oxidation is completely inhibited by the adsorbed carboxylate layer at the anode surface.⁶⁹ In addition, methanol is often chosen as it can be easily removed *in vacuo*, which is especially important when products have low molecular weights and low boiling points.⁵⁵

Both acetonitrile and dimethylformamide (DMF) have also been used as solvents for Kolbe electrolysis with good yield of the desired Kolbe product. Whilst the oxidation potential for DMF is higher than methanol (Table 2.2), DMF is often avoided as the oxidation product (*N*-acyloxy-*N*-methyl formamide) is more challenging to remove than the oxidation product of methanol which is ultimately CO₂.⁹⁵ Table 2.2 summarises some of the effects of solvent on the outcome of Kolbe electrolysis reported as the ratio between the Kolbe and non-Kolbe products for the electrolysis of cyclohexanecarboxylic acid (Scheme 2.8).⁹⁶ No base was added to this reaction as 25% of the acid added was either the sodium or tetrabutylammonium carboxylate salt.



Scheme 2.8 Kolbe electrochemical homo-coupling of cyclohexanecarboxylic acid in various solvents.⁹⁶

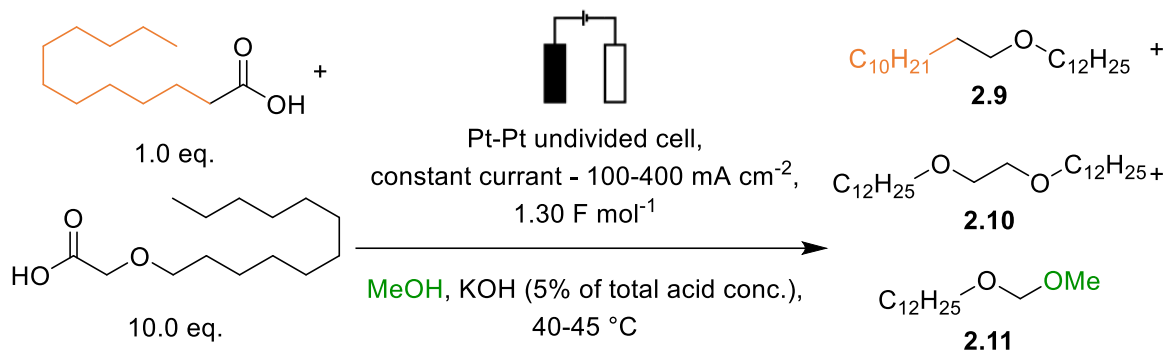
Table 2.2 The effect of solvent on the Kolbe:non-Kolbe product ratio.⁹⁶

Entry	Solvent	Approximate Oxidation Potential vs SCE / V ⁹⁵	Kolbe Product 2.8 :non-Kolbe Product Ratio
1	MeOH + H ₂ O (30% v/v) ^a	2.0 ^c	0.97:1.00
2	MeOH ^a	0.0	1.76:1.00
3	MeCN ^b	3.3	2.26:1.00
4	DMF ^b	1.6	4.32:1.00

^a sodium salt added, ^b tetrabutylammonium salt added, ^c oxidation potential for water

2.1.4.3 Current Density and Kolbe Electrolysis

To promote bimolecular radical-radical coupling in Kolbe electrolysis, a high radical concentration near the electrode surface is required. This can be achieved by a high current density, typically greater than 200 mA cm^{-2} .^{58,84} In one published study, at lower current densities (100 mA cm^{-2}) the yield for the non-Kolbe product **2.11** was observed to be 1.5 times greater than at 200 mA cm^{-2} (Scheme 2.9, Table 2.3).⁸⁴



Scheme 2.9 Kolbe electrochemical hetero-coupling of long chain fatty acids at various current densities.⁸⁴

Table 2.3 The effect of current density on the outcome of Kolbe electrolysis and the overall Kolbe:non-Kolbe product ratio.⁸⁴

Entry	Current Density / mA cm^{-2}	Yield Determined by GLC / %			
		Hetero-coupled product 2.9	Homo-coupled product 2.10	Non-Kolbe Product 2.11	Kolbe Product:Non-Kolbe Product Ratio
1	100	45	5	50	1.0:1.0
2	200	61	7	32	2.1:1.0
3	300	61	4	35	1.9:1.0
4	400	64	4	32	2.1:1.0

2.1.4.4 pH and the Amount of Base for Kolbe Electrolysis

A neutral or slightly acidic pH is used for Kolbe electrolysis to promote the formation of the desired Kolbe product. To maintain this pH a relatively small amount (5-10% of the total acid concentration) of an alkali metal hydroxide or alkoxide base is commonly added, although amine bases have also been used.^{58,97} An increase in non-Kolbe product formation at very low amounts of base (below 5%) has been observed.⁸⁴ This has been attributed to an insufficient coverage of the anode surface by carboxylate anions. This results in a low

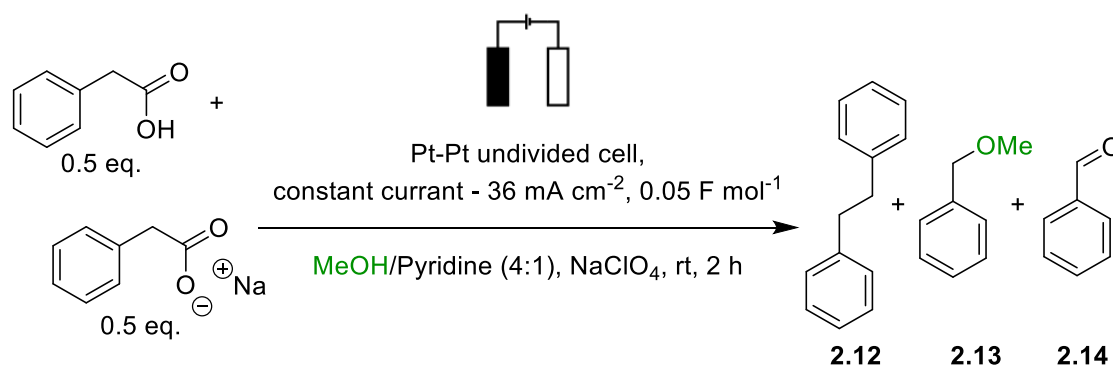
concentration of radicals near the electrode surface and hence a second electron oxidation to carbocations is favoured.⁸⁴

Some foreign cationic species which are believed to form a blocking oxide layers at the anode, e.g. Fe^{2+} or Co^{2+} can decrease the yield of the Kolbe product. Alkali and alkaline earth metal ions or alkylammonium ion appear to have no effect on Kolbe electrolysis and are subsequently used as counter ions for carboxylates.⁵⁸

In hetero-coupling reactions, where two different carboxylic acids with significantly different $\text{p}K_{\text{a}}$ values are used, 100% neutralisation is often used to avoid preferential deprotonation of one acid over the other, which would lead to homo-coupling.⁸⁴ In aqueous solutions, a high percentage of base is also used to convert all the carboxylic acid into carboxylate to improve the solubility of the starting materials.⁵⁸

2.1.4.5 Choice of Electrolyte for Kolbe Electrolysis

The addition of a supporting electrolyte to electrochemical reactions is common as it can significantly increase the current by reducing solvent resistance.⁵² However, Kolbe electrolysis is commonly performed without a supporting electrolyte. When tested, usually the addition of foreign anions results in lower yields of Kolbe products, and this is attributed to the disruption of the carboxylic acid layer at the anode.⁹¹ For instance, it was shown that the addition of high concentrations of NaClO_4 completely suppressed the formation of the Kolbe products from the homo-coupling of phenylacetate in favour of formation of benzylmethylether **2.13** (Scheme 2.10, Table 2.4).^{98,99} No base was added as 50% of the acid was added as to sodium carboxylate salt.



Scheme 2.10 Kolbe electrochemical coupling of phenylacetic acid with supporting electrolyte NaClO_4 .⁹⁸

Table 2.4 The effect of an supporting electrolyte (NaClO_4) on the outcome of Kolbe electrolysis and the Faradaic efficiencies⁹⁸

Entry	NaClO_4 / mM	Relative Peak Area in GLC / %			Kolbe:non-Kolbe product ratio
		Kolbe Product 2.12	Methoxylated non-Kolbe Product 2.13	Aldehyde Product 2.14	
1	0	68	27	5	2.52:1.00
2	0.65	42	53	5	0.79:1.00
3	1.77	18	75	7	0.24:1.00
4	5.18	0	91	9	0.00:1.00
5	15.80	0	94	6	0.00:1.00

To achieve the high current densities required for Kolbe electrolysis in the absence of a supporting electrolyte and with low base stoichiometry, a high concentration of carboxylic acid starting material is used (typically 0.5 M). To further minimise the effect of solvent resistance the anode and cathode are usual positioned close together.⁶⁹

2.1.4.6 Temperature and Kolbe Electrolysis

Kolbe electrolysis reactions are typically performed at room temperature.⁷⁷ Due to the increase in temperature during electrolysis (associated with solvent resistance), water baths or cooling jackets are often used to maintain a constant, controlled temperature.⁵⁵ Elevated temperatures can improve viscosity and mass transport, however, temperatures above 65 °C are usually avoided as side processes are favoured such as esterification.^{77,100}

However, in 2012 a high temperature was used in Kolbe electrolysis to create a thermomorphic system in which a non-polar cycloalkane phase and a polar pyridine/methanol/acetonitrile phase became monophasic during electrolysis.¹⁰¹ After electrolysis, the mixture was cooled to form the biphasic system. This method allowed for easy separation of the non-polar Kolbe products after electrolysis with good yields of the Kolbe product (> 69%).¹⁰¹

2.1.5 Broadening the Synthetic Scope of Kolbe Electrolysis

Traditionally, Kolbe electrolysis was developed for the homo-coupling or hetero-coupling of alkyl radicals generated from the electrochemical oxidation which has subsequently been used in the coupling of highly functionalised carboxylic acids.¹⁰² Alternatively, the intermediate radicals generated by oxidative decarboxylation can participate in other reactions such as inter- or intramolecular addition to alkenes.¹⁰³ The following sections outline some of the synthetic strategies developed which utilise Kolbe electrolysis.

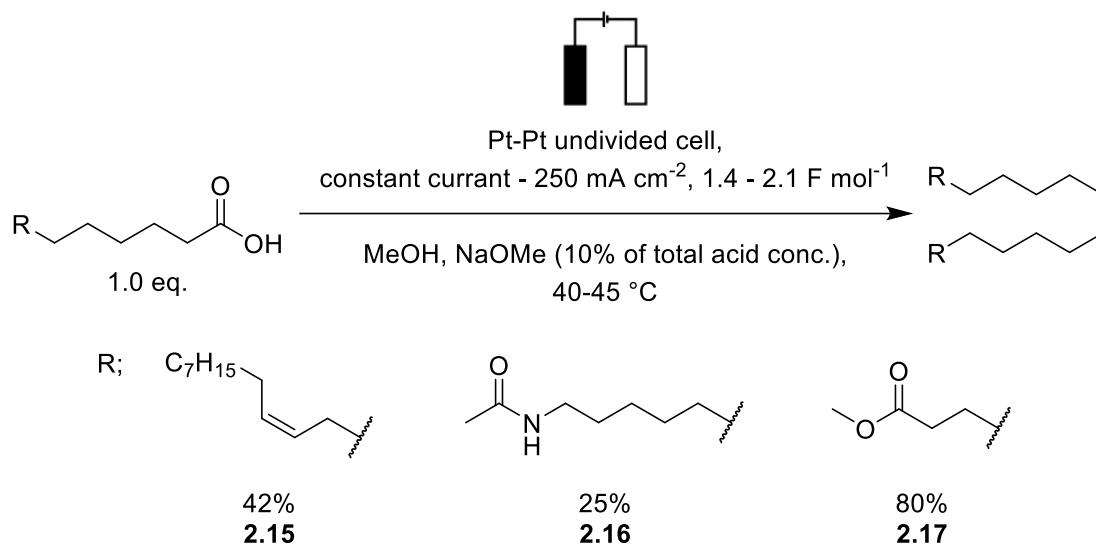
2.1.5.1 Homo-coupling of Alkyl Radicals Derived from Fatty Acids

Schäfer pioneered the revival of Kolbe electrolysis in the 1990s.⁵⁸ An example of this is presented in Scheme 2.11.¹⁰⁴ The conditions used for the reaction were consistent with those described previously to ensure homo-coupling of alkyl radicals. In a beaker-type electrochemical cell, carboxylic acids were electrolysed using platinum foil electrodes. The solvent was methanol, and the carboxylic acids were neutralised to an extent of 10% with sodium methoxide. The temperature was maintained between 40-45 °C. A high current density (200 mA cm⁻²) was held by varying the cell voltage between 60 and 110 V. The end point of the reaction was determined based on electrical charge, 1.3 F (total moles of acid)⁻¹ were passed during the reaction, meaning theoretically 0.3 equivalents of excess electrons were used. Passing a small theoretical excess of electrons is common in Kolbe electrolysis.¹⁰⁴

A moderate 42% yield for the homo-coupled product **2.15** was achieved when a 0.3 M solution of the corresponding fatty acid was electrolysed. A 15% yield for non-Kolbe disproportionation products were observed as a 1:1 mixture of alkene and H-abstraction products. Due to issues with solubility of the non-polar starting acid in methanol, 40% of the starting acid was recovered which contributed to the low yield for this example.¹⁰⁴

The conditions by Schäfer and co-workers using the beaker-type cell were extended to the reaction of more complex carboxylic acids demonstrating the structural diversity tolerated by Kolbe electrolysis.¹⁰⁴ Carboxylic acids bearing amides and esters have been electrolysed to give symmetrical homo-coupled products **2.16** and **2.17** in moderate and good yields respectively (Scheme 2.11). **2.16** was prepared in a 25% yield, after 2.13 F mol⁻¹ of charge, from 1.6 M solution of the corresponding amino acid. 15% of the starting material was recovered and 41% for the non-Kolbe products. In this example the amino acid was acetylated to protect the free amine from oxidation under the electrochemical conditions, however, poor yields were still attained showing some limitations of the reaction. After 1.4

$F \text{ mol}^{-1}$ at 220 mA cm^{-2} an excellent 80% yield for the homo-coupled product **2.17** was achieved after electrolysis of a 1.6 M solution of the corresponding acid. Only a 10% yield for the non-Kolbe products were achieved. This work utilised Kolbe electrolysis, under “standard” conditions, to generate simple primary alkyl radicals for homo-coupling reactions.¹⁰⁴



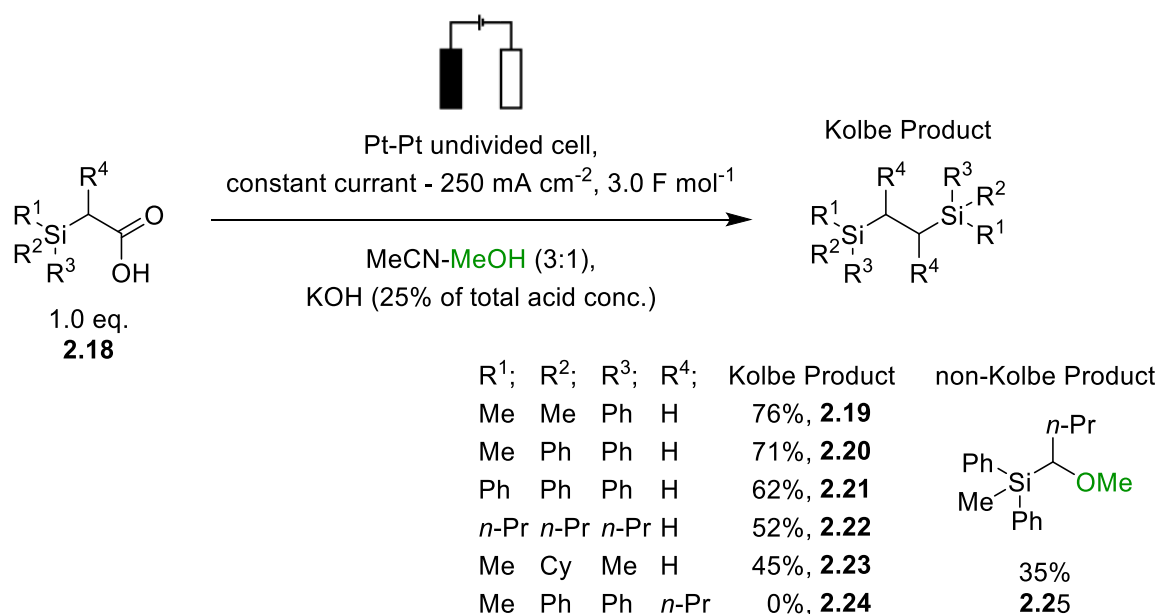
Scheme 2.11 Kolbe electrochemical homo-coupling of fatty acids by Schäfer and co-workers.¹⁰⁴

2.1.5.2 Homo-coupling of Alkyl Radicals Derived from Substituted Carboxylates

When subject to electrolysis, α -substituted carboxylates will typically form stabilised carbocations and consequently non-Kolbe products.⁵⁸ However, α -silyl carboxylic acids have been successfully used by Becker and co-workers in the preparation of symmetric 1,2-disilylethanes as the α -silyl groups stabilised the alkyl radicals (Scheme 2.12).^{105–107} Furthermore, the α -silicon effect destabilises developing positive charges and stabilises forming negative charges through the empty 3d atomic orbital on silicon which can further stabilise the α -silyl alkyl radicals relative to over-oxidation. α -Silylacetic acid derivatives (**2.18**, 0.13 M) were typically electrolysed in a methanol-acetonitrile co-solvent system (1:3 v/v) to aid solubility. With α -silylacetic acid bearing vinyl substituents, polymerisation at the electrode surface was observed and so dimethoxyethane (DME) was added as a sacrificial co-solvent in methanol (methanol-DME 1:2 v/v) which was preferentially electrolysed, suppressing polymerisation.¹⁰⁵

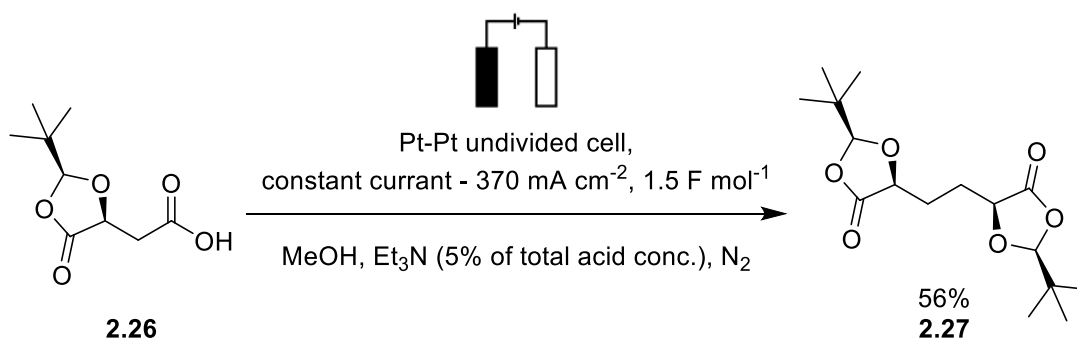
It was shown that increasing the steric bulk of the silyl substituent lowered the yield of the Kolbe homo-coupled product (Scheme 2.12, **2.19-2.24**).¹⁰⁵ This is attributed to increased steric hindrance of the silyl group disrupting the packing at the electrode surface. The alkyl radical concentration near the surface of the electrode will subsequently be lowered leading to reduced radical-radical coupling and increased over-oxidation and non-Kolbe products.¹⁰⁵ In contrast, the Schäfer group's work which used long chain fatty acids, allowed better packing at the electrode surface due to the increased flexibility in the chain and therefore higher yields for some examples were achieved.¹⁰⁴ The disruption of the carboxylate layer at the electrode surface caused by the bulky substituents may also lead to preferential solvent oxidation at the anode. Solvent oxidation would also explain the high 3 F mol^{-1} of charge needed for this reaction of α -silylacetic acid derivatives as the Faradaic efficiency is lowered by oxidation of non-carboxylate molecules.¹⁰⁵

Finally, in studies of α -silylacetic acid Kolbe reactivity, it was shown that the introduction of an electron donating group α -to the radical (in the R^4 position) completely suppressed the Kolbe pathway and led to a 35% yield of carbocation derived non-Kolbe product **2.25**. The radical underwent further oxidation to a carbocation at the electrode surface and nucleophilic attack, by the solvent (methanol), then delivered the non-Kolbe product **2.25**.¹⁰⁴



Scheme 2.12 Kolbe electrochemical homo-coupling of α -silyl carboxylic acids by Becker and co-workers.¹⁰⁵

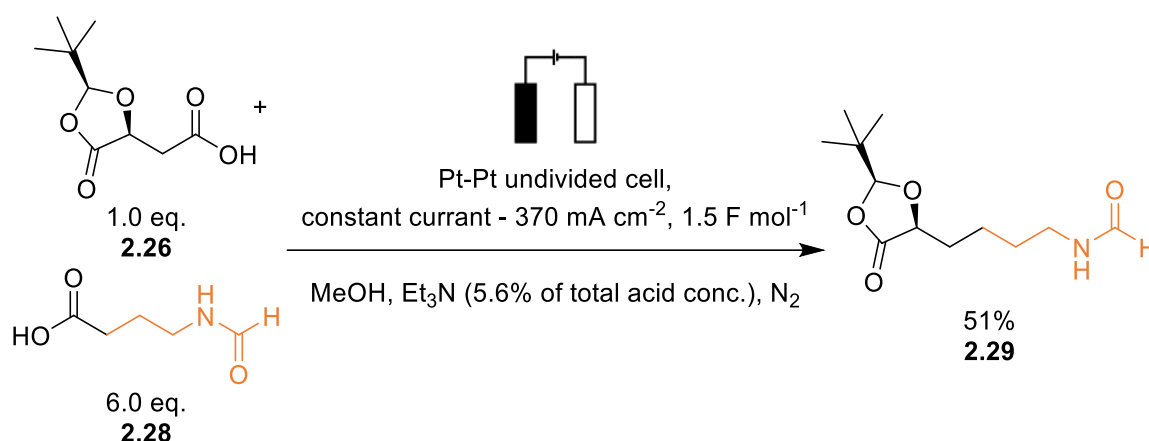
Other highly functionalised, chiral carboxylic acids have been reacted with good yields for Kolbe products, as shown in a publication by Seebach and co-workers in 1985. Malic acid derivative **2.26** (0.25 M) was electrolysed at platinum electrodes in an undivided cell, with methanol as the solvent, triethylamine as the base and dihydroxyadipic acid **2.27** was isolated in a 56% yield (Scheme 2.13). A high current density (370 mA cm^{-2}) was used for this reaction, which promoted a high concentration of radicals and thus favoured radical coupling. The reaction temperature was maintained between $10 \text{ }^{\circ}\text{C}$ and $20 \text{ }^{\circ}\text{C}$ to prevent esterification at increased temperatures. To avoid condensation of water from the air, reactions were performed under a nitrogen atmosphere.⁹⁷ As with the α -silylacetic acids with larger substituents (Scheme 2.12), the moderate yield for this example may be due to the steric hindrance of the bulky carboxylate disrupting the packing of adsorbed carboxylates at the electrode surface leading to less coupled product and further oxidation of radicals.



Scheme 2.13 Kolbe electrochemical homo-coupling of malic acid derivative **2.26** by Seebach and co-workers.⁹⁷

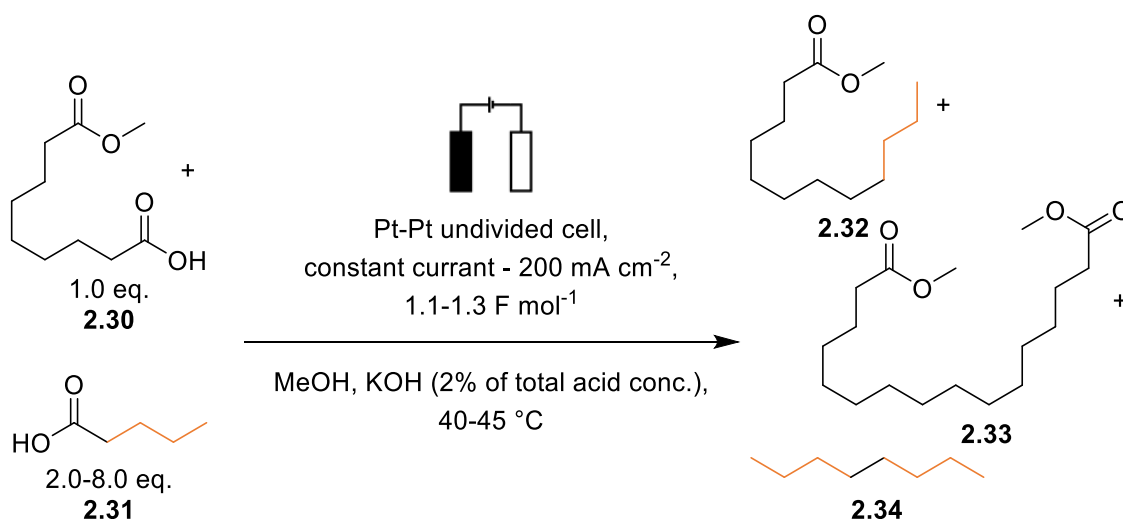
2.1.5.3 Hetero-coupling of Alkyl Radicals Derived from Carboxylates

The conditions by the Seebach group were extended to Kolbe electrochemical hetero-coupling of carboxylic acids to synthesise complex scaffolds (Scheme 2.14). Malic acid derivative **2.26** was electrolysed in the presence of an excess of *N*-formyl- γ -aminobutyric acid (**2.28**) leading to a 51% yield of **2.29**. In hetero-coupling reactions the acid in excess is typically referred to as the co-acid. The co-acid was in a 6-fold excess meaning the total acid concentration was 0.67 M. Triethylamine was added as the base at a level that was 5.6% of the total acid concentration (both **2.26** and **2.28**).⁹⁷



Scheme 2.14 Kolbe electrochemical hetero-coupling of malic acid derivative **2.26** and amide **2.28** by Seebach and co-workers.⁹⁷

In hetero-coupling reactions, the co-acid is often the less expensive acid and is typically used in a large excess to statistically favour the hetero-coupling over homo-coupling of the more costly acid. In the hetero-coupling of two fatty acids **2.30** and **2.31**, after decarboxylation the alkyl radicals either homo-coupled to form **2.33** and **2.34** or hetero-coupled to form **2.32** (Scheme 2.15).⁹¹ Increased equivalents of co-acid **2.31** led to an increase in yield of **2.32** from 53% to 79% (Table 2.5).



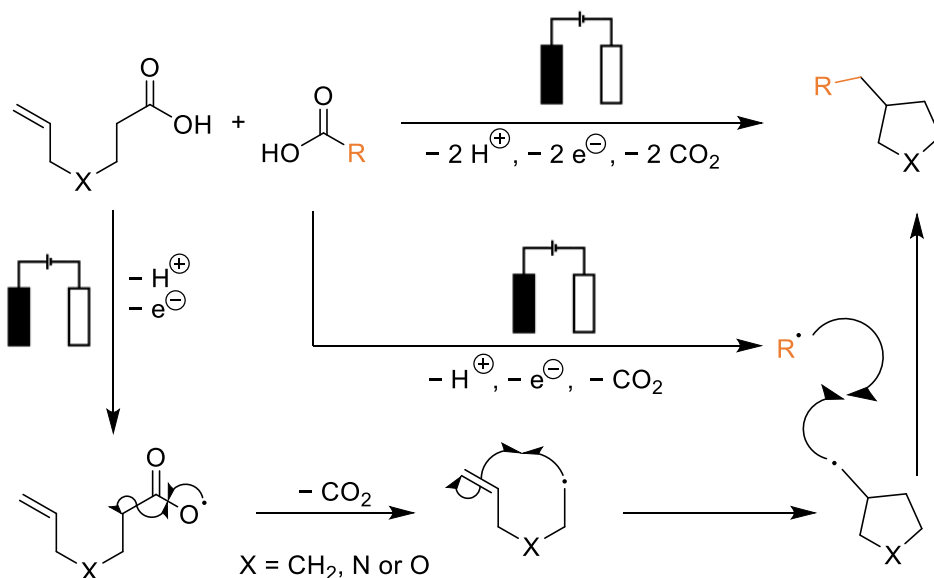
Scheme 2.15 Kolbe electrochemical hetero-coupling of by Schäfer and co-workers highlighting the effect of co-acid stoichiometry.⁹⁷

Table 2.5 The effect of increased amount of co-acid on the outcome of Kolbe electrolysis⁹¹

Entry	Ratio of 2.30 : 2.31	Yield of hetero-coupled product 2.32 based on conversion of 2.30 / %	
		GC yield based on 2.30	Isolated yield
1	1:2	56	53
2	1:4	72	67
3	1:8	83	79

2.1.6 Intramolecular Cyclisation

Kolbe electrolysis has been used to synthesise heterocyclic compounds *via* intramolecular radical cyclisations prior to coupling with another radical. Carboxylic acids bearing alkenes can decarboxylate to form alkyl radical which can undergo a rapid intramolecular cyclisation (typically a 5-exo-trig cyclisation) yielding another alkyl radical outside the newly formed ring. This radical then hetero-couples to another alkyl radical (Scheme 2.16).^{103,108,109} The rapid cyclisation often means fewer non-Kolbe side products are observed as it moves the radical away from the electrode surface.

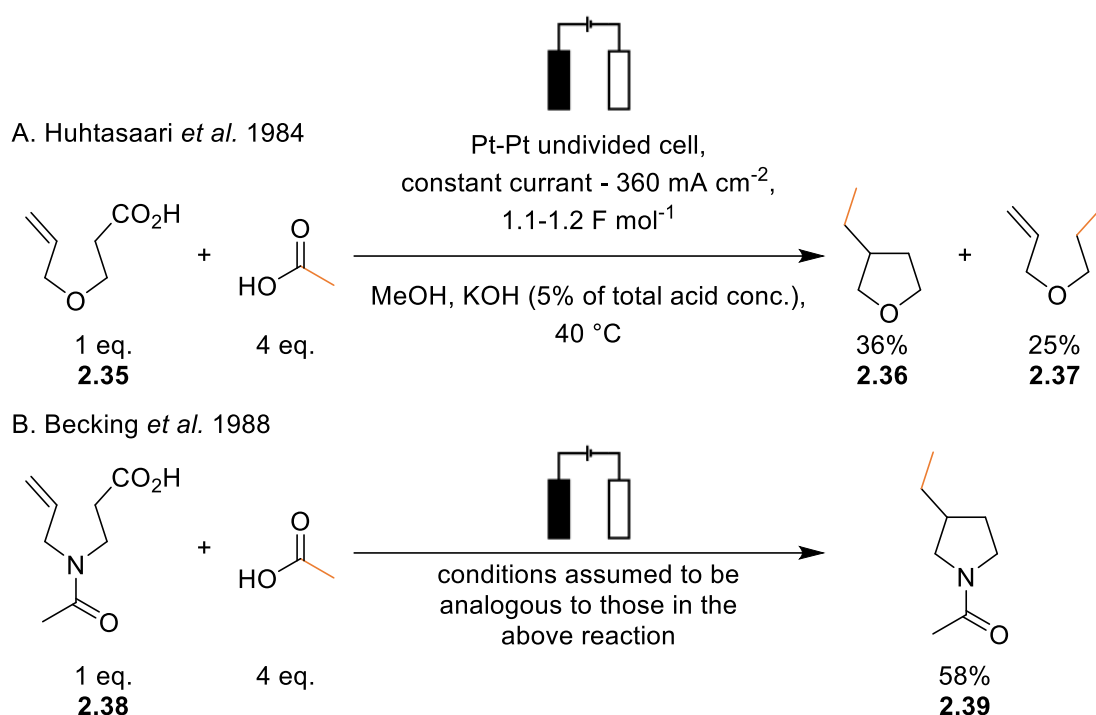


Scheme 2.16 General mechanism for Kolbe electrochemical 5-exo-trig cyclisation.

In general, for Kolbe electrochemical cyclisation reactions, the reaction conditions (total acid concentrations, amount of base and electrode material) are similar to those of hetero-

coupling reactions. This is because cyclisation reactions have a hetero-coupling reaction after the initial cyclisation.

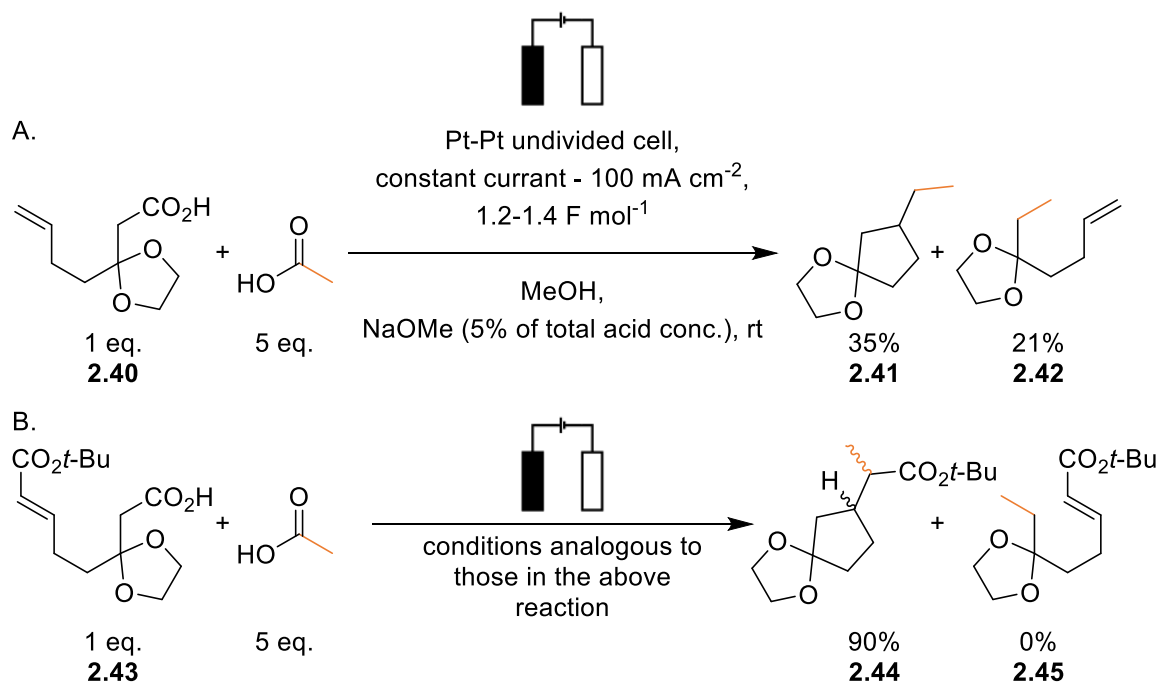
As part of work by the Schäfer group, Huhtasaari *et al.* performed cyclisation reactions to synthesise substituted tetrahydrofurans from unsaturated carboxylic acids (Scheme 2.17 A).¹⁰⁸ Acetic acid was added in 4-fold excess relative to the unsaturated acid **2.35**. Cyclised product **2.36** was obtained in a 36% yield along with 25% for the uncyclised hetero-coupled product **2.37**.¹⁰⁸ The work was then extended to the synthesis of substituted pyrrolidines (Scheme 2.17 B).¹⁰⁹ Due to the lack of experimental detail in the paper, it is assumed that analogous conditions were used for this work. Pyrrolidine **2.39** was prepared by electrolysis of unsaturated carboxylic acid **2.38** in a 58% yield.¹⁰⁹



Scheme 2.17 Kolbe electrochemical cyclisation reactions performed by Schäfer and co-workers.^{108,109}

In 2008 Markó and co-workers showed that the amount of Kolbe cyclised product could be increased by the introduction of electron-withdrawing substituents on the alkene, as the addition of an electron rich alkyl radical to an electron deficient alkene is more favoured.¹⁰³ Initially, Kolbe cyclisation product **2.41** was achieved in a 35% yield with a 21% yield for the uncyclised product **2.42** when unsaturated acid **2.40** was electrolysed (Scheme 2.18 A). However, the introduction of the electron-withdrawing *t*-butyl ester on the alkene (**2.43**)

increased the yield of the cyclised product **2.44** to 90% and completely suppressed the direct hetero-coupled product **2.45** (Scheme 2.18 B).¹⁰³



Scheme 2.18 Kolbe electrochemical cyclisation reactions performed by Markó and co-workers.¹⁰³

2.1.7 Non-Kolbe Oxidation Pathway

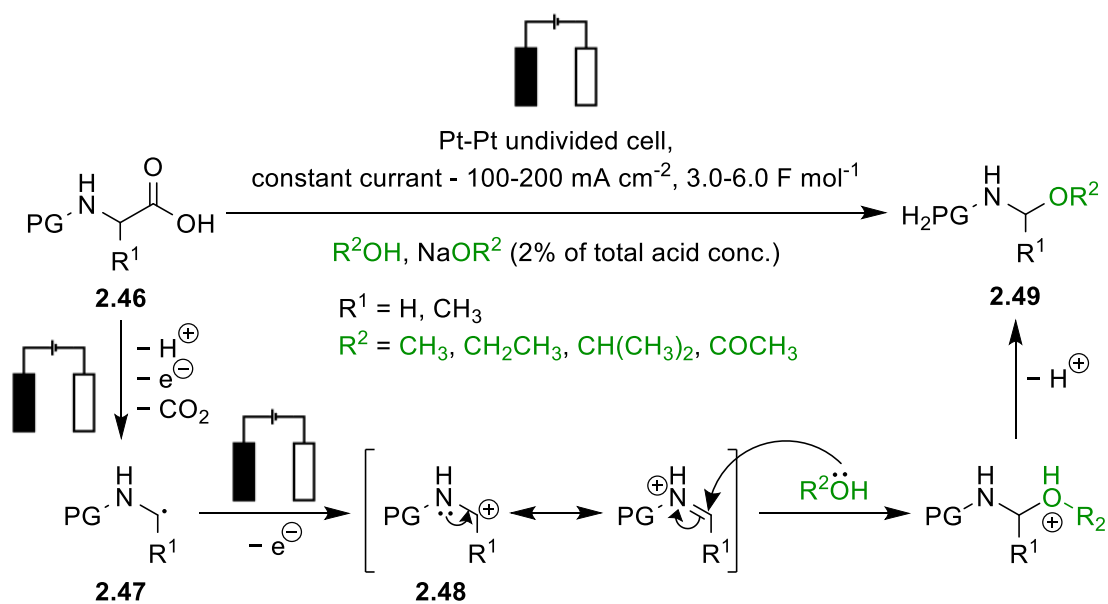
Many of the side products observed in Kolbe electrolysis are carbocation derived. As highlighted in the following sections, some researchers have optimised synthetic methodologies that utilise this carbocation rather than the alkyl radical intermediate.

As described, the non-Kolbe pathway is favoured at carbon electrodes and in experiments with lower current densities and in polar aprotic solvents. The selectivity of the non-Kolbe product also depends heavily on the structure of the carboxylic acid starting material.^{84,110} Starting materials that are known to form high yields of non-Kolbe products include amines, lactams, carbamates and *N*-acylated amino acids where the functional groups are located α to the radical formed from decarboxylation.¹¹¹ This can be rationalised by considering the electron impact ionisation potential of the radical formed by Kolbe electrolysis.⁸⁶ The ionisation potential is experimentally determined and is the minimum energy to remove the outermost electron, which in this case would convert the radical into the carbocation. This value contributes to the standard potential for oxidation of the radical to the carbocation and therefore the thermodynamics of the process. Non-Kolbe products have been observed for

radicals with ionisation potentials below 8 eV, e.g. secondary and tertiary aliphatic radicals and radicals with some α -functional groups. Primary aliphatic radicals and resonance-stabilised radicals have ionisation potentials above 8 eV and will typically favour the formation of the Kolbe products.^{58,65} The ionisation potential for alkyl radicals will also decrease with increased chain length.⁸⁶

2.1.7.1 Types of Non-Kolbe Products

The most common non-Kolbe products are derived from the addition of nucleophiles and nucleophilic solvents to carbocations. These non-Kolbe products are sometimes referred to as Hofer-Moest products or Hofer-Moest-type products, however, this is typically reserved for aqueous electrolysis where the nucleophile is water and the resulting Hofer-Moest product is an alcohol or ester. Work by Linstead *et al.* investigated the effect of solvent on the formation of non-Kolbe products derived from *N*-protected glycine and DL- α -alanine (**2.46**).⁸⁵ Platinum electrodes and high current densities were used, but as the radicals formed from decarboxylation (**2.47**) were α to nitrogen they readily underwent a second oxidation to resonance stabilised carbocations (**2.48**, Scheme 2.19). Nucleophilic addition of solvent then delivered a range of amino ethers (see Table 2.6). Particularly high yields were observed for the DL- α -alanine derivatives as the radicals formed were also secondary and therefore had lower ionisation potentials and were consequently easier to oxidise to carbocations than the glycine derivatives (Table 2.6, entries 5-6).⁸⁵

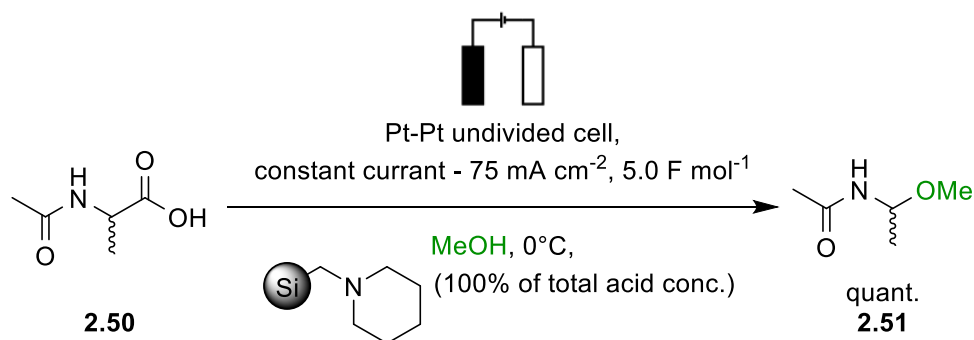


Scheme 2.19 Non-Kolbe pathway observed by Linstead *et al.* in various solvents.⁸⁵

Table 2.6 The effect of solvent on the outcome of the non-Kolbe pathway for α -amino acids by Linstead *et al.*⁸⁵

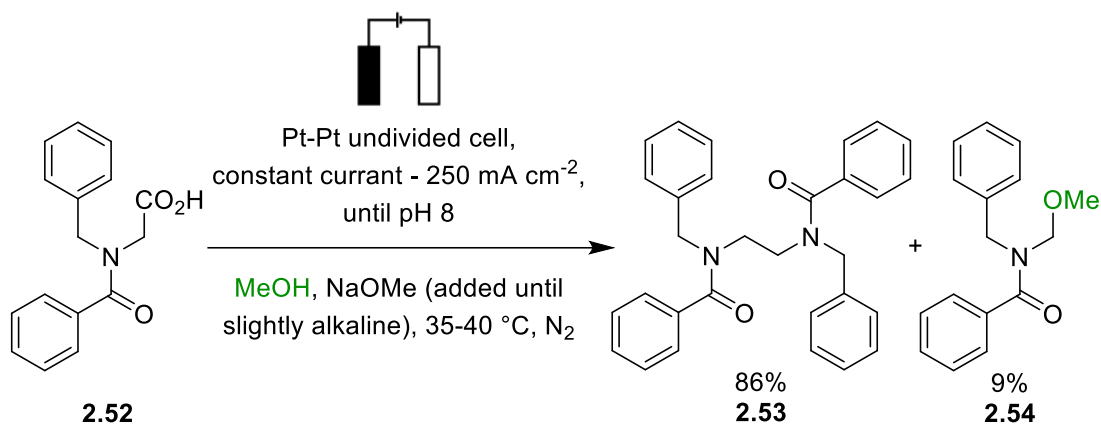
Entry	R	Protecting Group	Yield of Non-Kolbe Product 2.49 on Changing Solvent / %			
			Methanol	Ethanol	<i>Iso</i> -propanol	Acetic Acid
1	H	<i>N</i> -benzoyl	61	56	70	-
2	H	<i>N</i> -acetyl	78	-	-	-
3	H	<i>N</i> -carbobenzyloxy	74	-	-	-
4	H	<i>N</i> -phenylacetyl	-	-	-	38
5	CH ₃	<i>N</i> -benzoyl	91	76	-	-
6	CH ₃	<i>N</i> -acetyl	85	-	-	-

Excellent yields of non-Kolbe alkoxylation products have also been achieved by Fuchigami and co-workers using 100% neutralisation and solid supported bases, which could be re-used after filtration.¹¹¹ In the electrolysis of *N*-acetylated alanine **2.50** at platinum electrodes, a low current density was applied and the resulting α -methoxylated non-Kolbe product **2.51** was isolated in a quantitative yield (Scheme 2.20).¹¹¹

Scheme 2.20 Non-Kolbe pathway alkoxylation with solid supported bases by Fuchigami and co-workers.¹¹¹

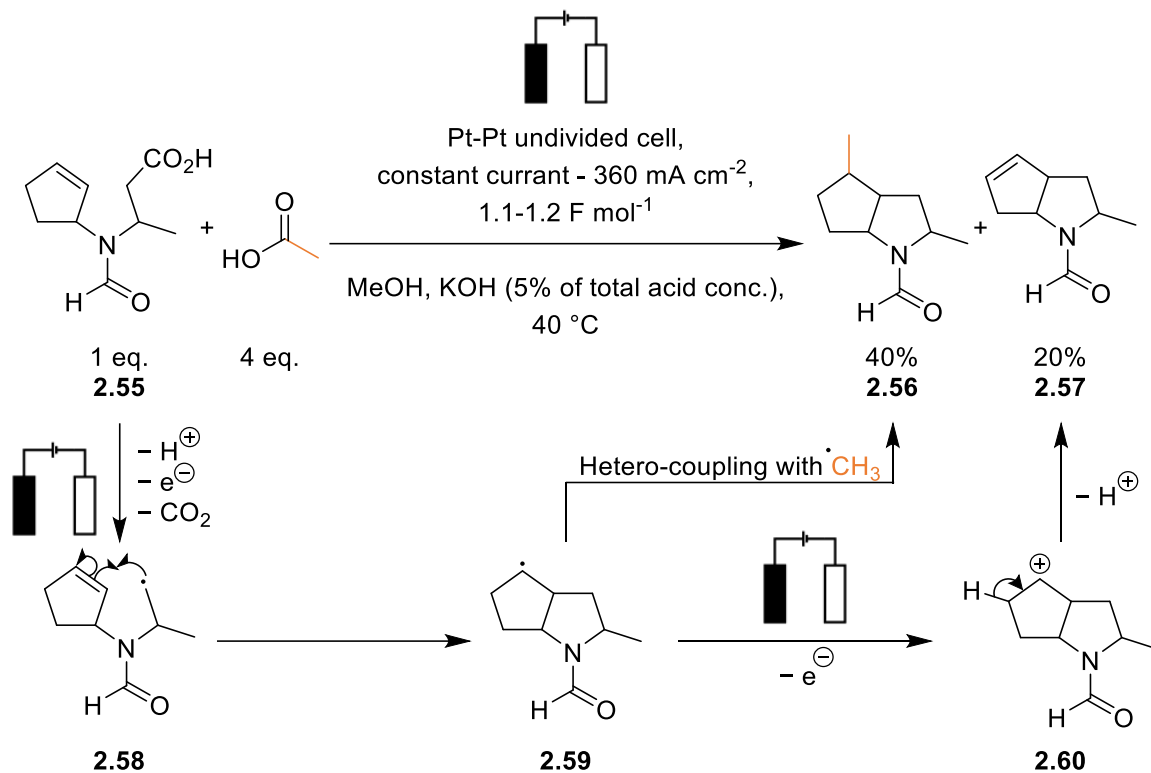
In fact, only one example of a successful Kolbe homo-coupling α to nitrogen could be found in the literature and is given in Scheme 2.21.¹¹² Kolbe product **2.53** was isolated in an 86% yield with only a 9% yield for solvated non-Kolbe product **2.54** in the electrolysis of **2.52**. Similar conditions were used to Linstead *et al.*, and the reason for the high yield of **2.53** is not obvious.⁸⁵ The reaction was performed at platinum electrodes with a high current density

and the authors suggest that the protected nitrogen reduced the electron-donating effect, making the radical intermediate less susceptible to over-oxidation.¹¹²



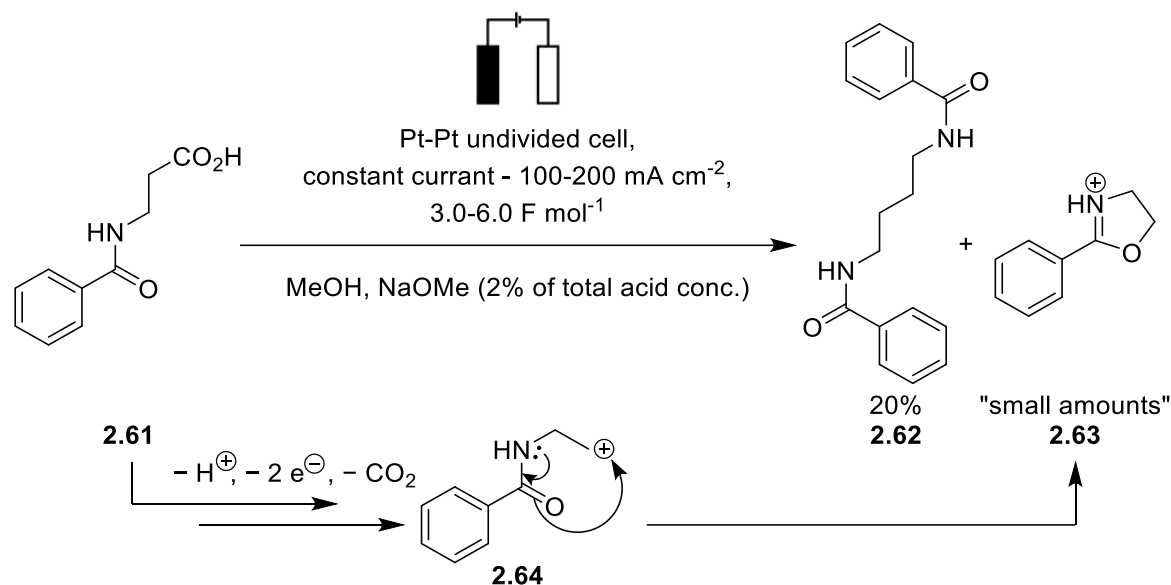
Scheme 2.21 Kolbe electrochemical homo-coupling of carboxylate **2.52** resulting in high yields of the Kolbe product and low yields of non-Kolbe methylation product **2.54** by Lateef and co-workers.¹¹²

Another common route to non-Kolbe products is *via* deprotonation of the carbocation. For example, in the electrochemical cyclisation of unsaturated amino acid **2.55**, along with a 40% yield for bicyclic pyrrolidine **2.56**, alkene **2.57** was isolated in a 20% yield (Scheme 2.22).¹⁰⁹ Here, the non-Kolbe product **2.57** was believed to be formed by further oxidation of the secondary radical **2.59** after the 5-exo-trig cyclisation. Oxidation of the secondary radical **2.59** would have been more favoured than oxidation of the initial primary alkyl radical **2.58**. Deprotonation β -to the carbocation gave alkene non-Kolbe product **2.57**.¹⁰⁹ As carbocation **2.60** is less stabilised than α to a heteroatom, such as nitrogen, it is likely that deprotonation is quicker than solvolysis of a more stabilised carbocation. In addition, previous examples of glycine derivatives do not have a β -proton to deprotonate.



Scheme 2.22 Kolbe electrochemical 5-exo-trig cyclisation of carboxylate **2.55** resulting in non-Kolbe alkene **2.57**.¹⁰⁹

Although uncommon, carbocations may undergo intramolecular process to form stabilised, charged species. “Small amounts” of **2.63** were observed along with homo-coupled product **2.62** in the electrolysis of protected β -alanine **2.61** (Scheme 2.23). It was believed **2.63** was carbocation derived after over-oxidation of the initial alkyl radical and as the carbocation **2.64** could not be directly stabilised by the hetero-atom, it underwent an intramolecular cyclisation through the carbonyl to stabilise the positive charge.⁸⁵



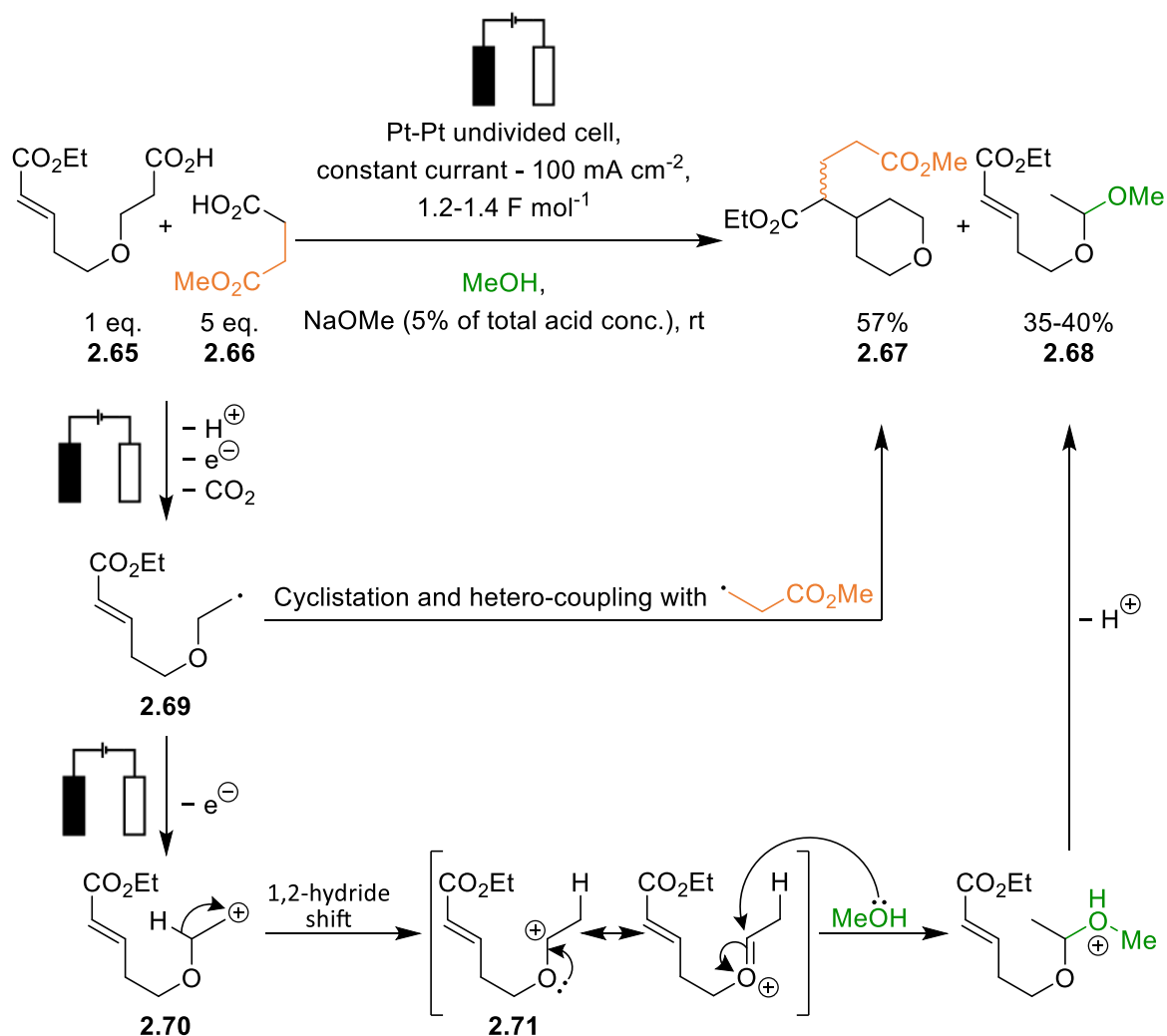
Scheme 2.23 Kolbe electrochemical homo-coupling of protected β -alanine **2.61** to give coupled product **2.62** and non-Kolbe product **2.63**.⁸⁵

2.1.7.2 Rearrangements of Intermediate Carbocations

Intermediate carbocations, formed by two-electron oxidation of a carboxylic acid starting material, have been known to undergo rapid rearrangements prior to further reactions. These rearrangements are not necessarily specific to Kolbe electrolysis but are derived from general carbocation reaction pathways. In the electrolysis of potassium octanoate in 1:1 acetonitrile/water at carbon electrodes, non-Kolbe product alcohols 1-heptanol, 2-heptanol and 3-heptanol were achieved in 18.5%, 43.8% and 37.7% yields respectively.⁸⁷ The regioisomers of heptanol were formed by rearrangements of the initial primary carbocation to more stabilised carbocations (primary carbocation less stable than secondary) before solvolysis.⁸⁷

Another example of carbocation rearrangement in the Kolbe reaction was observed by Markó and co-workers., methoxylated non-Kolbe product **2.68** was generated in a 35-40% during the electrolysis of unsaturated carboxylic acid **2.65** and co-acid **2.66**. A proposed mechanism for the formation of this product is given in Scheme 2.24. As the 6-exo-trig cyclisation was sufficiently slow, the intermediate alkyl radical **2.69** was long lived enough to undergo a second electron oxidation at the electrode surface to form carbocation **2.70**. This primary carbocation could then undergo a 1,2-hydride shift forming a more stable secondary carbocation **2.71**. Secondary carbocation **2.71** was further stabilised by resonance

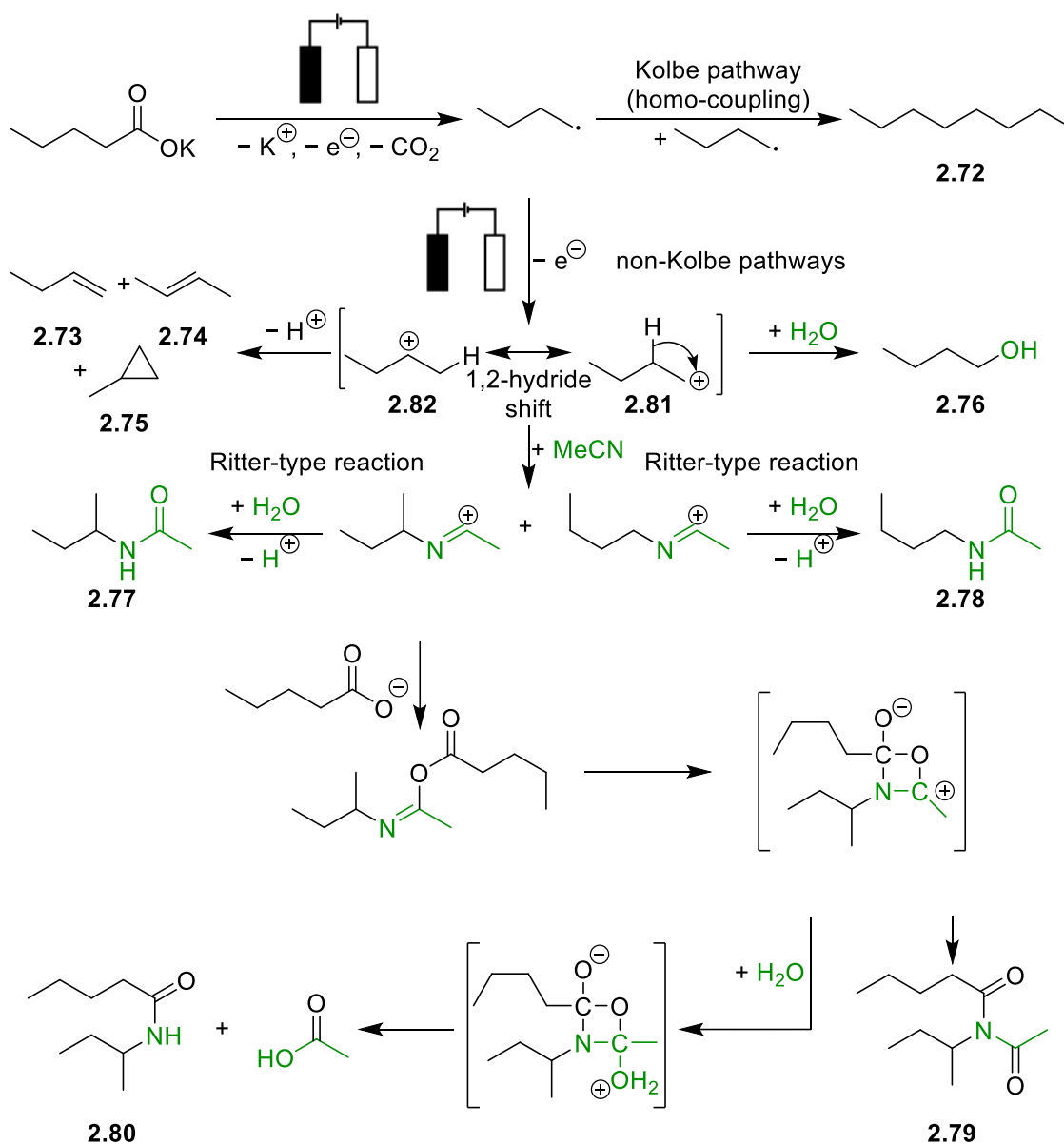
and finally, addition of methanol and deprotonation delivered non-Kolbe product **2.68** along with Kolbe product **2.67**.¹⁰³



Scheme 2.24 Kolbe electrochemical 6-exo-trig cyclisation reaction, carbocation formation, 1,2 hydride shift and non-Kolbe product formation from Markó and co-workers.¹⁰³

An approach for the electrochemical synthesis of *N*-alkylacetamides from simple alkyl carboxylate salts has been developed by Muck *et al.*⁸⁷ The reaction utilised the non-Kolbe pathway to carbocations, which subsequently underwent addition to acetonitrile, in a Ritter-type reaction (Scheme 2.25).¹¹³ A variety of acetamides were synthesised by this approach, derived from different rearrangements of the intermediate carbocations.⁸⁷ The pathways to acetamides (**2.77-2.80**) were also in competition with non-Kolbe elimination forming alkenes and cyclopropanes (**2.73-2.75**), direct addition of water to form alcohols (**2.76**), and the Kolbe pathway to simple alkanes (**2.72**). Intermediate carbocation **2.81** could initially undergo a 1,2-hydride shift, leading to secondary carbocation **2.82**. This meant both

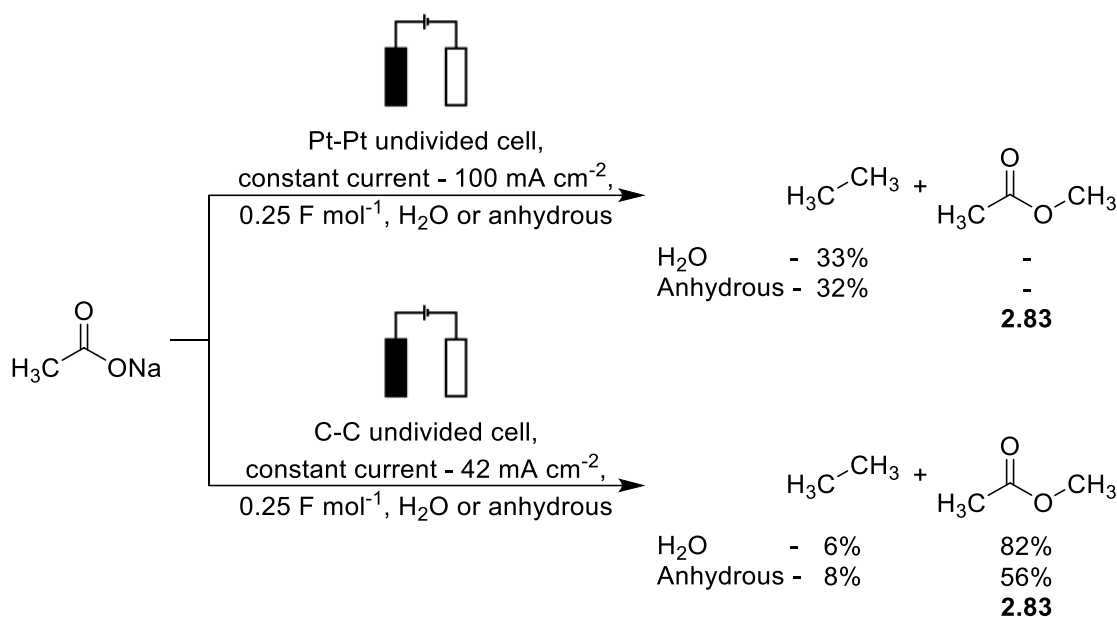
branched and linear acetamides were observed, however, as the secondary carbocation **2.82** was more inductively stabilised, more branched acetamide products (such as **2.77**) were observed. Typically, to further promote the two-electron pathway, these reactions were performed at carbon electrodes in an acetonitrile/water solvent mixture with a low current density.⁸⁷ Furthermore, the potassium carboxylate salt was used, meaning on dissociation in solution, all the acid was present as the free carboxylate. Yields of up to 50% for acetamide **2.77** were achieved by this approach and the Kolbe pathway was completely suppressed.⁸⁷



Scheme 2.25 Non-Kolbe carbocation formation and subsequent rearrangement to give Ritter-type products.⁸⁷

2.1.7.3 Competition of Kolbe and non-Kolbe Reactions

Some Kolbe reactions have been specifically designed to change the Kolbe versus non-Kolbe product selectivity. For example, in the electrolysis of sodium acetate, the Kolbe product was observed in moderate yields at platinum electrodes and the non-Kolbe ester **2.83** was not observed. However, at carbon electrodes and a reduced current density, the non-Kolbe product **2.83** was observed in yields of up to 82% with only low yields of the Kolbe product (Scheme 2.26).¹¹⁴

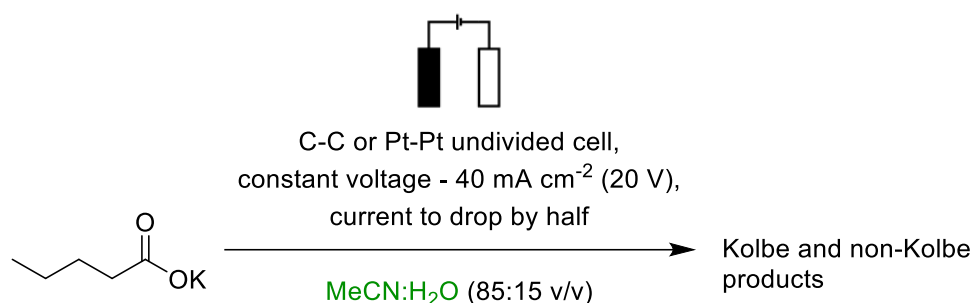


Scheme 2.26 Kolbe electrochemical homo-coupling of acetate at platinum and graphite electrodes showing the change in selectivity.¹¹⁴

The nature of the carbon electrode can also impact the outcome of the reaction. Muck *et al.* showed that, in aqueous acetonitrile, graphite and amorphous carbon electrodes favoured acetamide formation *via* Ritter-type reactions, whilst pyrolytic graphite favoured the elimination and deprotonation products (Scheme 2.27, Table 2.7).⁸⁷ It was theorised that the difference in product distribution was due to the structure of the electrode surface. Amorphous carbon and graphite electrodes are porous (apparent densities of between 1.42-1.53 g mL⁻¹ and 1.50-1.60 g mL⁻¹ respectively) and therefore have a high surface area, which results in a lower current density. At low current densities, there is a lower surface concentration of radicals, which favours the non-Kolbe pathway and the formation of carbocations, which react with solvent molecules that are present at the electrode surface as a non-uniform layer of carboxylate is formed. Pyrolytic graphite however, has a layered

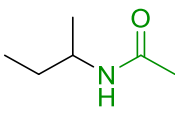
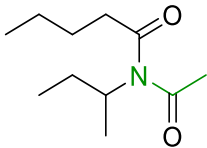
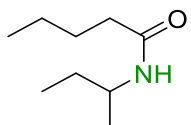
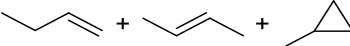
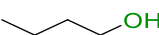
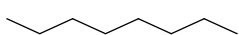
platelet structure, which is a harder surface (an apparent density between 2.20-2.23 g mL⁻¹) that results in a more ordered carboxylate layer at the electrode surface.⁸⁷ This prevented solvent molecules from being present at the electrode surface. Therefore on further oxidation, carbocations underwent elimination and deprotonation reactions forming alkenes.⁹²

A relatively low yield of Kolbe product was also obtained at platinum electrodes as, even though platinum favours a high radical concentration and radical coupling, the low current density and high neutralisation (100%) encouraged the formation of carbocations.⁸⁷ It has been suggested that at high neutralisation, the ionic strength of the solution increases, which in turn favours the formation of carbocations.⁸⁴



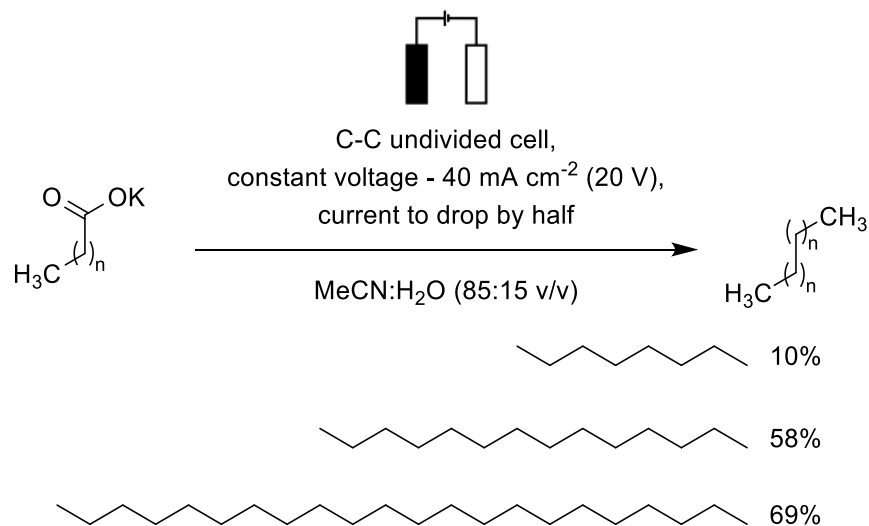
Scheme 2.27 Kolbe electrochemical homo-coupling using potassium valerate with platinum and carbon electrodes to give a range of Kolbe and non-Kolbe products.⁸⁴

Table 2.7 The effect of electrode material on the outcome of the non-Kolbe product distribution.⁸⁷

Entry	Type of Product	Yield of Product with Respect to Electrode Material / %			
		Graphite	Amorphous Carbon	Pyrolytic Graphite	Platinum
<i>N</i> -Alkylacetamide (non-Kolbe)					
1		49	50	29	19
<i>N</i> -Alkylacetamide (non-Kolbe)					
2		10	23	3	0
<i>N</i> -Alkylacetamide (non-Kolbe)					
3		10	8	12	6
Elimination (non-Kolbe)					
4		31	13	56	42
Alcohol (non-Kolbe)					
5		0	0	0	0
Homo-coupled product (Kolbe)					
6		0	6	0	33

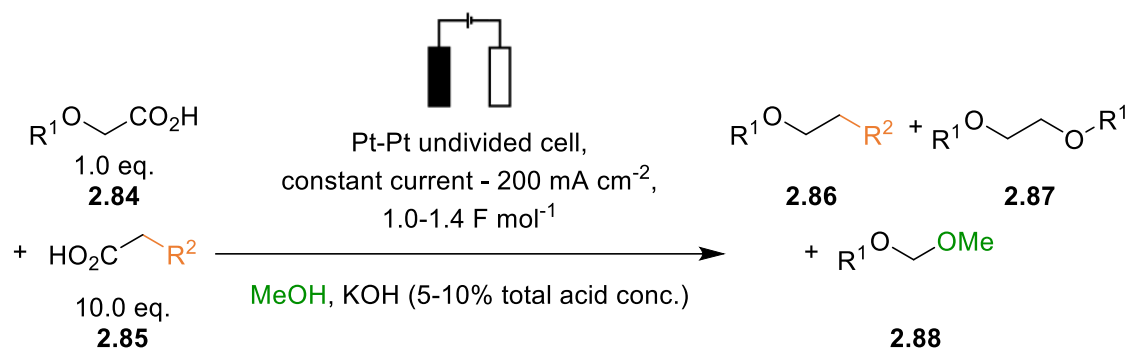
The structure of the carboxylate has an important role on the outcome of the reaction. With longer, linear alkane carboxylates, even at carbon electrodes which typically favour the non-Kolbe pathway, increased yields of homo-coupled products have been observed with increased chain length (Scheme 2.28), from a 10% yield with potassium butanoate to a 69% yield for the electrolysis of potassium undecanoate.⁸⁷ It was reasoned that the increase in yield was due to better ordering of the carboxylate monolayer and better packing of the carboxylates at the electrode surface. As the chain length increased, the van der Waals attractive forces between the hydrophobic alkyl chains increased and thus carboxylates arranged more orderly and stacked perpendicular to the electrode surface. On

decarboxylation, the alkyl radicals were closer in space and therefore more likely to couple, suppressing further oxidation to carbocations. For smaller carboxylates (below six carbons long), a random orientation was proposed which meant radicals formed may not have been close in space to other radicals and therefore underwent a second oxidation to a carbocation, giving a low yield of octane.⁸⁷



Scheme 2.28 Kolbe homo-coupling of various chain length alkyl carboxylates giving increased Kolbe product with increased chain length.⁸⁷

In a series of hetero-coupling reactions with alkoxyacetic acid, both longer and shorter carboxylic acids were electrolysed and the resulting product distribution calculated (Scheme 2.29, Table 2.8).⁸⁴ In the electrolysis of carboxylate ether **2.84** in the absence of a co-acid **2.85**, only non-Kolbe products were observed. This is because the radical formed, being α to a heteroatom, readily underwent a second oxidation to a carbocation which was quenched by methanol. The addition of a smaller co-acid in a 10-fold excess resulted in a 30-32% yield of the hetero-coupled Kolbe product and up to a 58% yield of the Kolbe product with a longer co-acid.⁸⁴ The authors concluded that the improved yield was due to increased order at the electrode surface and the perpendicular stacking of the carboxylates, which prevented the adsorption of the ether group onto the electrode surface which would promote the non-Kolbe two-electron pathway *via* over-oxidation.⁸⁴



Scheme 2.29 Kolbe electrochemical hetero-coupling of **2.84** and **2.85** showing the effect on the Kolbe:non-Kolbe selectivity with increased chain length.⁸⁴

Table 2.8 The effect of a co-acid on the outcome of Kolbe electrolysis.⁸⁴

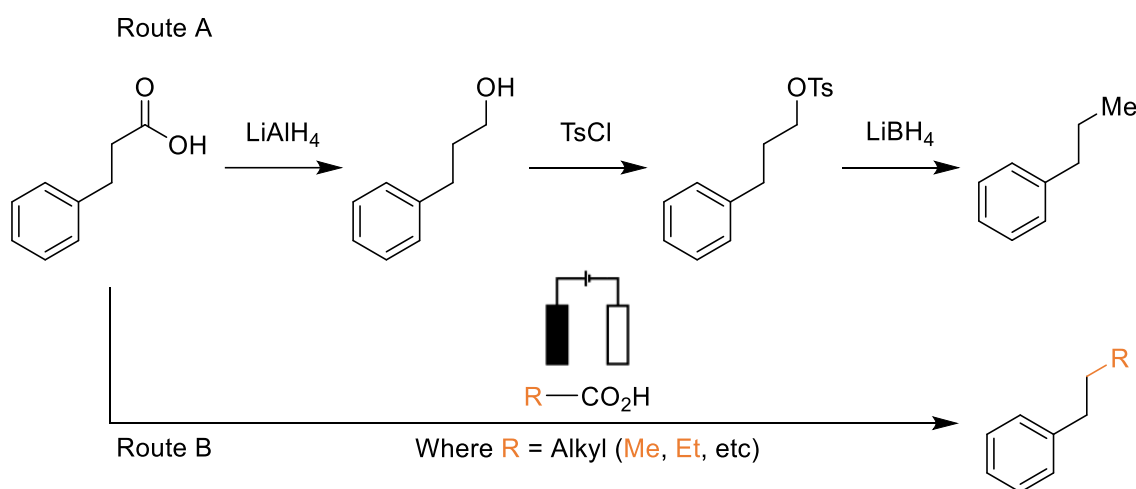
Entry	R ¹	R ²	Conversion of 2.84 / %	Yields of Kolbe Products with Respect to the Combination of Acids			Ratio Radical Coupling:Non-Kolbe Product
				Hetero-coupled Product 2.86	Homo-coupled Product 2.87	Non-Kolbe Product 2.88	
1	C ₆ H ₁₃	-	89	-	0	100	0.00:1.00
2	C ₁₂ H ₂₅	-	83	-	0	100	0.00:1.00
3	C ₆ H ₁₃	C ₄ H ₉	99	32	7	61	0.64:1.00
4	C ₁₂ H ₂₅	C ₄ H ₉	97	30	2	68	0.47:1.00
5	C ₆ H ₁₃	C ₁₀ H ₂₁	100	51	7	42	1.38:1.00
6	C ₁₂ H ₂₅	C ₁₀ H ₂₁	98	58	7	35	1.86:1.00

This demonstrates that regardless of the reaction conditions, ultimately, the structure of the carboxylate is critical to the outcome of the Kolbe electrolysis reaction. Carboxylates with electron-donating groups in the α position will lower the ionisation potential and therefore the radicals will have a lower thermodynamic barrier to over-oxidation. In addition, bulky substituents have been known to disrupt the packing at the electrode surface, which increases the distance between alkyl radicals, disfavours coupling and leading to the formation of carbocations.

2.1.8 Chapter Aims

The mechanism of Kolbe electrolysis has been well studied, with many of the reaction conditions established to achieve successful coupling of simple primary alkyl radicals. Whilst Kolbe electrolysis has been developed for the homo-coupling of fatty acids and simple carboxylates, including on an industrial scale, there is significant scope to expand the reaction for the synthesis of highly functionalised small molecules *via* the hetero-coupling of two alkyl radicals.

As an example of the proposed transformation with electrochemistry verses more traditional two electron approaches to synthesis, if the formation of *n*-propylbenzene is considered, Scheme 2.30. In Route A, reduction of a carboxylic acid to an alcohol, followed by tosylation and finally reduction with LiBH_4 would give a methylated product, *n*-propylbenzene in three steps.^{115–117} Alternatively, Kolbe electrolysis could theoretically provide a one-step route to a range of alkylated products *via* electrochemical hetero-coupling with a range of co-acids (Scheme 2.30, Route B).

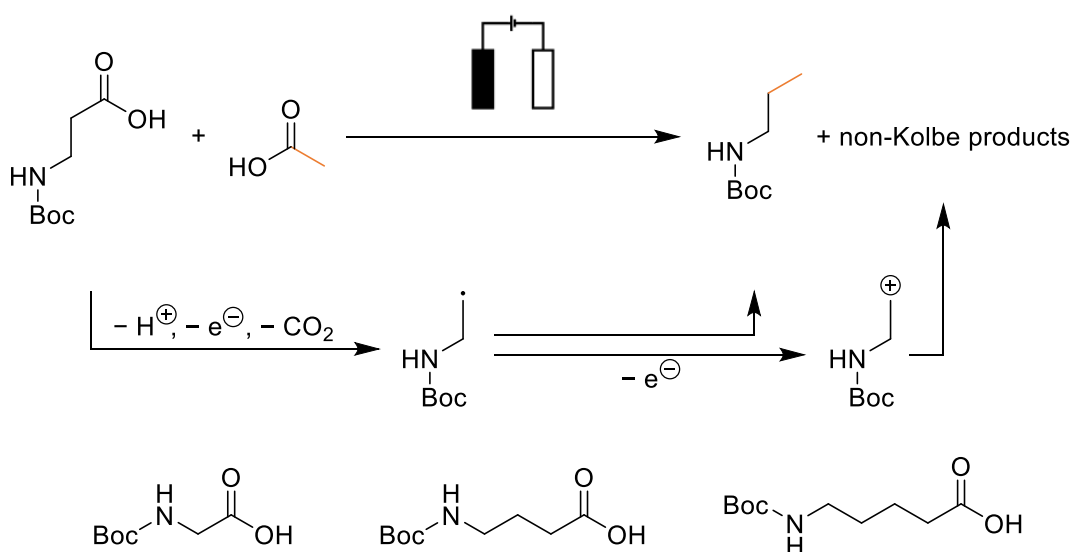


Scheme 2.30 Routes to *n*-propylbenzene: Route A – classical two electron approach requiring three steps and protecting groups. Route B – Kolbe electrolysis in one step where the R group of the co-acid can easily be varied.

The aim of this work is to determine the feasibility of using Kolbe electrolysis as a radical reaction for the functionalisation of simple protected amino acids. Radical reactions often show high functional group tolerance and reactivity. By generating the radicals electrochemically, mild conditions can be used in a greener approach to organic synthesis. Amino acids were chosen as they have the carboxylic acid group which will be oxidised at the anode and an amine which can be used for further diversification, and the distance

between the acid and amine can be varied by changing the amino acid and the subsequent outcome on product selectivity determined.

Furthermore, amino acids are inexpensive, commercially available, and good building blocks for synthetic chemistry making them the ideal starting materials. Shorter chain amino acids have previously been used in Kolbe electrochemical homo-coupling reactions and often the proximity of the radical formed to nitrogen resulted in high yields of non-Kolbe products.⁸⁵ By conducting detailed monitoring of the reaction progression, this work aims to achieve high yields of Kolbe hetero-coupled products from *N*-Boc amino acids starting materials such as those given in Scheme 2.31.



Scheme 2.31 Proposed hetero-coupling reaction of *N*-Boc linear amino acids and acetic acid.

To achieve high yields of the Kolbe product derived from amino acids, a bespoke electrochemical set-up will be developed to provide the necessary conditions, high current density and platinum electrodes. Based on the known mechanism, the conditions and starting acid will be varied to try and promote radical coupling over carbocation formation.

2.2 Results and Discussion

2.2.1 Electrochemical Set-Up and Reproducibility

In order to carry out Kolbe electrolysis at high current densities and at platinum electrodes, a bespoke in-house electrochemical set-up was assembled. The power supply, platinised titanium electrodes and associated 9 mL electrochemical cell (Sections 2.2.1.1 and 2.2.1.2) were previously developed in the group and will briefly be described below.¹¹⁸ An alternative set of platinum wire electrodes were also developed and will be discussed in Section 2.2.1.3.

2.2.1.1 Power Supply for Kolbe Electrolysis

A constant voltage was applied between the anode and cathode by two power packs with a maximum voltage of 15 V each (combined maximum voltage 30 V). A Labjack[®] was used to record the potential difference and the experimental current (Figure 2.2).

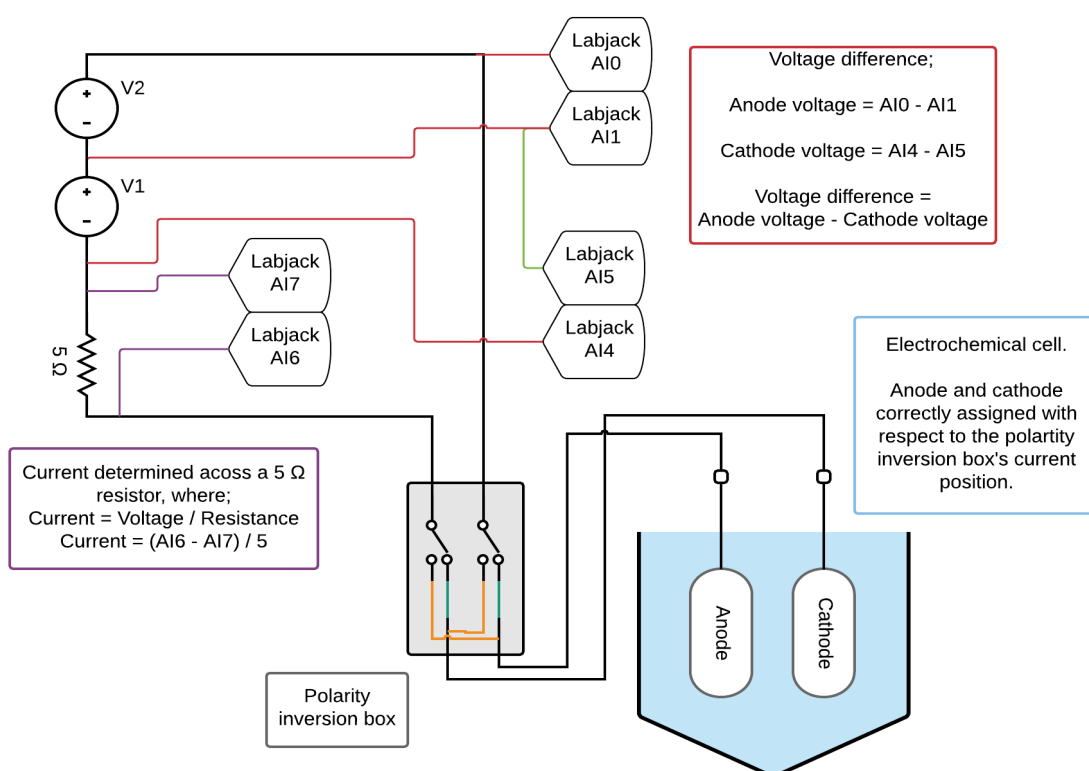


Figure 2.2 Circuit diagram for electrochemical set-up including powerpacks, Labjack[®], polarity inverter and electrodes

The current was determined by measuring the voltage drop across a 5 Ω resistor and applying Ohm's law (Equation 2.4). A limitation of the design was that only a constant voltage could

be achieved, as opposed to the constant current often seen in the literature for Kolbe electrolysis.⁷⁷ A polarity inverter was included which could periodically switch the anode and cathode potential to prevent passivation (see Section 2.1.4.1).

$$\text{Voltage (V)} = \text{Current (I)} \times \text{Resistance (R)} \quad \text{Equation 2.4}$$

2.2.1.2 Platinised Titanium Electrodes and 9 mL Electrochemical Cell

A set of electrodes were developed which used a platinised titanium mesh as a cost-effective way of achieving a large surface area of platinum (3.3 cm²).¹¹⁸ Platinised titanium has recently been shown to perform as well as pure platinum in the anodic decarboxylation of *n*-hexanoic acid to form *n*-decane.¹¹⁹ Both a labelled image and schematic of the electrodes and cell are given in Figure 2.3. The electrodes were held in place with a PTFE mount, which maintained a fixed spacing between the electrodes of 2 mm. PTFE was used for the mount as it is chemically resistant to methanol, the solvent that is typically used for Kolbe electrolysis. A small electrode spacing was used to minimise solvent resistance as Kolbe electrolysis is usually performed in the absence of supporting electrolyte. The temperature was monitored during the reaction and maintained at *ca.* 20 °C by a stirred water bath around the electrochemical cell. Reactions were stirred to aid mass transport.

A glass cell was made to accommodate the electrodes. A side arm allowed an inlet/outlet needle to be fitted so reactions could be performed under inert atmospheres. The cell was designed to hold 9 mL of solvent which sufficiently covered the electrodes whilst simultaneously not covering the wires connecting the electrodes to the powerpacks and allowing room for a stirrer bar at the bottom of the cell. 9 mL was chosen as the reaction volume as, due to the high concentrations of carboxylate used for Kolbe electrolysis, reasonable amounts of product could be isolated by column chromatography without being wasteful of starting materials. The relatively low volume of solvent also meant a high electrode surface area per solvent volume could be used (0.37 cm² mL⁻¹), allowing reactions to be performed on a reasonable timescale (*ca.* 90 minutes). A larger electrode surface area per solvent volume would result in shorter reaction times through an increase in the current.

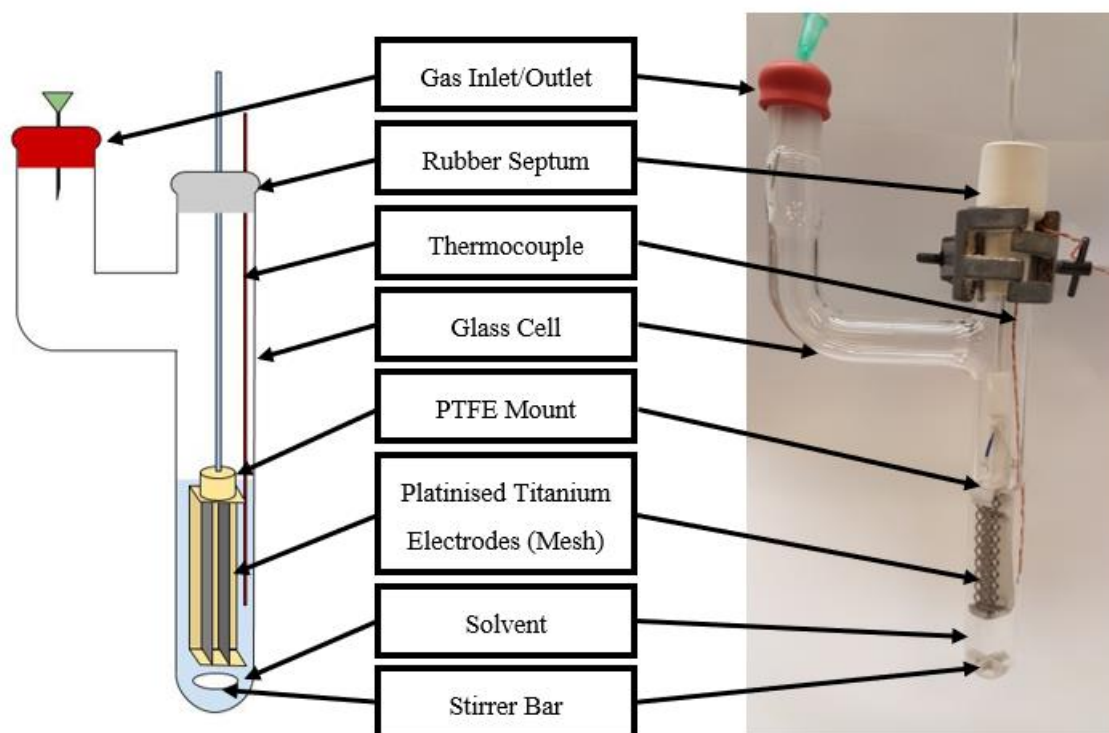


Figure 2.3 Labeled image (left) and photograph (right) of the platinised titanium electrodes in the 9 mL cell

2.2.1.3 Platinum Wire Electrodes and 2 mL Electrochemical Cell

A miniaturised electrochemical cell based on a Wheaton 2 mL sample vial containing a small stirrer bar permitted experiments to be conducted in a cost-effective manner using deuterated solvents (2 mL solvent volume). This cell was designed to allow direct analysis of the reaction mixtures by ^1H NMR spectroscopy, without the need for workups (Figure 2.4 for a labelled photo and schematic). Furthermore, aliquots taken for analysis by ^1H NMR spectroscopy, or gas chromatography (GC), represented a greater percentage of the reaction mixture (12.5% of the total reaction mixture was taken for quantification with ^1H NMR spectroscopy compared to 3.0% in the 9 mL cell). Reaction times in this cell were also generally quicker than with the platinised titanium electrodes in the 9 mL cell, as the electrode surface area per volume of solvent was larger ($0.42\text{ cm}^2\text{ mL}^{-1}$). Due to the simplicity of the design, reactions could not be performed under inert atmospheres. The electrodes in the miniaturised Kolbe electrolysis cell were made from pure platinum wire (0.2 mm diameter), which could be cleaned more easily than the platinised titanium electrodes, which gradually degraded by successive cleaning (see Section 2.2.1.4 for discussion of electrode cleaning to aid reproducibility). The platinum wire was wrapped around a modified glass microscope slide and connected to the power packs by crocodile

clips mounted on a plastic back board. The glass slide was cut to a size of 26 mm by 7 mm (1 mm thick). Two grooves were cut into the glass, a set distance apart, to hold the wire in place. Thus the anode-to-cathode electrode spacing could be as close as 0.8 mm (i.e. closer than for the platinised titanium electrodes in the 9 mL cell). Furthermore, the electrode spacing could be easily changed by simple replacement of the “grooved” glass slide. The platinum wires were wrapped around the slide multiple times to increase to surface area of platinum (measured at 0.84 cm²). The surface area for the wire electrodes was still significantly smaller than for the platinised titanium electrodes and consequently the current densities at the same potential were higher with the wire electrodes than the platinised titanium.

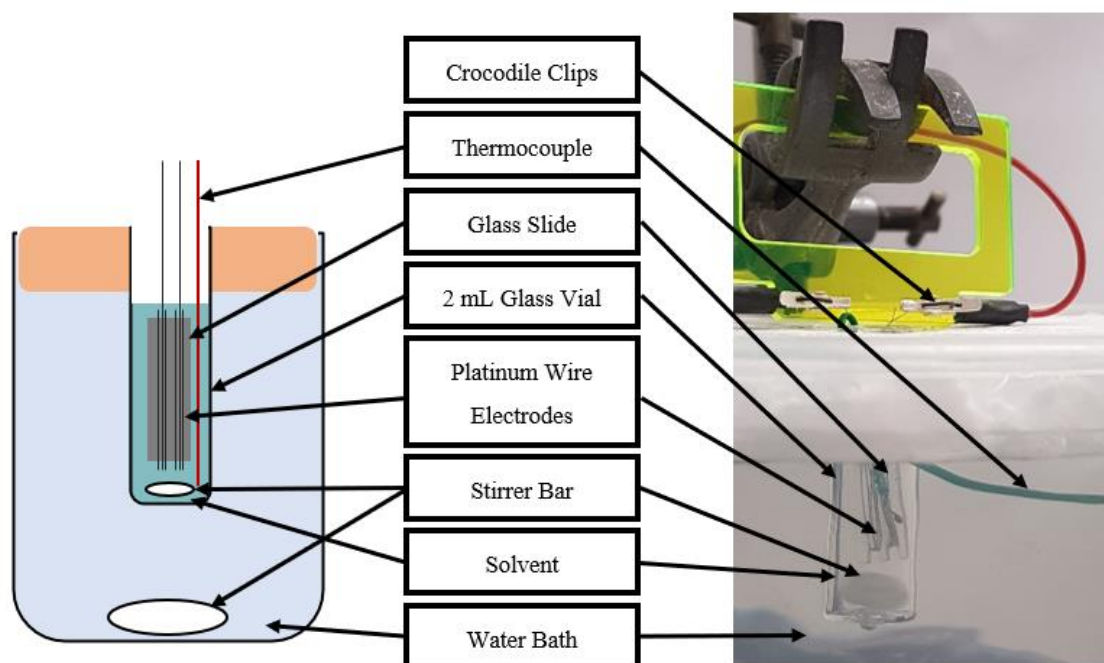


Figure 2.4 Labelled image (left) and photograph (right) of the platinum wire electrodes in the 2 mL cell

2.2.1.4 Electrolysis Conditions, Reproducibility and Electrode Cleaning

Two sets of general electrolysis conditions were used in this chapter and these are summarised in Table 2.9. General Procedure 2A was adapted from the Schäfer group and the cyclisation work by Huhtasaari *et al.* (Scheme 2.17), where unsaturated acid **2.35** underwent a Kolbe cyclisation, and the resulting radical was coupled to methyl radicals derived from acetic acid.¹⁰⁸ General Procedure 2B was adapted from the Kolbe hetero-coupling of functionalised carboxylic acid **2.26** with protected amino acid **2.28** performed

by Seebach and co-workers (Scheme 2.14).⁹⁷ In this literature, the experiments were performed under nitrogen to prevent the condensation of water at low temperatures.

In keeping with the standard Kolbe reaction conditions laid out in the introduction (Section 2.14), both sets of experimental conditions utilise platinum electrodes in undivided cells with methanol as the solvent. High carboxylate concentrations were used, which were partially neutralised with base. General Procedure 2A used a total acid concentration of 0.67 M and potassium hydroxide as the base (5.0%) whilst General Procedure 2B had a total acid concentration of 0.64 M with triethylamine as the base (5.6%). The ratio of acid to co-acid was higher for General Procedure 2B than General Procedure 2A, 1:6 and 1:4 acid:co-acid ratio respectively. When the platinised titanium electrodes were used in the 9 mL glass cell with General Procedure 2B, reactions were performed under nitrogen to match the literature.⁹⁷

Table 2.9 Summary of the two sets of Kolbe electrosynthesis conditions used in this chapter, General Procedure 2A and 2B; these are based on published work by Schäfer and co-workers¹⁰⁸ and Seebach and co-workers, respectively.⁹⁷

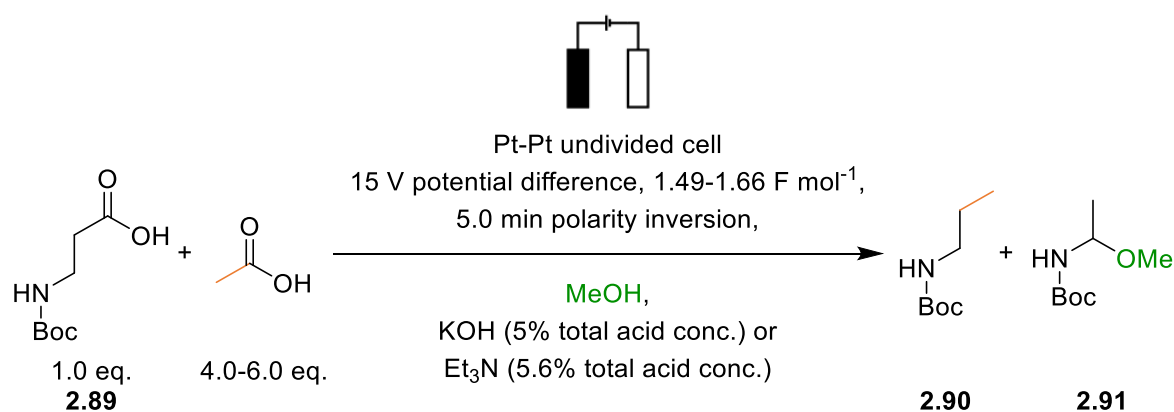
Conditions	General	General
	Procedure 2A ¹⁰⁸	Procedure 2B ⁹⁷
Solvent	Methanol	Methanol
Base	KOH	Et ₃ N
Neutralisation / %	5.0	5.6
Total Acid Concentration / mol dm ⁻³	0.67	0.64
Eq. of Co-Acid	4.0	6.0
Charge / F mol ⁻¹	1.6	1.5
Atmosphere	Air	N ₂
Average Current Density ^a / mA cm ⁻²	75	67

^a Using platinum wire electrodes and 2 mL cell.

The electrolysis of *N*-Boc β-alanine **2.89** with acetic acid as the co-acid, which forms Kolbe product **2.90** and non-Kolbe product **2.91**, was used to assess the reproducibility of the electrochemical set-up and conditions (Scheme 2.32). The results of electrolysis, with General Procedure 2A and 2B, each performed three times in the 2 mL cell with platinum wire electrodes are presented in Table 2.10. The reactions were quantified by ¹H NMR spectroscopy, using mesitylene as an external standard and integrating the CH₂N and CH₃ protons to quantify the Kolbe and non-Kolbe products respectively. Further details about

quantifying the reaction with ^1H NMR spectroscopy are given in Section 2.2.3 and the origin of non-Kolbe product **2.91** is discussed in Section 2.2.2.2.

Although the literature from which the experimental conditions are derived all reported similarly high current densities of $360\text{--}370\text{ mA cm}^{-2}$, in the experiments shown in Table 2.10 the applied 15 V cell potential only generated current densities of approximately 75 mA cm^{-2} for General Procedure 2A and approximately 67 mA cm^{-2} for General Procedure 2B.^{97,108} Despite this, all reactions generated products and the optimised electrolysis conditions resulted in good reproducibility using both General Procedure 2A (Table 2.10, entries 1-3) and 2B (Table 2.10, entries 4-6). The yield of the desired Kolbe hetero-coupling product **2.90** was reasonably high with both sets of conditions, giving an average yield of 69% with General Procedure 2A and 63% with General Procedure 2B. The selectivity of the Kolbe product over the non-Kolbe product was marginally higher for General Procedure 2A than for General Procedure 2B. The overall conversion and mass balance for both reactions were also high ($> 90\%$). Despite the slightly higher yield with General Procedure 2A, triethylamine (as used in General Procedure 2B) was a more useful base for monitoring the progress of the reactions and any consumption of base as it has protons visible in the ^1H NMR spectrum. Furthermore, by using triethylamine, direct aliquots of the reaction mixture could be taken for quantification by GC since the lack of inorganic base negated the need for a prior work-up.



Scheme 2.32 Kolbe electrochemical hetero-coupling of *N*-Boc β -alanine and acetic acid with General Procedure 2A and 2B.

Table 2.10 Yields of Kolbe product **2.90** and non-Kolbe product **2.91** by ^1H NMR spectroscopy after using either General Procedure 2A and 2B and the 2 mL electrochemical cell, as detailed in Scheme 2.32

Entry	General Procedure	Eq. of Charge / F mol ⁻¹	Average Current Density / mA cm ⁻²	Yield 2.90 by ^1H NMR spectroscopy / %	Yield 2.91 by ^1H NMR spectroscopy / %
1	2A	1.64	81	67	23
2	2A	1.64	75	72	25
3	2A	1.66	70	68	24
Average Yields for General Procedure 2A				69	24
4	2B	1.54	70	59	33
5	2B	1.49	76	64	31
6	2B	1.51	55	66	32
Average Yields for General Procedure 2B				63	32
7 ^a	2A	1.65	63	59	40
8 ^a	2B	1.54	57	58	28

^a no polarity inversion

As the reaction occurs at the electrode surface and is therefore considered a heterogeneous process, the nature of the electrode surface will have a significant impact on the reaction outcome. For example, passivation, the build-up of an insulating layer of insoluble organic material on the electrode surface, will change the electrode surface chemistry. Therefore, to improve reproducibility between reactions, after every Kolbe electrolysis run the platinum wire electrodes were cleaned *via* submerging in sulfuric acid (0.1 M) and application of a 3 V potential difference. S. Berrell found that after comparable experiments using the 9 mL volume cell and platinised titanium electrodes it was not possible to use the same acid-based electrode cleaning step because of electrode degradation.¹¹⁸ This has been previously reported in the literature, for example Neubert *et al.* reported finding detached platinum from platinised titanium electrodes in their final Kolbe electrolysis reaction mixtures.¹¹⁹ They reasoned that during electrolysis gas evolution, particularly at exposed areas of titanium, caused this de-platinisation.

As a control, reactions in the 2 mL cell were performed without polarity inversion (Table 2.10, entries 7 and 8). The results show slightly lower average current densities which implies a higher level of electrode passivation (Appendix A for overlay of current traces). Passivation reduces the current because the build up of the insulating passivation layer on

the electrode surface will increase the resistance, which at a fixed voltage, will decrease the current (based on Ohms law, Equation 2.4). This also correlated with lower yields of the Kolbe product and increased yields of the non-Kolbe product in the experiment using General Procedure 2A. This could be explained by the adsorption of carboxylate ions and alkyl radicals on the passivated layer, hindering desorption, and therefore radicals underwent a second electron oxidation to form carbocations. An alternative reason for the lower current densities without polarity inversion could be due to a lower radical concentration at the electrode surface due to poor mass transport. Once the Kolbe hetero-coupled product is formed, the diffusion from the electrode surface may be hindered resulting in less carboxylate at the surface whilst polarity inversion allows a new layer to form every 5 minutes. Radicals which do not couple at the surface would subsequently get further oxidised to carbocations forming non-Kolbe products.

Figure 2.5 shows a comparison of the experimental current vs time plots for an experiment conducted under General Procedure 2A and an experiment using General Procedure 2B. The spikes in Figure 2.5 every 5 minutes are associated with charging at the electrode and reforming the double layer on switching the polarity of the anode and cathode. These datasets reflect a general trend: after *ca.* 25 minutes the current density recorded for experiments using General Procedure 2B began to drop off, at which time $0.94 \text{ F (mol of total acid)}^{-1}$ of charge had been passed. Assuming a 100% Faradaic efficiency for both reactions, this would be sufficient to have consumed 75% of acid starting material based on 59:33 ratio of Kolbe to non-Kolbe product (a total of 1.25 F mol^{-1} of electrons were required as the non-Kolbe product requires a two-electron oxidation). Thus, the drop in current is attributed to the consumption of the majority of carboxylate, after which point insufficient carboxylate coverage could lead to triethylamine being preferentially oxidised, which may lead to passivation of the electrode surface and a drop in current. In contrast, as shown in Figure 2.5, experiments using General Procedure 2A show a relatively stable current density-time trace for 50 min. This could mean that at lower carboxylate concentrations, potassium hydroxide can either still facilitate Kolbe electrolysis or an alternative oxidation/reduction reaction, such as methanol oxidation, leading to a retention of the current density.

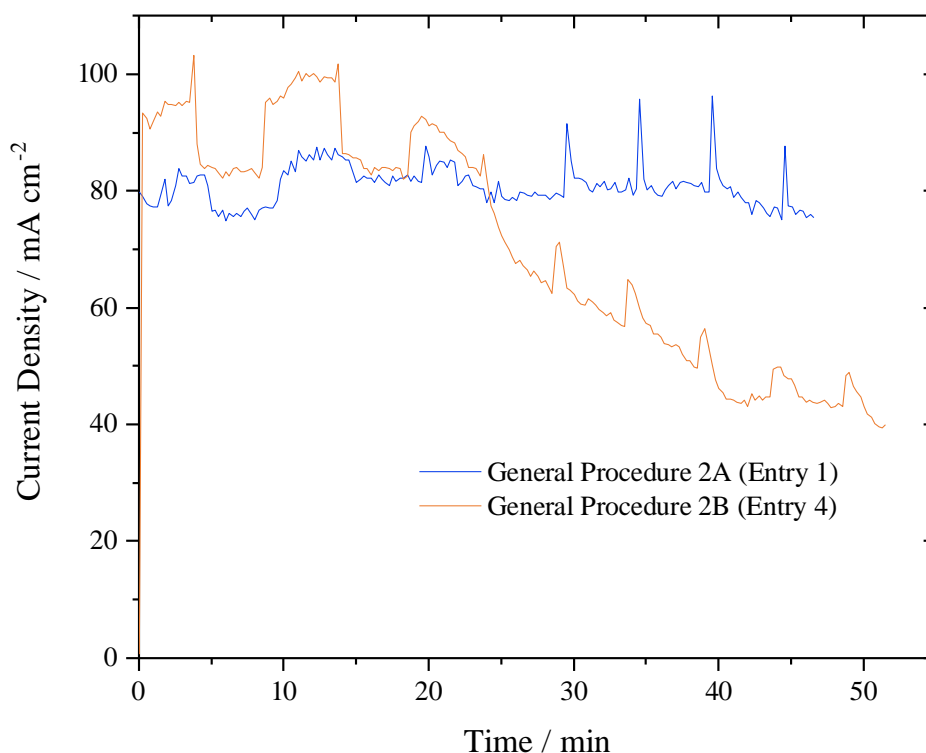


Figure 2.5 Overlay of current vs time plot for General Procedure 2A and General Procedure 2B, using Table 2.10, entries 1 and 4

Having established that the electrochemical set-ups and general reaction conditions produce reproducible data with a benchmark electrosynthetic Kolbe reaction, next the nature of the substrate was investigated.

2.2.2 Electrolysis of *N*-Boc Amino Acids

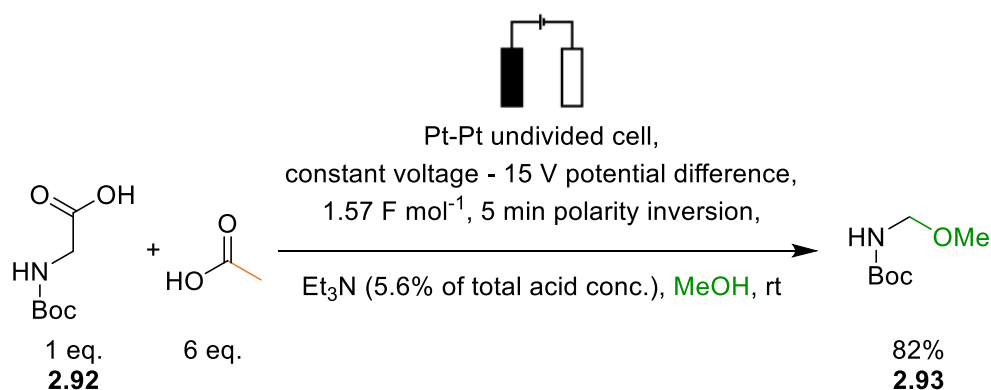
Linear amino acids, which would form primary alkyl radicals, were chosen to examine the effect of varying the distance between the heteroatom and carboxylate on the outcome of electrolysis. The amino acids were protected to prevent oxidation of the free amine and the Boc group was chosen as it is a synthetically relevant protecting group that can be easily removed.^{104,120–122} Acetic acid was used as the co-acid as it is inexpensive, readily available, and the homo-coupled product, ethane, would be removed from the reaction as a gas. Both General Procedure 2A and 2B were used for electrolyses which were performed using the 9

mL cell and platinised titanium electrodes so that sufficient quantities of both Kolbe and non-Kolbe products could be generated for characterisation.

In the following sections, where appropriate, comparison has been made to Kolbe decarboxylation of *N*-protected piperidine derived carboxylates with acetic acid, performed by a previous PhD student in the group, S. Berrell. For these reactions, the same platinised titanium electrodes and 9 mL electrochemical cell were used and related non-Kolbe products, derived from analogous carbocation rearrangements, were observed.¹¹⁸

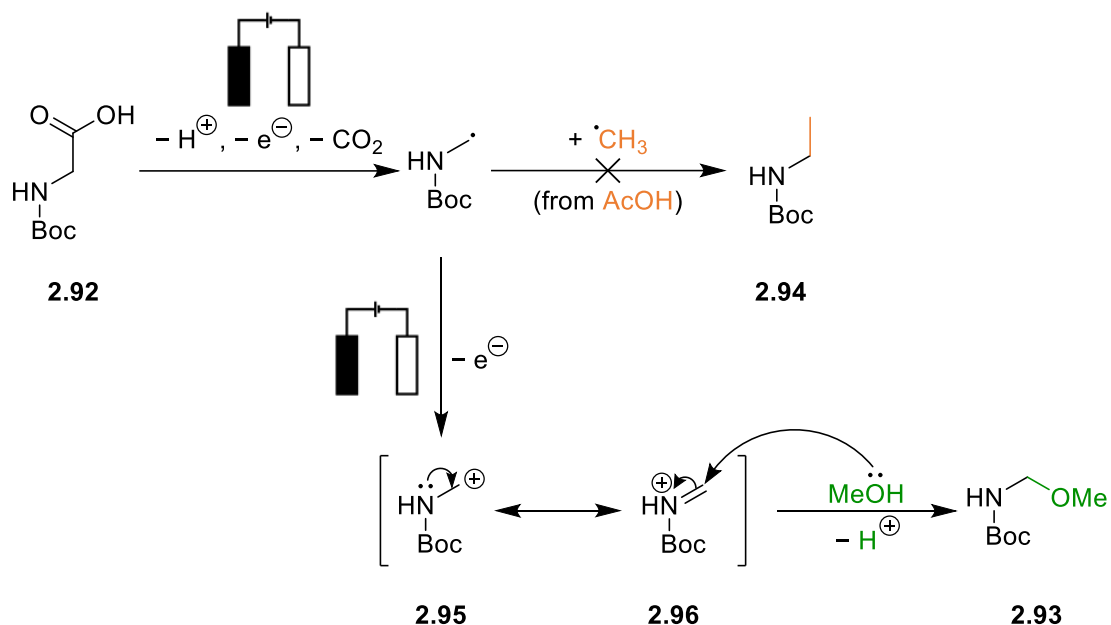
2.2.2.1 Electrochemical Oxidation of α -Amino Carboxylates

Electrolysis of *N*-Boc glycine (**2.92**) and acetic acid gave non-Kolbe amino ester **2.93** in an 82% isolated yield (Scheme 2.33) with no evidence for the formation of the desired Kolbe hetero-coupled product **2.94**.



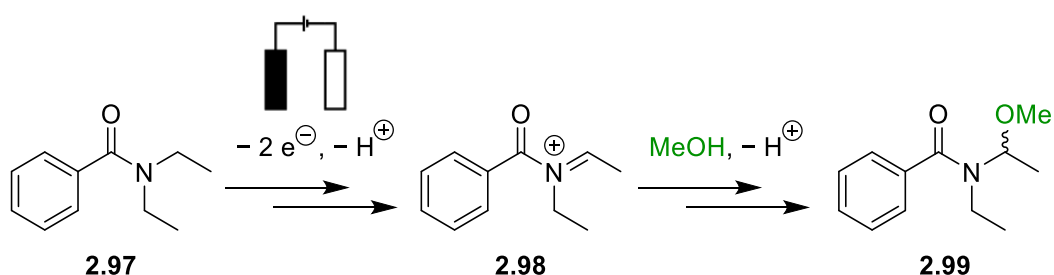
Scheme 2.33 Kolbe electrolysis of *N*-Boc glycine with acetic acid using General Procedure 2B.

Mechanistically, carbocation **2.95**, which formed *via* the two-electron oxidation pathway, is resonance stabilised as iminium ion **2.96**. Nucleophilic addition of methanol and deprotonation then delivered non-Kolbe product **2.93** (Scheme 2.34). This α -amino functionalised product **2.93** is analogous to a Shono-oxidation product; however, loss of the carboxylate group was reasonable evidence to support the non-Kolbe pathway. The Shono oxidation pathway will be briefly discussed below with reference to where it has been observed in Kolbe electrochemical coupling reactions as it is an alternative route to α -heteroatom functionalisation.



Scheme 2.34 Proposed mechanism for Kolbe electrolysis of *N*-Boc glycine with acetic acid.

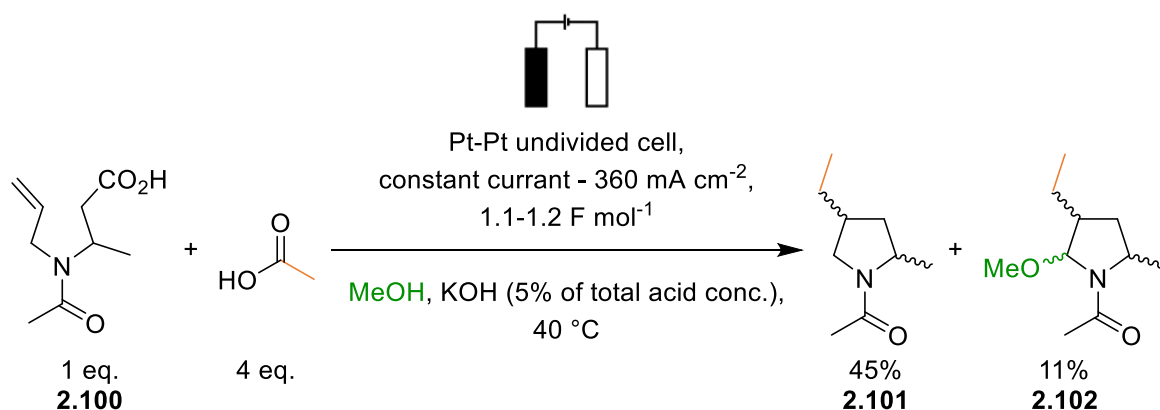
Shono oxidation is widely used for C-H functionalisation α to a nitrogen *via* iminium ions.¹²³ Mechanistically, in Shono electrolysis, oxidation of an amine such as **2.97** to a radical cation, followed by a proton loss and a second electron oxidation to forms iminium ion **2.98** (Scheme 2.35). The iminium ion is then trapped by a nucleophile, typically a solvent such as methanol, to form the Shono product **2.99**.¹²³ Typically, the Shono product is favoured by reticulated vitreous carbon (RVC) electrodes, methanol or acetonitrile as the solvent, and supporting electrolyte such as tetrabutylammonium perchlorate.¹²⁴ The conditions encourage adsorption to the electrode surface and thus multiple electrochemical oxidations.



Scheme 2.35 Example Shono oxidation by Jones *et al.*¹²⁴

Shono oxidation products have been observed in Kolbe electrolysis as unwanted side-products, lowering the yield of Kolbe product and Faradaic efficiency of the reaction. When

carboxylic acid **2.100** was electrolysed at platinum electrodes, along with the desired Kolbe product **2.101** in a 45% yield, side product methyl ether **2.102** was observed in 11% yield (Scheme 2.36).¹⁰⁹ The side product was believed to be formed *via* Shono oxidation rather than *via* a non-Kolbe pathway as the starting material underwent radical cyclisation, as the product no longer contained the carboxylate functional group, meaning the alkyl radical formed from decarboxylation underwent addition to the alkene and was not oxidised to a carbocation.¹⁰⁹



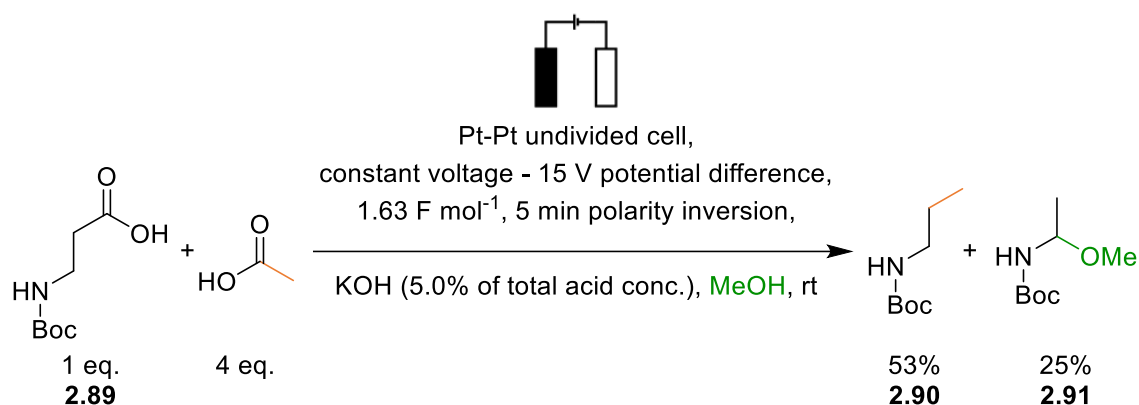
Scheme 2.36 Shono oxidation in Kolbe electrolysis (example from Becking *et al.*).¹⁰⁹

In the electrolysis of *N*-Boc glycine and acetic acid, the desired hetero-coupled product was not formed, despite some literature precedents (Scheme 2.21).¹¹² The high yield of non-Kolbe product was consistent with the majority of previous studies which have reported the electrochemical oxidation of α -amino radicals to carbocations under Kolbe electrolysis conditions.^{85,111} This is because α -amino radicals have low ionisation potentials, 5.9 eV for $\cdot\text{CH}_2\text{N}(\text{H})\text{Me}$ and, as predicted by Ebersson *et al.*, radicals with ionisation potentials below 8 eV readily over-oxidise to carbocations.^{86,125-127}

2.2.2.2 Electrochemical Oxidation of β -Amino Carboxylates

As previously described, when the radical was formed β to nitrogen, in the electrolysis of *N*-Boc β -alanine, both the one and two-electron products were observed. Hetero-coupled product **2.90** and non-Kolbe methoxylated product **2.91** were isolated in a 53% and 25% yield respectively, with Kolbe:non-Kolbe product ratio of 2.1:1.0 (Scheme 2.37). The reaction was also reproduced at York by S. Berrell, using the platinised titanium electrodes and 9 mL cell, with isolated yields of 50% and 18% for **2.90** and **2.91** respectively.¹¹⁸

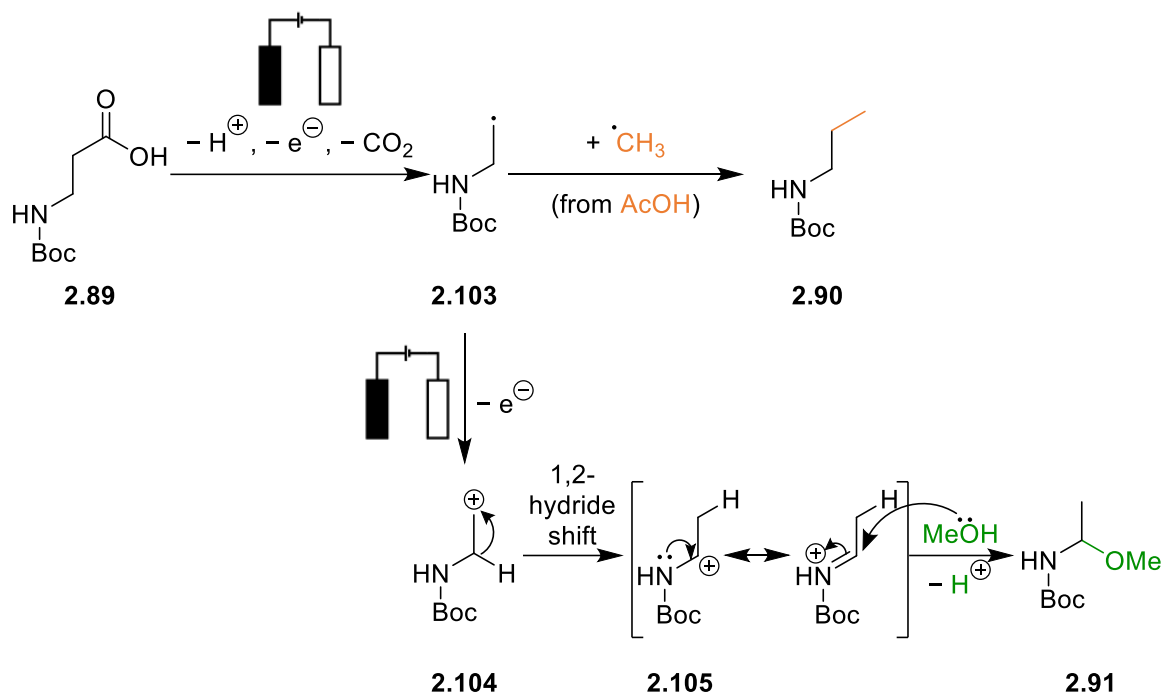
Gratifyingly, this result was consistent with the yields determined by ^1H NMR spectroscopy using the platinum wire electrodes and 2 mL cell (Section 2.2.1.4).



Scheme 2.37 Kolbe electrolysis of *N*-Boc β -alanine with acetic acid using General Procedure 2A.

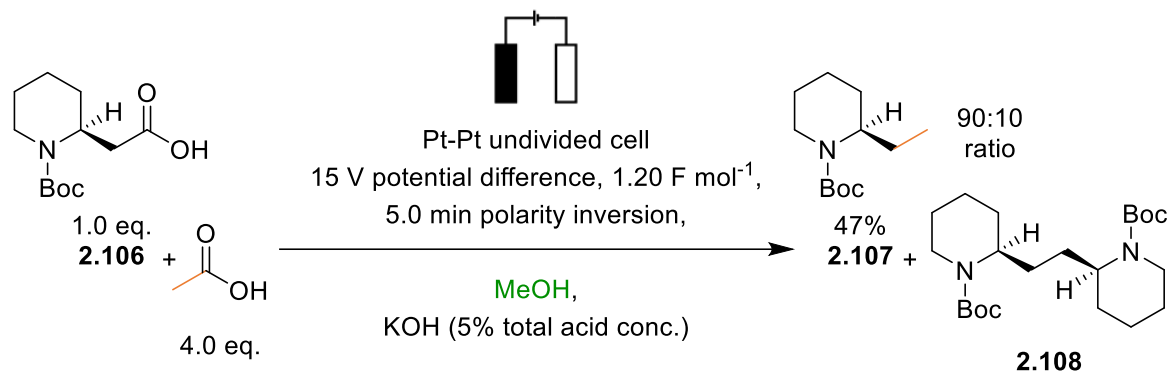
Whilst the ionisation potential for a radical β to nitrogen, such as **2.103** (Scheme 2.38) is not known, it is likely to be close to or less than 8 eV as carbocation derived products were observed. The ionisation potential can be predicted by comparing to the ionisation potentials for hydroxymethyl radicals ($\cdot\text{CH}_2\text{OH}$) and hydroxyethyl radicals ($\cdot\text{CH}_2\text{CH}_2\text{OH}$), which have been determined at 7.56 eV and 8.35 eV respectively.^{127–129} Therefore, as amino methyl radicals ($\cdot\text{CH}_2\text{NH}_2$) have ionisation potentials of 6.2 eV, less than hydroxymethyl radicals, it is reasonable to conclude that amino ethyl radicals will be close to or even lower than 8.35 eV.¹²⁵ Furthermore, the ionisation potential for an ethyl radical was determined to be 8.38 eV, which is comparable to hydroxyethyl radicals, therefore the distal hetero-atom may have little effect on the ionisation potential when it is not α to the radical.¹³⁰ If this is the case, all subsequent linear amino acids should show some level of over-oxidation as the ionisation potential decreases with increased chain length for linear alkyl radicals (1-heptyl radicals have an ionisation potential of 8.10 eV).¹³¹

Methoxylation was believed to occur α -to nitrogen, rather than β -to nitrogen, as carbocation **2.104** underwent a rapid 1,2-hydride shift to form a more stabilised secondary carbocation **2.105**, which was further resonance stabilised as an iminium ion (Scheme 2.38). Nucleophilic addition of methanol and deprotonation resulted in non-Kolbe product **2.91** being formed. An analogous carbocation rearrangement was observed in a Kolbe cyclisation reaction by Markó and co-workers for a carbocation formed β to oxygen (Scheme 2.24). A similar Kolbe:non-Kolbe product ratio was also achieved (1.4-1.6:1.0).¹⁰³



Scheme 2.38 Proposed mechanism for Kolbe electrolysis of *N*-Boc β -alanine with acetic acid.

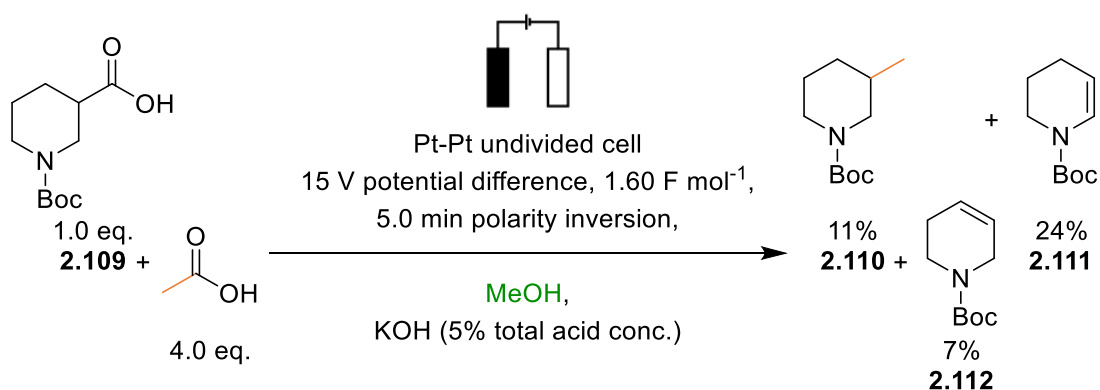
The results described above for *N*-Boc β -alanine can be compared with the electrochemical oxidation of piperidine derivative **2.106**, which resulted in an isolated yield of 47% for the Kolbe hetero-coupled product **2.107** (Scheme 2.39).¹¹⁸ Again, a primary radical was formed β to nitrogen which resulted in a similar yield of the hetero-coupled product with methyl radicals derived from acetic acid. Surprisingly, further oxidation of the β -amino radical was not observed, despite a possible lowering of the ionisation potential relative to radical **2.103** (*iso*-butyl radicals have ionisation potentials of 8.01 eV).¹³⁰ One possible reason could have been that the increased steric hinderance of the piperidine ring favoured rapid desorption from the electrode surface which would prevent a second electron oxidation and carbocation formation. In the ¹H crude NMR spectrum for the electrolysis of piperidine derivative **2.106**, homo-coupled product **2.108** was observed in a 10:90 ratio with Kolbe hetero-coupled product **2.107**, showing that homo-coupling of β -amino radicals is possible even with a large excess of co-acid.



Scheme 2.39 Kolbe electrochemical hetero-coupling of **2.106** and acetic acid performed by S. Berrell.¹¹⁸

Further comparison can be made to the electrochemical oxidation of piperidine derivative **2.109** and acetic acid (Scheme 2.40).¹¹⁸ Despite also forming a β -amino radical, this reaction resulted in high yields of non-Kolbe products relative to the Kolbe product with an overall Kolbe:non-Kolbe product ratio of 0.35:1.00. This was attributed to the fact that secondary radicals have lower ionisation potentials, 7.55 eV for $\text{CH}_3\dot{\text{C}}\text{HCH}_3$, and are therefore more readily oxidised to more stabilised carbocations.¹³⁰

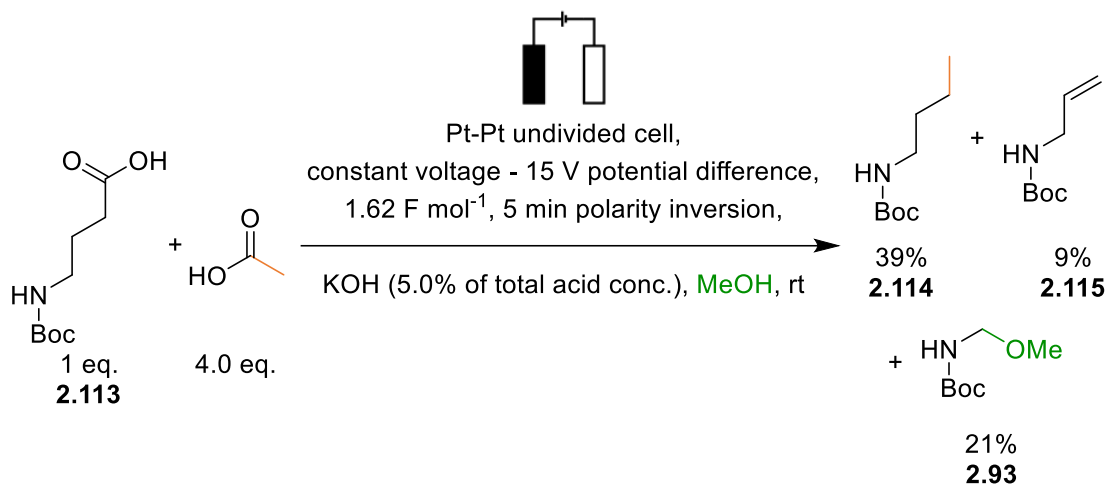
The hetero-coupled product **2.110** was isolated in an 11% yield, with two non-Kolbe alkenes, **2.111** and **2.112**, derived from deprotonation of either β -proton, isolated in 24% and 7% yields, respectively. A higher yield of non-Kolbe product **2.111** was observed, which may be because the proton α to nitrogen was more acidic than the proton γ to nitrogen, therefore the α -proton underwent preferential deprotonation.



Scheme 2.40 Kolbe electrochemical hetero-coupling of **2.109** and acetic acid performed by S. Berrell.¹¹⁸

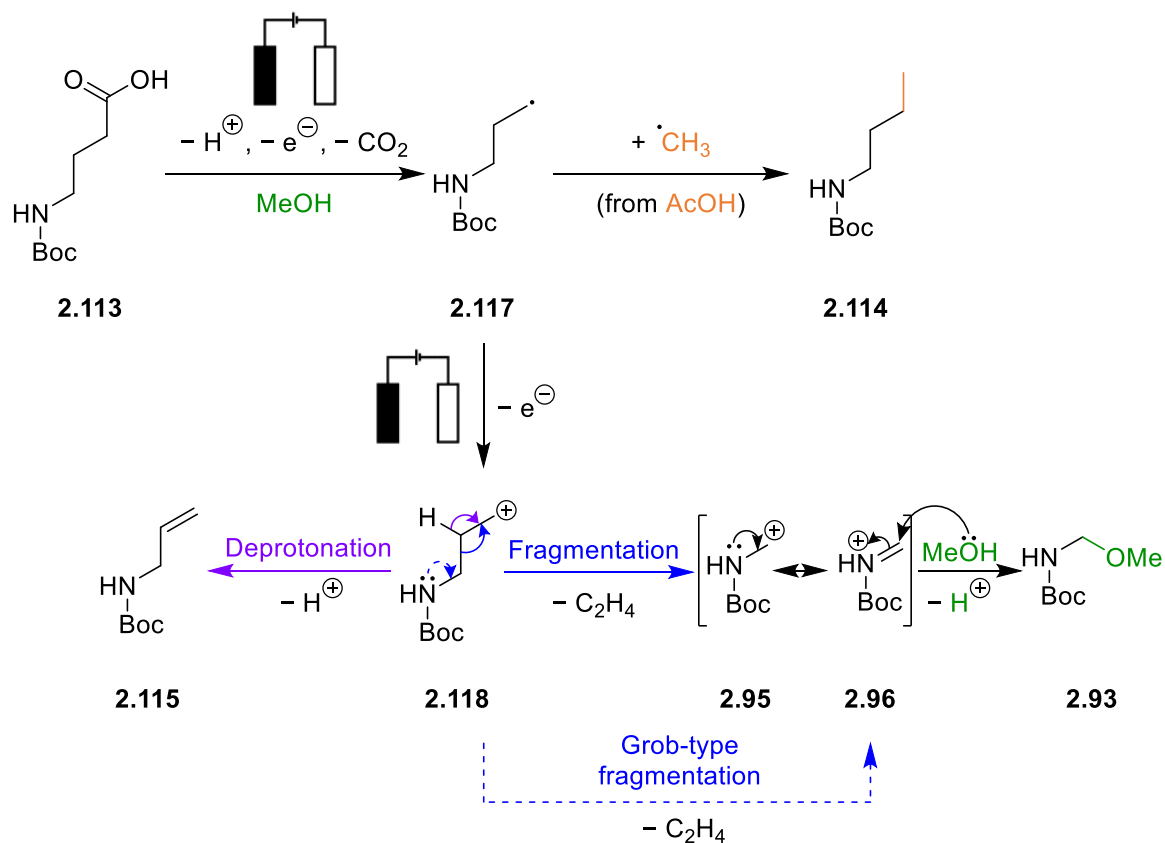
2.2.2.3 Electrochemical Oxidation of γ -Amino Carboxylates

The Kolbe electrolysis of *N*-Boc γ -aminobutyric acid **2.113** should result in a radical formed γ to nitrogen, **2.117** (as illustrated in Scheme 2.41). In support of this, the desired Kolbe product **2.114** was isolated in a 39% yield. In addition, two non-Kolbe products were isolated, **2.115** and **2.93** (Scheme 2.41). Again, this can be rationalised by consideration of ionisation potentials. Although values for the ionisation potential of a radical γ to a hetero-atom could not be found, *n*-propyl radicals are reported to have an ionisation potential of 8.10 eV.¹³⁰ Thus, even without the hetero-atom having any stabilising influence at all, over-oxidation of the alkyl radical should readily occur, leading to the generation of non-Kolbe products.



Scheme 2.41 Kolbe electrolysis of *N*-Boc γ -aminobutyric acid with acetic acid using General Procedure 2A.

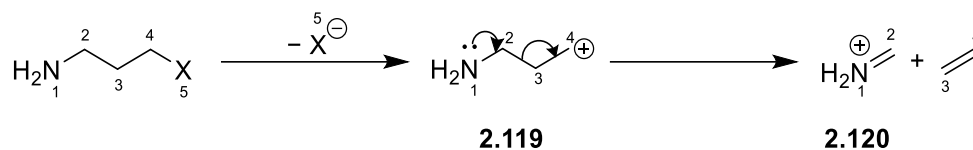
Oxidation of radical **2.117** would lead to primary carbocation **2.118**. Deprotonation of a β -proton would give alkene **2.115**, providing a rationale for the isolation of this product in a 9% yield (Scheme 2.42). This transformation is analogous to a classical E1 elimination mechanisms of an alkyl halide with base where initially a halide is lost, forming a carbocation, followed by deprotonation of a β -hydrogen.¹³² Alkenes have also been prepared by oxidative decarboxylation using phenyliodine bis(trifluoroacetate) and microwave radiation.^{133,134}

Scheme 2.42 Proposed mechanism for Kolbe electrolysis of *N*-Boc γ -aminobutyric acid with acetic acid.

The fact that Kolbe electrolysis of *N*-Boc γ -aminobutyric acid gives rise to methoxylated non-Kolbe product **2.93** in a 21% yield also suggests that a stabilised carbocation α to nitrogen, **2.95**, was formed as an intermediate in the reaction; this would require fragmentation and the loss of ethene, as in Scheme 2.42. The mechanism for formation of this carbocation could either be a stepwise elimination of ethene, where the resulting carbocation **2.95** was further stabilised by resonance as the iminium ion **2.96** (Scheme 2.42 solid blue line), or a concerted Grob-type fragmentation process, forming iminium ion **2.96** and losing ethene in one step (Scheme 2.42 dashed blue line).

As shown in Scheme 2.43, Grob fragmentation is known for γ -aminohalides producing three fragments: an electrofuge (atoms 1 and 2), an unsaturated component (atoms 3 and 4) and an anion, (atom 5, the nucleofugal/leaving group).¹³⁵ One possible Grob fragmentation pathway proceeds *via* initial loss of the leaving group (X^-) forming a carbocation **2.119**, followed by rapid elimination of the alkene component (ethene) and formation of a charged iminium ion **2.120**. As with unimolecular substitution ($\text{S}_{\text{N}}1$) or elimination ($\text{E}1$), this two-step mechanism is favoured when a stabilised carbocation is formed, and ionisation of the γ -

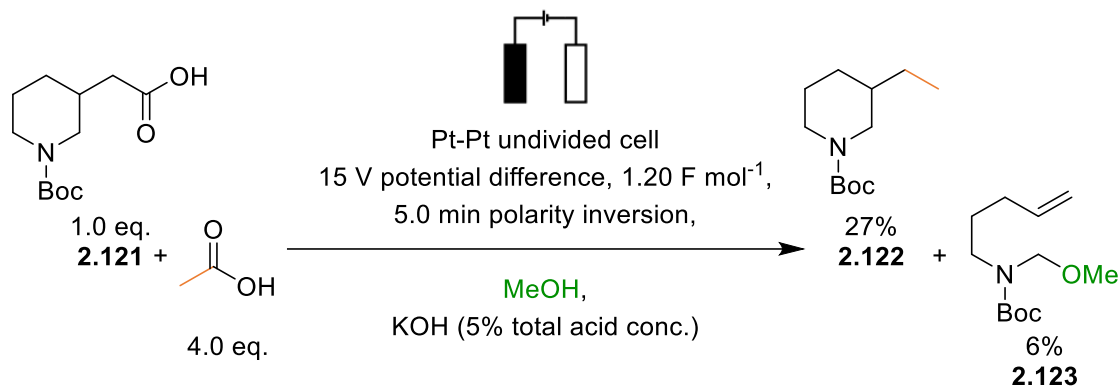
aminoaldehydes is the rate-determining step.¹³⁶ This could therefore be an alternative route for the formation of methyl ether **2.93** via iminium ion **2.96**.



Scheme 2.43 Possible fragmentation pathway adapted from Grob 1969.¹³⁶

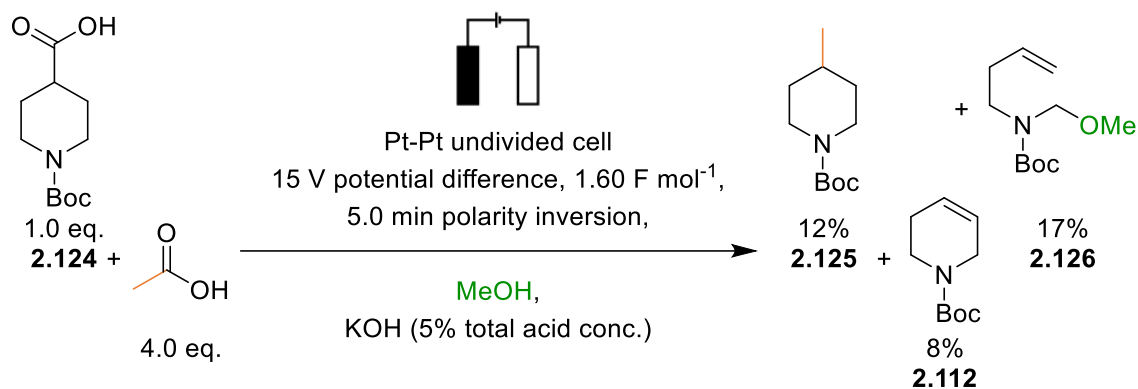
In the electrolysis of *N*-Boc γ -aminobutyric acid and acetic acid, relative to alkene **2.115**, increased yields of the methoxylated non-Kolbe product **2.93** were observed as a more stabilised carbocation intermediate was formed through the rapid Grob-type fragmentation. Furthermore, the low percentage base used in Kolbe would have disfavoured the deprotonation pathway.

As summarised in Scheme 2.44, work conducted at York by S. Berrell explored the Kolbe electrolysis of *N*-Boc protected piperidine derivative, **2.121**, and this is comparable to the electrolysis of *N*-Boc γ -aminobutyric acid **2.113**. The Kolbe:non-Kolbe ratio is much higher for the reaction with piperidine derivative **2.121** (4.5:1.0) than linear amino acid **2.113** (1.3:1.0). However, in the piperidine reaction the total product yield was lower, meaning starting acid may have been lost to passivation if the radicals did not couple sufficiently quickly. This could possibly be attributed to the fact that linear carboxylates would form a better layer at the electrode surface. In S. Berrell's work, the observation of a 6% yield of non-Kolbe product, **2.123**, is further evidence of similar carbocation rearrangements which occur after oxidation of a primary radical formed γ to nitrogen.¹¹⁸ Notably, in the electrolysis of piperidine derivative **2.121** non-Kolbe products derived from elimination of protons were not observed, it is hypothesised that deprotonation may have been hindered because this would need to occur at a tertiary substituted carbon.



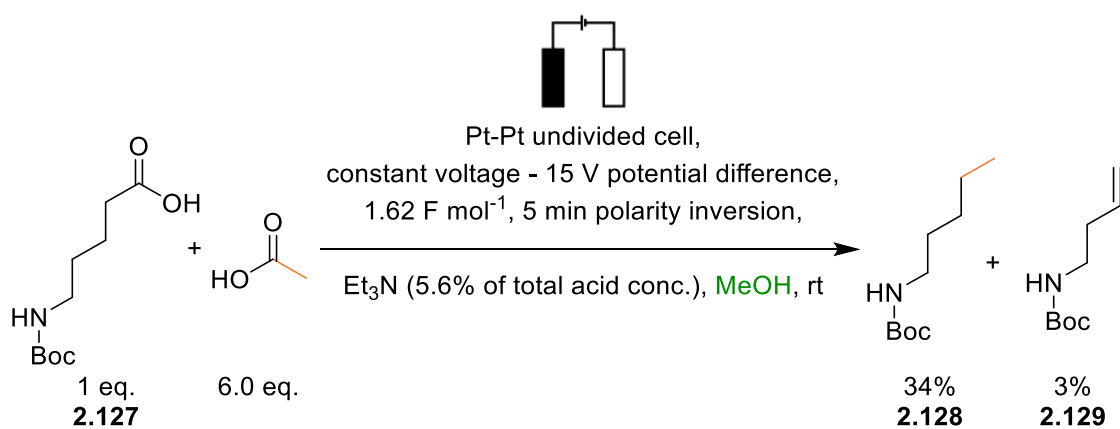
Scheme 2.44. Kolbe electrochemical hetero-coupling of **2.121** and acetic acid performed by S. Berrell.¹¹⁸

Also comparable to the electrolysis of *N*-Boc γ -aminobutyric acid, S. Berrell carried out the electrolysis of piperidine derivative **2.124** and acetic acid (Scheme 2.45).¹¹⁸ Hetero-coupled product **2.125** was isolated in a 12% yield, with non-Kolbe products generated at an 8% yield for alkene **2.112** and a 17% yield for methyl ether **2.126**.¹¹⁸ Thus, increased yields of non-Kolbe product were observed relative to the reaction shown in Scheme 2.44. This is thought to be because the resulting radical underwent more facile oxidation to the carbocation due to the lower ionisation potential (8.01 eV for a *iso*-butyl radical vs 7.55 eV for a secondary radical).¹³⁰ Because a symmetrical intermediate carbocation could be formed *via* oxidation of the radical intermediate, elimination of either β -proton would result in alkene **2.112** (Scheme 2.45). The origin of the second non-Kolbe product is attributed to a ring opening, comparable to that assumed to occur in Scheme 2.44. This generated a carbocation α to nitrogen which is subsequently methoxylated to give methyl ether **2.126**. A higher selectivity for the ring opening product methyl ether **2.126** over the deprotonation alkene product **2.112** is again attributed to the concentration of the base and stability of the intermediate carbocation formed α to nitrogen.

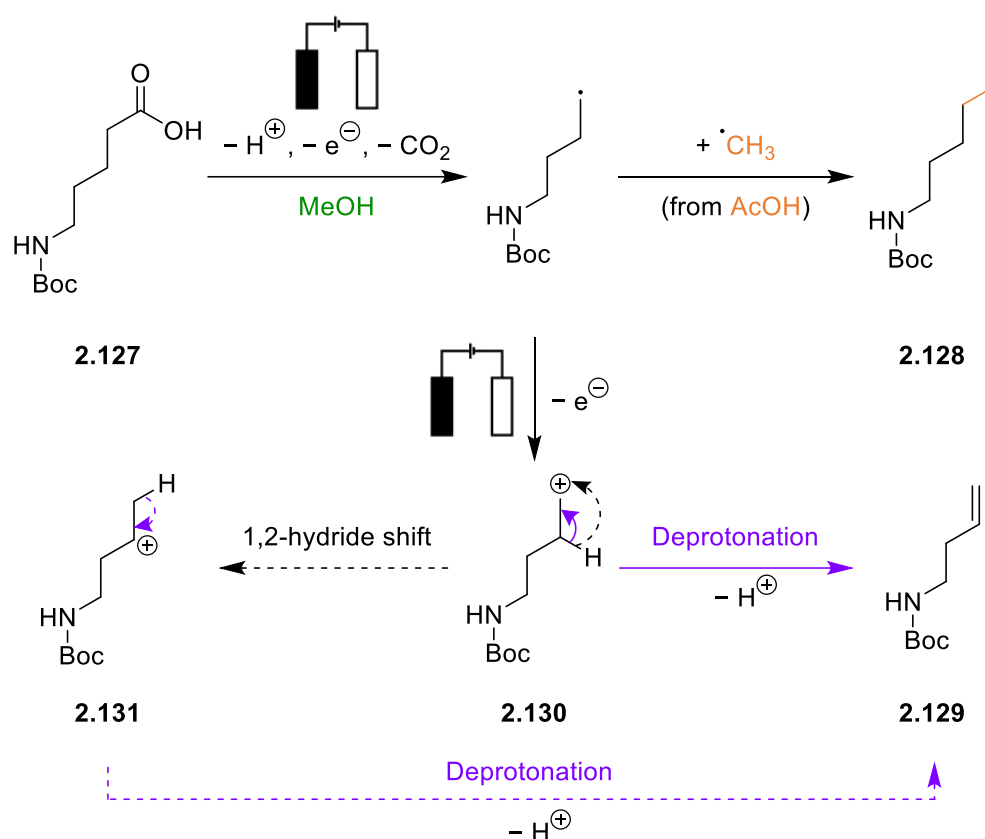
Scheme 2.45. Kolbe electrochemical hetero-coupling of **2.124** and acetic acid performed S. Berrell.¹¹⁸

2.2.2.4 Electrochemical Oxidation of δ -Amino Carboxylates

It was theorised that extending the alkyl chain of the linear acid starting material by one more carbon to *N*-Boc 5-aminopentanoic acid **2.127** should result in Kolbe electrolysis which generates a radical with such a high ionisation potential (above 8 eV) that it will be stable with respect to further oxidation, ensuring very little carbocation formation and minimal yields of associated non-Kolbe products. In practise, this was found to be true, the Kolbe product **2.128** was isolated in a moderate 34% yield, with only a 3% yield for non-Kolbe product **2.129**; this is equivalent to a very high Kolbe:non-Kolbe product ratio of 11.3:1.0 (Scheme 2.46). Similar yields of Kolbe product, 23-38%, were also observed by Linstead *et al.* in the homo-coupling of protected aminohexanoic acids.⁸⁵ In both cases, the overall recovery of products means that starting material must be consumed in other pathways, such as passivation.

Scheme 2.46 Kolbe electrolysis of *N*-Boc 5-aminopentanoic acid with acetic acid using General Procedure 2B.

The non-Kolbe product in Scheme 2.47, alkene **2.129**, could be derived from deprotonation of a proton β to carbocation **2.130**. Alternatively, a more stabilised secondary carbocation **2.131** could have been generated from a 1,2-hydride shift on the same intermediate, and subsequent deprotonation of a proton on the least hindered CH_3 group would then result in the same alkene **2.129**. 1,3- and 1,4-hydride shifts would also have been possible rearrangements. The 1,4-hydride shift would have resulted in a more stabilised α -amino carbocation, however it was probably not observed as the energy barrier is relatively high ($7.5 \text{ kcal mol}^{-1}$), compared to $3.9 \text{ kcal mol}^{-1}$ and $4.2 \text{ kcal mol}^{-1}$ for the 1,2- and 1,3-hydride shifts, respectively.¹³⁷



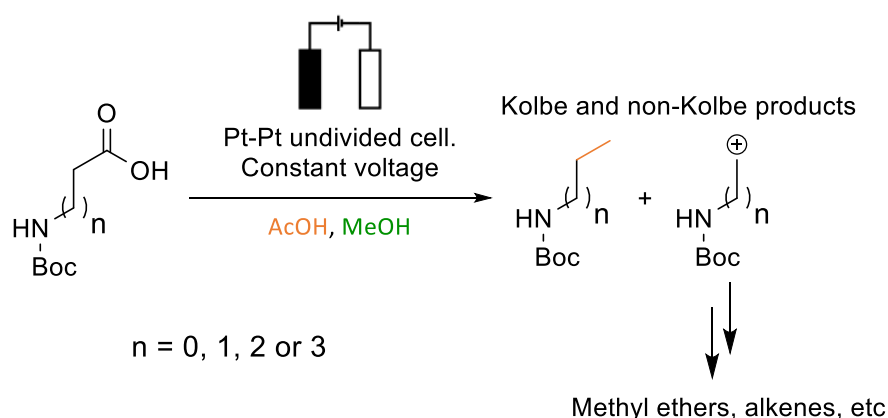
Scheme 2.47 Proposed mechanism for Kolbe electrolysis of *N*-Boc 5-aminopentanoic acid with acetic acid.

Notably, non-Kolbe products derived from solvolysis were not observed in the electrolysis of *N*-Boc 5-aminopentanoic acid reaction (Scheme 2.46). This implies a sufficient layer of carboxylates formed at the electrode surface, blocking methanol reaction with the carbocation.⁸⁴ Furthermore, fragmentation did not occur, presumably because cleaving the

bond β to the carbocation would not have resulted in a significantly more stabilised carbocation.

2.2.2.5 Summary of the Electrochemical Oxidation of Varying Chain Length Amino Acids

For the series of linear *N*-Boc amino acids from glycine to 5-aminopentanoic acid, increasing the chain length generally decreased the amount of non-Kolbe side products formed, consequently increasing the Kolbe:non-Kolbe product ratio (Scheme 2.48, Table 2.11). However, the electrolysis of all the amino acids studied resulted in some degree of non-Kolbe product formation. This is attributed to the fact that the ionisation potentials for the radicals were not significantly higher than 8 eV.⁸⁶



Scheme 2.48 General scheme for the study into Kolbe electrolysis of various length *N*-Boc protected amino acids.

Table 2.11 Table showing Kolbe product yields, total non-Kolbe product yields and the ratios of Kolbe:non-Kolbe product for *N*-Boc amino acids

n	Kolbe product yield / %	Total non-Kolbe product yield / %	Ratio Kolbe:non-Kolbe
1	-	82	0.00:1.00
2	53	25	2.12:1.00
3	39	30	1.30:1.00
4	34	3	11.3:1.00

The nature of the carbocation derived non-Kolbe side products changed with increasing chain length. Carbocations which could undergo facile rearrangements to form stabilised

carbocations α to nitrogen typically resulted in solvolysis products due to the lack of β -protons. Longer chain amino acids that formed carbocations tended to either fragment, forming more stabilised carbocations near nitrogen, which then reacted to form solvolysis products. Alkene products were observed as the only carbocation derived non-Kolbe products when stabilised carbocations could not be formed easily by classical carbocation rearrangements.

Overall, it appeared that the stability of the carbocations dictated the product formed. Stabilised carbocations gave solvolysis products whilst unstabilised carbocations yielded elimination products. This could be because the stabilised carbocations were able to diffuse away from the electrode surface into the bulk solution to react with methanol, whilst the unstabilised carbocation underwent rapid deprotonation at the electrode surface.

Next, the effect of reaction conditions was assessed to try and change the selectivity between the Kolbe and non-Kolbe product. Since the electrolysis of *N*-Boc β -alanine resulted in good yields of the Kolbe product and only one non-Kolbe product, this was selected as the reaction to study in more detail. Initially, reaction monitoring was used to probe the formation of products and consumption of starting material. Then, Kolbe electrolysis was subject to various changes to the conditions to determine the effect on the outcome and Kolbe:non-Kolbe product ratio.

2.2.3 Monitoring Kolbe Electrolysis by ^1H NMR Spectroscopy

Having established the electrolysis of *N*-Boc β -alanine as an appropriate reaction to study in-depth, a method of reaction monitoring and quantification was developed with the initial aim of understanding the relative Kolbe and non-Kolbe product formation. The Kolbe and non-Kolbe products could be formed at different stages of the reaction, and therefore it is possible that the selectivity may change during the course of the reaction. This information about how the reaction develops over time could then be used to identify possible methods of improving the selectivity of the reaction in favour of the Kolbe product.

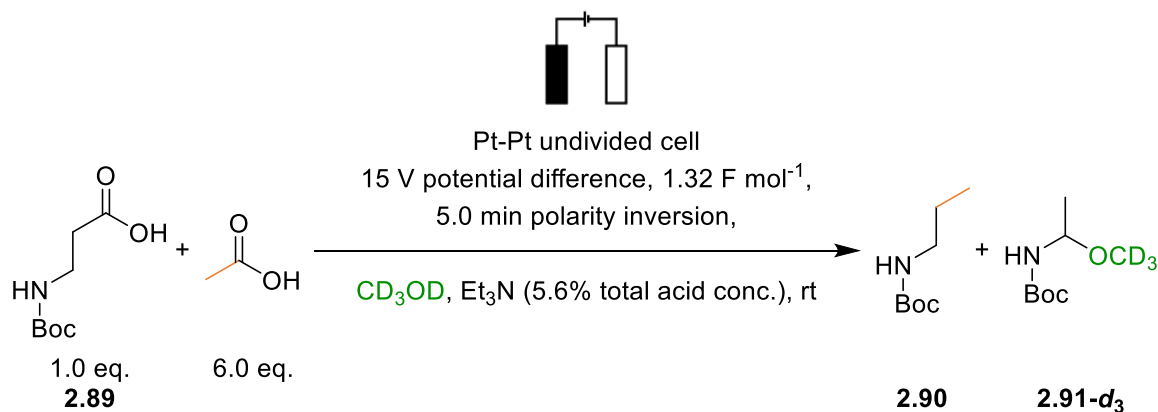
2.2.3.1 Developing a Method of Monitoring the Progress of Kolbe Electrolysis

First, the electrolysis of *N*-Boc β -alanine **2.89** and acetic acid was performed in the 9 mL cell for a total of 90 minutes (equivalent to $1.32 \text{ F (mol of the total acid concentration)}^{-1}$), with the platinised titanium electrodes and deuterated methanol (9 mL) as the solvent

(General Procedure 2B, Scheme 2.49). These reaction conditions were chosen so that any possible consumption of triethylamine base could be observed. Aliquots of the reaction mixture were taken every 10 minutes and analysed by ^1H NMR spectroscopy with mesitylene as an external standard (see Experimental General Procedure 2C).

Figure 2.6 shows sections of the aryl and alkyl regions of the resultant ^1H NMR spectra. Both products (**2.90** and **2.91-*d*₃**) and reagents (*N*-Boc β -alanine, acetic acid and triethylamine) had distinct signals in the crude ^1H NMR spectrum that could be reliably integrated, with little evidence of any other side products. The 3H singlet of the methoxylated non-Kolbe product **2.91**, usually observed at δ_{H} 3.31 ppm, was not visible in the crude ^1H NMR spectrum because it was derived from addition of deuterated methanol, therefore the methyl group of the ether was deuterated (**2.91-*d*₃**).

Once the carboxylic acids had been consumed in the reaction and the pH of the solution became basic, the triplet signal from unprotonated triethylamine overlapped with the doublet from the methoxylated product **2.91-*d*₃**. Therefore, benzoic acid (50 μL , 0.57 M in deuterated methanol) was added to the NMR samples prior to recording the ^1H NMR spectrum to keep the crude mixture acidic and the peaks separate.



Scheme 2.49 Kolbe electrochemical hetero-coupling of *N*-Boc β -alanine and acetic acid in deuterated methanol.

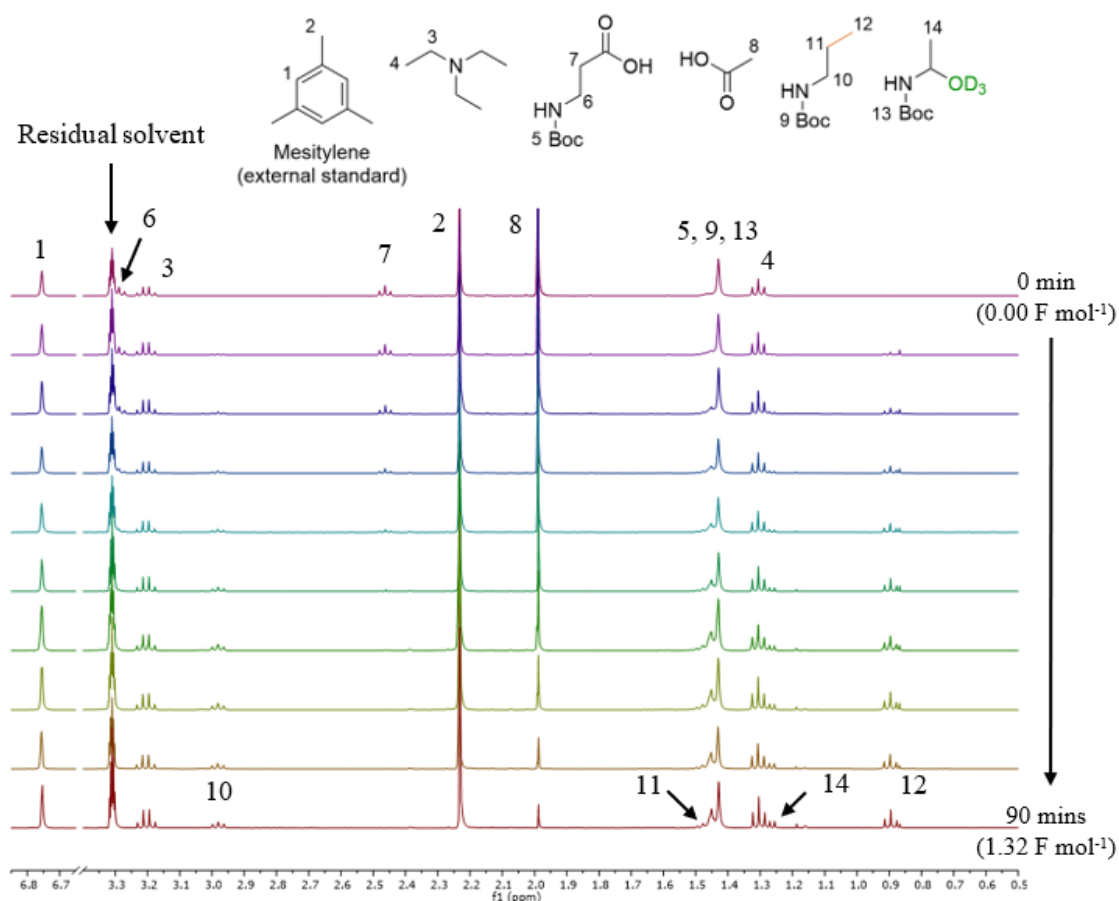


Figure 2.6 Stacked ^1H NMR spectra showing the formation of Kolbe product **2.90** and non-Kolbe product **2.91- d_3** , recorded every 10 minutes during Kolbe electrolysis of *N*-Boc β -alanine **2.89** and acetic acid

The percentage starting material and yields of products, determined by reference to the integral of the external standard (mesitylene), were then quantified from each ^1H NMR spectrum and plotted against time, along with the equivalents of charge passed in F mol^{-1} (Figure 2.7). More Kolbe product **2.90** (Figure 2.7, purple triangles) had formed at each interval compared to non-Kolbe methoxylated product (Figure 2.7, green diamonds). This is attributed to the fact that β -amino radicals generated at the electrode surface preferentially couple to methyl radicals, derived from acetic acid, as opposed to undergoing a second electron oxidation, leading to the non-Kolbe product.

At the end of the reaction, once *N*-Boc β -alanine **2.89** was consumed, the formation of both products **2.90** and **2.91- d_3** plateaued. The amount of triethylamine (and ultimately protonated triethylamine, $\text{Et}_3\text{N}^+\text{H}$) remained constant throughout the reaction indicating that acetic acid is preferentially oxidised at the anode. After 90 minutes, according to the ^1H NMR

spectroscopy analysis the yield for the Kolbe product **2.90** was 62% and the yield for the non-Kolbe product **2.91-d₃** was 30% (Table 2.12, entry 1). This is in agreement with experiments described above (see Table 2.10) and the isolated yields in Section 2.2.2.2, Scheme 2.37.

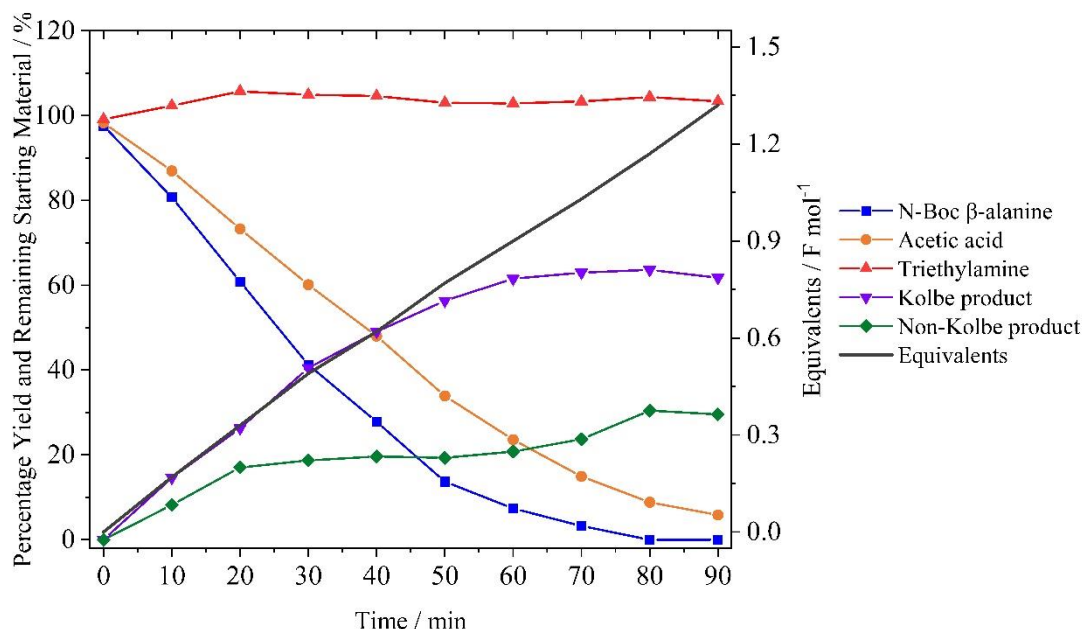


Figure 2.7 Plot of Kolbe product **2.90** and non-Kolbe product **2.91-d₃** yields and starting material remaining as quantified by ¹H NMR spectroscopy using mesitylene and an external standard. Also plotted is the equivalents of charge in F mol⁻¹

2.2.3.2 Monitoring Kolbe Electrolysis and the Effect of Changing the Conditions

Next, small changes were made to the reaction conditions to determine the effect on the progress of the reaction. The reaction was monitored using General Procedure 2A. After 90 minutes, the yields for the Kolbe and non-Kolbe products **2.90** and **2.91-d₃** were 60% and 28%, respectively (Table 2.12, entry 2), and therefore comparable to General Procedure 2B. As with General Procedure 2B, more Kolbe product was formed compared to non-Kolbe product **2.91-d₃** at each time interval and both products started to form from the start of the reaction. As the base was potassium hydroxide, it could not be monitored by ¹H NMR spectroscopy (Figure 2.8, graph B).

In an attempt to increase the current density, and thus increase the radical concentration at the electrode surface, the applied potential difference was raised from 15 V to 30 V (all other experimental conditions as in General Procedure 2B) and the reaction was monitored (Table 2.12, entry 3). Due to the associated increase in current, the reaction time was shortened to

45 minutes, by which point 1.24 F mol⁻¹ had been passed, and aliquots were taken every 5 minutes (Figure 2.8, graph C). The increase in applied potential did not impact how the starting material was consumed, the products were formed or the selectivity of the reaction, as a 59% yield for **2.90** and 27% yield for **2.91-d₃** was achieved (Table 2.12, entry 3).

Finally, using General Procedure 2B, the water bath was removed from the reaction, and the reaction mixture was allowed to heat up from solvent resistance, which resulted in a final temperature of 50 °C. Aliquots were taken every 10 minutes and the results are given in Figure 2.8, graph D. The graph shows that more of each product (**2.90** and **2.91-d₃**) was formed and after 50 minutes, nearly all the *N*-Boc β-alanine had been consumed and the formation of Kolbe product **2.90** and non-Kolbe product **2.91-d₃** had plateaued. After this time, triethylamine was then oxidised at the anode (Figure 2.8, graph D, red triangle). At the end of the 90 minutes, the yield for the Kolbe product **2.90** was 72% and the yield for the non-Kolbe product **2.91-d₃** was 31% by quantitative ¹H NMR spectroscopy. This equates to a physically impossible total yield of greater than 100%. This error is attributed to solvent evaporation at the higher reaction temperature.

Table 2.12 Yields of Kolbe product **2.90** and non-Kolbe product **2.91-d₃** after 90 or 45 minutes in the electrolysis of *N*-Boc β-alanine and acetic acid, quantified with ¹H NMR spectroscopy using mesitylene as an external standard

Entry	Graph in Figure 2.8	Conditions	Equivalents of Charge / F mol ⁻¹	Yield of Kolbe Product (2.90) / % ^a	Yield of non-Kolbe Product (2.91-d₃) / % ^a
1	A	General Procedure 2B	1.32	62	30
2	B	General Procedure 2A	1.16	60	28
3	C	General Procedure 2B, 30 V potential difference	1.24	59	27
4	D	General Procedure 2B, no water bath	1.49	72	31

^a Determined by quantitative ¹H NMR spectroscopy using mesitylene as an external standard

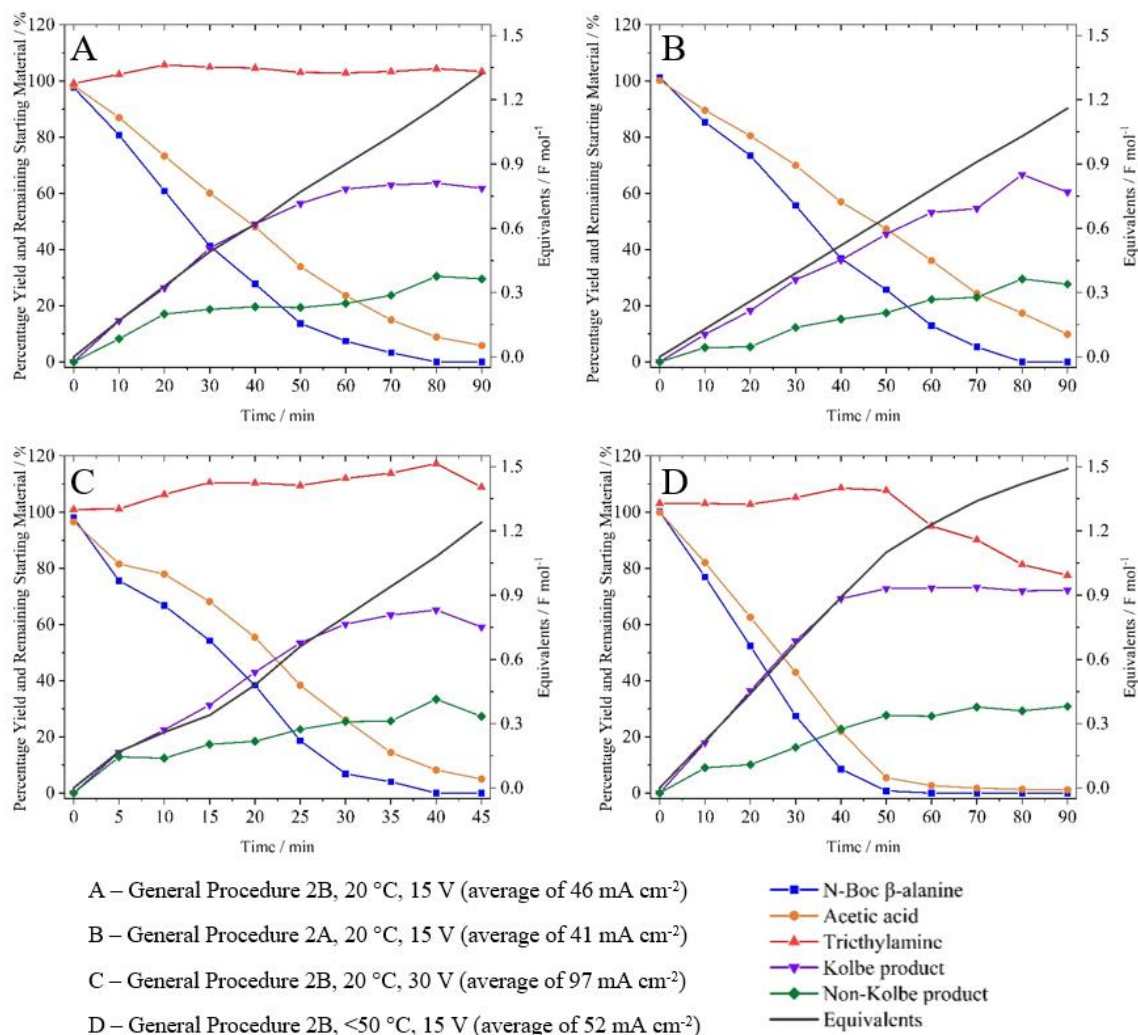


Figure 2.8 Plots of reagent and product time-traces as quantified by ¹H NMR spectroscopy using mesitylene as an external standard from reactions carried out under various electrolysis conditions, as summarised in Table 2.12. Also plotted is the equivalents of charge in F mol⁻¹

The current density and voltage vs time plots for the high temperature experiment indicate that once the starting material is consumed and triethylamine oxidation commences there is a drop in the current/current density (Figure 2.9). This indicates that the oxidation of the base is a less facile reaction. Alternately, poor mass transport could result reduced oxidation and reduced current once the anions at the electrode surface have been consumed (more quickly) or when the concentration of carboxylate is lower at the surface. However, the graph in Figure 2.8, D showing the consumption of carboxylate after 40 minutes favours the former argument (overall consumption of carboxylate).

In Figure 2.9, the small spikes upwards (increased current density) on the current trace every 5 minutes are associated with charging at the electrode surface on polarity inversion. The

larger spikes in the current trace every 10 minutes (decreased current density), which coincide with spikes in the voltage trace e.g. 70 minutes, are due to turning to power supply off to take an aliquot of the reaction mixture.

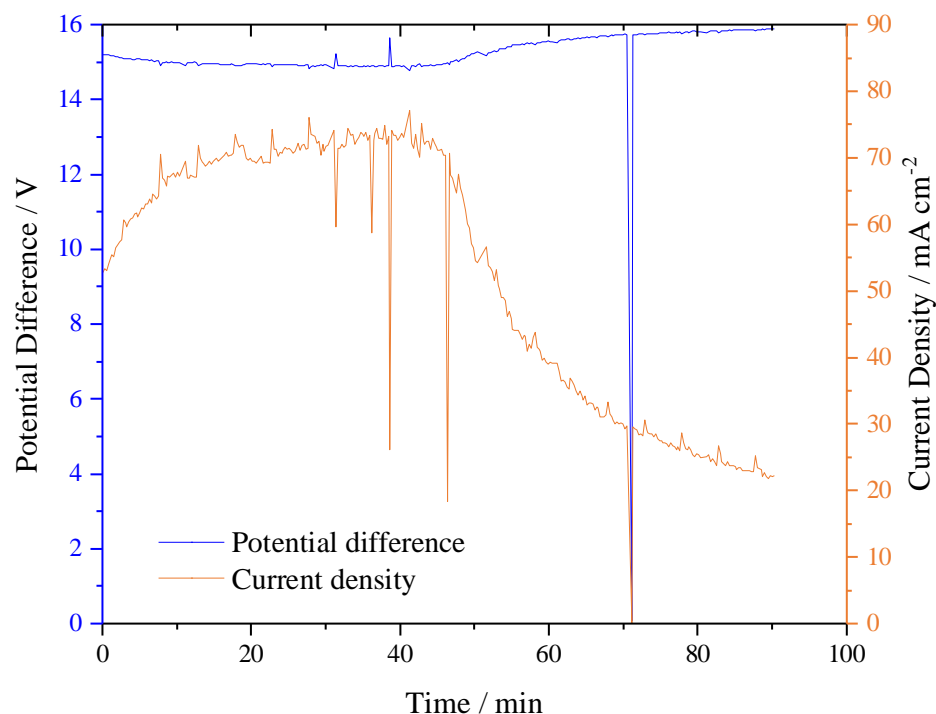


Figure 2.9 Recorded potential difference and current density plotted against time for the electrolysis of *N*-Boc β -alanine and acetic acid with no water bath (uncontrolled temperature)

Overall, the results of monitoring Kolbe electrolysis showed that both the Kolbe product and non-Kolbe products were formed simultaneously and so the selectivity cannot be tuned by changing the reaction time. Under conditions that favour the Kolbe pathway (platinum electrodes, high current density etc.), radical coupling preferentially occurred over further oxidation of alkyl radicals and so more Kolbe product was observed at the end of the reaction. For the electrolysis of *N*-Boc β -alanine with acetic acid, the average yield for the Kolbe product **2.90** was 63%, whilst the average yield for the non-Kolbe product **2.91-d₃** was 29% as determined by quantitative ^1H NMR spectroscopy. The overall recovery for the reaction was high, typically ca. 90%, meaning most of the starting acid formed either the Kolbe or non-Kolbe product.

As shown previously, both reaction General Procedures 2A and 2B performed equally well. Although it did not change the reaction selectivity, increasing the applied potential difference from 15 V to 30 V reduced the reaction time by increasing the current density and the concomitant rate of product formation. To avoid solvent losses leading to yields of over

100%, which could not be possible, a water bath will be used to maintain room temperature reactions.

2.2.4 Further Optimising Conditions for Kolbe Electrolysis

In the literature, the impact of the Kolbe electrolysis reaction conditions has been studied using simple alkyl or aryl carboxylates starting materials which lack functionality, carboxylates with distal functional groups, or carboxylates with α -substituents which either stabilise the radical or lower the ionisation potential, making the radicals more prone to over-oxidation.^{84,87} To complement this insight, the electrolysis of *N*-Boc β -alanine with acetic acid was probed to gain new understanding into the selectivity of the Kolbe reaction. Unless stated otherwise, reactions were performed with the platinum wire electrodes and in the 2 mL electrochemical cell. Gas chromatography (GC) was used to quantify Kolbe product **2.90** and non-Kolbe product **2.91** in the crude reaction mixtures based on calibration curves of isolated products. By using gas chromatography rather than ¹H NMR spectroscopy, large quantities of deuterated solvents were avoided, and reaction mixtures did not have to be acidified prior to quantification. As GC was used to quantify reaction mixtures, General Procedure B was used (with triethylamine) so the reaction mixture could be directly analysed, because with General Procedure A, NaOH had to be removed prior to analysis. The temperature and reagent concentrations were controlled to ensure accurate and reproducible results. Some reactions have been performed multiple times, and average values for the yields are reported.

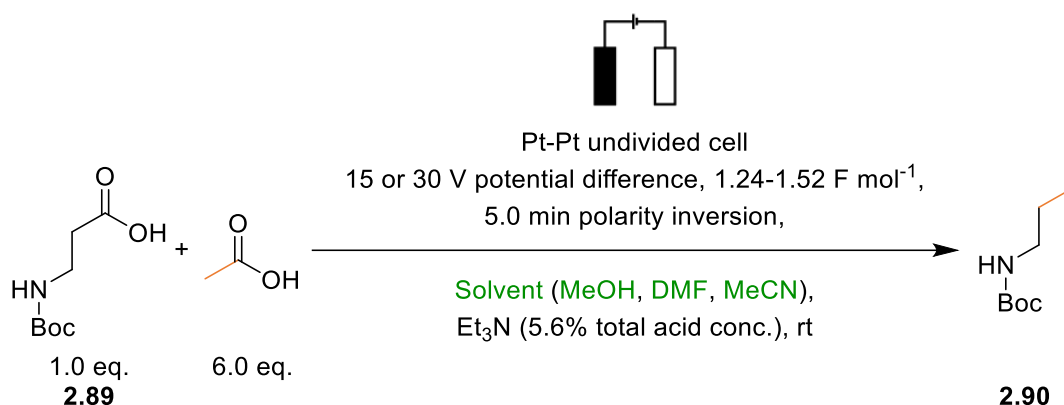
2.2.4.1 The Effect of Solvent on the Outcome of Kolbe Electrolysis

Methanol is by far the most common solvent for Kolbe electrolysis, because above the critical potential methanol oxidation is inhibited by the formation of a carboxylate layer at the platinum anode. Furthermore, methanol and the oxidation products of methanol are easily removed from the reaction *in vacuo*, which is particularly important when low boiling products are formed.⁹⁶ However, good yields of Kolbe products have also been reported with other alcohol solvents, such as ethanol or *iso*-propanol.⁸⁵ Despite their ability to stabilise carbocations, polar aprotic solvents such as dimethylformamide and acetonitrile have also been shown to give good yields of the Kolbe product.^{77,84,96,138,139}

The electrolysis of *N*-Boc β -alanine **2.89** and acetic acid was performed in both dimethylformamide and acetonitrile to determine the effect on the yield of the Kolbe product

(Scheme 2.50). Only the Kolbe product **2.90** was quantified during these reactions as the non-Kolbe product **2.91** was derived from addition of methanol, which was not added. The change in solvent resulted in a 46% and 21% yield for Kolbe hetero-coupled product **2.90** with dimethylformamide and acetonitrile, respectively (Table 2.13, entries 2 and 3).

One way the solvent could have affected the outcome of electrolysis was through a change in the pK_a value of the starting acid. Carboxylic acids have an approximate pK_a value of 5 in water, this shifts to 10, 13 and 22 in methanol, dimethylformamide and acetonitrile, respectively.^{140,141} This is because methanol, dimethylformamide and acetonitrile have lower dielectric constants than water and so are less good at stabilising the charged species formed.¹⁴² If less carboxylate is formed in acetonitrile and dimethylformamide than methanol, this would explain the decreased current densities which result in a lower radical concentration and correspondingly less hetero-coupled product **2.90**.



Scheme 2.50 Kolbe electrochemical hetero-coupling of *N*-Boc β -alanine and acetic acid with different solvents.

Table 2.13 Table showing the applied potential difference, average current densities and yield of Kolbe hetero-coupled product **2.90** determined by GC for the electrolysis of *N*-Boc β -alanine and acetic acid using various solvents

Entry	Solvent	Potential Difference / V	Average Current Density / mA cm ⁻²	Yield of Kolbe Product (2.90) / % ^a
1	MeOH	15	73	58
2	DMF ^b	30	17	46
3	MeCN	15	27	21

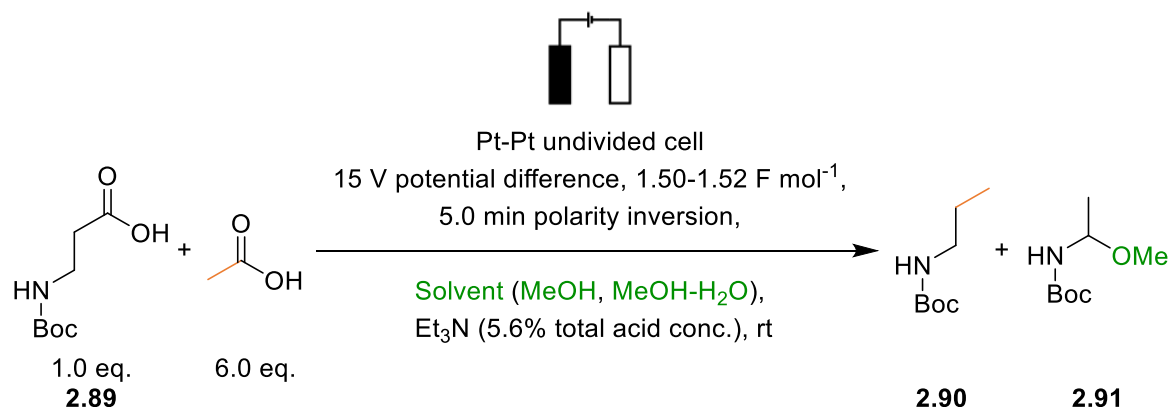
^a Reaction quantified with GC calibration curves ^b Performed on 9 mL scale, result is an average from two reactions.

Comparable yields for a different homo-coupled Kolbe product were achieved by Finkelstein and co-workers who used 40% neutralisation to achieve a 41% yield of 2,3-diphenylbutane from the homo-coupling of diphenylacetic acid in dimethylformamide.¹³⁹ They used increased neutralisation to favour carboxylate formation and try to drive to formation of a high radical concentration at the electrode surface and increase the ion transport in solution. Despite this only moderate yields of the product were formed.¹³⁹

When acetonitrile has been used as the Kolbe reaction solvent, usually a carboxylate salt is added as a starting material to favour the formation of a stabilised carboxylate mono-layer and compensate for the high pK_a value of alkyl carboxylates in acetonitrile.^{140,143} In the electrolysis of potassium butanoate in acetonitrile at platinum electrodes, only a 33% yield for the Kolbe product octane was observed by Muck and co-workers (Scheme 2.27, Table 2.7).⁸⁷

Kolbe electrolysis has been reported using methanol-water mixtures.¹⁴⁴ However, the addition of water has been shown to lower the yield of the Kolbe product, presumably by stabilising the formation of carbocation intermediates.⁹⁶ To explore this, the electrochemical oxidation of **2.89** with acetic acid was performed both with the addition of water (2.5% volume) and with dried methanol (Scheme 2.51). The results are summarised in Table 2.14.

With the methanol-water mixture, comparable yields of both the Kolbe and non-Kolbe product were achieved (Table 2.14, entry 2), showing that a small amount of additional water in the reaction made no appreciable difference and implying that water does not disrupt carboxylate binding to the electrode surface. Dry methanol also gave a similar yield for the Kolbe product, but the non-Kolbe product yield fell slightly from 27% to 19% (Table 2.14, entry 3). This could imply that water will compete with methanol to act as the nucleophile, the Hofer-Moest reaction, which couples to the carbocation. Since the yield of Kolbe product was not affected by small changes to the amount of water, methanol was used for future reactions without further drying.



Scheme 2.51 Kolbe electrochemical hetero-coupling of *N*-Boc β -alanine with methanol and methanol water mixtures.

Table 2.14 Table showing the yield of Kolbe hetero-coupled product **2.90**, non-Kolbe product **2.91** and Kolbe:non-Kolbe product ratio determined by GC for the electrolysis of *N*-Boc β -alanine and acetic acid using methanol, dried methanol and methanol with water

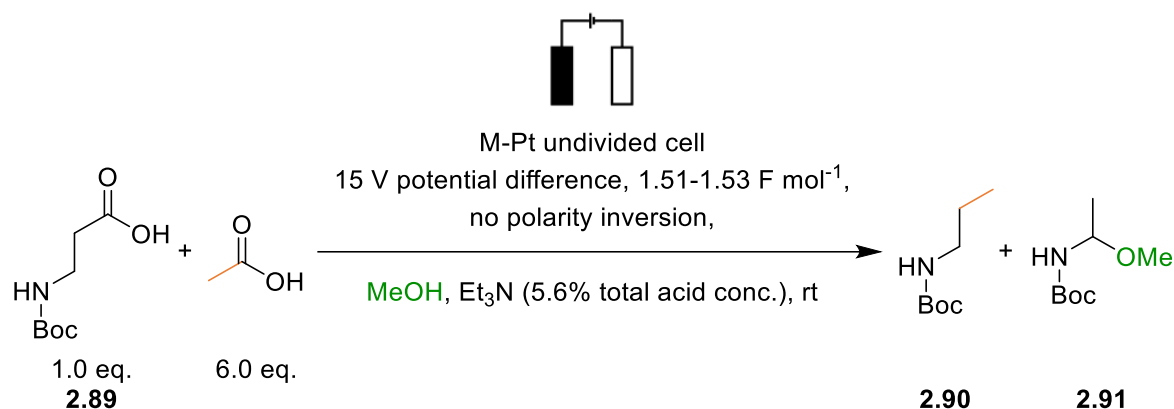
Entry	Solvent	Yield of Kolbe Product (2.90) / % ^a	Yield of non-Kolbe Product (2.91) / % ^a	Ratio Kolbe:non-Kolbe
1	MeOH	58	27	2.15:1.00
2	MeOH-H ₂ O (2.5%)	55	27	2.04:1.00
3	Dry MeOH	54	19	2.84:1.00

^a Reaction quantified with GC calibration curves

2.2.4.2 The Effect of Electrode Material on the Outcome of Kolbe Electrolysis

As described in the Chapter Introduction (Section 2.1.4.1), the anode material is critical to the outcome of Kolbe electrolysis.¹⁴⁵ Platinum, gold and palladium have all previously been used to study carboxylate double layer formation and adsorbed intermediates in Kolbe electrolysis using acetic acid.^{88,114,146} Therefore, the platinum wire electrode set-up was modified to accommodate gold and palladium anodes. Carbon was not used as the anode material as it is well documented that the non-Kolbe product will form preferentially at some carbon surfaces, and it was not possible to include carbon as the anode material in the developed cell.⁸⁷ Platinum was used as the cathode material as it is efficient at facilitating hydrogen reduction. As a result of using a different anode and cathode, the polarity of the electrodes was not inverted during electrolysis.

In the electrolysis of *N*-Boc β -alanine **2.89** with acetic acid (Scheme 2.52), when gold was used as the anode a 41% yield of the hetero-coupled product **2.90** was achieved and a 51% yield of the methoxylated product **2.91** was also observed (Table 2.15, entry 2). When palladium was used, only a 19% yield of the hetero-coupled product **2.90** was achieved and a 29% yield of the methoxylated product **2.91** (Table 2.15, entry 3). At the end of the reaction using the palladium anode 50% of the starting material remained. Taken together, this means that alkyl radicals can still be generated *via* oxidative decarboxylation of *N*-Boc β -alanine at both gold and palladium electrodes, as well as platinum. With gold and palladium anodes, a lower Kolbe:non-Kolbe product ratios, 0.80:1.00 and 0.66:1.00, respectively, indicates the second electron oxidation is favoured over radical coupling.



Scheme 2.52 Influence of different anode materials on the Kolbe electrochemical hetero-coupling of *N*-Boc β -alanine and acetic acid.

Table 2.15 Table showing average current densities, the yield of Kolbe hetero-coupled product **2.90**, non-Kolbe product **2.01** and Kolbe:non-Kolbe product ratio determined by GC for the electrolysis of *N*-Boc β -alanine and acetic acid using various anode materials; platinum, gold and palladium

Entry	Anode Material (M)	Average Current Density / mA cm ⁻²	Yield of Kolbe Product (2.90) / %	Yield of non-Kolbe Product (2.91) / %	Ratio Kolbe:non-Kolbe
1	Pt ^a	73	58 ^b	27 ^b	2.15:1.00
2	Au	45	41 ^c	51 ^c	0.80:1.00
3	Pd	59	19 ^c	29 ^c	0.66:1.00

^a Polarity inverted ^b Reaction quantified with GC calibration curves ^c Reaction quantified with ¹H NMR spectroscopy using mesitylene as an external standard

The results with *N*-Boc β -alanine are consistent with those reported for the electrolysis of acetic acid in methanol when it was shown that both platinum and gold gave reasonable yields for the Kolbe product, ethane (98% and 88% current efficiencies respectively), whilst reduced yields of ethane were observed with a palladium anode (45% current efficiency). The authors reasoned that the decreased yield of the Kolbe product with palladium was due to preferential methanol oxidation at the anode. Evidence included increased levels of formaldehyde, from methanol oxidation, detected by GC. Compared to platinum, increased levels of formaldehyde production, were also detected with the gold anode, particular at lower applied potentials. When glacial acetic acid was used as the solvent, all three anode materials performed equally well (98%, 95% and 95% current efficiencies for Pt, Au and Pd respectively).¹⁴⁷ Furthermore, a separate study has shown that methanol oxidation at a palladium anode has a lower onset potential than at platinum (-0.52 V vs SCE and -0.62 V vs SCE respectively), therefore oxidation of methanol is more thermodynamically favourable at palladium.¹⁴⁸ The preferential oxidation of methanol at palladium would account for the high starting material recovery (50%) in the electrolysis of *N*-Boc β -alanine and acetic acid.

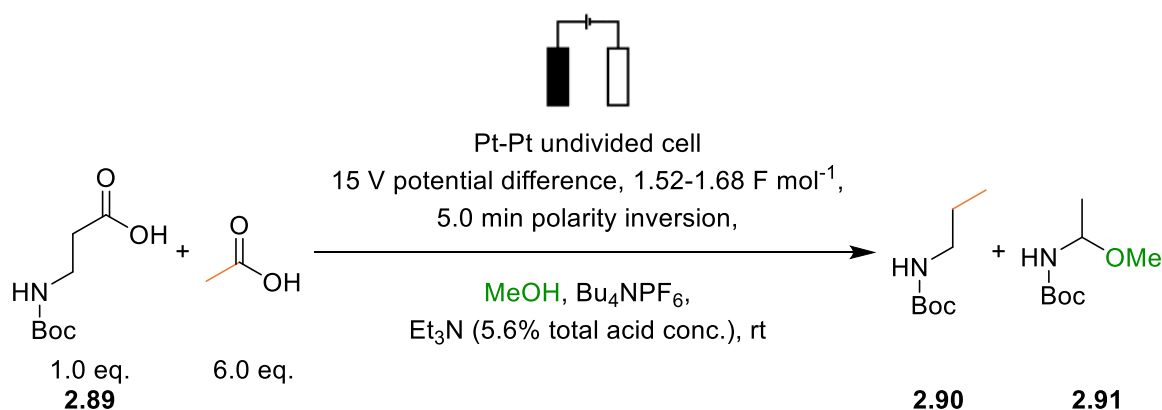
2.2.4.3 The Effect of Changing Current Density on the Outcome of Kolbe Electrolysis

In the literature, an increase in current density has been shown to improve the yield of the radical derived Kolbe product in electrolysis, presumably due to a greater radical concentration at the electrode surface. Typically, current densities of greater than 200 mA cm^{-2} have shown high selectivity for the Kolbe product over carbocation derived non-Kolbe side products.⁸⁴ One method of increasing current density is by adding supporting electrolyte, which decreases the solution resistance by increasing the number of charged species in solution. However, it has been reported that foreign anions tend to result in reduced Kolbe product yields by disrupting the carboxylate layer at the electrode surface and lowering the surface radical concentration.⁹¹ To observe the effect of supporting electrolyte on the outcome of the electrolysis of *N*-Boc β -alanine and acetic acid, tetrabutylammonium hexafluorophosphate (Bu_4NPF_6) was added (Scheme 2.53). Bu_4NPF_6 was chosen as the supporting electrolyte as it is commonly used in organic electrochemistry and shows high solubility in polar solvents.⁵² Furthermore, the cationic component was an ammonium ion, therefore not dissimilar to the base used in the reaction (triethylamine). The supporting electrolyte is typically used in excess of the electroactive reagents and so both 0.67 M and

1.33 M supporting electrolyte in methanol concentrations were tested. The results are presented in Table 2.16.

Despite significantly increasing the current density (to greater than 300 mA cm^{-2}), the addition of supporting electrolyte caused a total drop in the production of Kolbe hetero-coupled product **2.90**. Non-Kolbe product **2.91** was observed in a 24% yield when 0.67 M tetrabutylammonium hexafluorophosphate was used, however, only trace amounts were detected when the supporting electrolyte concentration was increased to 1.33 M. In addition, substantial amounts of the *N*-Boc β -alanine starting material remained unreacted in the crude GC trace of experiments that included supporting electrolyte.

These results are interpreted as showing that with 1.0 eq. (total acid concentration) of supporting electrolyte, some carboxylate was able to reach the electrode surface and undergo decarboxylation to form an alkyl radical. However, as hexafluorophosphate anions were also present at the electrode surface, disrupting the carboxylate layer, radicals did not readily couple and instead underwent a second electron oxidation to carbocations which were repelled from the anode, into the bulk and formed non-Kolbe product **2.91**. Furthermore, with a competing anion at the electrode surface, not all carboxylate was oxidised during the reaction and so some starting material was left in the crude mixture. With 2.0 eq. (total acid concentration) of supporting electrolyte, the zero percent yield for both the Kolbe and non-Kolbe product is attributed to even more substantial suppression of carboxylate layer formation at the anode.



Scheme 2.53 Influence of supporting electrolyte on Kolbe electrochemical hetero-coupling of *N*-Boc β -alanine with acetic acid.

Table 2.16 Table showing the average current densities and yield of Kolbe hetero-coupled product **2.90**, non-Kolbe product **2.91** and remaining starting material **2.89** determined by GC for the electrolysis of *N*-Boc β -alanine and acetic acid in methanol using tetrabutylammonium hexafluorophosphate (Bu_4NPF_6) as supporting electrolyte

Entry	Supporting Electrolyte Concentration / M	Average Current Density / mA cm^{-2}	Yield of Kolbe Product (2.90) / % ^a	Yield of non-Kolbe Product (2.91) / % ^a	Remaining Starting Material (2.89) / % ^a
1	None	73	58	27	0
2	0.67	379	0	24	44
3	1.33	343	0	Trace (0.1%)	30

^a Reaction quantified with GC calibration curves

The results in Table 2.16 were consistent with those reported in the literature for the electrochemical homo-coupling of phenyl acetic acid with sodium perchlorate (NaClO_4), Scheme 2.10, Table 2.4.⁹⁸ The addition of the supporting electrolyte promoted the non-Kolbe pathway over radical coupling, although in the work by Coleman and co-workers a complete drop off in both the Kolbe and non-Kolbe products was not observed.⁹⁸ This could be because a lower relative concentration of supporting electrolyte was added (less than 0.64 eq.).

Next, attempts were made to increase the current density by reducing the surface area of the anode and cathode from 0.84 cm^2 to 0.29 cm^2 (Scheme 2.54). At an applied potential difference of 15 V, this resulted in an increased average current density of 134 mA cm^{-2} (Table 2.17, entry 2), and an increased reaction time of 83 minutes, compared to 53 minutes with the 0.84 cm^2 wire electrodes (Table 2.17, entry 1). Whilst the yield of Kolbe product **2.90** was comparable, there was a slight lowering of the yield of non-Kolbe product **2.91**, which resulted in an increased Kolbe:non-Kolbe product ratio.

Next, the applied potential difference was raised from 15 V to 30 V. At a fixed solution resistance, for example the same concentration of carboxylate, base and solvent, an increase in voltage would lead to an increase in the current according to Ohm's law (Equation 2.4). Both the larger and smaller surface area platinum wire electrodes were used and increased average current densities of 171 mA cm^{-2} and 331 mA cm^{-2} (Table 2.17, entries 3 and 4) were achieved, corresponding to a 2.3- and a 2.5-fold current density increase, respectively.

The increase in current density did not lead to an increase in the yield of the Kolbe product **2.90**, as a slightly lower yields were observed with both sets of electrodes.

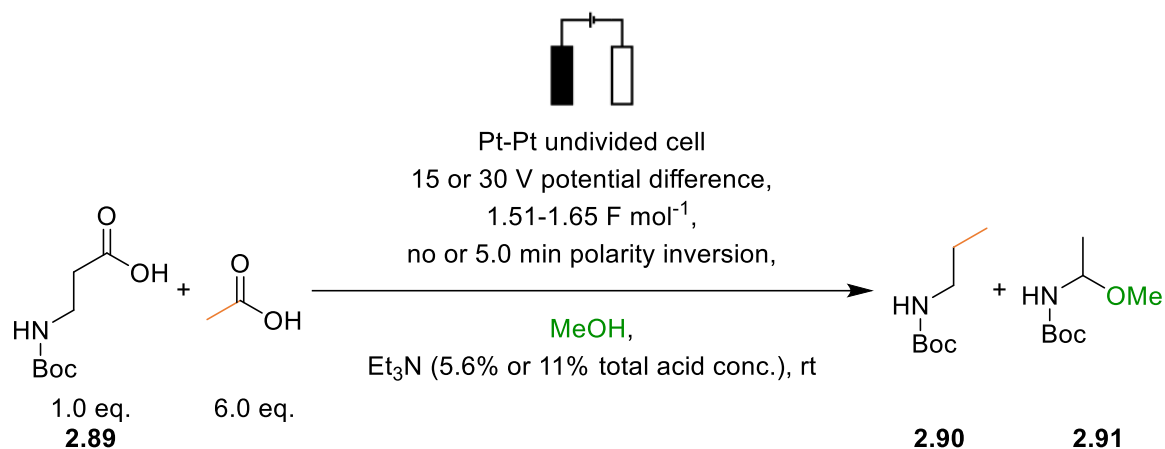
In both reactions using the reduced surface area electrodes, Table 2.17, entries 2 and 4, lower yield of non-Kolbe product were achieved compared to the larger surface area electrodes. The decrease in non-Kolbe product yield may be due to the formation of a more uniform carboxylate monolayer as there was less electrode surface area to cover, which in-turn would disfavour the carbocation pathway in favour of radical coupling. Additionally, the higher current density would favour a higher radical concentration in the vicinity of the electrode which would also favour radical coupling. However, the yield of the Kolbe product **2.90** did not increase accordingly.

It was theorised that with the smaller surface area electrodes the cathodic process, hydrogen reduction, might limit the current. Therefore, a set of electrodes were made that had an anode surface area of 0.28 cm² but a cathode surface area of 0.84 cm². Again, a 30 V potential difference was applied but because the anode and cathode surface areas were different, polarity inversion was not used in this reaction. The increased cathode area did not increase the average current density, and a slow decrease in the current density, attributed to electrode passivation, is thought to have contributed to the lower yields of the Kolbe and non-Kolbe products (Table 2.17, entry 5).

The degree of neutralisation typically used for Kolbe electrolysis is between 5-10%.⁵⁸ Therefore an *N*-Boc β-alanine and acetic acid electrolysis experiment was conducted using base at 11% of the total acid concentration to investigate the impact of doubling the concentration of the carboxylate anions.⁹⁷ When the larger platinum wire electrodes (surface area 0.84 cm²) were used with a 15 V potential difference, the average current density was increased to 124 mA cm⁻² but the yield of the Kolbe product was only 48% (Table 2.17, entry 6). Whilst the overall recovery of products was slightly lower, the Kolbe:non-Kolbe product ratio was comparable to when 5.6% base was used (Table 2.17, entry 1), which suggests that although increasing the amount of base can be used to speed up the reaction time, it does not significantly impact on the selectivity of the radical coupling reaction.

Finally, to generate the maximum average current density the smaller surface area platinum wire electrodes (0.29 cm²) were used with an applied potential difference of 30 V and 11% neutralisation (Table 2.17, entry 7). This resulted in an average current density of 409 mA cm⁻², however a yield of only 43% of Kolbe product **2.90** was achieved. The

Kolbe:non:Kolbe product ratio was comparable to the standard reaction conditions (Table 2.17, entry 1).



Scheme 2.54 Influence of applied potential and base concentration on the Kolbe electrochemical hetero-coupling of *N*-Boc β -alanine and acetic acid.

Table 2.17 Table showing the applied potential difference, degree of neutralisation (*N*), anode surface area, average current density and the yield of Kolbe hetero-coupled product **2.90**, non-Kolbe product **2.91** and Kolbe:non-Kolbe product ratio determined by GC for the electrolysis of *N*-Boc β -alanine and acetic acid

Entry	Potential Difference / V	<i>N</i> / %	Anode Surface Area / cm ²	Average Current Density / mA cm ⁻²	Yield of Kolbe Product (2.90) / % ^a	Yield of non-Kolbe Product (2.91) / % ^a	Kolbe:non-Kolbe product ratio
1	15	5.6	0.84	73	58	27	2.15:1.00
2	15	5.6	0.29	134	57	22	2.59:1.00
3	30	5.6	0.84	171	46	29	1.59:1.00
4	30	5.6	0.29	331	50	21	2.38:1.00
5 ^b	30	5.6	0.28	282	41 ^c	22 ^c	1.86:1.00
6	15	11	0.84	124	48	23	2.09:1.00
7	30	11	0.29	409	43 ^c	21 ^c	2.05:1.00

^a Reaction quantified with GC calibration curves ^b Cathode surface area 0.84 cm², no polarity inversion ^c average value taken over multiple reactions

Overall, changing the current density by changing the electrode surface area, applied potential and degree of neutralisation did not have a substantial impact on the outcome of the Kolbe reaction of *N*-Boc β -alanine and acetic acid. This suggests that in the electrolysis

of *N*-Boc β -alanine, current densities of *ca.* 70 mA cm⁻² are sufficient to generate a high enough concentration of radicals at the electrode surface, and the reaction is limited by the ability of the radicals to diffuse away from the electrode surface.⁸⁴

2.2.4.4 Summary of Changes to Electrolysis Conditions

The largest factors that affected the selectivity between the Kolbe and non-Kolbe products across the whole study of *N*-Boc β -alanine and acetic acid reactivity were solvent and the electrode material. Although the current density was successfully increased, improved yields of the Kolbe product were not observed. The addition of supporting electrolyte suppressed the Kolbe reaction, presumably by preventing carboxylate layer formation, and increased potential differences or larger quantities of base had little effect. This indicates that the most important determinant in selectivity between the Kolbe and non-Kolbe process is the inherent reactivity of the substrate.

2.3 Conclusions and Future Work

In conclusion, Kolbe electrolysis has been shown to be a useful electrochemical reaction, capable of forming intermolecular carbon-carbon bonds from two different carboxylic acid starting materials. Using conditions from the literature, Kolbe and non-Kolbe products have been achieved for the electrolysis of a range of *N*-Boc amino acids and the results show that the reaction selectivity is highly substrate dependant.

High yields, of up to 82%, of non-Kolbe products were observed with α -amino carboxylates, and this is attributed to the low ionisation potential of the radical intermediate. Kolbe hetero-coupled products were observed for β -, γ -, and δ -amino acids, indicating that the radicals formed were more stable to further oxidation and so underwent the desired coupling with methyl radicals (derived from acetic acid). However, carbocation derived non-Kolbe products were still observed and carbocations underwent rearrangements, such as hydride shifts and fragmentations, to form more stabilised intermediates. Substrates capable of forming stabilised α -amino carbocations tended to result in solvolysis products whilst unstabilised primary carbocations underwent deprotonation to form alkenes.

The electrolysis of *N*-Boc β -alanine and acetic acid provided an excellent reaction to study in more detail as it resulted in high yields of a Kolbe product and formed only one non-Kolbe side product that was easily and reliably quantified. Furthermore, amines are synthetically useful building blocks and so this system provided a relevant reaction to explore. ^1H NMR spectroscopy data of the Kolbe reaction over time revealed that both the Kolbe and non-Kolbe products are formed simultaneously during electrolysis. The results also showed that when the majority of carboxylate was consumed, amine bases were then oxidised, causing a lowering in the current density, possibly through an electrode passivation mechanism. With alkaline metal bases, a constant current was maintained, which implied an alternative oxidation pathway was facilitated at low carboxylate concentration.

Finally, the impact of experimental condition on the Kolbe reaction was explored. Overall, changes to the solution-electrode interface, such as variation in solvent or electrode material, had a large effect on the outcome of the reaction. In particular, the introduction of high concentrations of supporting electrolyte entirely suppressed the Kolbe reaction. Together, this is taken to show that the progress of the reaction is highly sensitive to a disruption in the packing of carboxylate at the anode surface. Conversely, trying to drive the reaction selectivity by increasing the rate of radical formation through increasing the current density

beyond 70 mA cm^{-2} did not increase the amount of Kolbe product of the ratio of Kolbe:non-Kolbe product. This is interpreted as showing that beyond a threshold concentration of radical formation, the amount of Kolbe to non-Kolbe product formation is mainly dictated by the ionisation potential of the radical.

Future developments to Kolbe electrolysis of protected amino acids would involve structural changes, such as changing the protecting group or increasing the length of the acid, to increase the ionisation potential of the radical formed so that it will not undergo a facile second oxidation. With respect to the electrolysis of *N*-Boc β -alanine, increased temperature seemed to improve the rate of coupling (although solvent evaporation resulting in inaccurate analysis measuring greater than 100% yield), therefore it may be interesting to see the effect of a lower reaction temperature which may impede diffusion and radical coupling.

Chapter 3: Synthesis of Sterically Hindered Tertiary Amines using Electrochemically Generated α -Amino Radicals

3.1 Introduction

The development of new synthetic methods for constructing amines is of importance to synthetic chemists. Free radical reactions offer promising routes to functionalised amines under mild conditions.²³ Recent photocatalytic work has highlighted a reductive route to synthesise medicinally relevant amines *via* reactive α -amino radicals.¹⁴⁹ Such radicals can be initiated photocatalytically, chemically with strong reducing agents, or electrochemically. Radicals can undergo radical-radical couplings, intra- or intermolecular additions to electrophiles or hydrogen atom transfers to produce α -functionalised amines.¹⁵⁰ The discovery of new methods for the construction of amines with α -tertiary centres is of particular importance because these functional groups are abundant across the pharmaceutical and agrochemical sector.¹⁵¹ This work aims to develop an electrochemical approach to the synthesis of sterically hindered tertiary amines *via* α -amino radicals. This chapter begins with a review of the current synthetic methods for forming α -amino radicals, then the development of a new electrosynthetic reaction is described, and the scope of the reaction outlined.

3.1.1 General Methods for the Synthesis of Amines

Amines and nitrogen containing heterocycles are abundant in many pharmaceuticals and agrochemicals. A study of FDA approved pharmaceuticals from 2014 found that 84% of unique drugs contained at least one nitrogen atom and 59% included at least one nitrogen containing heterocycle.¹⁵² Figure 3.1 highlights a number of drug molecules bearing amines, focusing on tertiary amines and cyclic tertiary amines. Aliphatic amines, and particularly tertiary alkyl amines, are valuable as drug components; the lone pair of electrons is important for hydrogen bonding and alkyl groups can be selected to improve lipophilicity and tune the electronics.¹⁵⁰

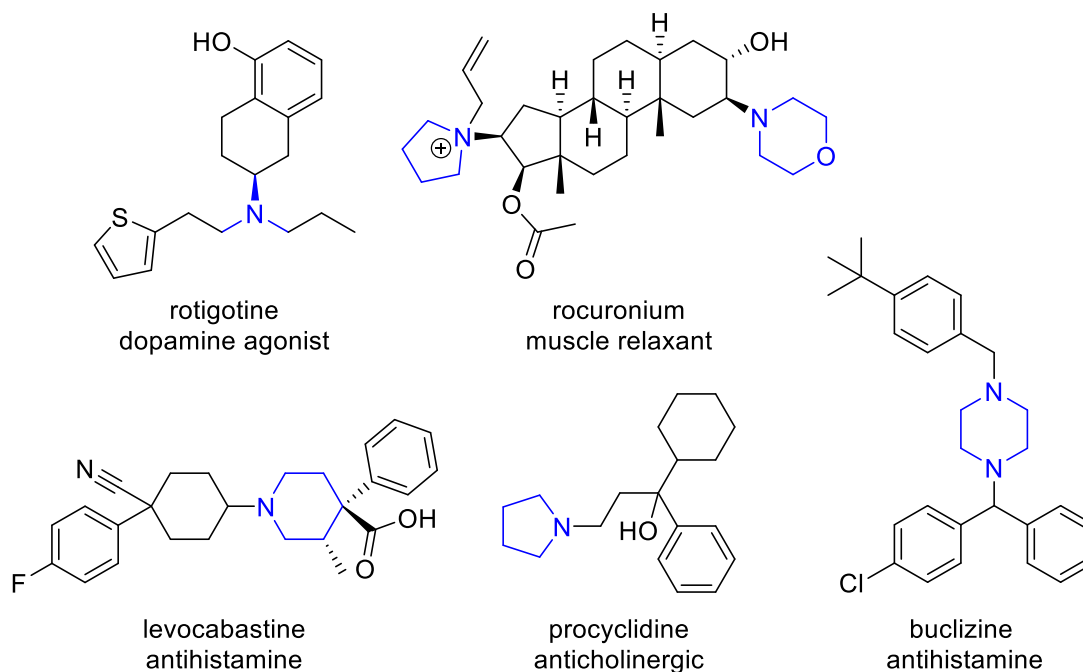
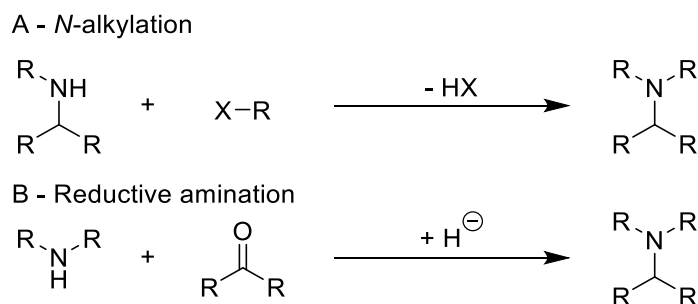


Figure 3.1 Various tertiary amines used in pharmaceuticals.¹⁵²

Widely used methods of amine synthesis include traditional *N*-alkylation and reductive amination approaches.¹⁵³ For the synthesis of aliphatic amines, *N*-alkylation offers a simple approach. By combining primary or secondary amines with alkyl (pseudo)halides, complex secondary or tertiary amine products can be made (Scheme 3.1 A). Overalkylation, i.e. the addition of the amine to multiple alkyl (pseudo)halides, can be a problem with this method, leading to the formation of quaternary ammonium salts. Even when a large excess of amine is used, poor yields of the desired amine can result.

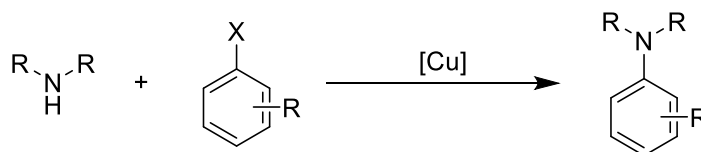
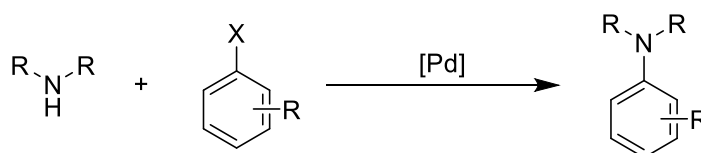


Scheme 3.1 Classical methods for synthesis of amines.

Reductive amination approaches offer an alternative to *N*-alkylation for the formation of amines (Scheme 3.1 B). In a direct reductive amination pathway, an aldehyde or ketone is

reacted with an amine to form a hemiaminal. With either a primary amine or ammonia, upon loss of water, an intermediate imine is formed which is reduced to the target amine. Alternatively, with a secondary amine, the hemiaminal can either undergo direct reduction or form an intermediate iminium ion which is reduced.¹⁵⁴ Typically, a borohydride complex acts as the hydride source for the reduction step. Alternatively, catalytic hydrogenation techniques with hydrogen gas and either platinum, palladium, or nickel are used. Whilst hydrogenation is economical, particularly for large scale, it should be avoided when substrates contain readily reducible functional groups such as nitro, cyano or C-C multiple bonds. Hydride reducing agents, such as NaBH_3CN , $\text{NaBH}(\text{OAc})_3$ or NaBH_4 , offer better selectivity for the protonated imines over aldehydes and ketones at pH 6-8. However, these reactions require hazardous borohydride reagents which in some cases can produce toxic byproducts (for example HCN or NaCN with NaBH_3CN) and they often require a large excess of amine.¹⁵⁵ Neither of the approaches outlined in Scheme 3.1 are particularly useful for the synthesis of sterically hindered amines.

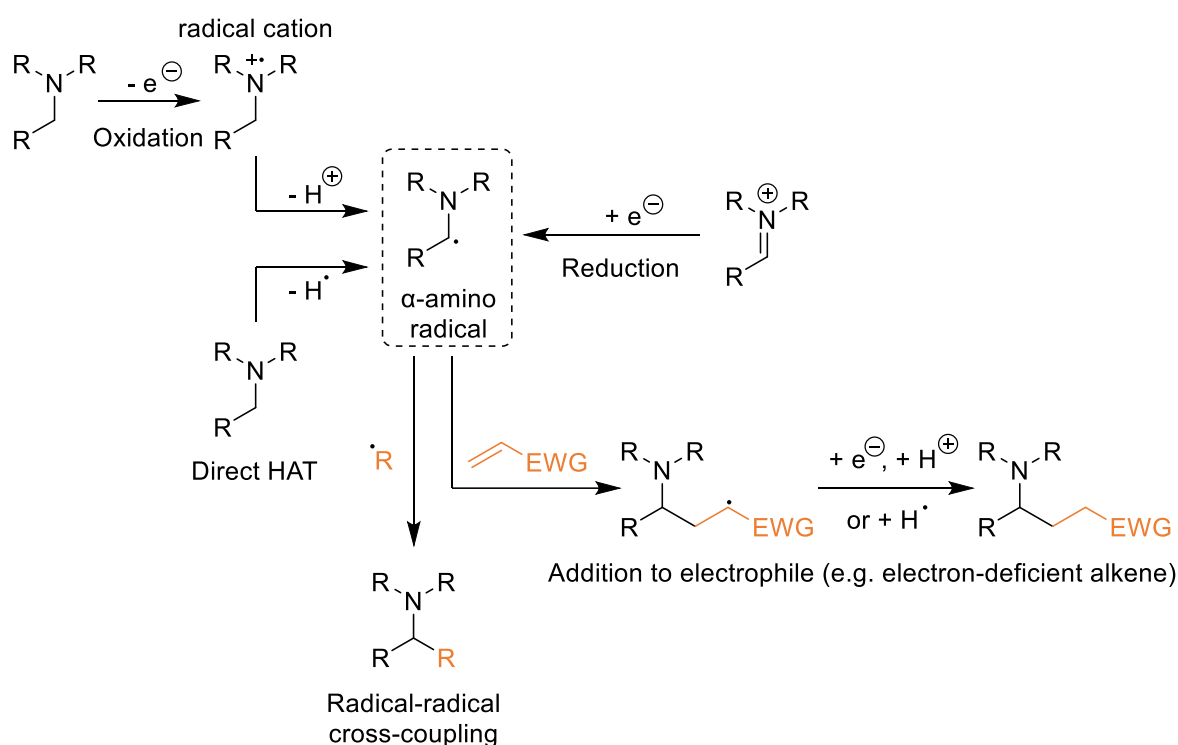
Other methods for forming amines rely on transition metal catalysts.¹⁵⁰ Copper catalysed Ullmann-Type reactions (Scheme 3.2 A) and palladium catalysed Buchwald-Hartwig amination (Scheme 3.2 B) offer synthetically useful methods of $\text{C}(sp^2)\text{-N}$ bond formation from amines and aryl (pseudo)halides.^{156,157} The high functional group tolerance has made them key reaction in medicinal chemistry.¹⁵⁸ However, these metal mediated cross-coupling reactions are typically limited by sp^2 hybridised starting materials, meaning complex α -tertiary amine products cannot be achieved.¹⁵⁷

A - Ullmann-Type coupling - *N*-arylationB - Buchwald-Hartwig amination - *N*-arylation

Scheme 3.2 Transition metal mediated cross-coupling routes for synthesis of amines.

Since the late 2000s there has been an increase in the number of publications which utilise light and either transition metal (typically ruthenium or iridium) or organic photocatalysts for the synthesis of complex amines *via* radicals. Radicals show high levels of functional group tolerance and partake in reaction pathways that are inaccessible by classical ionic approaches.²³ Radical-based methods address some of the disadvantages mentioned above and, in particular, sterically congested α -tertiary centres can be made.

α -Amino radicals are valuable intermediates in the synthesis of α -functionalised amines. They can be prepared oxidatively from amines *via* radical cations, by redox neutral direct hydrogen atom transfer (HAT) mechanisms or through the reduction of imines, imine derivatives and iminium ions. The resultant electron-rich radicals can participate in a variety of C-C bond forming reactions including radical-radical couplings, and additions to electrophiles (Scheme 3.3).^{149,150} As the α -amino radicals are nucleophilic, they will undergo facile addition to alkenes which have electron withdrawing groups and are therefore electron deficient. This is because the SOMO-LUMO energy gap is small, as the SOMO of an electron rich radical is higher in energy than a non-electron rich radical and electron-withdrawing group lowers the LUMO energy of the alkene.¹⁵



Scheme 3.3 Single electron routes to α -amino radicals and subsequent reactions of α -amino radicals.

In order to provide context for the work described in this chapter, the following sections will highlight the importance of α -amino radicals as key intermediates for the synthesis of α -substituted amines. Methods for radical generation will be grouped into a brief discussion of oxidative and redox neutral approaches followed by reductive approaches including photocatalytic reductions of imines and iminium ions, chemical reductions using samarium(II) iodide and finally electrochemical reductions of iminium ions. Both radical-radical coupling and addition to electrophiles will be covered.

3.1.2 Oxidative Approaches for α -Amino Radical Formation

Tertiary amines with low oxidation potentials have traditionally been used as a source of electrons (“sacrificial electron donors” or SEDs) in photochemical and electrochemical reactions such as H_2 production and CO_2 photoreduction.¹⁵⁹ The chosen amines are often cheap, readily available and easily oxidised (Figure 3.2), and can therefore be used to facilitate desired reductions.¹²⁰ Reactive intermediates, such as α -amino radicals or iminium ions, can be generated from tertiary amines. Until recently, these reactive intermediates have not been used as building blocks for the preparation of more complex α -functionalised amines.¹⁶⁰ This section will briefly describe methods of α -functionalising amines *via* oxidatively generated α -amino radicals.

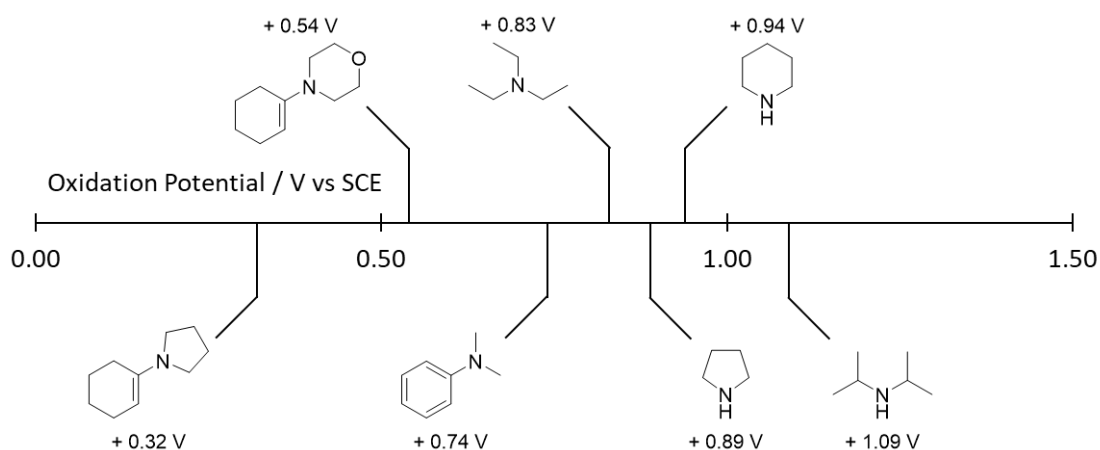
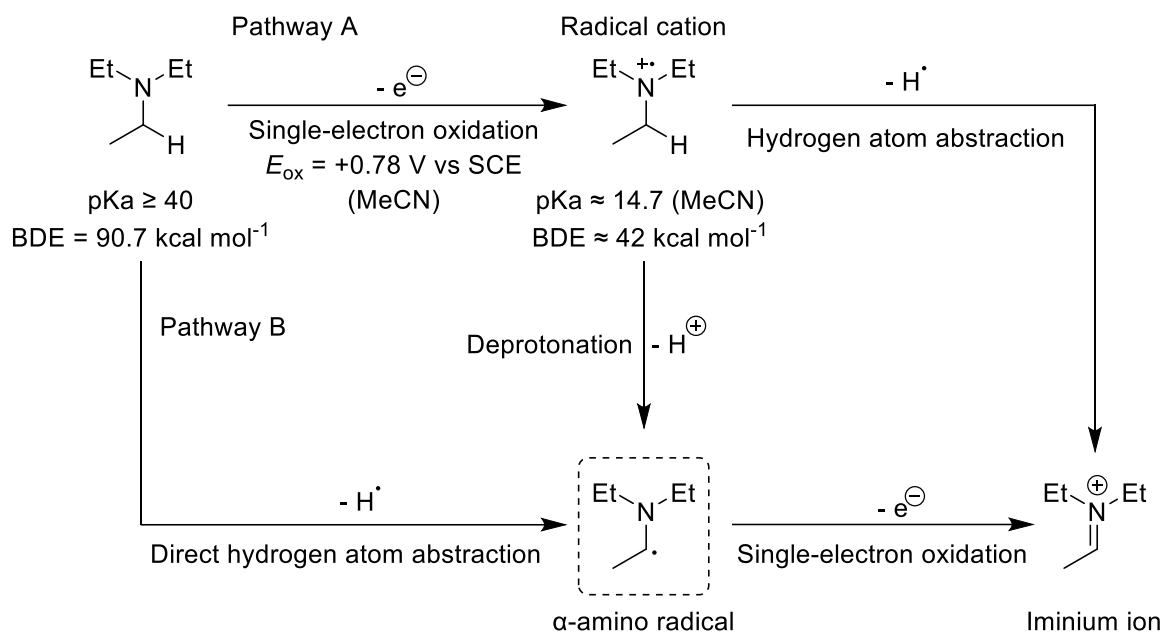


Figure 3.2 Oxidation potentials for various amines.¹²⁰

The single-electron oxidation of an amine forms a radical cation, acidifying the α -C-H bond (Scheme 3.4 Pathway A).¹⁶¹ This allows the radical cation to undergo deprotonation to form an α -amino radical. Alternatively, hydrogen atom abstraction from the radical cation would generate an iminium ion. Iminium ions may also be generated through further single electron

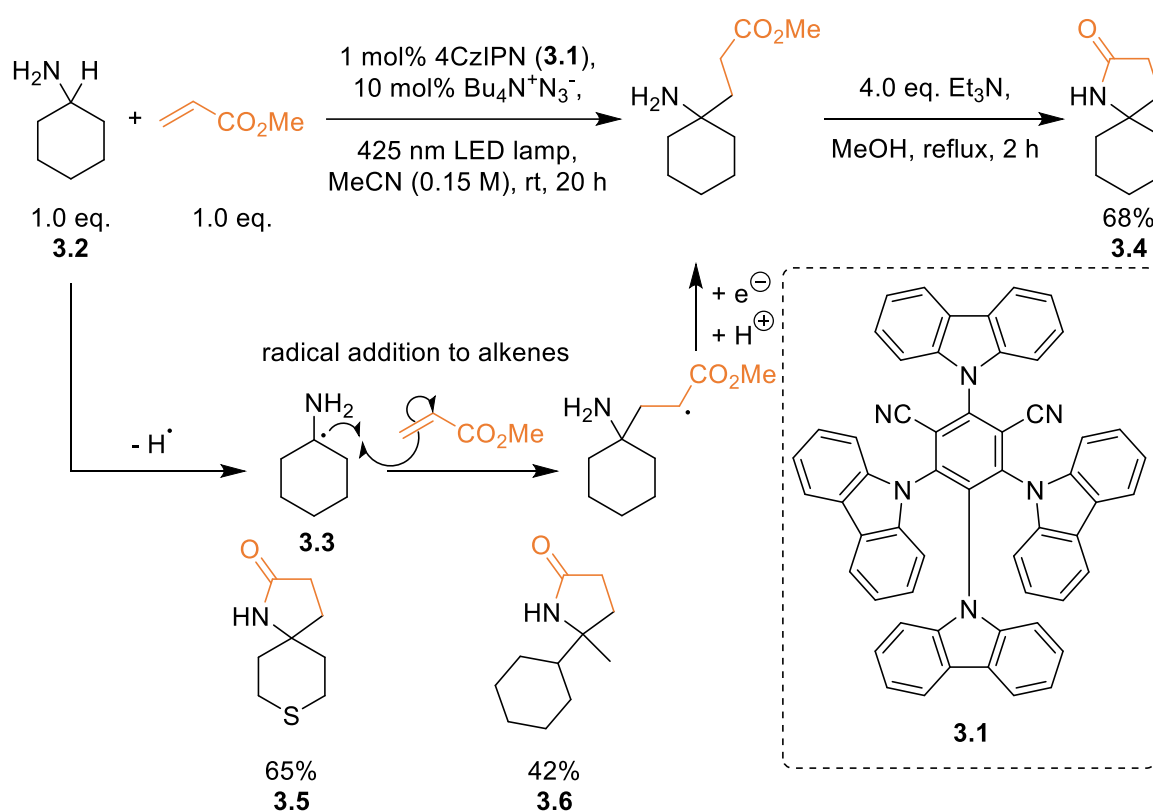
oxidation of α -amino radicals.¹⁶⁰ Using an appropriate HAT catalyst, amines may also undergo direct HAT to α -amino radicals (Scheme 3.4 Pathway B).



Scheme 3.4 Triethylamine single electron oxidation pathways.¹⁶⁰

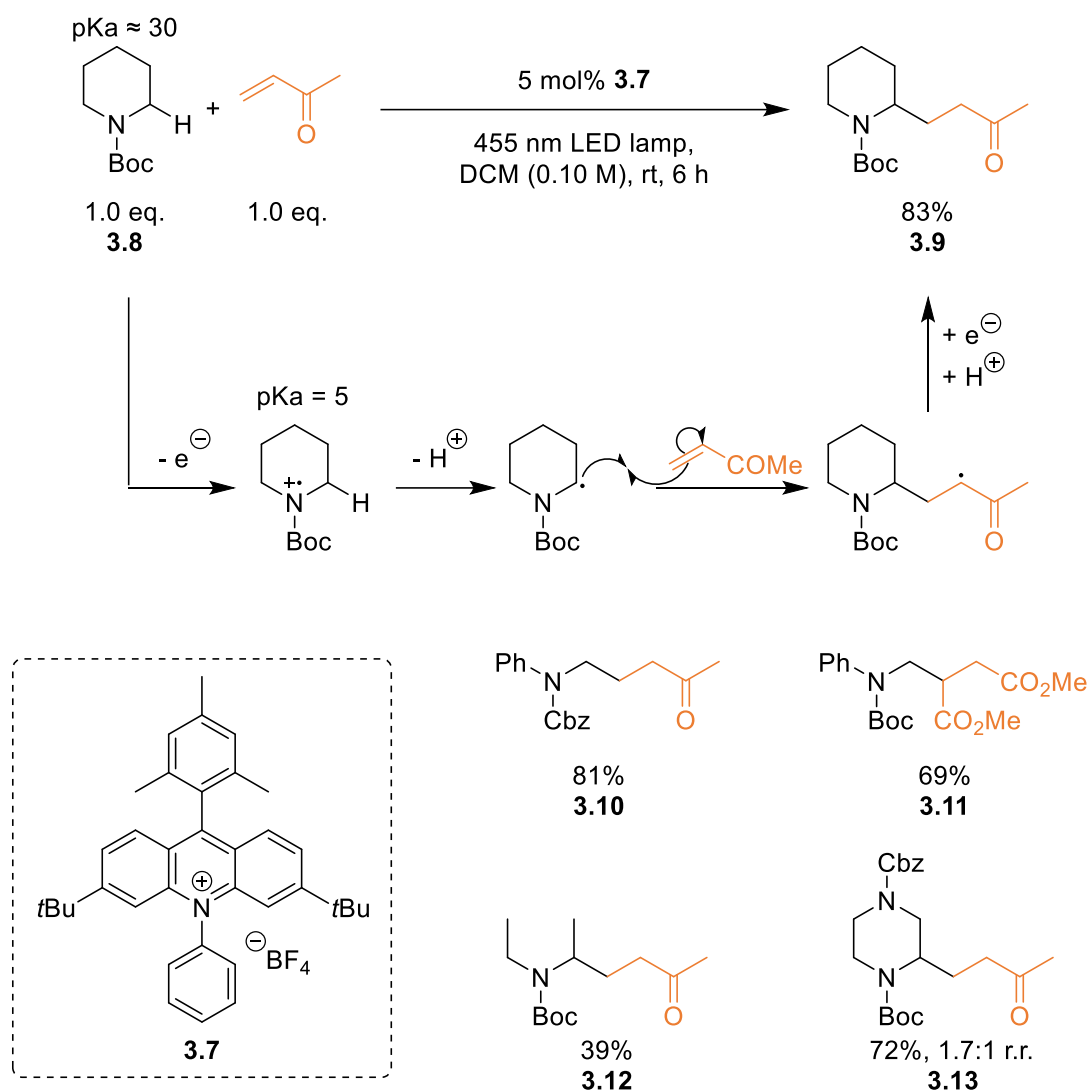
3.1.2.1 α -Amino Radical Formation by Direct HAT of Amines

One example of a HAT catalyst is an azide ion. Azide ions can be oxidised to azidyl radicals by excited photocatalysts such as 1,2,3,5-tetrakis(carbazole-9-yl)-4,6-dicyanobenzene (4CzIPN, **3.1**). The resulting azidyl radicals are potent oxidants and can readily abstract hydrogens from unactivated alkanes.¹⁶² This strategy was employed by the Cresswell group as a method of providing direct access to α -tertiary amines and their corresponding γ -lactams from unprotected primary amines and electron-deficient alkenes (Scheme 3.5).¹⁶³ Lactam **3.4** was prepared in a 68% yield from primary amine **3.2** *via* α -amino radical **3.3**. The reaction showed good functional group tolerance and a variety of amine starting materials were found to be compatible with the conditions (see **3.5** and **3.6** for representative examples).

Scheme 3.5 Direct HAT of amines by the Cresswell group.¹⁶³

3.1.2.2 Addition of Oxidatively Generated α -Amino Radicals to Alkenes

Nicewicz and co-workers prepared a series of α -functionalised carbamates from protected piperidines and piperazines and electron-deficient alkenes, typically vinyl ketones (Scheme 3.6). The highly oxidising acridinium-based organic photocatalysts such as **3.7** employed had oxidation potentials for the excited state between +1.62 and +2.15 V vs SCE.¹⁶⁴ Such an oxidising photocatalyst was needed as, unlike the amines in Figure 3.2, the half wave potential ($E_{p/2}$) for *N*-Boc piperidine **3.8** is +1.96 V vs SCE.¹⁶⁵ The reaction conditions were compatible with a range of protecting groups **3.9** and **3.10** and Michael acceptors **3.11** but lower yields were observed with acyclic aliphatic amines **3.12**.¹⁶⁵ The reaction proved to be site-selective for piperazines bearing two different protecting groups **3.13**.¹⁶⁶



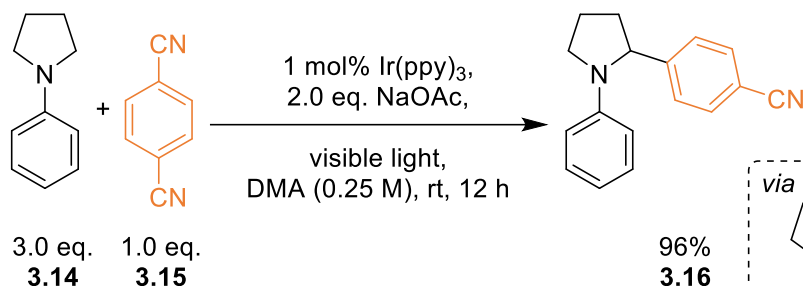
Scheme 3.6 Oxidative generation of α -amino radicals and subsequent reaction with electron-deficient alkenes by Nicewicz and co-workers.^{164,165}

3.1.2.3 Radical-Radical Coupling of Oxidatively Generated α -Amino Radicals with Reductively Generated Aryl Radicals

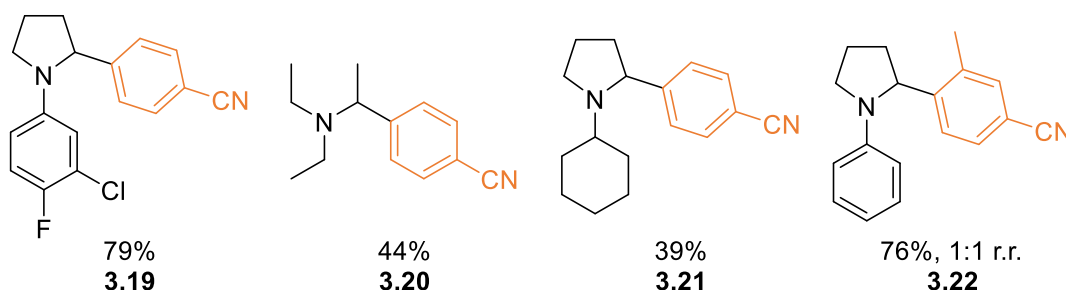
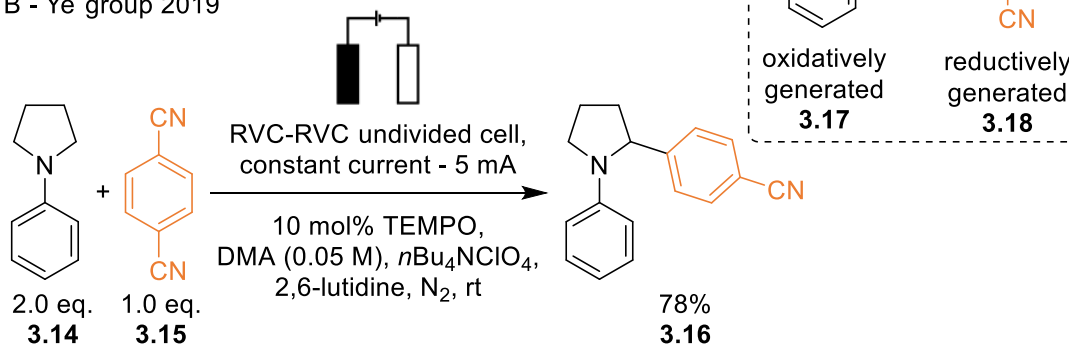
In 2011, the MacMillan group reported a high-yielding method for α -amino C-H arylation *via* photochemically generated α -amino radicals in excellent yields (Scheme 3.7 Radical-radical coupling of transient α -amino radicals and persistent cyanoarene derived radicals by the MacMillan group and the Ye group.^{167,169} A).^{167,168} In 2019, the Ye group reported an alternative electrochemical approach where instead of expensive iridium photocatalysts, reticulated vitreous carbon (RVC) electrodes were used.¹⁶⁹ At the anode, single electron oxidation of TEMPO formed an active species, which oxidised amine **3.14** to a radical cation which on deprotonation formed α -amino radical **3.17** (Scheme 3.7 Radical-radical coupling

of transient α -amino radicals and persistent cyanoarene derived radicals by the MacMillan group and the Ye group.^{167,169} B). The radical underwent radical-radical coupling with **3.18**, generated by electrochemical reduction of **3.15**. On elimination of cyanide, arylated amine **3.16** was achieved.

A - MacMillan group 2011



B - Ye group 2019



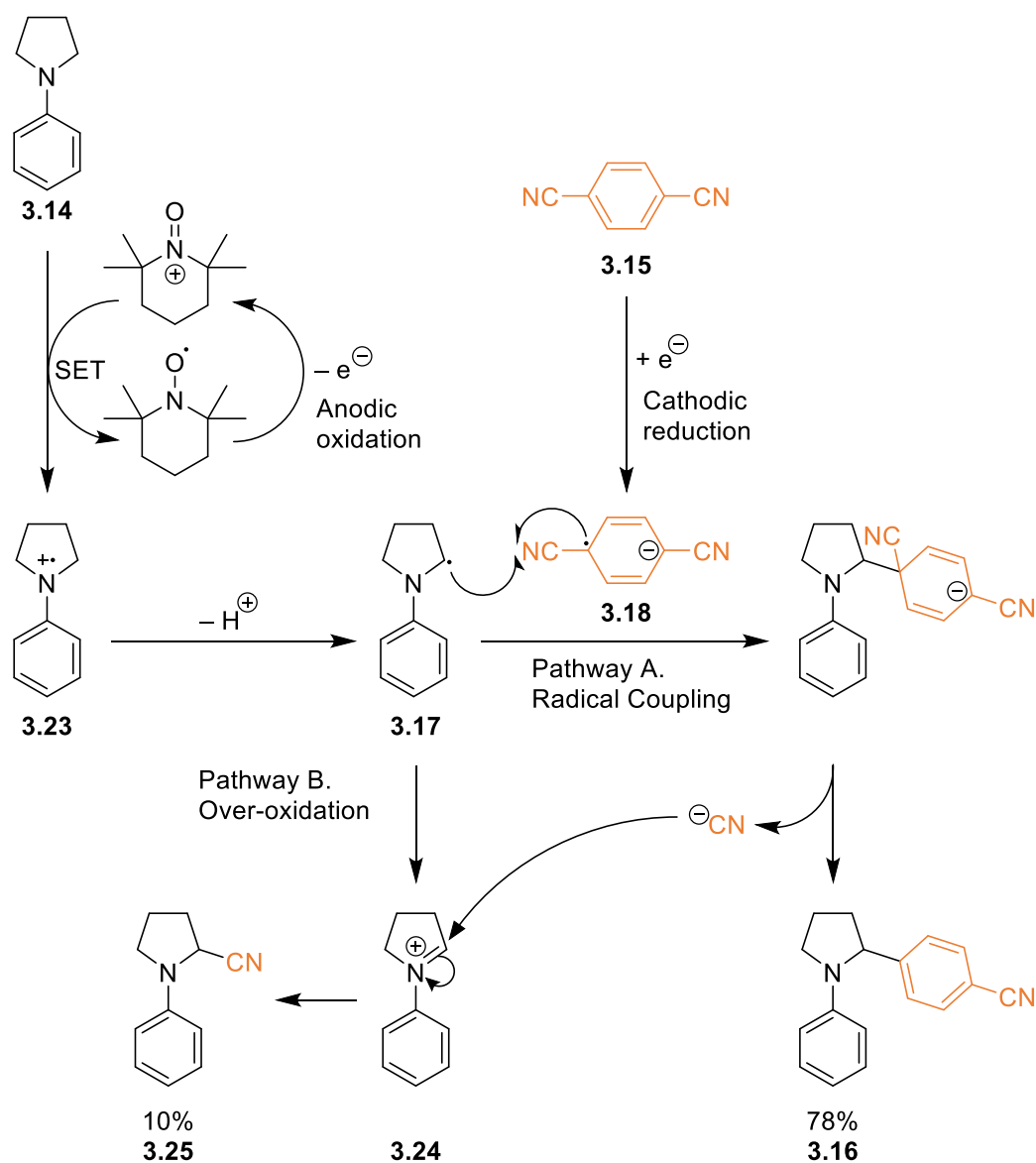
Scheme 3.7 Radical-radical coupling of transient α -amino radicals and persistent cyanoarene derived radicals by the MacMillan group and the Ye group.^{167,169}

In the electrochemical study, moderate to excellent yields were achieved for a large range of *N*-aryl pyrrolidine-based amines bearing weakly electron-withdrawing substituents **3.19**. When triethylamine was oxidised, only a 44% yield was observed for arylated product **3.20**. The lower yield with the acyclic amine was attributed to a decrease in nucleophilicity of the α -amino radical, due to reduced orbital overlap between the radical and nitrogen lone pair.¹⁷⁰ Arylation occurred preferentially on the pyrrolidine ring for *N*-alkyl examples, such as **3.21**, and lower yields were achieved.

In total, only six cyanoarenes bearing electron-withdrawing groups were explored in the study by the Ye group, two of which are given in Scheme 3.7 Radical-radical coupling of transient α -amino radicals and persistent cyanoarene derived radicals by the MacMillan group and the Ye group.^{167,169} As cyanide elimination is not regioselective, **3.22** was isolated as a 1:1 mixture of two regioisomers. Electron-deficient heteroaromatics (for example 4-cyanopyridine) were not compatible with the reaction conditions.¹⁶⁹ A lower yield of 78% was achieved for **3.16** compared to the photochemical example. A constant current of 10 mA was applied and TEMPO (10 mol%) was used as a mediator to successfully arylate tertiary amines.^{167,169}

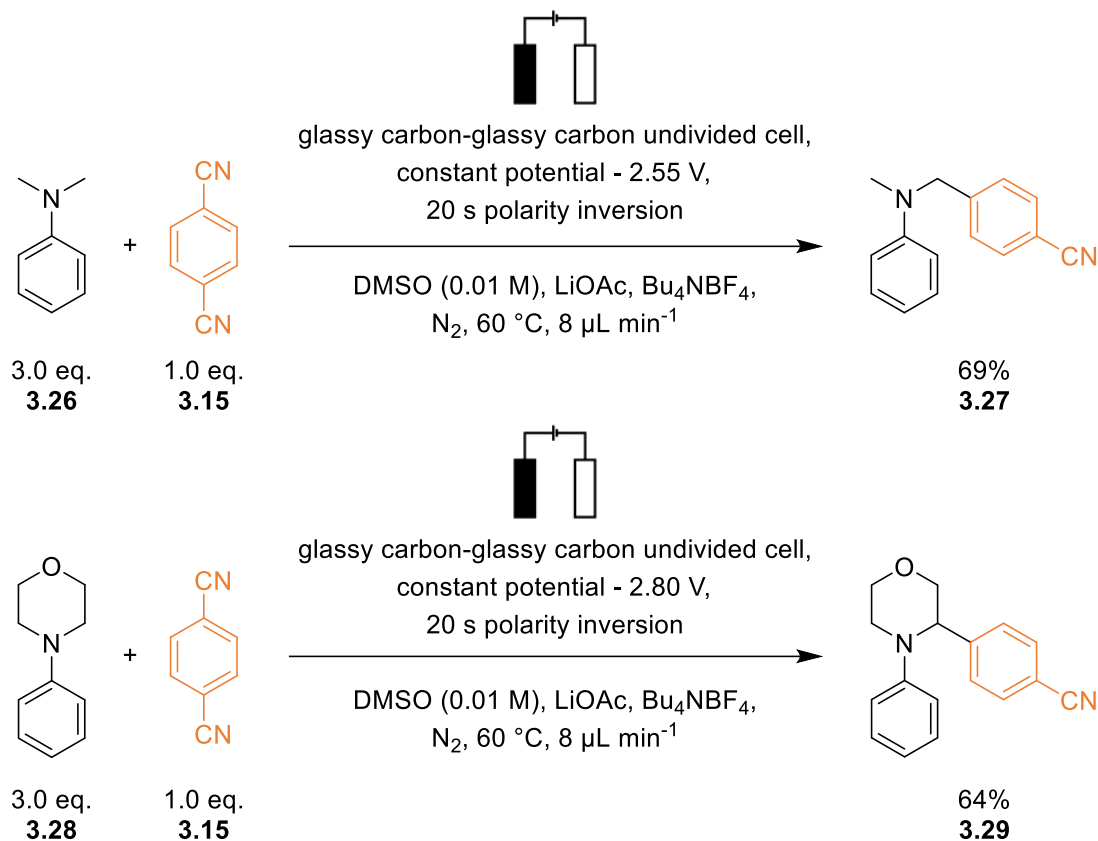
A recent mechanistic study into the photochemical reaction has suggested that 1,4-dicyanobenzene (**3.15**) acts as the primary proton acceptor for the radical cation **3.23** formed from the oxidation of amine **3.14**. This was because the rate of deprotonation, measured electrochemically, was unchanged by the addition of sodium acetate (used as the base by the MacMillan group). It was proposed that initially 1,4-dicyanobenzene deprotonates radical cation **3.23** before itself being deprotonated by the base additive. Therefore, cyanoarenes which are less good proton acceptors may inhibit the reaction.¹⁷¹

In the electrochemical example, the desired radical-radical coupling (Scheme 3.8 Proposed mechanism for the oxidation of arylated pyrrolidine **3.14** and subsequent radical-radical coupling.¹⁶⁹ Pathway A) was in competition with further oxidation of the α -amino radical **3.17** to an iminium ion **3.24** (Scheme 3.8 Proposed mechanism for the oxidation of arylated pyrrolidine **3.14** and subsequent radical-radical coupling.¹⁶⁹ Pathway B). α -Cyanation side product **3.25** was observed in a 10% yield, derived from addition of a cyanide anion to the iminium ion. Only a 35% yield of desired product **3.16** was observed without TEMPO as a mediator in the electrochemical example. TEMPO was necessary as it moved the oxidation away from the electrode surface and avoided over-oxidation. In examples where the desired product was not observed, high yields of iminium ion derived products were isolated as the second oxidation was more facile. Moreover, TEMPO was required as a mediator because the transient α -amino radical lifetime would be much less than the time required to diffuse from the anode to the cathode. This means radical **3.17** would be less likely to couple with the persistent radical **3.18** if they formed on opposite electrodes, on opposite sides of the electrochemical cell. With TEMPO as a mediator, the oxidation of **3.14** to radical **3.17** moves into the bulk solution and closer to the cathode where radical **3.18** is generated and therefore radical-radical coupling can occur instead of further oxidation to iminium ion **3.24**.¹⁶⁹



Scheme 3.8 Proposed mechanism for the oxidation of arylated pyrrolidine **3.14** and subsequent radical-radical coupling.¹⁶⁹

Another variation of this reaction was published by Buchwald, Jensen and co-workers in 2020 using a narrow gap cell with the products of direct oxidation and direct reduction coupling (Scheme 3.9). It was theorised that if the lifetime of the persistent radical derived from the cyanoarene (**3.15**) was longer than the diffusion time across the cell then radical-radical coupling was possible. A cell was designed so that two glassy carbon electrodes had a 25 μL gap between them. An excess of the transient radical was used to ensure radical-radical coupling. Oxidation of **3.26** and reduction of **3.15** successfully delivered coupled product **3.27** in a 69% yield and with *N*-aryl morpholine derivative **3.28** a 64% yield of **3.29** was achieved.¹⁷²



Scheme 3.9 Narrow gap electrolysis, oxidation of arylated amines by Buchwald, Jensen and co-workers.¹⁷²

3.1.2.4 Summary of α -Amino Radicals Generated by Oxidation of Amines

In summary, both photoredox chemistry and synthetic electrochemistry have been used to access α -amino radicals from amines *via* direct hydrogen atom transfers and oxidation of tertiary amines and carbamates. In the photochemical approaches, oxidising photocatalysts were needed to access radical cations which, due to the increase in acidity, were deprotonated to form α -amino radicals. Arylated products were achieved through radical couplings with cyanoarenes and alkylated products from radical addition into electron deficient alkenes. This radical addition pathway is possible as the α -amino radicals formed are nucleophilic.

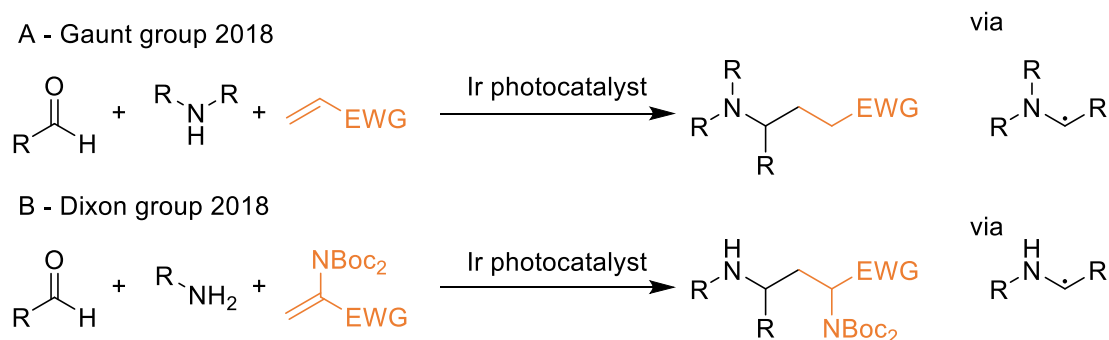
Generally, improved yields were observed with cyclic amines and aniline derivatives and reduced yields were achieved with acyclic amines (**3.9** compared to **3.12**, Scheme 3.6). A new carbon-carbon bond was formed on the less hindered side and, as a result, more sterically congested α -tertiary centres were not attained by this method of functionalisation.

As opposed to photochemical oxidation of amines, which uses expensive photocatalysts, synthetic electrochemistry provided an alternative approach to analogous tertiary amines

(3.16). In the electrochemical oxidation of **3.14**, overoxidation of the α -amino radical was found to be a competing side reaction. The introduction of a mediator, TEMPO, resulted in high yields of the radical-radical coupling products as the radical formation was moved away from the anode and the site of over-oxidation, meaning less iminium ion derived products were observed. Furthermore, the transient α -amino radical did not have to diffuse from the anode to the cathode to couple with persistent radicals derived from cyanoarenes meaning radical-radical coupling was more likely. In the work by Buchwald, a mediator was avoided by using a narrow gap cell, where the diffusion rate was less than the transient radical lifetime. Highly oxidising conditions, overoxidation and the need for a mediator can be avoided by using an alternative reductive approach to α -amino radicals.

3.1.3 Photocatalytic Reduction of Iminium Ions and Imines

Recent photocatalytic work has shown that imines and iminium ions, formed *in-situ*, can be reduced with iridium photocatalysts to α -amino radicals.^{173–176} These radicals can undergo addition into electron-deficient alkenes forming tertiary, and secondary amine products (Scheme 3.10 A and B).^{173–175} This approach to amine synthesis offers an operationally simple way of making complex α -substituted tertiary amines from readily available primary or secondary amines, carbonyl components and alkenes.



Scheme 3.10 Photocatalytic routes to amines via α -amino radicals.^{173–175}

Relative to the parent aldehydes and ketones, the imines and iminium ions are more readily reduced. Typical reduction potentials for iminium ions range between -0.8 V and -2.0 V vs SCE depending on the number and nature of the substituents (Figure 3.3).^{177,178} Increased conjugation, in the form of aromatic substituents, helps to lower the barrier to reduction, shifting reduction potentials to more positive values.^{177,178} Tetra-alkyl iminium ions are

harder to reduce (*ca.* -1.95 V vs SCE) as they are not conjugated and therefore require highly reducing photocatalysts.¹⁷³

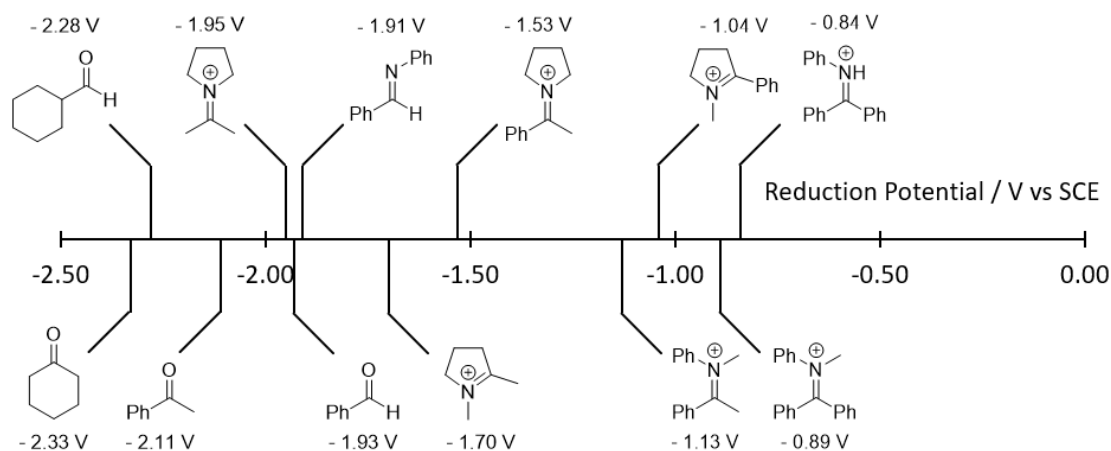
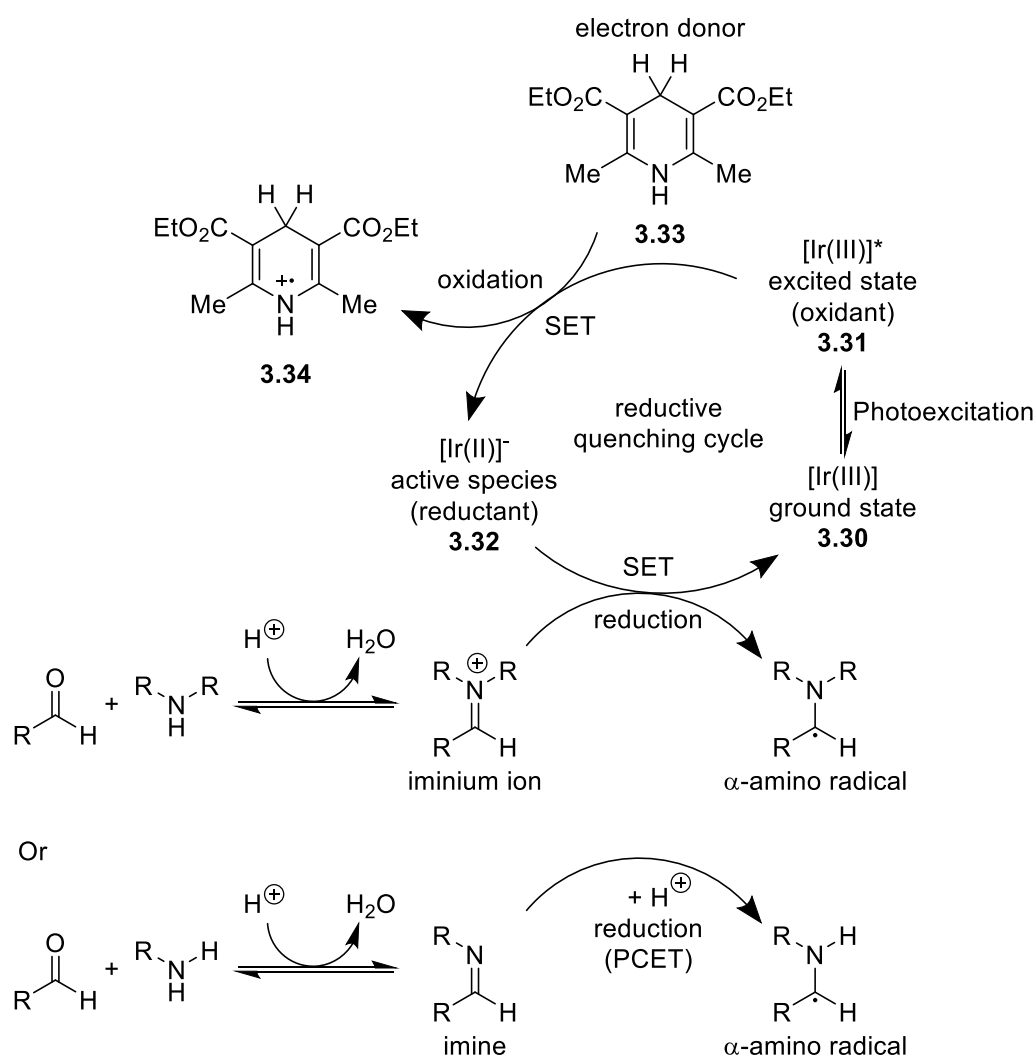


Figure 3.3 Reduction potentials for various aldehydes, ketones, imines and iminium ions.^{120,173,177,178}

3.1.3.1 Mechanism of Photocatalytic Reductive α -Amino Radical Formation

For the single-electron reduction of imines and iminium ions to α -amino radicals, Ir(III) photocatalysts are commonly employed.¹⁵⁰ The mechanism generally proceeds *via* photoexcitation of the catalyst **3.30** to a triplet excited species **3.31**, that is reduced to the active catalytic species **3.32** by a suitable electron donor, often a Hantzsch ester **3.33**. The active iridium species **3.32** then undergoes a single electron transfer into the π^* -orbital of the imine/iminium ion, reducing it to an α -amino radical (Scheme 3.11 Photocatalytic mechanism for iminium ion/imine reduction performed by the Gaunt group.¹⁷³). With imines, Brønsted acids facilitate the reduction through proton coupled electron transfer (PCET) mechanisms. A proton is transferred to the imine, raising the reduction potential (less negative value), and a one-electron reduction occurs.¹⁴⁹

Scheme 3.11 Photocatalytic mechanism for iminium ion/imine reduction performed by the Gaunt group.¹⁷³

3.1.3.2 Addition of Photocatalytically Generated α -Amino Radicals to Alkenes

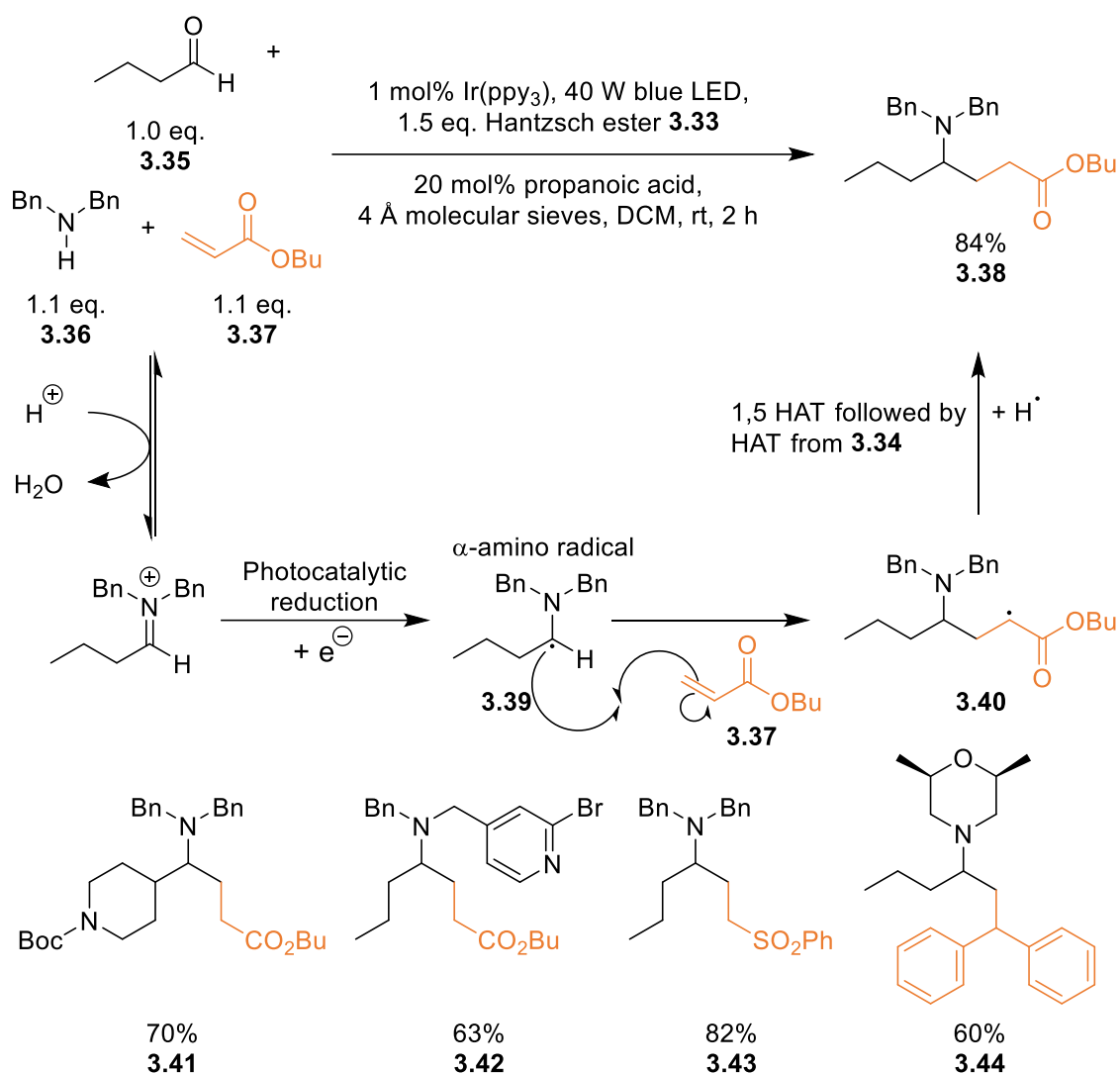
Reductively generated α -amino radicals can of course undergo addition to alkenes in the same way that oxidatively generated ones can. Historically, the scope and nature of formation of α -amino radicals has been different, therefore the oxidative and reductive reactions are discussed in different sections.

In 2014, it was shown that α -amino radicals, generated from pre-formed imines, could undergo coupling reactions with benzylic ethers.¹⁷⁹ However, the scope of imines was limited to conjugated aromatics. In 2018, independent publications by the Dixon group and the Gaunt group reported the functionalisation of amines with aldehydes and electron-deficient alkenes *via in-situ* imine/iminium ion formation, photocatalytic single-electron reduction, and addition into electron-deficient alkenes. Mechanistically, in the *in-situ*

approach an initial condensation reaction between the amine and aldehyde, catalysed by acid and driven forward by removal of water by 4Å molecular sieves, formed either the imine or iminium ion prior to photochemical reduction (Scheme 3.11 Photocatalytic mechanism for iminium ion/imine reduction performed by the Gaunt group.¹⁷³). A related photochemical reductive amination approach was published by Wenger and co-workers in 2018. *In-situ* formed iminium ions were reduced to α -amino radicals prior to hydrogen atom transfer from 3-mercaptopropionic acid to give reductive amination products in good to excellent yields.¹⁸⁰

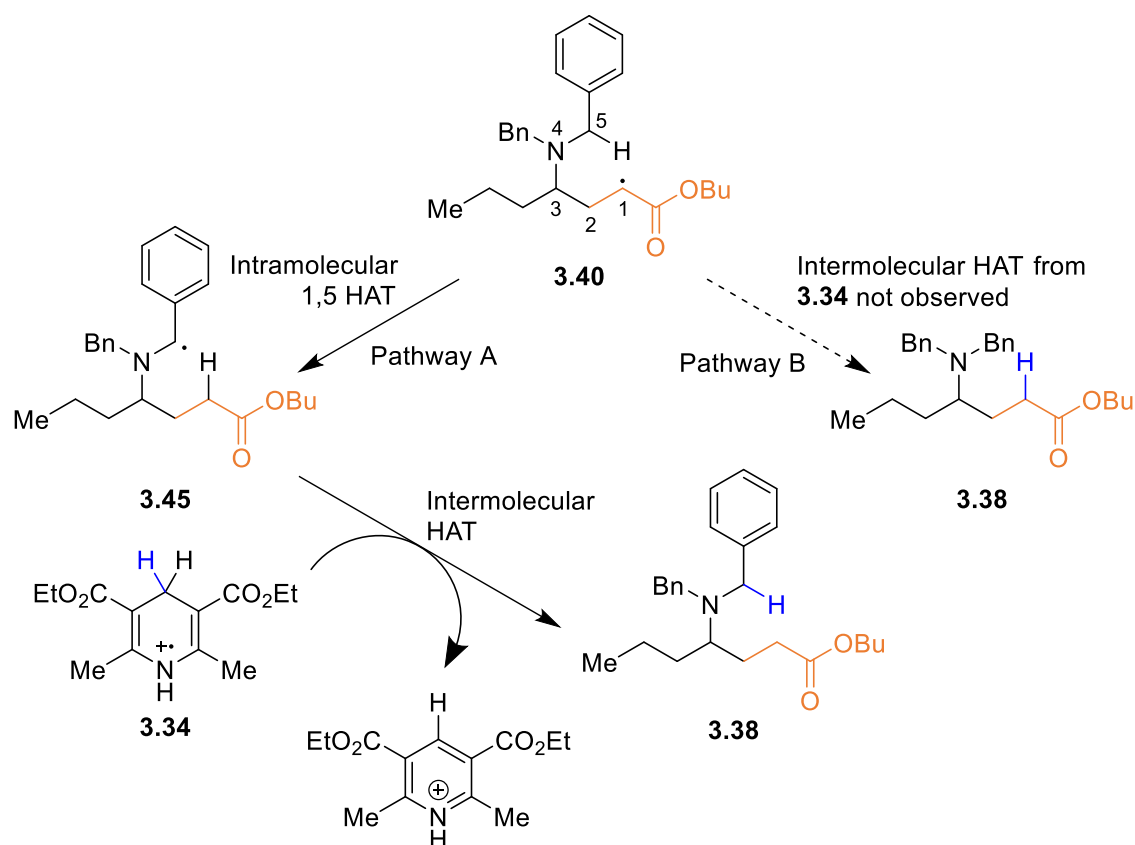
An example synthesis for tertiary amine **3.38** by the Gaunt group is given in Scheme 3.12. Premixing aldehyde **3.35**, amine **3.36** and acrylate **3.37**, in dichloromethane, with catalytic acid and irradiating in the presence of an iridium photocatalyst and Hantzsch ester **3.33** gave amino ester **3.38** in 84% yield. Propanoic acid catalysed iminium ion formation and highly reducing Ir(ppy)₃ photocatalyst was used to generate α -amino radical **3.39**. The electron-rich radical **3.39**, underwent Giese-type radical addition to electron-deficient alkene **3.37** leading to α -ester radical **3.40** and the formation of a new sp^3 - sp^3 , carbon-carbon bond. Hantzsch ester radical cation **3.34** was used as a source of hydrogen in the final step to give product **3.38** (Scheme 3.12).¹⁷³

The transformation showed good scope for aldehydes bearing both aryl and alkyl substituents including heterocycles **3.41**. Using dialkylamines with at least one benzyl substituent resulted in a range of tertiary amines with yields of between 24% and 84% and showed the reaction conditions were compatible with heteroaryl substituents (for example **3.42**). Radical addition occurred for a wide range of electron-deficient alkenes including more hindered examples and different heteroatoms **3.43**. On moving away from benzylamines to cyclic amines, less electron-deficient alkenes were used to avoid oligomerisation. Morpholine **3.44** was successfully synthesised in a 60% yield from a morpholine derivative and 1,1-diphenylethylene.¹⁷³



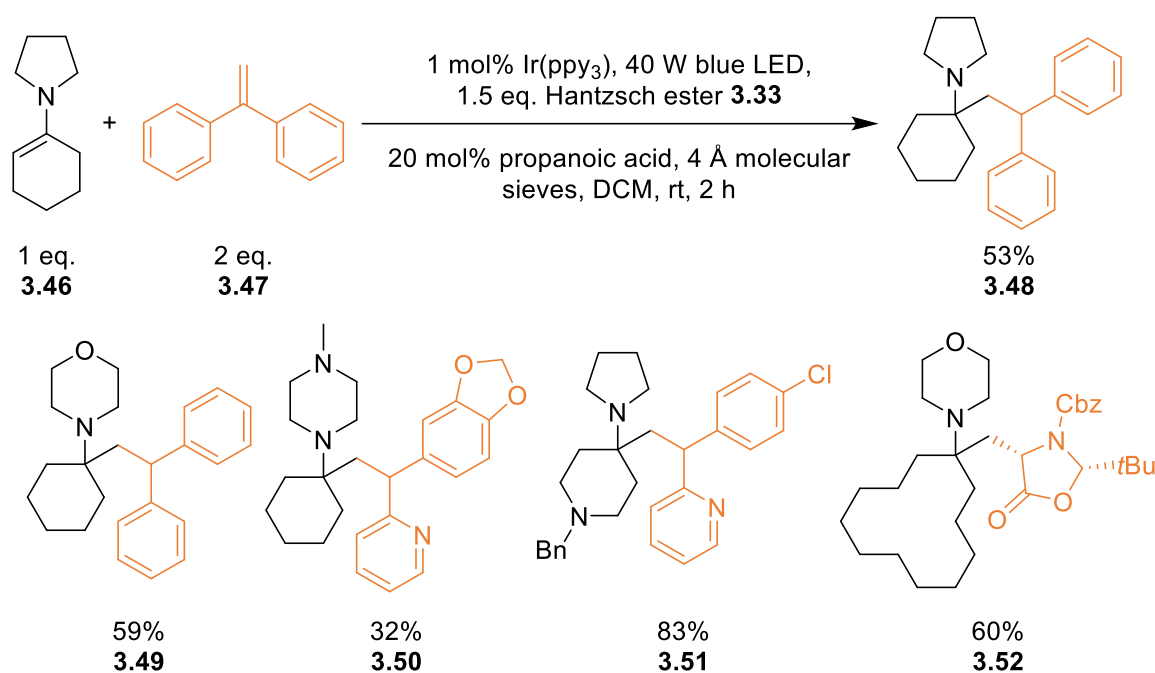
Scheme 3.12 Photochemical reduction of in-situ formed iminium ions to α -amino radicals and subsequent addition to electron-deficient alkenes by the Gaunt group.¹⁷³

In examples where benzylic amines were used, the authors proposed that an intramolecular 1,5-hydrogen atom transfer (HAT) preceded the intermolecular HAT from Hantzsch ester-radical cation **3.34** (Scheme 3.13 Pathway A rather than Pathway B). This was suggested as benzyl radical **3.45** is more stabilised than radical **3.40**.¹⁷³ Furthermore, as this radical is more stabilised it is less likely to undergo oligomerisation, which is a common problem with this type of radical addition.¹⁸¹ Deuterium labelling of the Hantzsch ester confirmed Pathway A.¹⁷³



Scheme 3.13 Proposed mechanism for intramolecular 1,5 HAT by the Gaunt group.¹⁷³

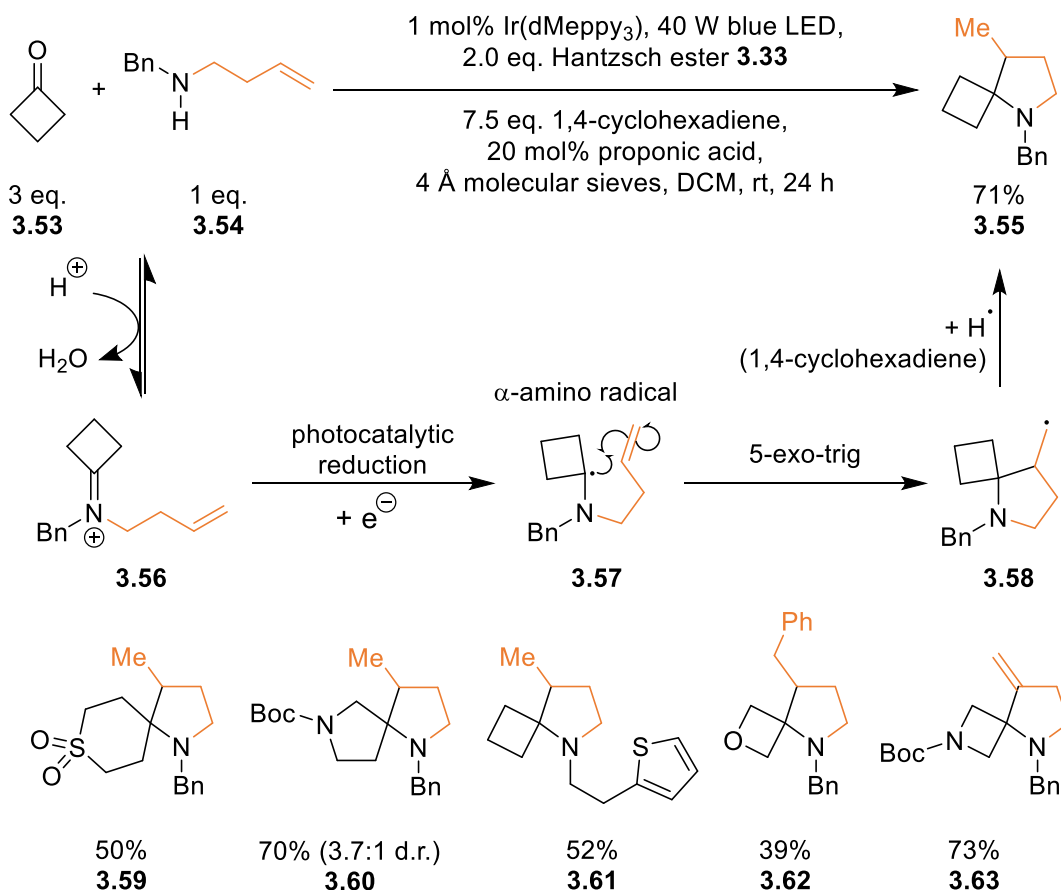
Dialkylketones were explored as the carbonyl component to synthesise α -tertiary amines. Enamines were protonated to generate ketiminium ions *in-situ*. This approach was taken as the condensation of amines and ketones often requires more forcing conditions than with aldehydes, such as azeotropic distillation.^{155,182} In the photochemical reduction, the alkene was also changed to less electrophilic 1,1-diphenylethylene **3.47** (and related adducts) to avoid oligomerisation. α -Substituted tertiary amine **3.48** was isolated in a 59% yield under the optimised photoredox conditions from enamine **3.46**. The extent of the scope with preformed enamines is shown in Scheme 3.14 (**3.49-3.52**). A limited number of enamines were used, likely due to the difficulty in forming them, and yields ranges from 32% to 83%. Both cyclic amines and ketones with heteroatom substituents on the ring were compatible and successfully coupled to bi-arylethylenes.¹⁷³



Scheme 3.14 Photochemical reduction of pre-formed enamines to α -amino radicals and subsequent addition to electron-deficient alkenes by the Gaunt group.¹⁷³

An intramolecular variant of this reaction was published in the following year by the same research group (Scheme 3.15). Homoallylic amines were coupled to cyclic ketones to synthesise spirocyclic tertiary amines under photoredox conditions. Spirocycle **3.55** was synthesised in a 71% yield from commercially available dialkyl ketone **3.53** and allylamine **3.54**. The longer reaction times (24 h) meant that the iminium ion had time to form using molecular sieves *in-situ*. α -Amino radical **3.57** was generated upon photocatalytic reduction of *in-situ* formed iminium ion **3.56** which then underwent 5-exo-trig cyclisation leading to substituted pyrrolidine **3.55**. For this transformation, a more reducing iridium photocatalyst was needed to drive the reaction forward. Excess 1,4-cyclohexadiene was used to facilitate the HAT to the resultant alkyl radical **3.58**, whilst the Hantzsch ester **3.33** was used for the reduction of the Ir(IV) species, generated after SET to the iminium ion, back to the initial Ir(III) photocatalyst.¹⁷⁴

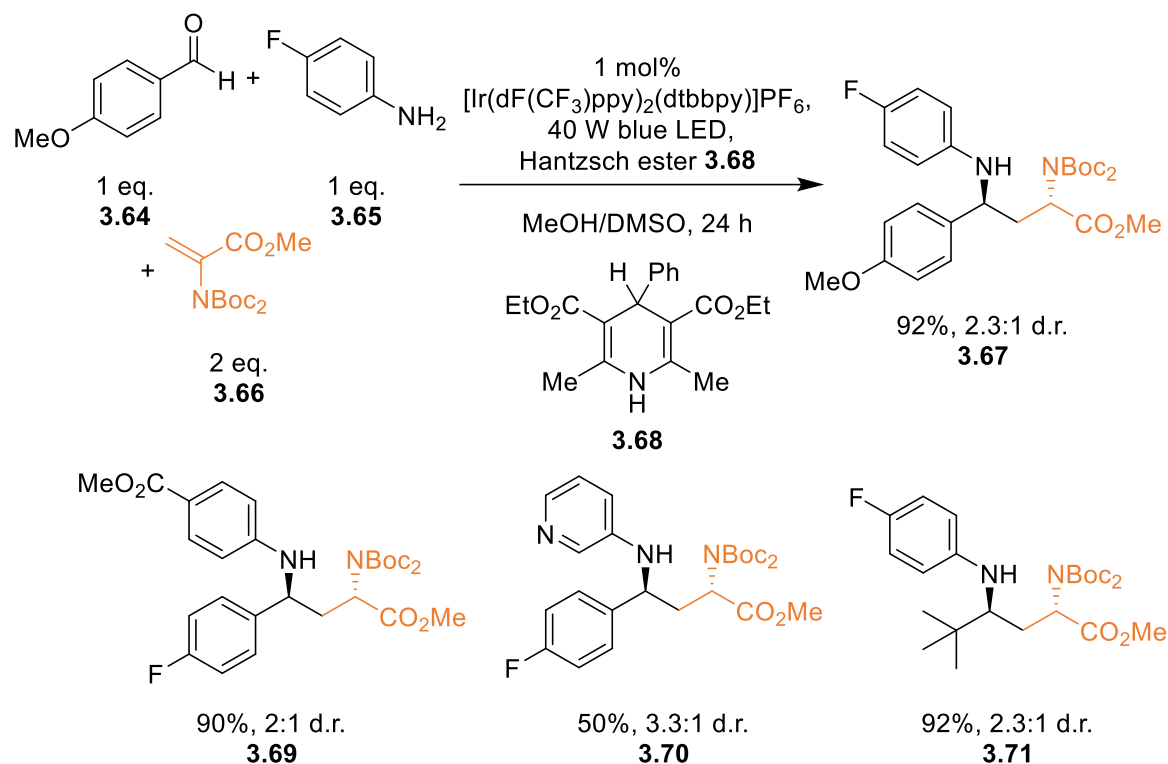
The reaction showed good compatibility with a range of heterocyclic ketones (such as in **3.59** and **3.60**) and allylic amines (such as in **3.61** and **3.62**) achieving high yields for a range of tertiary amine spirocycles. The reaction was also compatible with aldehydes and alkynyl amines to give tertiary amine products containing allyl functionalities (**3.63**) which could be used for further diversification.¹⁷⁴



Scheme 3.15 Photochemical reduction of *in-situ* formed iminium ions to α -amino radicals and subsequent intramolecular addition to alkenes to make spirocyclic amines by the Gaunt group.¹⁷⁴

An analogous approach to the synthesis of secondary amines was published by the Dixon group, in which *in-situ* formed aromatic imines were photocatalytically reduced to α -amino radicals in the presence of a highly reducing iridium photocatalyst and a Hantzsch ester. Aniline adducts were used with a range of commercially available, typically aryl, aldehydes to make the imines and a bis-*N*-Boc dehydroalanine derivative **3.66** was used as the electron-deficient alkene. Diamine **3.67** was isolated in a 92% yield with 2.3:1 d.r. from aldehyde **3.64**, primary amine **3.65** and alkene **3.66** (Scheme 3.16). Improved yields of the 1,3-diamine products were reported when the imine was formed *in-situ* and improved diastereoselectivity was achieved by using a mixed solvent system of methanol/dimethyl sulfoxide (3:2) and a substituted Hantzsch ester (**3.68**). The reaction was compatible with a range of substituted anilines (to make **3.69** and **3.70**) and aldehydes, typically aryl aldehydes. By using anilines and aryl-aldehydes, the reduction potential of the imine would have been higher (more easily reduced) than an “all-alkyl” equivalent. However, the reaction still proceeded with alkyl-aldehydes, such as **3.71**. The scope with respect to the alkene was not explored. Interestingly,

only a 50% yield of **3.70** was achieved after 48 h which implied that imine formation with aminopyridine was less favourable than for the other anilines.¹⁷⁵

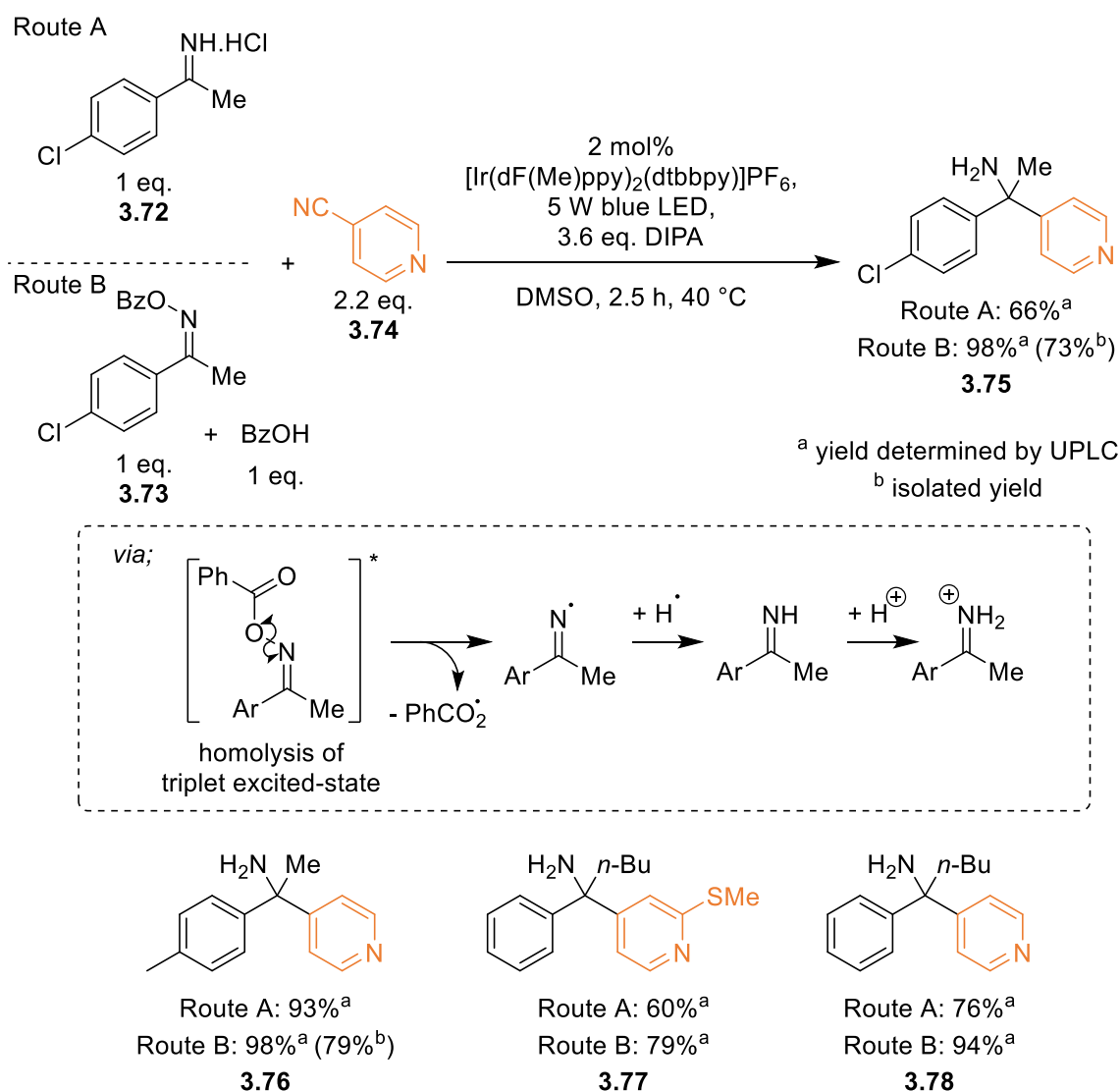


Scheme 3.16 Photochemical reduction of in-situ formed imines to α -amino radicals and subsequent addition to electron-deficient alkenes by the Dixon group.¹⁷⁵

3.1.3.3 Radical Coupling of Photocatalytically Generated α -Amino Radicals with Cyanoarenes

As well as radical addition, reductively generated α -amino radicals have undergone radical-radical coupling reactions. To synthesise α -functionalised primary amines, the Rovis group photochemically reduced pre-formed iminium chloride salt **3.72** in the presence of an iridium photocatalyst, and a cyanoarene **3.74** (Scheme 3.17, Route A). Alternatively, protonated oxime **3.73** was used as an iminium ion precursor (Scheme 3.17, Route B). With oxime **3.73** the yield by ultra performance liquid chromatography (UPLC) of amine **3.75** was 98% (73% yield isolated) but with iminium salt **3.72**, the yield by UPLC was lower at 66%. This one-electron reductive pathway utilised bench stable starting materials to access α -tertiary primary amines. Conditions were initially optimised for the reduction of oximes, but the authors found that they could also reduce iminium chloride salts under the same conditions.¹⁷⁶

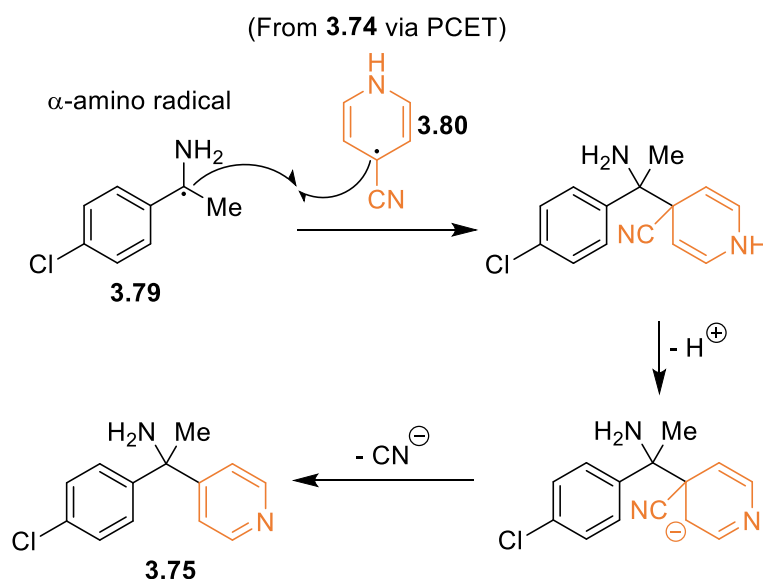
A range of primary amines were synthesised by this method from the corresponding oximes and iminium hydrochlorides. The reaction conditions accommodated changes to the aryl and alkyl groups of the oxime or iminium hydrochloride and led to a range of functionalised cyanoarenes (including **3.76** and **3.77**). Longer alkyl groups, *n*-butyl, resulted in very good yields by either route (**3.78**), however a more sterically demanding *t*-butyl substituents was not compatible with oximes but gave an 84% yield of the primary amine *via* Route A.¹⁷⁶



Scheme 3.17 Photochemical reduction of oximes (A) and iminium hydrochlorides (B) to α -amino radicals and the subsequent radical-radical coupling by the Rovis group.¹⁷⁶

Mechanistically, the α -amino radical **3.79** formed from reduction of either of **3.72** or **3.73** underwent a radical-radical hetero-coupling reaction with a persistent radical **3.80** derived from reduction of **3.74** (Scheme 3.18). The cyanopyridine underwent a proton coupled electron transfer (PCET) step to form radical **3.80**. This radical coupling was possible

because **3.80** is a persistent radical which is relatively stable and will not undergo self-termination, only cross-coupling. Therefore coupling of transient radical **3.79** was possible.¹⁸³ After radical coupling, the cyano group was lost in the re-aromatisation of the pyridine ring to give primary amine product **3.75**.¹⁷⁶ The loss of cyanide means this approach to amines synthesis has an increased safety risk associated with it as cyanide is toxic and the protonated form (hydrogen cyanide) is extremely toxic. The safety concerns linked with this reaction makes it less attractive, particularly on scale.

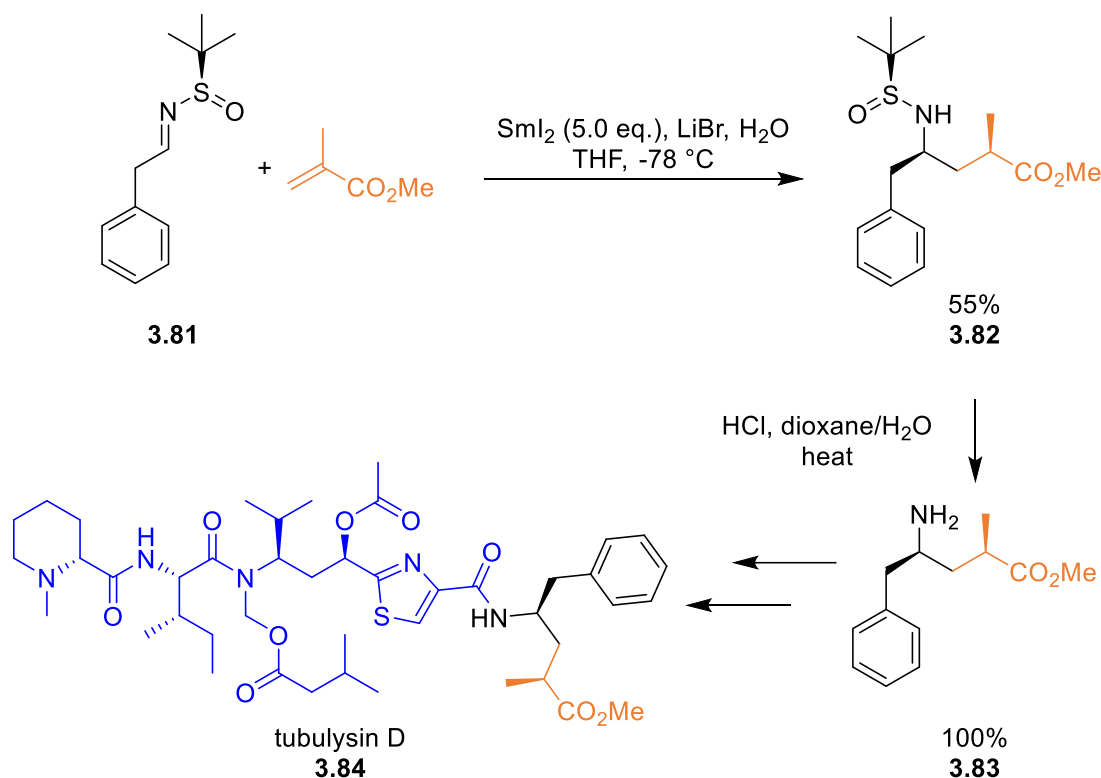


Scheme 3.18 Mechanism for the radical-radical coupling of alkyl radicals derived from cyanopyridines and α -amino radicals formed from the reduction of oximes or iminium hydrochlorides by the Rovis group.¹⁷⁶

3.1.4 Reduction of Iminium Ion and Imines with Samarium(II) Iodide

Related reductive transformations have also been performed with chemical reductants, rather than using photochemistry. Samarium(II) iodide (SmI_2), typically used in stoichiometric amounts, is a versatile reducing agent ($E_{\text{red}} -0.98 \text{ V vs SCE}$) in organic chemistry often used for the generation of ketyl radicals from carbonyl groups.^{184–186} Using SmI_2 , α -amino radicals have been formed from imines and iminium ions, and also from oximes, oxime esters, hydrazones and nitrones. However, due to the lower reactivity of imines relative to carbonyls, a large excess of reagents, high temperatures or additives are often required.¹⁸⁵ Additives such as hexamethylphosphoramide (HMPA), a Lewis base, can lower the reduction potential by *ca* 0.8 V ($\text{SmI}_2(\text{HMPA})_4 E_{\text{red}} -1.75 \text{ V vs SCE}$).^{187,188} The area of imine reduction with samarium(II) remains underexplored.

An early example of a SmI₂ mediated reduction of a *N*-*tert*-butanesulfinyl imine was published by Ellman *et al.* as part of the total synthesis of tubulyisin D **3.84** (Scheme 3.19). With 5 eq. of SmI₂, the imine **3.81** was reduced to the corresponding α -amino radical before subsequent addition into the alkene to give diastereomerically pure **3.82** in a moderate 55% yield. As part of the synthesis, removal of the *N*-*tert*-butanesulfinyl group with acid led to the enantiomerically pure amine **3.83**.¹⁸⁹

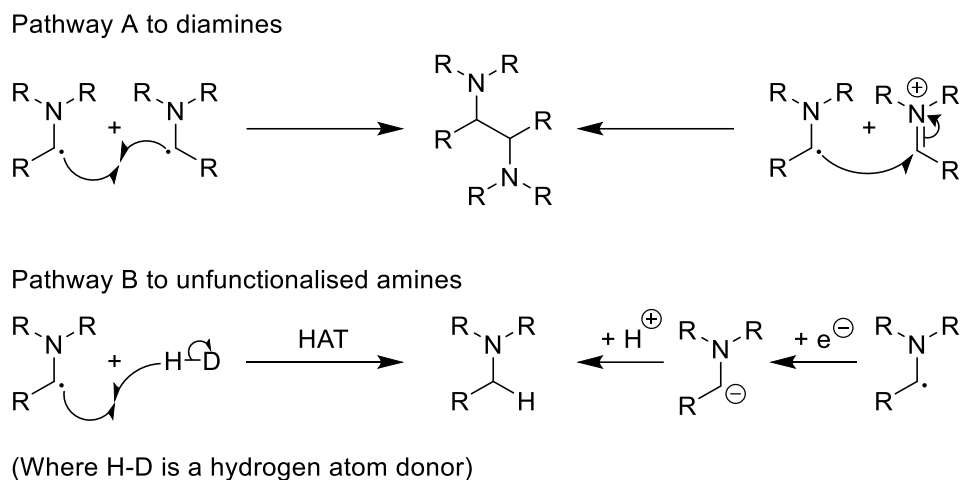


Scheme 3.19 Selected steps in the total synthesis of tubulyisin D showing the reduction of imine **3.81**.¹⁸⁹

3.1.4.1 Samarium(II) Generated α -Amino Radical Homocoupling for the Synthesis of Diamines

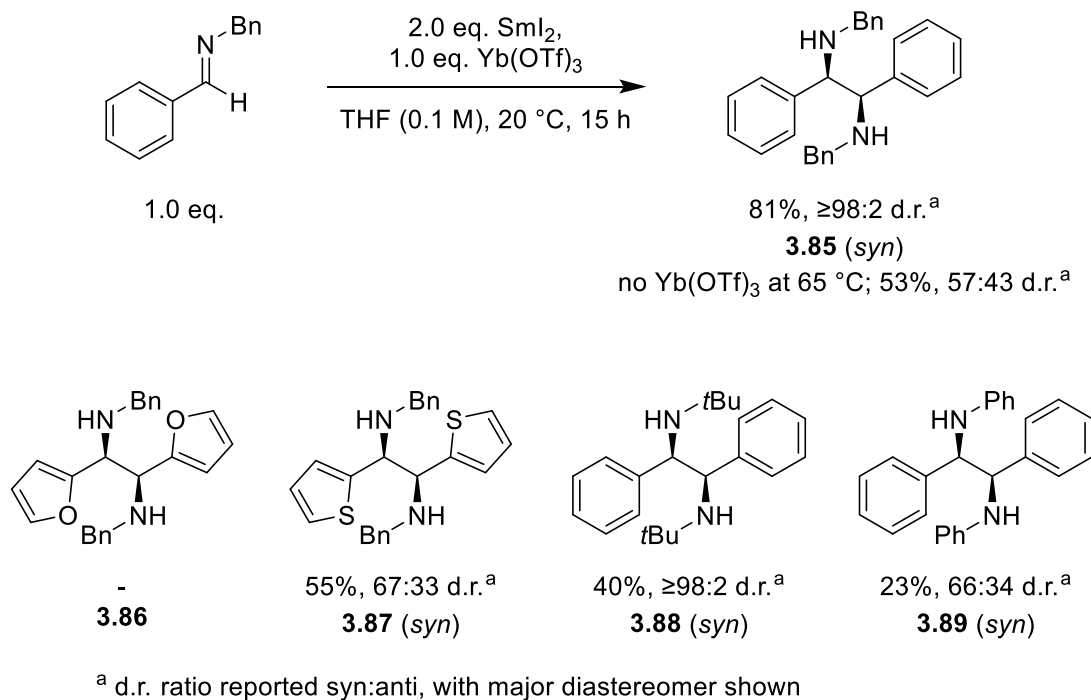
In the examples presented thus far, typically an excess of alkene or aryl radical precursor has been added to ensure the formation of the α -functionalised product. Common side-products include diamines from the homo-coupling of the α -amino radicals or radical addition into the iminium ion or imine π^* molecular orbital (Scheme 3.20 Pathway A), and unfunctionalised amines which failed to couple with alkenes or other radicals. The amines can either form by a HAT process or *via* protonation of an anion generated by over reduction (Scheme 3.20 Pathway B). Whilst such diamines and amines are often unwanted in the

formation of α -functionalised products, some procedures have been optimised to form them in reasonable yields.



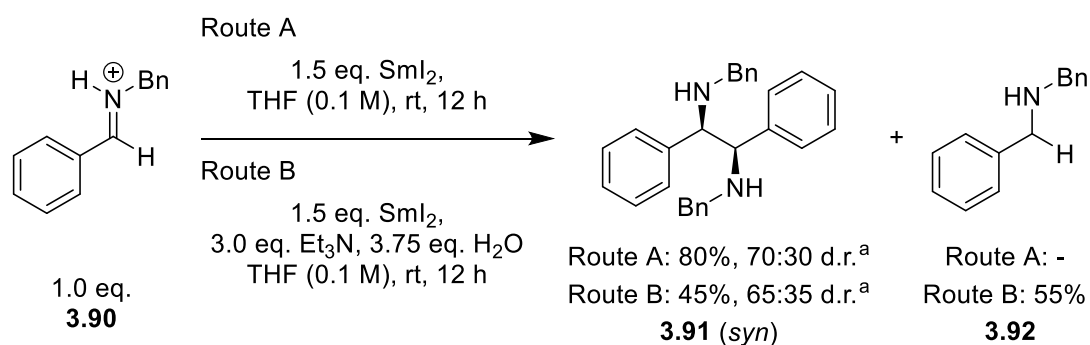
Scheme 3.20 Single electron reductive routes to diamines and amines from imines.

1,2-Diamines have been prepared by reduction of imines using samarium(II) based reagents in intermolecular homo-coupling reactions (Scheme 3.21).¹⁹⁰ The reaction temperature was successfully lowered from 65 °C to 20 °C by using a Lewis acid, Yb(OTf)₃, to coordinate to the imine, aiding reduction.¹⁹¹ The introduction of Yb(OTf)₃ also improved the stereoselectivity of the reaction. The reaction conditions were compatible with a range of aryl substitutions on *N*-benzylimines, achieving up to 85% yield with $\geq 98:2$ d.r. for **3.85** favouring the *syn* diastereomer. Due to the radical nature of the reaction, when a furylimine was used, a complex mixture of products was obtained due to the high reactivity of furans, and the desired product **3.86** was not observed. Lower yields were achieved with thiophenylimine derivatives **3.87**, cyclohexyl substituted heteroaromatics and examples with electron donating groups. With *N*-substituted benzaldimines, it was concluded that an *sp*³ carbon bonded to the nitrogen of the imine was required for both good yields and stereoselectivity (e.g. **3.88**) as only a 23% yield (66:34 d.r.) was achieved for phenyl substituted **3.89** at 20 °C.¹⁹⁰



Scheme 3.21 Reduction of imines with SmI₂ and subsequent radical-radical coupling to form diamines by Raimondi and co-workers.¹⁹⁰

Work by Flowers and co-workers focused on the nature of the samarium(II) reagent for the reduction of aldimines, ketimines and iminium ions.¹⁹² At room temperature, it was found that SmI₂ reduced iminium ion **3.90** to the α -amino radical, which formed diamine **3.91** in an 80% yield preferentially as the *syn* diastereoisomer (Scheme 3.22 Route A). Reactions with iminium ions were complete within 1 minute and thus stronger reducing agents or more forcing conditions were not required. However, when a highly reducing combination of SmI₂/Et₃N/H₂O (which can reduce conjugated double bonds and ketones) was used, along with a 45% yield of diamine **3.91**, amine **3.92** was isolated in a 55% yield (Scheme 3.22 Route B).

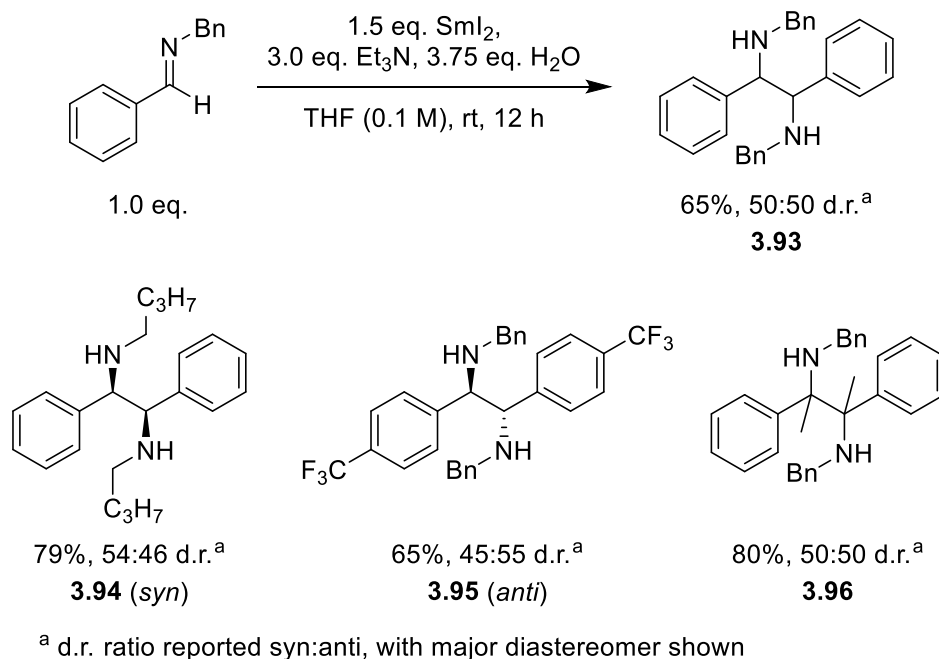


^a d.r. ratio reported syn:anti, with major diastereomer shown

Scheme 3.22 Reduction of iminium ions with SmI_2 and subsequent radical-radical coupling to form diamines by Flowers and co-workers.¹⁹²

Amines, such as **3.92**, are common side products in reductive radical reactions. They are either derived from a HAT to the α -amino radical or, under strongly reducing conditions, a second single electron reduction to the anion can occur followed by protonation. It is likely that with the stronger reducing $\text{SmI}_2/\text{Et}_3\text{N}/\text{H}_2\text{O}$ conditions, the mechanism to **3.92** is through further reduction and protonation.¹⁹² These amines are analogous to the ones obtained by classical two-electron reduction strategies such as reductive amination with borohydride reducing agents.¹⁵⁵ Reduced amine side products are typically avoided by trapping the radical with either an alkene or another radical (as seen the previous photochemical reactions, Section 3.1.3).^{173,176}

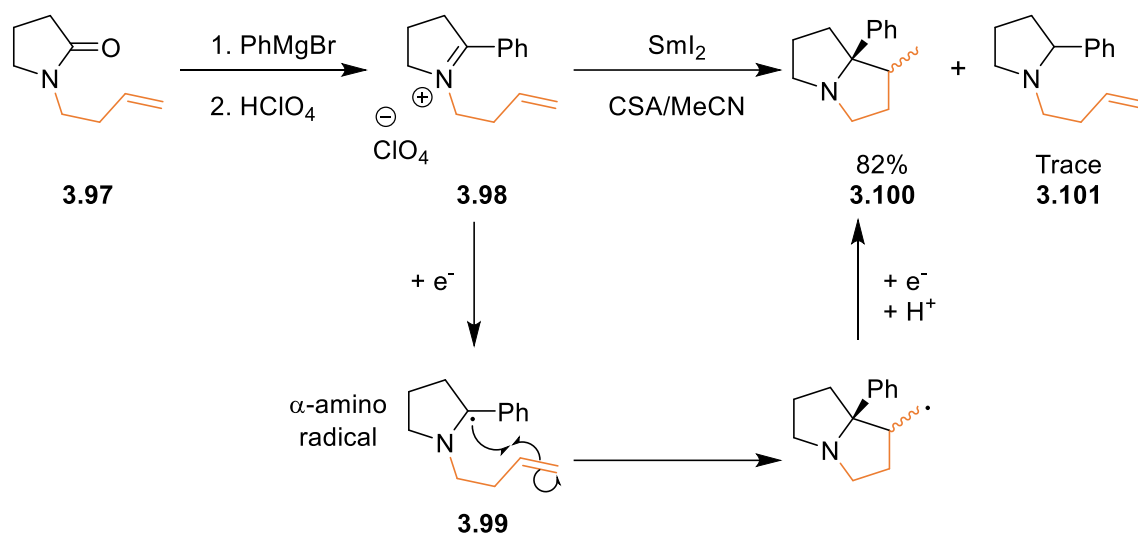
Moving to aldimines and more sterically congested ketimines, more strongly reducing conditions were required such as SmBr_2 , $\text{Sm}\{\text{N}[\text{Si}(\text{CH}_3)_3]_2\}_2$ or the combination of $\text{SmI}_2/\text{Et}_3\text{N}/\text{H}_2\text{O}$ (Scheme 3.23).¹⁹² Using the combination of $\text{SmI}_2/\text{Et}_3\text{N}/\text{H}_2\text{O}$, imines were readily reduced and coupled to form the corresponding diamines, with minimal reduced side-product. Yields of up to 80% were reached for a range of imines and ketimines (**3.93** – **3.96**), but the diastereomeric ratios were worse than those achieved with $\text{Yb}(\text{OTf})_3$.¹⁹²



Scheme 3.23 Reduction of imines with SmI₂ and subsequent radical-radical coupling to form diamines by Flowers and co-workers.¹⁹²

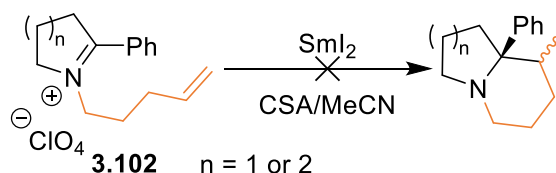
3.1.4.2 Samarium(II) Generated α -Amino Radical Generation and Intramolecular Addition

α -Amino radicals, generated from iminium ions with SmI₂, have undergone intramolecular additions (Scheme 3.24).¹⁹³ Iminium ion **3.98** was generated by treating lactam **3.97** with PhMgBr followed by work-up with aqueous perchloric acid. Then, reaction of perchlorate salt **3.98** with samarium iodide generated α -amino radical **3.99** which underwent a 5-exo-trig cyclisation to give the desired bicyclic amine **3.100** in 82% yield and trace amounts of amine **3.101**, formed by direct reduction of the iminium ion.¹⁹³

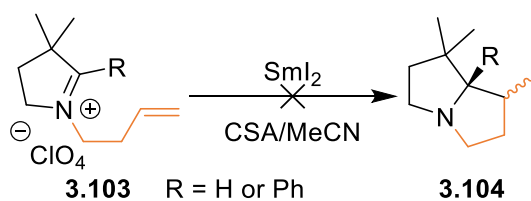


Scheme 3.24 Reduction of imine **3.97** with SmI_2 and subsequent intramolecular radical addition.¹⁹³

The scope of this cyclisation reaction was limited to 5 and 6 membered lactams, as these underwent rapid, favourable intramolecular cyclisations, and the cyclisation failed when *N*-4-pentenyl derivatives **3.102** were used (Scheme 3.25). Increased steric bulk, in the form of dimethyl groups **3.103**, slowed the cyclisation down and product **3.104** was not observed (Scheme 3.26).¹⁹³



Scheme 3.25 Reduction of imine **3.102** with SmI_2 which failed to undergo intramolecular addition.¹⁹³



Scheme 3.26 Reduction of imine **3.103** with SmI_2 which failed to undergo intramolecular addition.¹⁹³

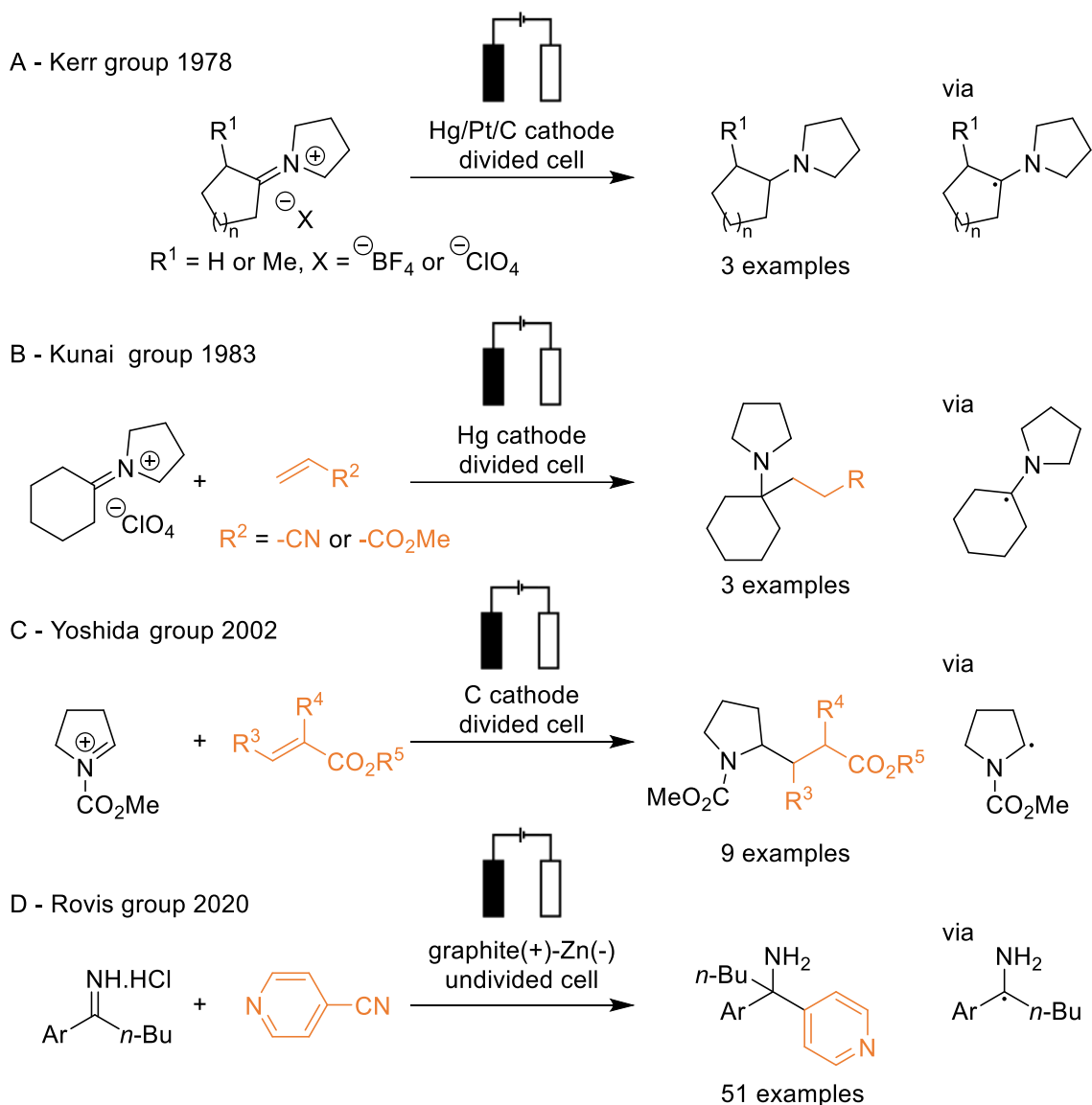
The approaches presented using samarium(II) reagents have delivered the desired amine products in good to excellent yields and show a reasonable level of functional group tolerance. Much of the scope focused on imines or iminium ions with at least one aryl

substituent in efforts to increase the reduction potential so samarium could facilitate reduction. Radicals formed have either undergone intermolecular addition into alkenes, intermolecular homo-couplings or intramolecular radical addition into alkenes. Due to the low reactivity of imines with respect to reduction, at room temperature, a Lewis acid additive often required to achieve the reduction products. Because iminium ions have higher reduction potentials compared to imines, the reductions often proceeded rapidly at room temperature without the need for additives, although stoichiometric amounts of reducing agents were still required.

3.1.5 Electrochemical Reductions of Iminium Ions

Synthetic electrochemistry offers an alternative to previously described methods for the generation of α -amino radicals as it avoids expensive iridium catalysts, forcing temperatures and stoichiometric amounts of reducing agents. Using electrons as reagents, imines and iminium ions can be reduced directly to α -amino radicals in a more sustainable way and with good atom economy.

A large amount of literature has been published detailing the electrochemical properties of iminium ions with various alkyl and aryl substituents.^{177,178} Preparative electrochemical reductions at controlled potentials have been used as methods of elucidating reduction pathways. A few electrochemical approaches, investigating the scope of amine synthesis *via* α -amino radicals, have also been reported (Scheme 3.27).^{194–197}

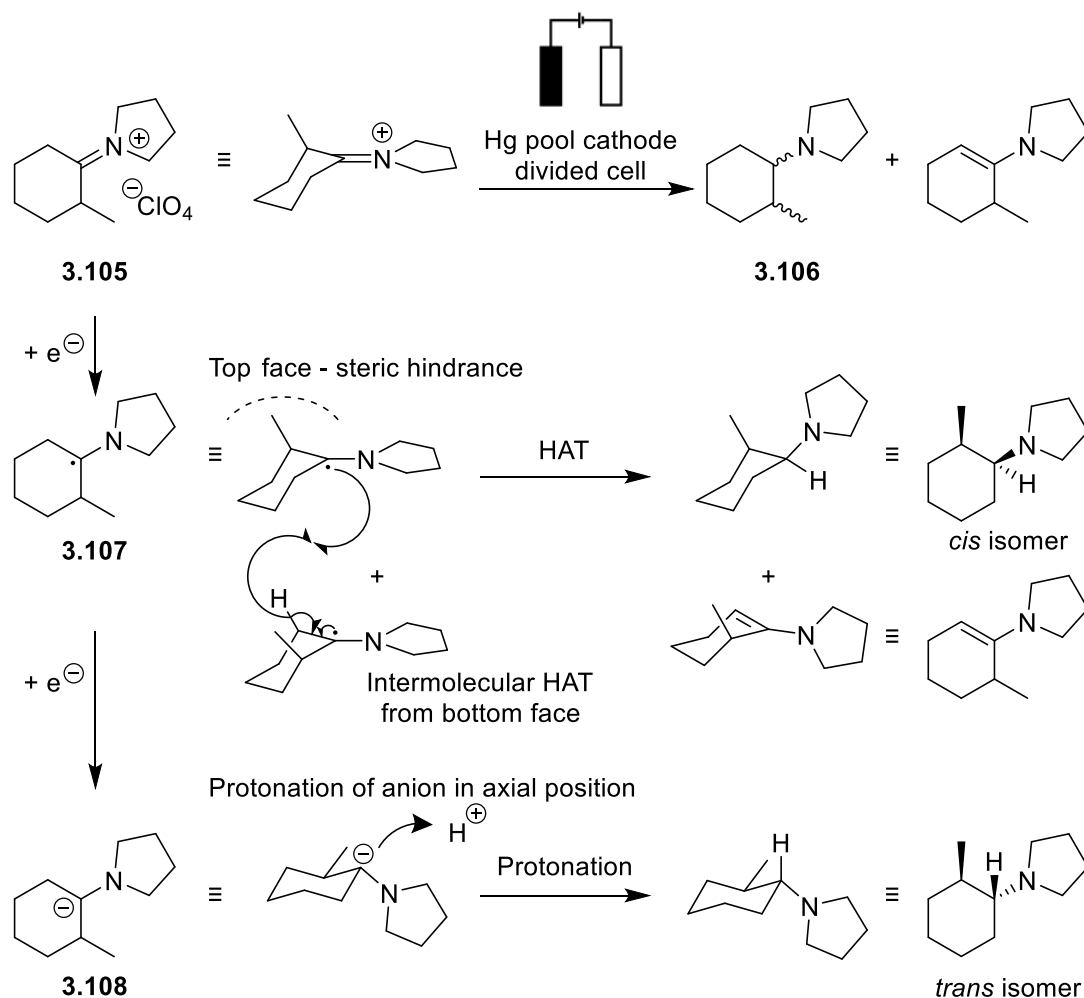
Scheme 3.27 Various examples of electrochemically reducing iminium ions.^{194–197}

3.1.5.1 Mechanism for the Electrochemical Reduction of Iminium Ions to α -Amino Radicals

Work published by Savéant and co-workers used polarography and cyclic voltammetry to determine the reduction potentials for a range of iminium ions.¹⁷⁸ Reduction potentials have been reported for *N*-cycloalkylpyrrolidine-derived iminium ions, some of which, recorded by Kovacic and co-workers, have been included in Figure 3.3.^{177,194,195} The data suggests the largest changes in reduction potential are observed by changing the substituents on the carbon of the C=N group.

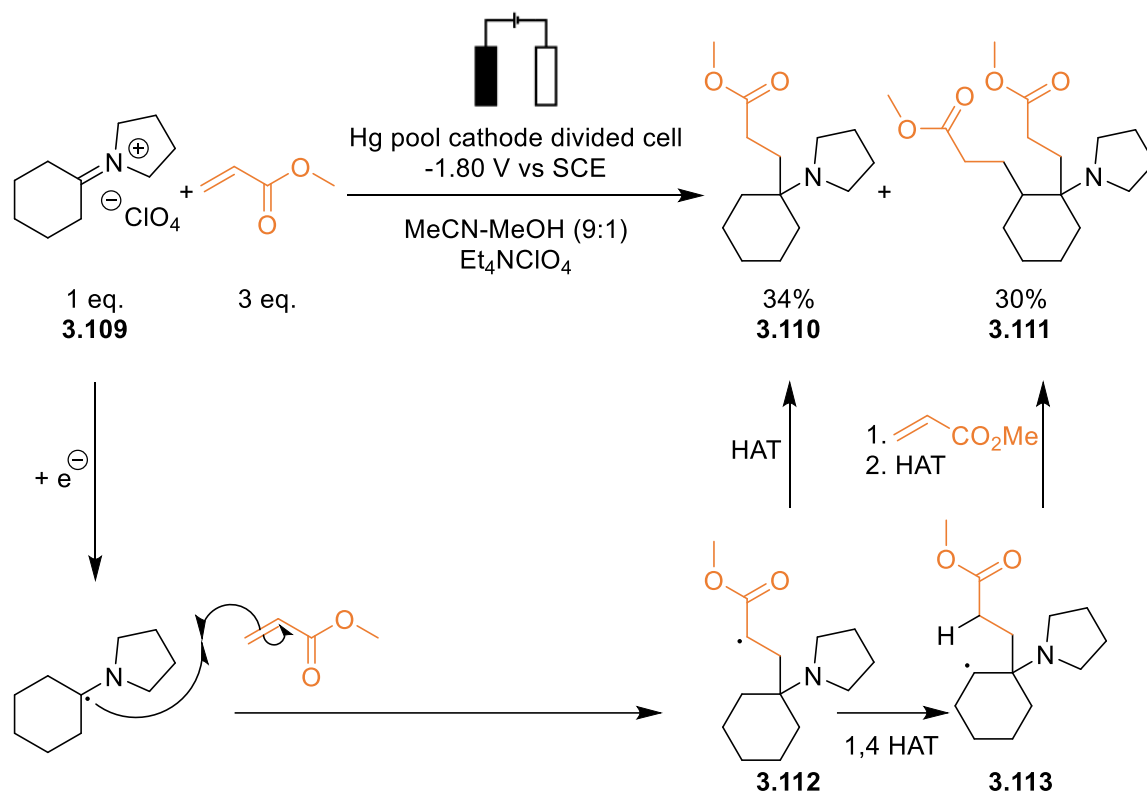
The Savéant group found that for an iminium ion where both carbon substituents were aromatic, in the absence of oxygen, a stabilised free radical could be detected by EPR upon electrochemical reduction.¹⁷⁸ The introduction of oxygen subsequently destroyed the α -amino radical, resulting in the formation of benzophenone. Other iminium ions, that did not have aromatic substituents on the carbon atom, underwent radical-radical homo-coupling reactions upon electrochemical reduction and the α -amino radical could not be observed spectroscopically.¹⁷⁸

Separate work by the Kerr and Kunai groups used polarography, cyclic voltammetry, and the results of controlled potential electrolysis to identify the key steps in the reduction of iminium ions.^{194,195} Kerr and co-workers particularly focused on the reduction of substrate **3.105** as it resulted in a tertiary amine **3.106** as a mixture of diastereoisomers (Scheme 3.28).¹⁹⁴ As the conditions were changed, the ratio between the *trans* and *cis* stereoisomers was measured and used to provide indirect evidence for one-electron and two-electron reduction pathways. The authors reasoned that the *cis* product was derived from an intermolecular HAT to α -amino radical **3.107**. The hydrogen atom was either from a second equivalent of α -amino radical **3.107** (as shown in Scheme 3.28) or from iminium ion **3.105**. It was delivered on the bottom face, resulting in the *cis* isomer, as the methyl substituent hindered transfer on the top face. The *trans* product was hypothesised to be derived from an intermediate anion **3.108**. The lone pair of electrons of the anion can either be in the axial or equatorial position. However, the most stable anion will have the lone pair of electrons in the axial position, with the methyl group and pyrrolidine ring *trans* to each other. This means that protonation of the axial lone pair will retain the stereochemistry, resulting in the *trans* diastereoisomer. Typically a high *cis:trans* ratio was observed and thus the authors concluded that the mechanism is likely radical.¹⁹⁴



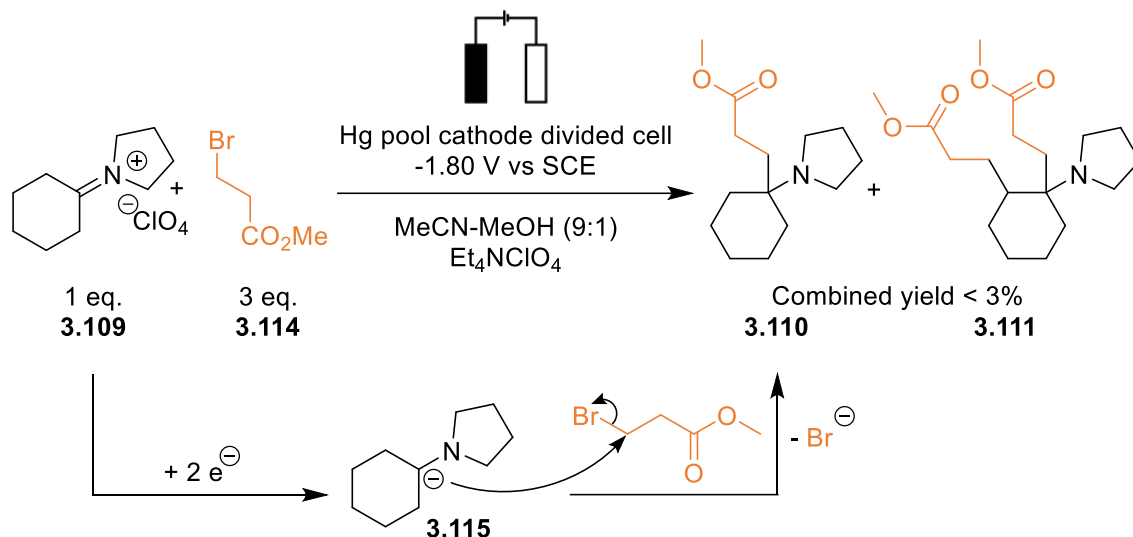
Scheme 3.28 Proposed pathways to *cis* and *trans* product via electrochemical single electron reductions of iminium ion **3.105**.¹⁹⁴

Kunai and co-workers used electron-deficient alkenes to trap radicals generated from the electrochemical reduction of iminium ions and protonated imines (Scheme 3.29).¹⁹⁵ Controlled potential electrolysis of iminium perchlorate **3.109** in the presence of methyl acrylate resulted in a 34% yield of α -functionalised product **3.110**. Product **3.111** (30% yield) was believed to be formed from a 1,4-hydrogen atom transfer, forming radical **3.113**, prior to addition to a second equivalent of acrylate. As the paper only reported IR and MS fragmentation data for compound **3.111**, there is a possibility this could have been a regioisomer. As opposed to undergoing an intramolecular 1,4 HAT step, alkyl radical **3.112** could have added directly into another equivalent of methyl acrylate prior to HAT. However due to the lack of spectroscopic data, the structure could not be confirmed either way.¹⁹⁵



Scheme 3.29 Electrochemical reduction of iminium ion **3.109** and subsequent radical addition into methyl acrylate by Kunai and co-workers.¹⁹⁵

Product **3.110** could either be derived from radical addition (as shown in Scheme 3.29) or Michael addition of an anion to methyl acrylate. To probe the reaction, methyl acrylate was replaced by methyl-3-bromopropionate **3.114** (Scheme 3.30).¹⁹⁵ The combined yield of **3.110** and **3.111** was less than 3%. This provided further evidence that the reduction likely proceeded *via* α -amino radicals and thus a radical addition mechanism as previously discussed was proposed. If high yields of the amines were achieved, then the mechanism could have proceeded *via* an anion **3.115** as the intermediate would be capable of S_N2 -type nucleophilic substitution with the electron-deficient alkene.¹⁹⁵



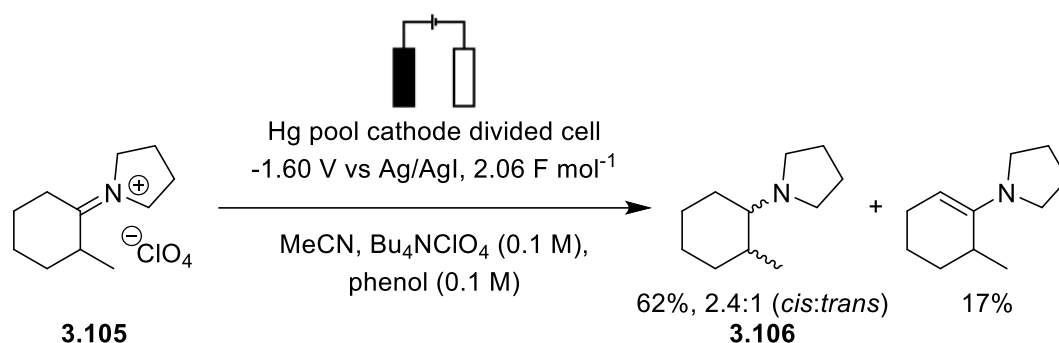
Scheme 3.30 Electrochemical reduction of iminium ion **3.109** in the presence of **3.114** to determine if the reaction proceeded through a radical or anion mechanism by Kunai and co-workers.¹⁹⁵

The electrode facilitates the single electron transfer, and as such, the electrode material play an important role in the electrolysis.¹⁴⁵ Both research groups typically used mercury hanging drop electrodes (MHDE) to reduce iminium ions, achieving up to 62% yields for amine **3.106**.^{194,195} In the electrolysis of **3.105**, Kerr and co-workers observed a high *cis:trans* ratio for amine **3.106** with graphite electrodes (5.3:1.0, 37% yield) and a low *cis:trans* ratio for amine **3.106** with platinum electrodes (2.0:1.0, 42% yield). The authors hypothesised that the increase in *trans* isomer was due to adsorption of the radical onto the metal electrode surface as a low amount of *trans* isomer was observed for graphite. Adsorption of radicals is a phenomenon not observed with photoredox or chemical reductions. The proposed mechanism for increased *trans* isomer was that adsorption of the radical onto the electrode could facilitated the second electron reduction to an anion, which as previously discussed would be protonated with the lone pair of electron of the anion in the axial position, therefore resulting in an increase in the *trans* isomer (Scheme 3.28).¹⁹⁴ The work described has shown that the electrochemical reduction of iminium ions proceeds *via* α -amino radical intermediates and that the radicals formed can adsorb onto the electrode surface.

3.1.5.2 Addition of Electrochemically Generated α -Amino Radicals to Alkenes

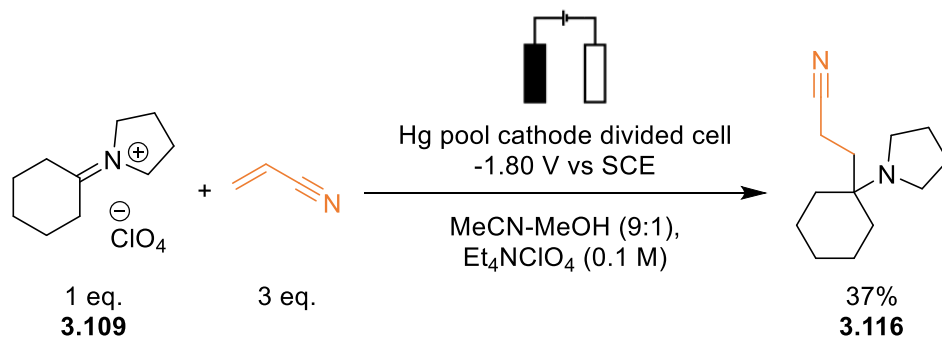
From the work described by the Kerr and Kunai groups (reactions A and B in Scheme 3.27), there was only a handful of examples in which amines were synthesised. Neither paper focused on applying the methodology for amine synthesis; rather, these studies used the

results of electrolysis to understand the mechanism of reduction.^{194,195} The highest yield for amine **3.106** was achieved when **3.105** (0.1 M) was electrolysed at a hanging mercury drop electrode (-1.6 V vs Ag/AgI) (Scheme 3.31).¹⁹⁴ Tetrabutylammonium perchlorate (0.1 M) in acetonitrile was used as the electrolyte solution and phenol (0.1 M) was added as a source of protons. The reaction was performed until the current dropped from 300 mA to zero (2.06 F mol⁻¹) and the yield of amine **3.106** was 62% by gas-liquid chromatography (GLC) in a 2.4:1 *cis:trans* ratio.¹⁹⁴



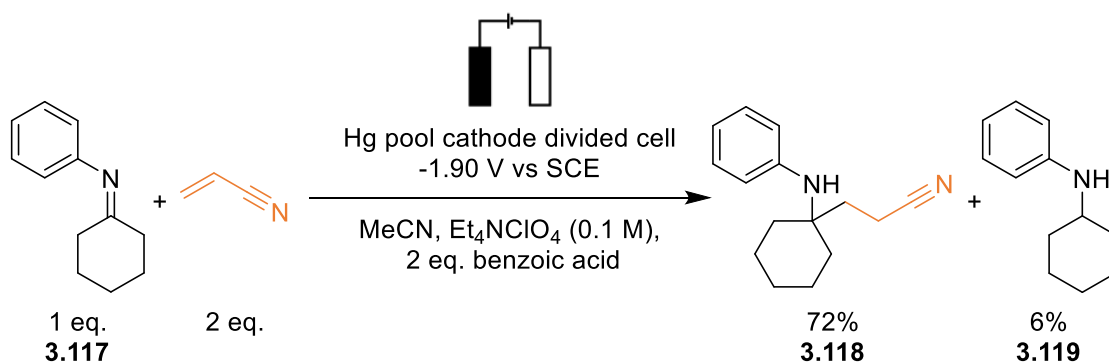
Scheme 3.31 Electrochemical reduction of iminium ion **3.105** by Kerr and co-workers.¹⁹⁴

Amine **3.116** was successfully synthesised in a 37% yield when 10% methanol in acetonitrile was used (Scheme 3.32).¹⁹⁵ The electrolysis of *N*-cyclohexylidene-pyrrolidinium perchlorate (**3.109**, 0.1 mmol) was performed in a divided cell with a mercury pool cathode in acetonitrile or acetonitrile/alcohol mixture (100 mL). A divided cell could have been used to prevent the oxidation of amine **3.116** to a radical cation. Acrylonitrile (3 eq., 0.3 mmol) was used as the electron-deficient alkene and the cell potential was set at -1.80 V vs saturated calomel electrode (SCE). An advantage of synthetic electrochemistry over using photocatalysts is that the cell potential can be tuned. The cyclic voltammograms and polarographic data showed a reduction peak for **3.116** at around -1.80 V vs SCE and that acrylonitrile and methyl acrylate had reduction potentials below -2.2 V vs SCE. Therefore, setting the cell potential to -1.80 V vs SCE, selectively reduced the iminium ion over the alkene. When the current dropped (after *ca.* 1 F mol⁻¹ of electricity), the reaction was stopped.¹⁹⁵



Scheme 3.32 Electrochemical reduction of iminium ion **3.109** and subsequent radical addition into acrylonitrile by Kunai and co-workers.¹⁹⁵

Imines were also successfully electrolysed to give α -functionalised products in higher yields. For the electrolysis of *N*-cyclohexylideneaniline (**3.117**, 0.1 mmol), reactions were conducted in the same electrochemical set-up as **3.109**.¹⁹⁵ Benzoic acid (2.0 eq.) was used to protonate the imine, shifting the reduction potential to a less negative value, making it easier to reduce. The cell potential was set at -1.90 V vs SCE. With acrylonitrile (2.0 eq.), a 72% yield of **3.118** was isolated (Scheme 3.33). This reaction also gave a 6% yield of reduced product **3.119**, which was observed in a 66% yield in the absence of acrylonitrile.¹⁹⁵

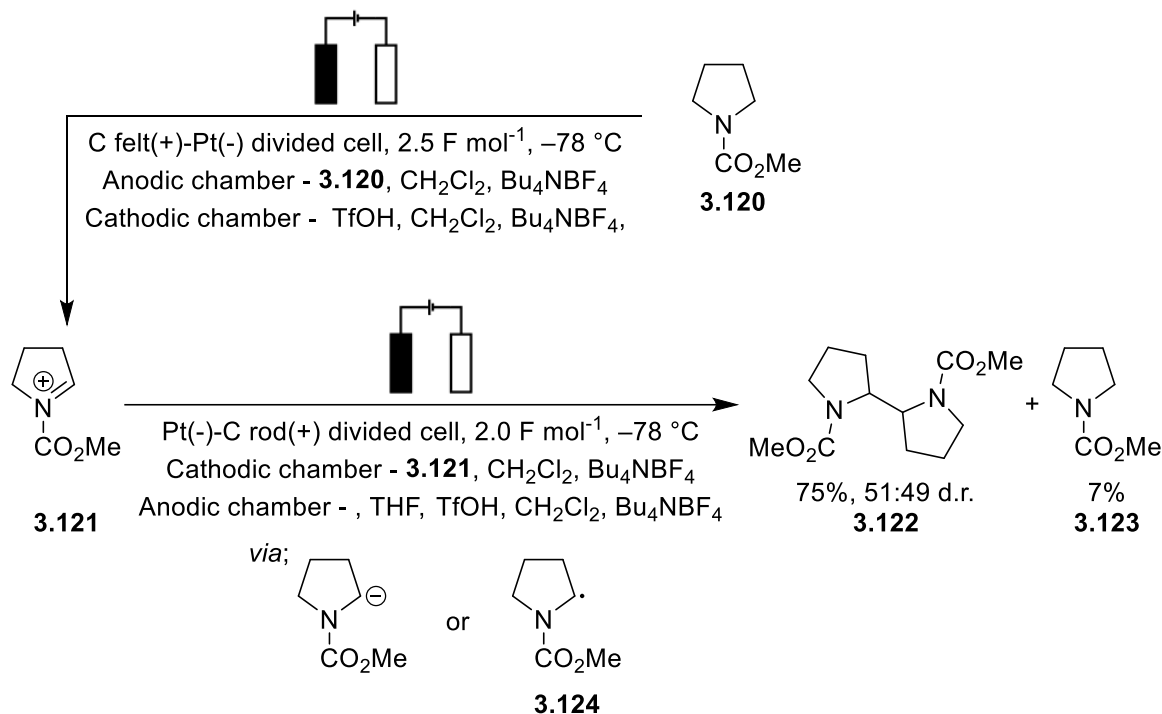


Scheme 3.33 Electrochemical reduction of imine **3.117** and subsequent radical addition into acrylonitrile by Kunai and co-workers.¹⁹⁵

A method of electrochemical α -amino radical formation from iminium ion reduction, which applied a “cation pool”, was developed by Yoshida and co-workers in 2002. In a cation pool, high concentrations of cations are generated by anodic oxidation, typically at low temperatures to avoid side reactions, prior to further reactions.^{198,199} Initially, anodic oxidation of *N*-acyl amine **3.120** at a carbon felt electrode resulted in the formation of

iminium ion **3.121**.¹⁹⁶ The cathodic process was the reduction of protons to hydrogen at a platinum cathode. The reduction potential of acyliminium ion **3.121**, determined by cyclic voltammetry, was -0.85 V vs Ag/AgCl and therefore easier to reduce than the previously reported “all-alkyl” iminium ions, likely due to conjugation in the methyl carbamate group (Figure 3.3). Iminium ion **3.121** was generated anodically and then cathodically reduced. Protected diamine **3.122** was isolated in a 75% yield with 51:49 d.r. (Scheme 3.34).¹⁹⁶ Tetrahydrofuran was added to the anodic chamber of the divided cell prior to the second electrolysis as the sacrificial electron donor.¹⁹⁶

A control reaction was performed using zinc metal as a two-electron reductant from which a 54% yield of amine **3.123** was obtained. This result implied that the electrolysis proceeded *via* a one-electron radical pathway as different major products were observed.¹⁹⁶ Since α -amino radical **3.124** was secondary, and located on the pyrrolidine ring, it was less sterically hindered than in the examples by the Kerr and Kunai groups which proceeded through tertiary radical intermediates. This means radical **3.124** could readily homo-couple to give product **3.122**, whereas in the electrolysis of **3.105** and **3.109**, homo-coupling was not observed.^{194–196}

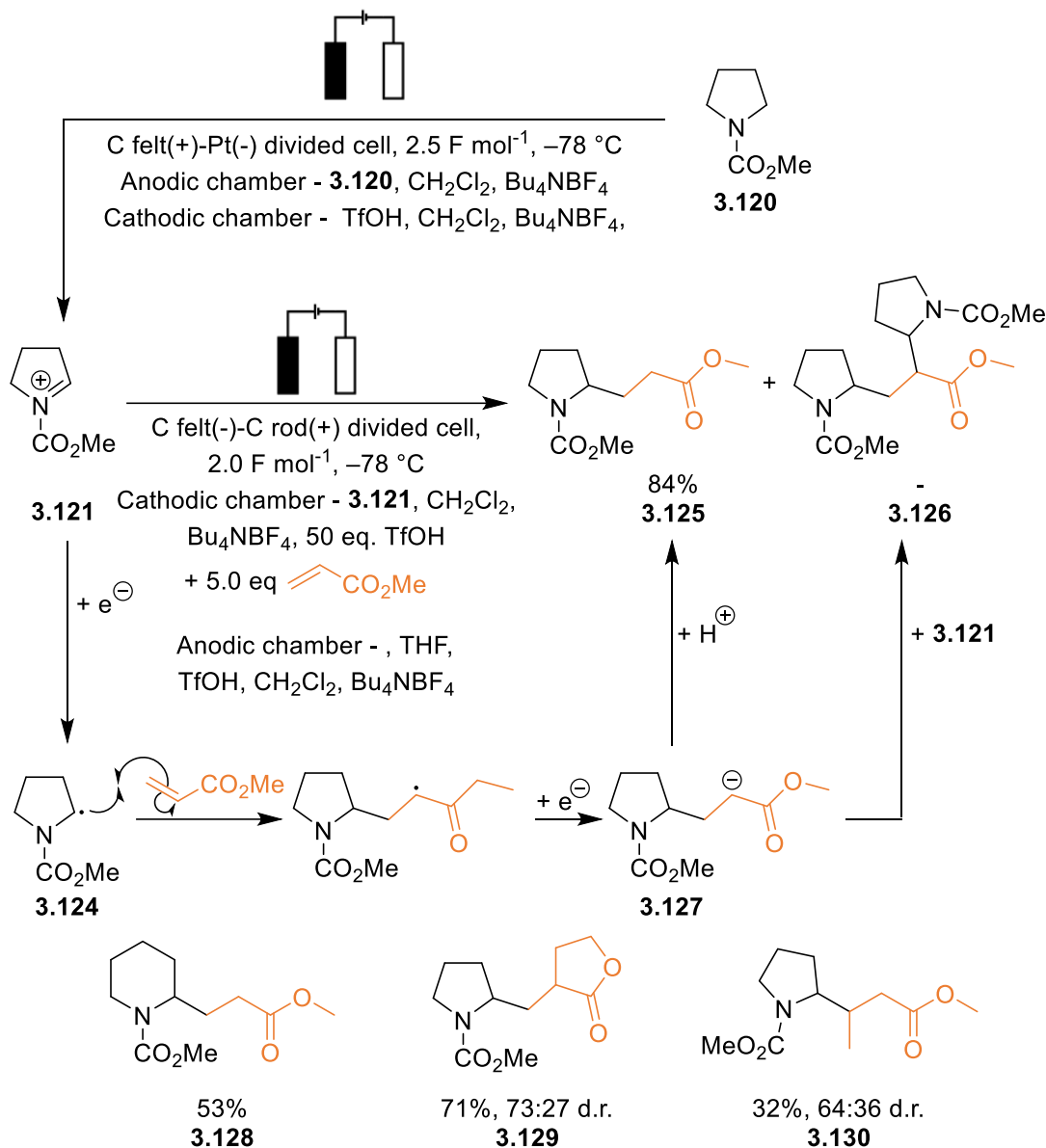


Scheme 3.34 Cation pool oxidative generation of iminium ion **3.121** and subsequent electrochemical reduction by Yoshida and co-workers.¹⁹⁶

The electrolysis of acyliminium ions in the presence of a range of acrylates was then studied by Yoshida and co-workers (Scheme 3.35). Tetrahydrofuran was used as the electron donor but unlike in the homo-coupling reaction, a carbon felt cathode was used to perform the desired reduction of acyliminium ion **3.121**. The yield of **3.125** (84%) was significantly improved, and side product **3.126** was avoided by using between 5-8 eq. of acrylate and the addition of up to 50 eq. trifluoromethanesulfonic acid (TfOH). TfOH acted as a source of protons to trap anion **3.127** and prevent reaction with acyliminium ion **3.121** leading to side product **3.126**.¹⁹⁶

As in the work by the Kunai group two pathways for addition to the alkene can be proposed.¹⁹⁵ As the amount of amine **3.125** did not increase with increased TfOH, Michael addition of the anion was rejected in favour of Giese radical addition, which further supports the previous conclusions.

Good yields for coupled products were achieved with other carbamates (**3.128**) and simple acrylates (**3.129**). However, more sterically congested alkenes resulted in lower yields (**3.130**). The overall transformation from amine **3.120** to **3.125** provides an attractive method for amine synthesis through C-H functionalisation α -to nitrogen under mild conditions.¹⁹⁶



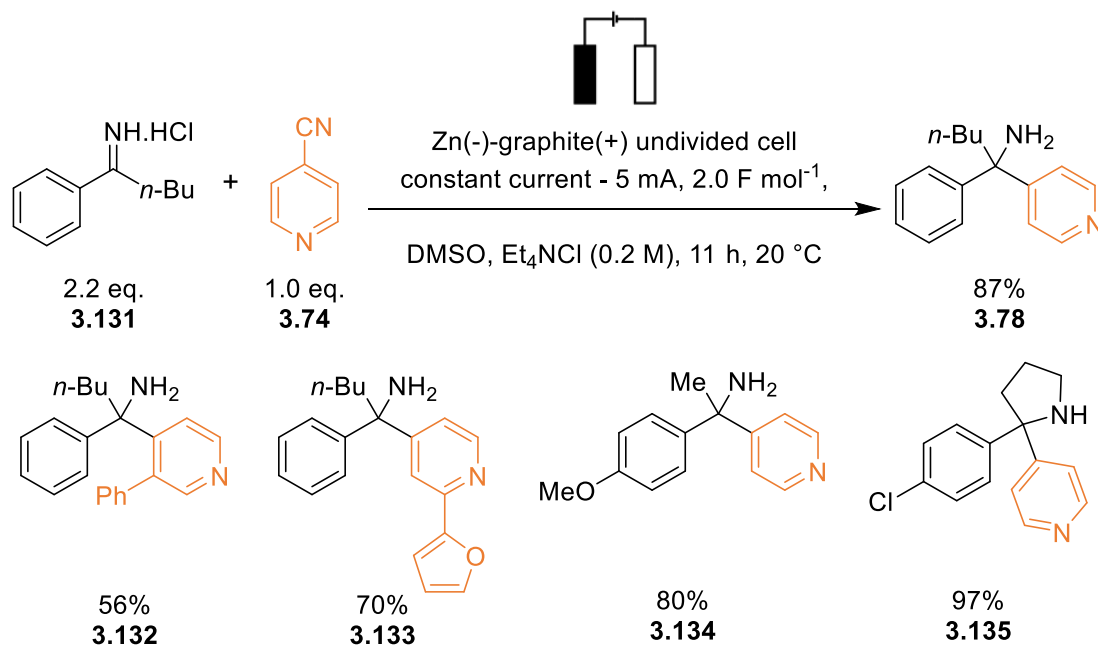
Scheme 3.35 Cation pool oxidative generation of iminium ions and subsequent electrochemical reduction in the presence of electron-deficient alkenes by Yoshida and co-workers.¹⁹⁶

3.1.5.3 Radical Coupling of Electrochemically Generated α -Amino Radicals with Cyanoarenes

In 2020, the electrochemical reduction of iminium ions to α -amino radicals and subsequent radical-radical coupling to persistent radicals formed from cyanopyridines was reported (Scheme 3.36).¹⁹⁷ The reduction was performed at a zinc working electrode. Cathodes with low overpotentials for the reduction of protons to hydrogen (e.g. platinum) resulted in poor yields of the product due to competing proton reduction. Aromatic iminium ions were used in the electrolysis. Relative to tetra-alkyl iminium ions, the reduction potentials were less

negative (*ca.* -1.02 V vs SCE), and therefore were easier to reduce. Graphite was used as the anode. The authors hypothesised that the oxidative process likely involved the oxidation of chloride to a chlorine radical (Cl^- to Cl^\cdot) which either abstracted hydrogen to form hydrogen chloride or coupled to form chloride gas.¹⁹⁷ Unlike in previous examples, this work successfully used a commercially available undivided cell to reduce iminium ion **3.131**, providing a more operationally simple approach to amine synthesis rather than a divided cell.²⁸ As primary amines are harder to oxidise than tertiary amines, an undivided cell was likely not needed.¹²⁰

As in the photochemical equivalent (Scheme 3.17), scope for this reaction was explored. Moderate to excellent yields of the primary and secondary amines were achieved with a range of iminium ions and cyanoarenes. Whilst the reaction conditions were not compatible with non-heterocyclic arenes, both *meta*- and *ortho*-substituents gave good yields for quite sterically hindered α -tertiary primary amines (**3.78** and **3.132-3.133**). The iminium ion scope was also explored. The aryl component could have both electron-donating and withdrawing substituents (**3.134**) and *N*-alkyl iminium ions gave excellent yields for very hindered secondary amines (**3.135**) (Scheme 3.36).¹⁹⁷



Scheme 3.36 Electrochemical reduction of iminium ions in the presence of cyanoarenes by the Rovis group.¹⁹⁷

3.1.5.4 Summary of Electrochemical Iminium Ion Reductions

Much of the electrochemical work on iminium ion reduction described focuses on the mechanism of iminium ion reductions and therefore the reaction and the nature of the α -amino radicals are well understood. The reduction potentials for iminium ions have been measured by cyclic voltammetry and typically iminium ions bearing aryl substituents require less reducing conditions than alkyl iminium ions. Iminium ions have been successfully reduced at the surface of mercury, graphite, and zinc cathodes. Electrolysis has been performed in both divided and undivided cells which implies that the amines formed are relatively electrochemically stable under the applied conditions.

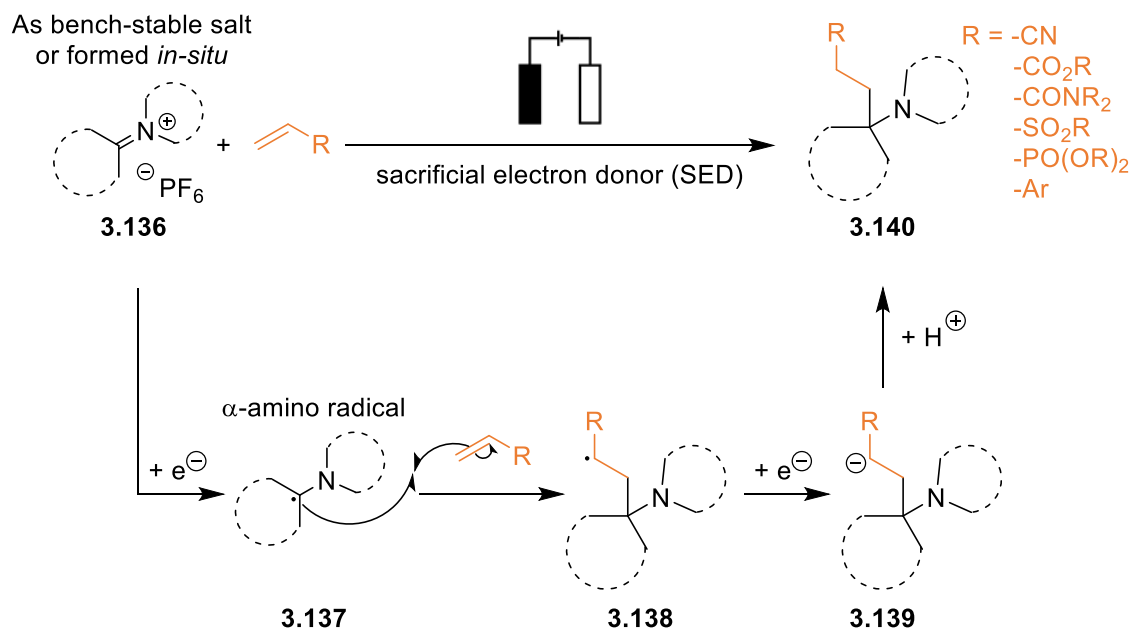
There is currently a gap in the literature for a synthetic electrochemical approach to tertiary alkyl amine synthesis which couples α -amino radicals with a range of different electron-deficient alkenes. Unlike in the photochemical reduction of iminium ions, the synthetic scope of electrochemical iminium ion reduction and coupling with Michael acceptors remains somewhat underexplored.^{173,175} The Rovis group has shown that a range of primary and secondary amines can be made by reduction of iminium ions and radical-radical coupling of the α -amino radicals with radicals derived from cyanoheteroarenes.¹⁹⁷ Simple electron-deficient alkenes, such as acrylates and acrylonitriles, have been added and used to trap the radicals in moderate to good yields which has shown that α -amino radicals are nucleophilic.

3.1.6 Chapter Aims

Reductive approaches to amine synthesis have been exploited as convenient methods for the synthesis of highly functionalised primary, secondary and tertiary alkyl and aryl amines. The reaction has shown high functional group tolerance and has been used for the late-stage functionalisation of pharmaceutical agents. α -Amino radicals have been generated photochemically, chemically or by electrolysis and have subsequently undergone a variety of reactions from radical-radical homo-couplings and hetero-couplings to radical addition with a range of electron-deficient alkenes. Synthetically, the scope for the reaction has been well explored for the photochemical generation of α -amino radicals. In contrast, the electrochemical variant remains significantly underexplored.

The aim of this work is, building on the historical electrochemical understanding, to develop an effective synthetic electrochemical procedure for the reduction of iminium ions and subsequent radical addition to alkenes. In particular, the synthesis of aliphatic tertiary amines with sterically hindered α -tertiary carbons will be developed. This should be a useful methodological development since the published electrochemical literature suggests that using electrons as reagents enables the generation of reactive intermediate α -amino radicals. By using synthetic electrochemistry, a suitably reducing environment may be generated to reduce “all-alkyl” iminium ions using mild reaction conditions, without expensive iridium photocatalysts or stoichiometric amounts of reductants and in good atom economies. Scheme 3.37 Proposed mechanism for the electrochemical reduction of various iminium ions in the presence of electron-deficient alkenes. summarises the proposed scope of this chapter with a range of alkenes and iminium ions typically derived from cyclic ketones and amines.

The proposed mechanism is a single electron reduction of the iminium ion **3.136** at the cathode to an α -amino radical **3.137** followed by addition to an electron-deficient alkene to give alkyl radical **3.138**. As the cathode should be reducing enough to form an anion, the alkyl radical will then undergo a second cathodic reduction to form anion **3.139**. This will then be protonated, delivering amine **3.140** (Scheme 3.37). This approach will avoid the addition of a HAT agent, which is required in the photochemical methodologies.



Scheme 3.37 Proposed mechanism for the electrochemical reduction of various iminium ions in the presence of electron-deficient alkenes.

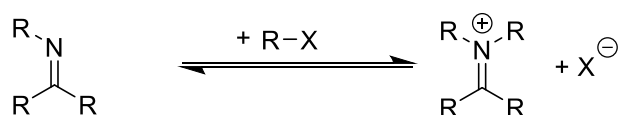
To achieve this, a simple and general method of forming iminium ion starting materials will be used which can be applied to make a range of cyclic and acyclic iminium ions and a variety of functional groups. The feasibility of using either an *in-situ* method of iminium ion formation (starting from easily accessible amines and ketones) or preformed bench stable iminium ion salts as starting materials will be compared. The α -amino radicals formed will undergo coupling to a range of alkenes bearing strongly and weakly electron-withdrawing groups to probe the electronic effect. Both simple and more sterically hindered electron-deficient alkenes will also be used to form sterically hindered amine products. The practicality of using the commercially available electrochemical set-up, the ElectraSyn 2.0, will also be investigated to ensure this methodology can be easily set-up and reproduced in any synthetic lab.²⁸

3.2 Results and Discussion

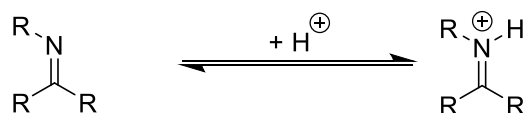
3.2.1 Methods for Iminium Ion Synthesis

To synthesise tertiary aliphatic amines from iminium ions *via* a reductive radical approach, a reliable method of iminium ion preparation first needed to be established. Ideally, a way of forming iminium ions which avoided time consuming purification steps would make the approach more synthetically attractive. Typical methods for preparing iminium ions include protonation or alkylation of imines. This method is simple and often high yielding; however, it relies on the availability of imines (Scheme 3.38 A and B).²⁰⁰ Iminium ions can also be prepared by elimination reactions from amino ethers (Scheme 3.38 C) or amino nitrates by treatment with silver nitrate (Scheme 3.38 D).²⁰¹ The purification of charged iminium salts can be challenging and is often restricted to recrystallisation. Condensation reactions of secondary amines with ketones or aldehydes can offer a direct route to iminium ions from a wide range of commercially available starting materials (Scheme 3.38 E).²⁰²

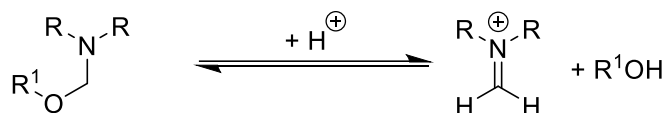
A - N-alkylation of imines



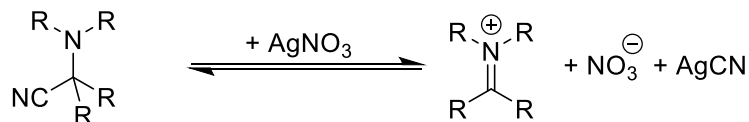
B - Protonation of imines



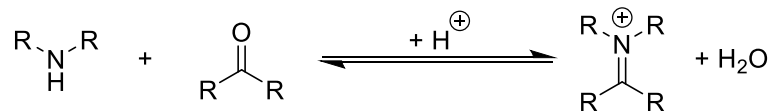
C - Protonation of amino ethers



D - Treatment of amino nitrile with AgNO₃



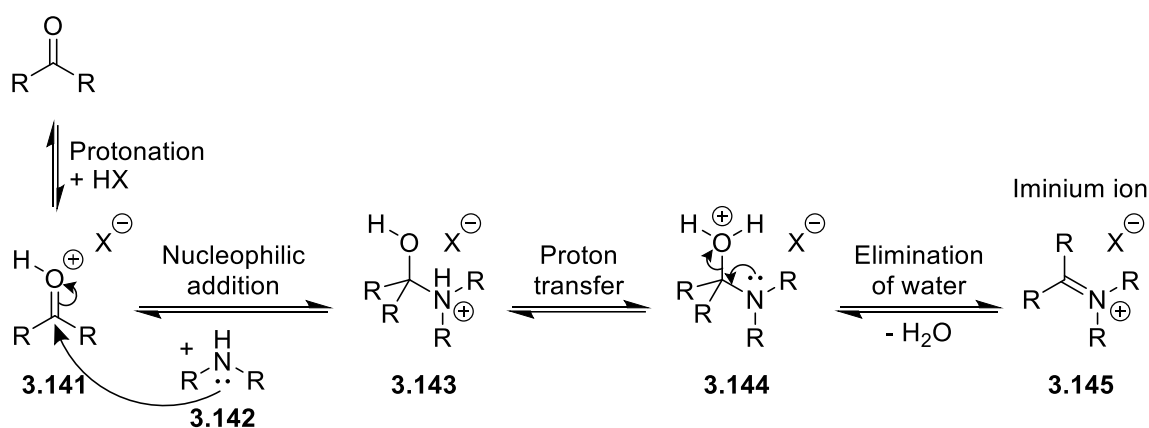
E - Condensation of amine and ketone



Scheme 3.38 Various routes for the synthesis of iminium ions.²⁰⁰⁻²⁰²

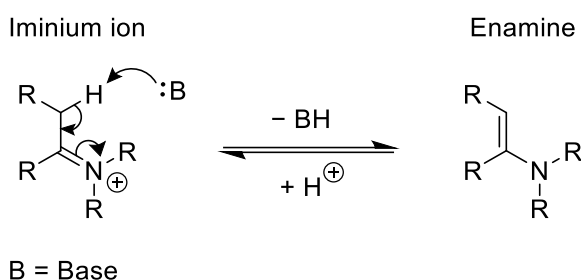
In the condensation of ketones and amines, mechanistically, amine **3.142** adds into the protonated carbonyl **3.141** forming carbinolamine **3.143** (Scheme 3.39). After a proton transfer, **3.144** eliminates water, and forms iminium ion **3.145**. The whole reaction is reversible and driven forward by the removal of water. The pH of the reaction is critical and dictates the rate determining step.²⁰³ Condensation reactions between ketones or aldehydes and amines are accelerated by the addition of general acid, with the rate maxima occurring between pH 4.5 and 5.0. At this pH, the carbonyl is partially protonated, increasing the electrophilicity of the carbonyl carbon, but the amine component is not fully protonated and therefore can still undergo nucleophilic addition. Below pH 4, the rate determining step is amine attack as the loss of water is rapid, whilst at more alkaline pH (above pH 5), the dehydration of the carbinolamine becomes the rate determining step.²⁰⁴ Generally, the reactions between amines and ketones or aldehydes are fast, and equilibrium is quickly established.²⁰³ Because of this, future evaluation of iminium ion synthesis will be discussed in terms of thermodynamic stability of the product.

Iminium ions can be stabilised by charge delocalisation across aromatic substituents.²⁰⁵ Therefore, aromatically functionalised iminium ions will be slow to react with nucleophiles and will not readily hydrolyse back to the corresponding amines and ketones or aldehydes.²⁰⁶



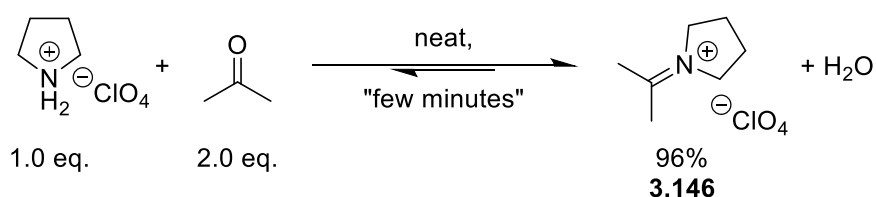
Scheme 3.39 Mechanism for iminium ion formation from amines and ketones or aldehydes.

In the presence of base, often as excess amine, iminium ions with β -hydrogens can be deprotonated to form neutral enamines (Scheme 3.40).²⁰⁷ Deprotonation is rapid and the resulting enamine will not undergo reduction to α -amino radicals. Therefore, in order to maintain the iminium ion, acid is typically added, particularly when a large excesses of amine is used.^{182,208,209}

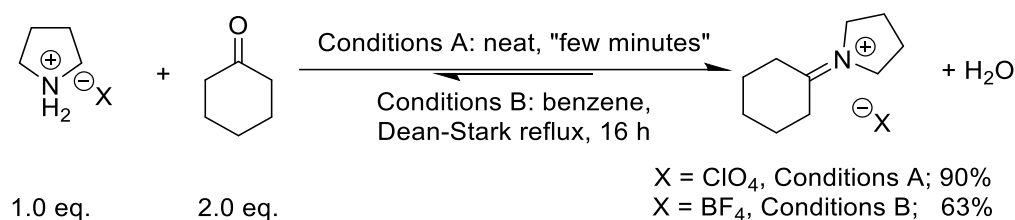


Scheme 3.40 Enamine formation from iminium ions.

In 1963 Leonard and Paukstelis published a procedure for the synthesis of alkyl iminium perchlorates by mixing aldehydes and ketones with secondary amine salts. The amine perchlorates were formed by reacting the free amine with perchloric acid in ethanol. The reactions were often rapid, and the desired iminium ions were achieved in excellent yields when there was little steric interference. For example, iminium ion **3.146** was isolated by recrystallisation in a 96% yield (Scheme 3.41).²⁰²

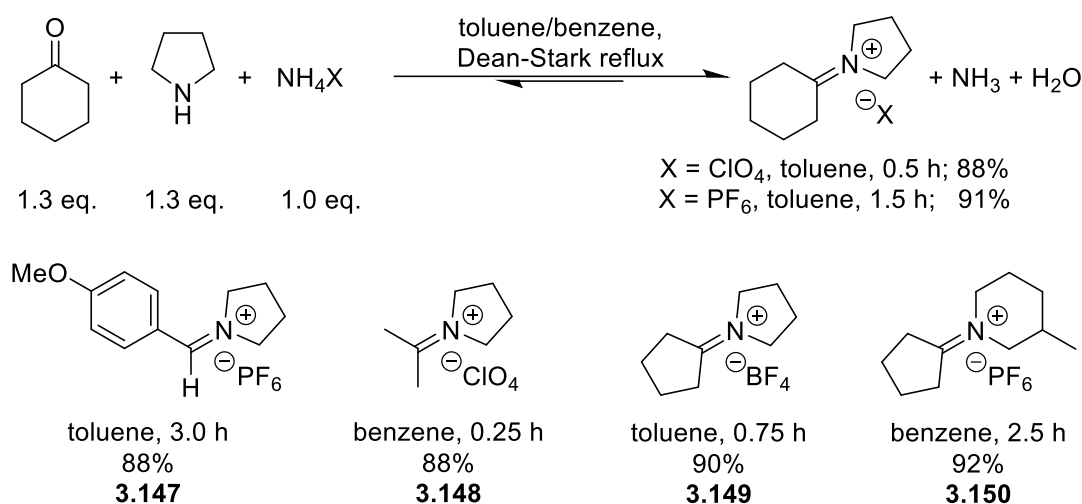
Scheme 3.41 Iminium perchlorate synthesised by Leonard et al. 1963.²⁰²

Perchlorate salts were chosen as they were easily crystallised, non-hygroscopic and perchlorate is non-nucleophilic. The reaction with perchlorate was performed with a range of aldehydes, cyclic and acyclic ketones. Pyrrolidine, morpholine and dimethylamine were successfully used as the amine component. In order to form reasonable amounts of iminium ion, reactions required heating in benzene with azeotropic distillation for more efficient water removal (Scheme 3.42).²⁰² Compared to perchlorate, tetrafluoroborate was less effective at forming iminium ions. However, tetrafluoroborate salts pose less of a safety concern than perchlorates, which are known to be explosive. “Simple” anions (e.g., chloride or bromide) performed poorly.²⁰²

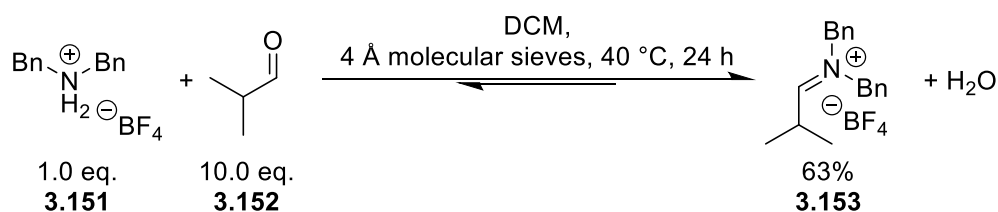


Scheme 3.42 Iminium perchlorate and tetrafluoroborate synthesised by Leonard et al. 1963.²⁰²

As opposed to pre-forming the amine salt, a one-pot procedure for iminium ion synthesis was developed by Saba and co-workers in 2008.²¹⁰ Stable iminium salts were prepared from the corresponding aldehyde or ketone, amine, and an ammonium salt. The role of the ammonium salt was twofold: the ammonium cation is sufficiently acidic to facilitate the condensation whilst the counter anion (either ClO₄⁻, BF₄⁻ or PF₆⁻) becomes the counter ion of the iminium salt. The reagents were heated at reflux for between 0.5 and 4 h and water was continuously removed by using a Dean-Stark trap. Different ammonium salts required different reflux times to attain high yields of iminium ions. Often the reaction with ammonium perchlorate was quicker than with either tetrafluoroborate or hexafluorophosphate (Scheme 3.43).²¹⁰ This is because different compounds have different equilibrium constants and therefore require different amounts of water to be removed to achieve the iminium ions. The resultant crude iminium salts were isolated and purified by crystallisation techniques. The authors used either toluene or benzene as the solvent and no apparent trends in solvent choice were reported. Aldehydes (for example **3.147**), acyclic amines and ketones (for example **3.148**), and different ring sizes (for example **3.149** and **3.150**) were successfully synthesised with this approach but the scope was somewhat limited to amines and carbonyls without heteroatoms or increased steric hinderance. The authors commented that they “reported a sampling of those that could easily be purified by crystallisation, affording non-hygroscopic crystalline products”. Therefore, whilst this approach was operationally simple, it may not be possible to prepare and isolate a wide range of iminium ions using this procedure.²¹⁰

Scheme 3.43 Various iminium salts synthesised by Saba et al. 2008.²¹⁰

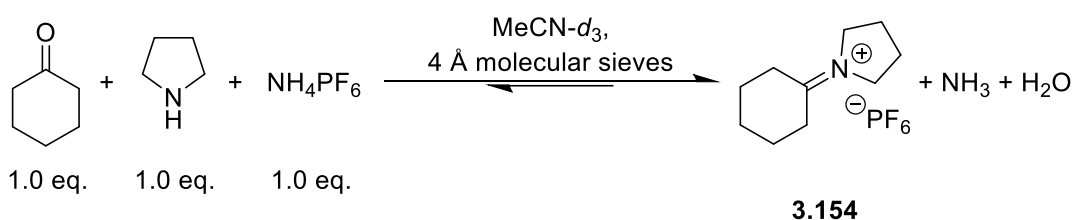
As opposed to azeotropic distillation, molecular sieves have also been used as a method of removing water during enamine and iminium ion synthesis.^{173,207} 4 Å molecular sieves were also used by the Gaunt group as the method for forming iminium ions *in-situ* prior to photochemical reduction. The reaction times were between 24 and 72 h showing that water removal using molecular sieves can require long reaction times.^{173,174} Iminium ion **3.153** was synthesised in a 63% yield from the ammonium tetrafluoroborate salt **3.151** and isobutyraldehyde **3.152** (Scheme 3.44).¹⁷³ The reaction was carried out in a glove box and required heating at 40 °C for 24 hours in order to form iminium ion **3.153**. As **3.153** was moisture sensitive and prone to hydrolysis, it had to be stored and used under nitrogen in a glove box.¹⁷³

Scheme 3.44 Iminium tetrafluoroborate synthesised by Trowbridge et al. 2018.¹⁷³

3.2.2 Iminium Ion Synthesis with 4 Å Molecular Sieves

N-Cyclohexylpyrrolidinium hexafluorophosphate **3.154** (Scheme 3.45) was chosen as the initial iminium ion to study as the electrochemistry has previously been reported for the perchlorate salt and related cyclic iminium ions.^{194,195} It was decided that hexafluorophosphate salts would be investigated as, like perchlorate, the hexafluorophosphate anion is only very weakly nucleophilic and is electrochemically inert in the proposed applied electrochemical potential window. Hexafluorophosphate salts can also be handled with greater assurance of safety compared to perchlorates which are known to be highly reactive oxidants and can be explosive.²⁰² Iminium ion **3.154** contains pyrrolidine and cyclohexyl rings, both of which are common in natural products and pharmaceuticals, and substituted versions are commercially available allowing for easy diversification.¹⁵²

To begin with, cyclohexanone (1.0 eq.), pyrrolidine (1.0 eq.), and ammonium hexafluorophosphate (1.0 eq., 0.03 M) were mixed in deuterated acetonitrile and the initial position of the equilibrium was measured by ¹H NMR spectroscopy (Figure 3.4, Spectrum 1). Ammonium hexafluorophosphate was sufficiently acidic to protonate pyrrolidine, therefore in the ¹H NMR spectra, pyrrolidine was present as the pyrrolidinium salt and the peaks (H⁸ and H⁹) were shifted downfield (H⁶ and H⁷). After the addition of 4 Å molecular sieves, aliquots of the reaction mixture were taken, and the position of equilibrium was monitored by observing the formation of iminium ion **3.154** by ¹H NMR spectroscopy for 20 h (Figure 3.4, Spectra 2-4).



Scheme 3.45 Monitoring the formation of iminium ion **3.154** with 4 Å molecular sieves by ¹H NMR spectroscopy.

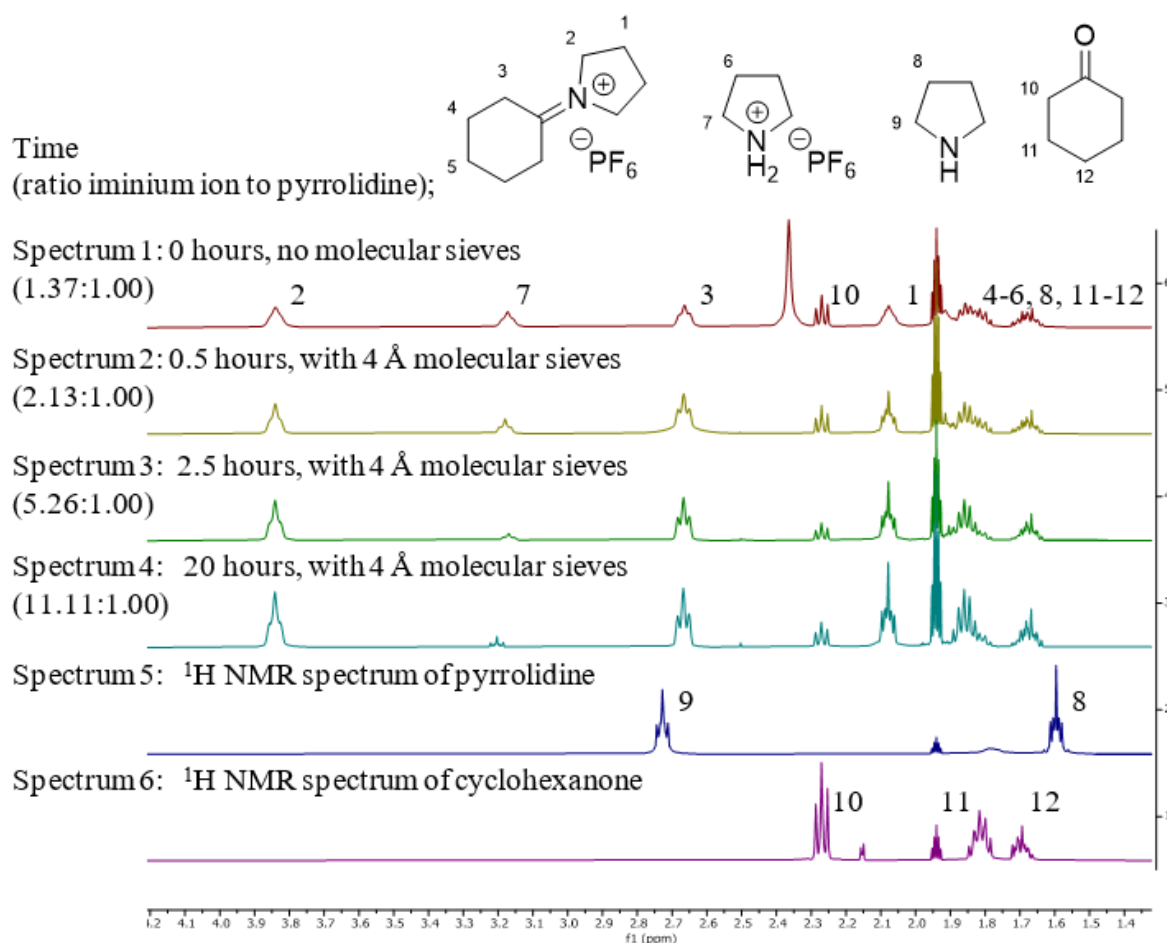
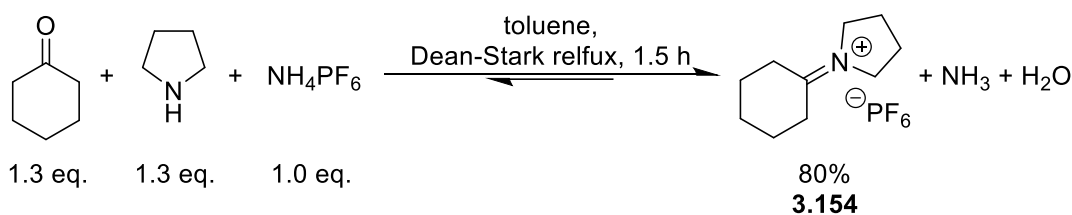


Figure 3.4 Stacked ^1H NMR spectra showing the formation of iminium ion 3.154 over 20 h with and without 4 Å molecular sieves

The equilibrium ratio of iminium ion to pyrrolidinium salt in the absence of 4 Å molecular sieves is 1.37:1.00 showing that the equilibrium is established very quickly. After addition of the 4 Å molecular sieves, the equilibrium shifted in favour of formation of the iminium ion. After 20 hours, the ratio of iminium ion to pyrrolidinium salt was 11.11:1.00 (peak H² to peak H⁷) suggesting that much of the amine and ketone have formed iminium ion and that the equilibrium in Scheme 3.45 has shifted far to the right. Whilst the equilibrium was established quickly, subsequent water removal was slow. 4 Å molecular sieves were tried in conjunction with electrolysis to form iminium ions *in-situ* prior and during electrochemical reductions and these results are discussed in Section 3.2.7. Unfortunately, achieving reproducible yields with 4 Å molecular sieves proved challenging due to unwanted water entry. Therefore, an alternative azeotropic distillation method, based on the work by Saba and co-workers, was explored to preform iminium ions.²¹⁰

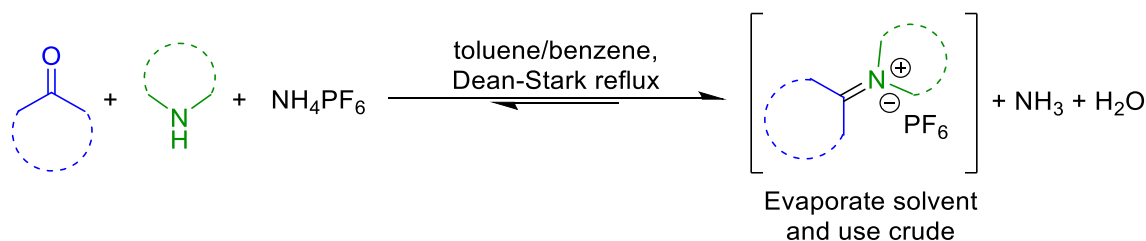
3.2.3 Iminium Ion Synthesis with Azeotropic Distillation

Following the procedure by Saba and co-workers, pyrrolidine (1.3 eq.), cyclohexanone (1.3 eq.), and ammonium hexafluorophosphate (1.0 eq., 0.5 M) were heated at reflux in toluene for 1.5 h, with the continuous removal of water with a Dean-Stark trap.²¹⁰ The resultant mixture was cooled in ice and the solid formed was recrystallised from ethanol-acetonitrile (Scheme 3.46) to give **3.154** in an 80% yield.



Scheme 3.46 Synthesis of iminium ion **3.154** by azeotropic distillation.

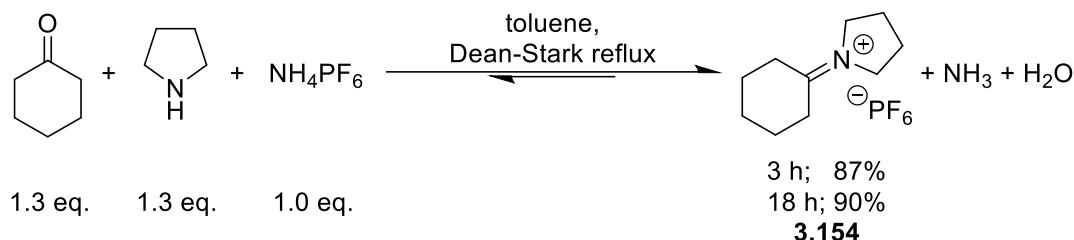
In order to simplify the synthesis and broaden the range of iminium ions beyond those that can be purified by recrystallisation, it was decided that after reflux, the solvent would be removed *in vacuo* (along with any volatile starting materials).¹⁷³ The iminium ions that formed would be stored under nitrogen, quantified by ¹H NMR spectroscopy and used as a crude mixture in the subsequent electrolysis experiments. Scheme 3.47 shows the general approach to iminium ion synthesis using (typically cyclic) ketones and amines.



Scheme 3.47 Synthesis of various iminium ions by azeotropic distillation.

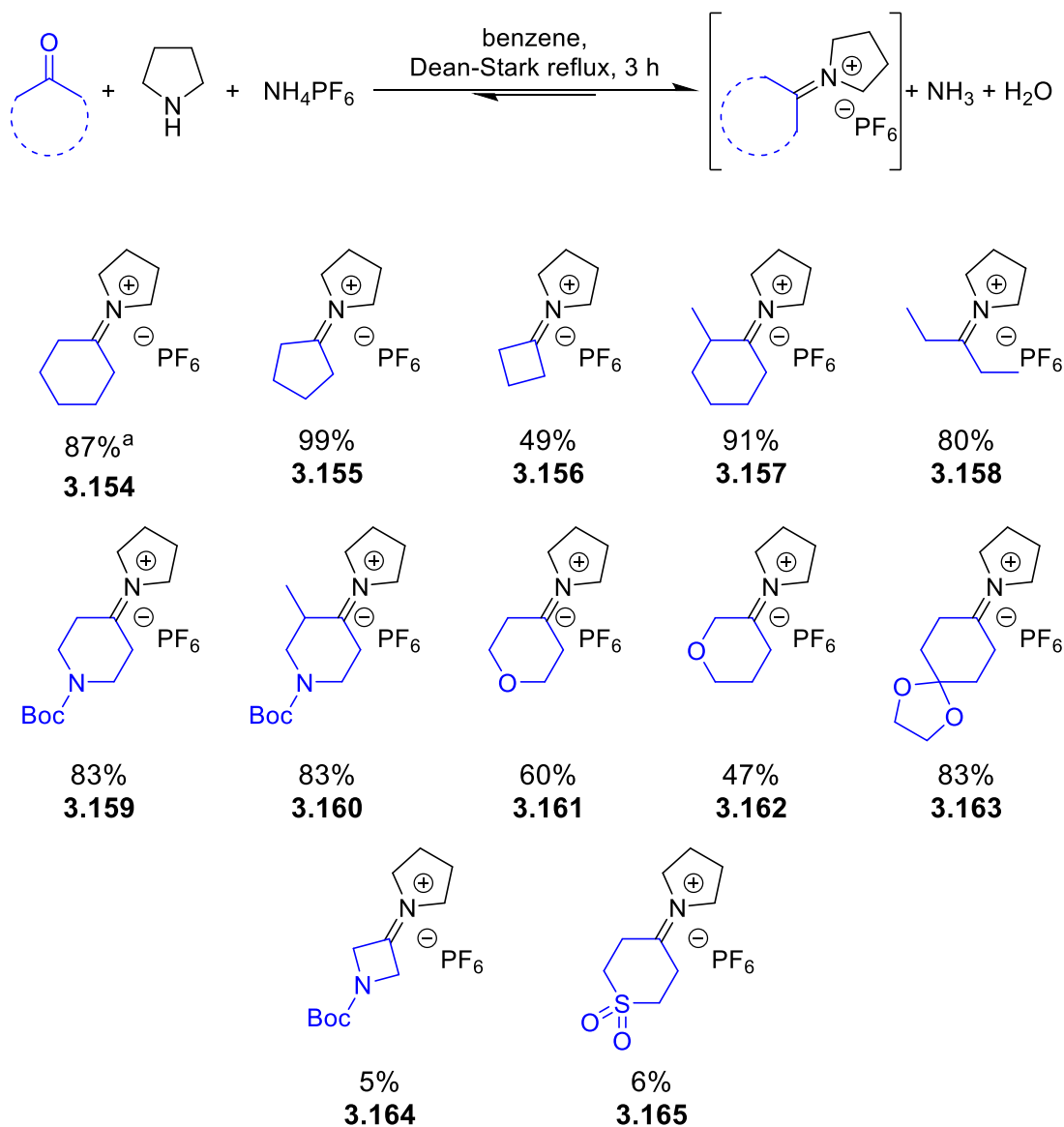
The effect of varying the reflux time was briefly explored as increasing the time for azeotropic distillation may help to form more iminium ion because water removal can be slow. Cyclohexanone (1.3 eq.), pyrrolidine (1.3 eq.), and ammonium hexafluorophosphate (1.3 eq., 0.5 M) were mixed in toluene and heated at reflux for 3 h and 18 h. The yield for iminium ion **3.154** was 87% after 3 h and 90% after 18 h as determined by quantitative ¹H NMR spectroscopy using dibromomethane as an external standard (Scheme 3.48). The yield

of the reaction did not significantly increase upon leaving the reflux longer. **3.154** is known to be a relatively stable iminium ion which means that less water would need to be removed to achieve reasonable yields of the iminium ion.^{194,195} It was decided that future iminium ion forming reactions would be performed for 3 h. In some examples, benzene proved to be the preferred solvent due to the lower azeotrope temperature.²¹¹



Scheme 3.48 Effect of distillation time on iminium ion **3.154** formation.

Initially, the ketone component was varied using pyrrolidine as the amine to prepare a range of iminium ions (Scheme 3.49). An excellent yield was observed with cyclopentanone (99%, **3.155**). However, on moving to more strained cyclobutanone, only a 49% yield of iminium ion **3.156** was achieved after a 3 hour reflux. This was unsurprising since cyclobuteniminium ions are known to be relatively unstable and they have previously been formed *in-situ*, with subsequent reactions occurring without isolation of the iminium ion.^{174,212} High yields were achieved for two cyclic ketones with α -substituents, for example the unsymmetrical iminium ion **3.157** was formed in a 91% yield from 2-methylcyclohexanone. An acyclic ketone was also found to be compatible with the reaction. When 3-pentanone was used as the ketone, iminium ion **3.158** was formed in an 80% yield.



^a toluene as solvent

Scheme 3.49 Synthesis of various iminium ions by azeotropic distillation, changing the ketone component.

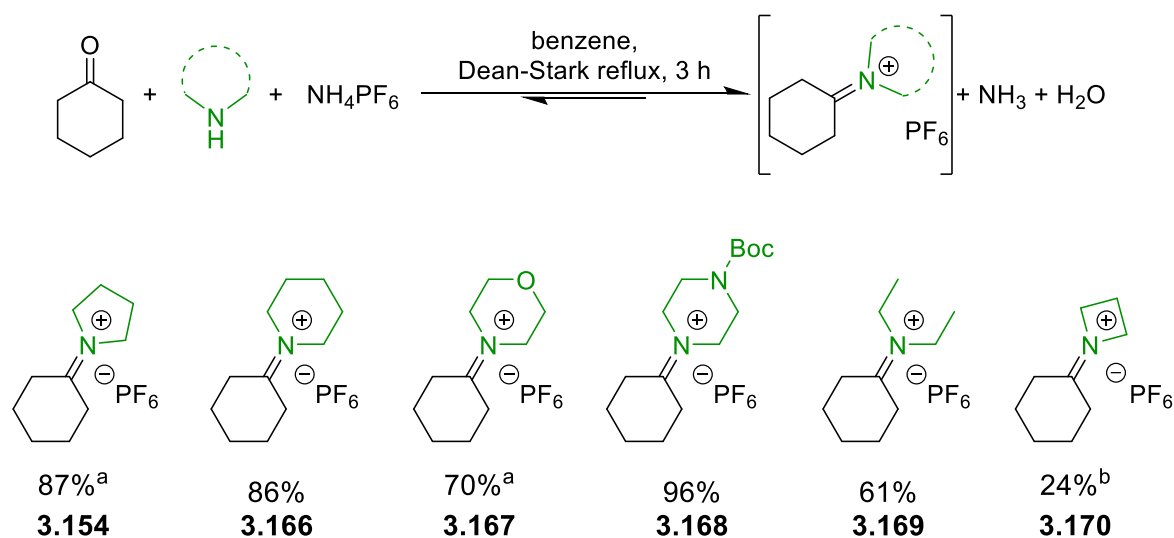
Finally, cyclic ketones bearing heteroatoms were also investigated (Scheme 3.49). Piperidines are a common and useful functionality in medicinal chemistry and therefore Boc protected piperidinones were studied as the ketone component. Both *N*-Boc-4-piperidineone and the 2-methyl derivative resulted in 83% yields for iminium ions **3.159** and **3.160**. Tetrahydropyrans were also compatible with the reaction conditions and yielded symmetrical and unsymmetrical iminium ions **3.161** and **3.162** respectively. Overall, the introduction of mildly electron-withdrawing heteroatoms on the ketone component destabilised the iminium ions, resulting in lower yields. This is because the carbon of the C=N has a partial positive charge and removing electron density from the bond will make

the iminium ion more unstable. As a result, relatively, lower yields were achieved with tetrahydropyrans compared to piperidines because the oxygen, being more electronegative, destabilised the iminium ion more than nitrogen. A 60% yield was achieved for **3.161** versus an 83% yield for **3.159**. Moving the oxygen closer to the C=N further destabilised the iminium ion so only a 47% yield of **3.162** was achieved. Similarly, when using azetidinone, the proximity of the nitrogen to the C=N results in an unstable iminium ion and therefore a very low yield for **3.164**. Additionally, the introduction of a strongly electron-withdrawing sulfone significantly destabilised the iminium ion and only a 6% yield for **3.165** was observed.

Ketals were compatible even under these mildly acidic reaction conditions, delivering iminium ion **3.163** in an 83% yield from the mono-protected diketone. The ketal provides a handle for further functionalisation.

To explore the scope of the iminium ion synthesis route with respect to the amine component, iminium ions were synthesised from cyclohexanone and a range of cyclic and acyclic secondary amines (Scheme 3.50). Increasing the ring size of the amine from pyrrolidine to piperidine resulted in an 86% yield for **3.166**, relative to 87% in the reaction with pyrrolidine. Morpholine and *N*-Boc piperazine resulted in 70% and near quantitative 96% yields for iminium ions **3.167** and **3.168** respectively. The lower yield for **3.167** with morpholine compared to **3.168** with piperidine was due to the additional electron withdrawing effect of the ether which destabilised the nitrogen positive charge. The Boc-protected nitrogen of the piperazine did not have the same destabilisation effect as morpholine, as the group is less electron withdrawing. Only a small substituent effect on iminium ion formation has been reported with substituted anilines.²⁰³

Use of acyclic diethylamine as a reagent only resulted in a 61% yield of iminium ion **3.169**. This was attributed to as the increased steric bulk from the flexible ethyl groups, which destabilised the iminium ion. Finally, azetidine was used as a smaller cyclic amine as it is a useful functional group in medicinal chemistry.^{213,214} However, as it is reasonably volatile (60 °C) and therefore only commercially available as the azetidine hydrochloride, iminium ion **3.170** was generated from the salt *in-situ* and only a 24% yield was achieved.²¹⁵



^a toluene as solvent, ^b azetidine was added as the hydrochloride salt

Scheme 3.50 Synthesis of various iminium ions by azeotropic distillation, changing the amine component.

3.2.4 Electrolysis of an Iminium Ion

To determine the reaction parameters for electrolysis, **3.154** was used as it was a stable iminium ion that could be easily purified. The unpurified iminium ions would be used for exploring the scope of the reaction (see Section 3.2.8).

Cyclic voltammetry was used to ascertain the reduction potential of iminium ion **3.154** to determine the potential to be applied to the working electrode so that during synthetic electrolysis the iminium ion would be reduced to the desired radical. The conditions used for the cyclic voltammogram (CV) were based on the electrochemical reduction of iminium ions by Kunai *et al.*: 10% methanol in acetonitrile as the solvent and 0.1 M iminium salt.¹⁹⁵ The CV (Figure 3.5) shows a non-reversible peak for reduction of iminium ion **3.154** with the reduction maxima, E_{red} , at -1.60 V vs Ag/AgCl. This value is comparable to previously reported reduction potentials for all-alkyl iminium ions.^{177,178,194,195}

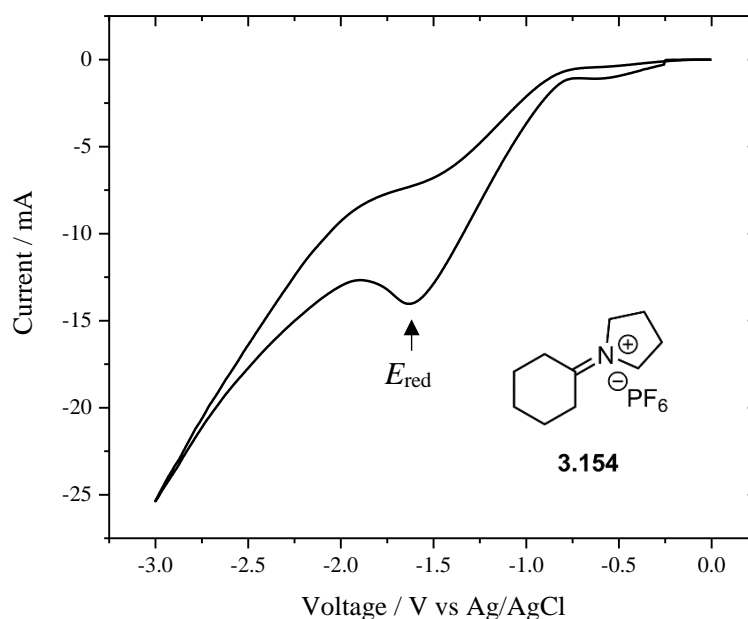


Figure 3.5 Cyclic voltammogram (CV) for iminium ion **3.154**. Recorded using platinum wire working and counter electrodes and an Ag/AgCl reference electrode. The CV was performed with an EmStat potentiostat with 10% methanol in acetonitrile as the solvent and 0.1 M iminium salt. Reduction maxima at -1.60 V vs Ag/AgCl, scan rate 50 mV s^{-1} .

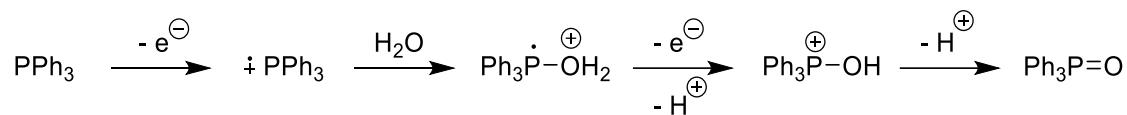
3.2.5 Iminium Ion Reduction and Reaction with Acrylonitrile: Optimisation of Electrolysis Conditions

3.2.5.1 Initial Electrochemical Conditions

The electrolysis of iminium ion **3.154** was conducted using the ElectraSyn 2.0 potentiostat, 10 mL cell and rectangular graphite working electrode (5.8 cm² of electrode in solution), rectangular platinum plated copper counter electrode (5.8 cm² of electrode in solution) and Ag/AgCl reference electrode. The potential for the working electrode was set to -1.80 V vs Ag/AgCl to ensure that reduction of iminium ion **3.154** would occur. Acrylonitrile was used as the electron-deficient alkene and initially 6 equivalents were added to ensure radical addition. The reaction was performed in acetonitrile as this solvent has previously been used for the electrochemical reduction of iminium ions that are similar to **3.154**.¹⁹⁵ The iminium ion acted as a non-innocent electrolyte and therefore the reaction did not require additional supporting electrolyte.

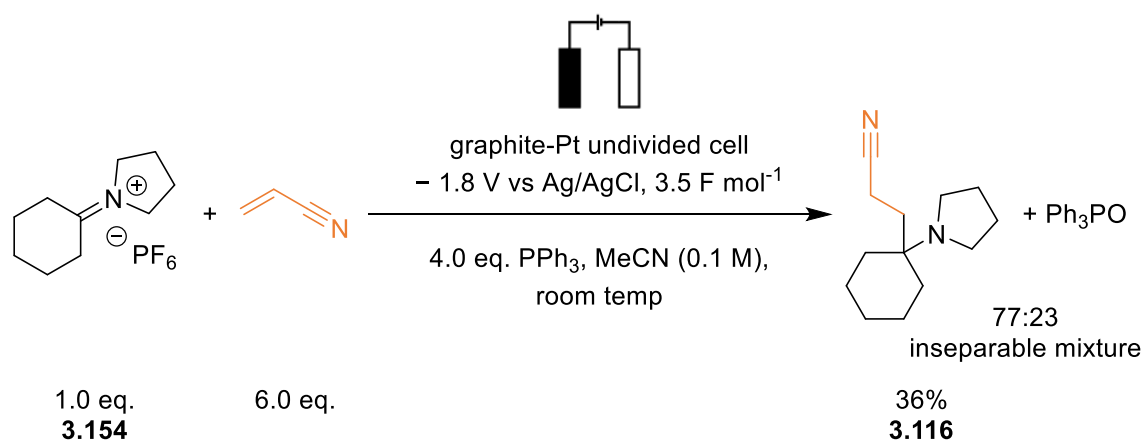
In order to reduce the iminium ion at the cathode, an appropriate reagent needed to be added to donate the electrons at the anode. Such reagents are often referred to as sacrificial electron donors (SEDs) and are chosen so they do not participate in the chemistry at the working

electrode.¹⁵⁹ Triphenylphosphine (4.0 eq.) was added as the SED, this can be oxidised by a two-electron process and reaction with water to yield triphenylphosphine oxide (Scheme 3.51).²¹⁶



Scheme 3.51 Proposed mechanism for oxidation of triphenylphosphine to triphenylphosphine oxide.²¹⁶

After 3.5 F (moles of iminium ion)⁻¹ of electrons had been consumed, the reaction was stopped. 3.5 F mol⁻¹ was chosen as 2 equivalents of electrons were required to form the desired amine **3.116**. However, other reducible species may compete for electrons and so an extra 1.5 equivalents of electrons was passed to prevent the amount of electrons limiting the reaction. Gratifyingly, the desired tertiary amine product **3.116** was isolated by column chromatography in a 36% yield (Scheme 3.52). Triphenylphosphine oxide proved difficult to separate from the desired amine product **3.116** (a 77:23 inseparable mixture of product **3.116** to triphenylphosphine oxide was obtained) and this is attributed to the fact that triphenylphosphine oxide is known to tail on silica.²¹⁷



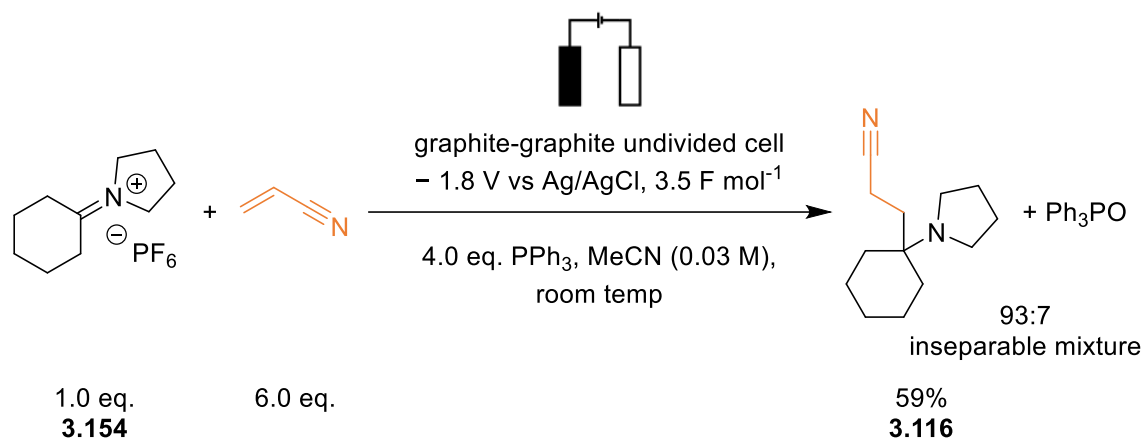
Scheme 3.52 Synthesis of amine **3.116** by electrochemical reduction of iminium ion **3.154** with graphite-platinum undivided cell.

An alternative method of purification was developed to separate the product from triphenylphosphine oxide. The amine product **3.116** was protonated with acid (2 M HCl_(aq)), loaded onto a silica plug and the less polar contaminants including PPh₃ and Ph₃PO were eluted with ethyl acetate. The amine was then deprotonated and eluted with an ammonium

hydroxide:ether:dichloromethane mixture (typically 1:25:25, v/v/v). If the product was not pure by ^1H NMR spectroscopy after the silica plug, it was further purified by column chromatography.

The concentration of the reaction was reduced to 0.03 M to keep the current below 100 mA, which is the maximum current for the ElectraSyn 2.0. The counter electrode was also changed to graphite as the platinum plating (on copper) was stripped during electrolysis exposing the copper below.

Using the newly developed silica plug purification and the changes to concentration and electrode material, the desired product **3.116** was isolated in a 59% yield as a 93:7 inseparable mixture of desired product and triphenylphosphine oxide (Scheme 3.53). The ^1H NMR spectrum for amine product **3.116** is given in the appendix (Appendix B).



Scheme 3.53 Synthesis of amine **3.116** by electrochemical reduction of iminium ion **3.154** with graphite-graphite undivided cell and modified purification.

3.2.5.2 Preventing Electrode Passivation

During the electrolysis of iminium ion **3.154**, when a constant voltage of -1.80 V vs Ag/AgCl was applied to the graphite working electrode, a steady drop in reductive current was observed over the first 15 minutes of the experiment (from approximately -40 mA to -15 mA). This was attributed to the formation of an insulating, so-called “passivation”, layer at the surface of the working electrode. Indeed, graphite electrodes could only be re-used after abrasion with emery paper to remove the surface layer and, if there were high levels of passivation, the electrodes were challenging to clean after multiple reactions. Potential sources of passivation include the α -amino radical forming and reacting at the working

electrode surface, or the electrochemical polymerisation of alkenes.^{144,215} To counteract the latter process, the amount of acrylonitrile was reduced to 3.0 eq.

To prevent and counteract passivation, polarity inversion was investigated. Inverting the polarity of the electrodes prevents the build-up of insulating films on the electrode surface, which would otherwise stop it functioning efficiently.⁹³ Polarity inversion works as the layer formed at the cathode is anodically removed on inversion and *vice versa*.²¹⁹ Additionally, inverting the polarity disrupts the formation of insulating layers on the electrode surface which increases the lifetime of the electrodes and therefore the electrodes do not need to be replaced as often.⁹⁴

When using the ElectraSyn 2.0, polarity inversion is only possible in a two-electrode anode-cathode constant voltage configuration, i.e. it is only possible to define a cell potential (E_{cell}) value of the voltage difference between the anode and the cathode, and a reference electrode cannot be used.⁹⁴ In the earlier three-electrode experiments using a Ag/AgCl reference electrode, when a potential of -1.80 V vs Ag/AgCl was applied to the working electrode, a potential difference of between 4 and 5 V was measured between the working and counter graphite electrodes. Therefore, an applied two-electrode cell potential of 5 V should provide an environment that is reducing enough for the iminium ion, whilst still allowing for the oxidation of triphenylphosphine. When this was tested (Table 3.1, entry 1), the experiment showed similar yields to those achieved using the previous three-electrode configuration where the working electrode was defined relative to the Ag/AgCl reference. While the overall reductive current was higher, the same decay was observed, indicating that electrode passivation was still occurring (Figure 3.6, orange line). This meant that the time required to pass the total required charge is significant and that the electrodes required significant abrasive cleaning.

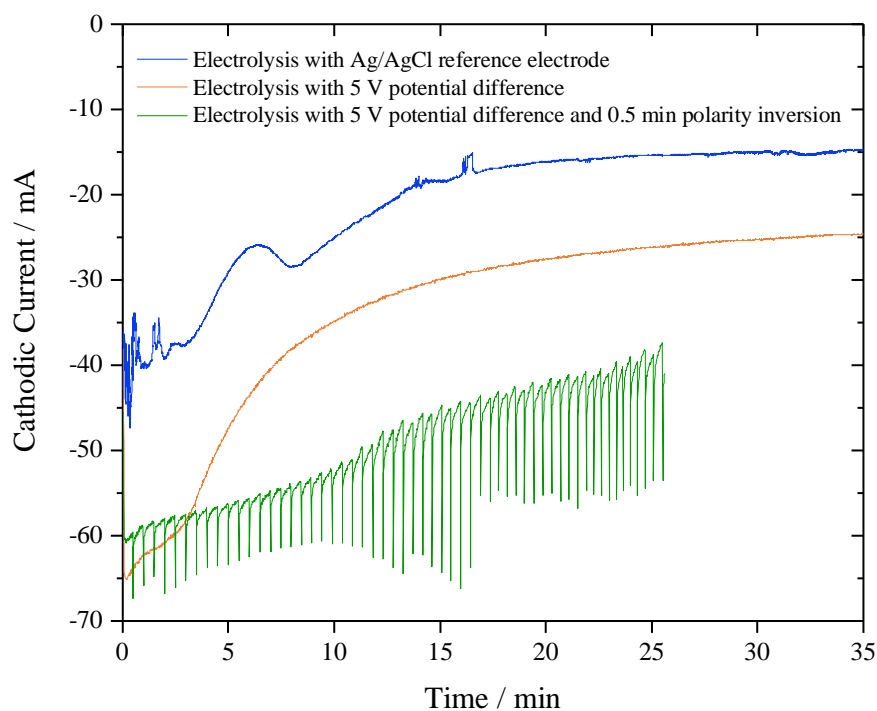
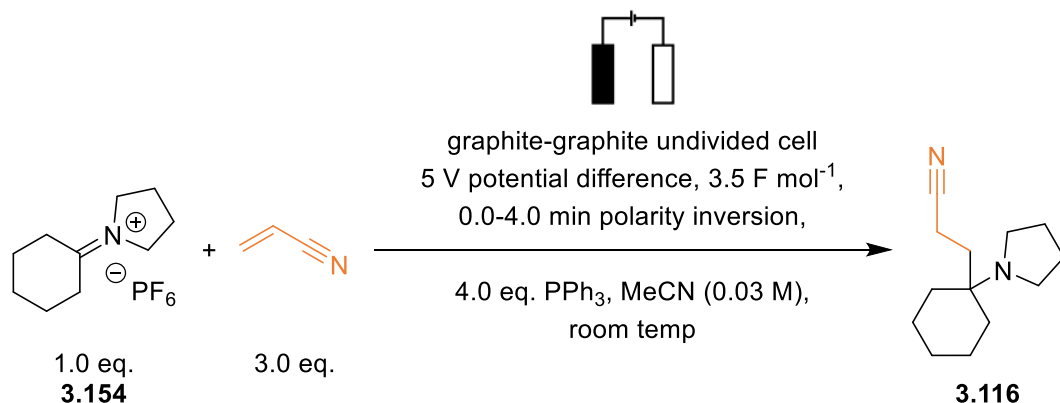


Figure 3.6 A graph showing negative absolute current vs time, for the first 35 minutes, for a series of electrochemical reductions of iminium ion **3.154** with and without a reference electrode and at 0.5 min polarity inversion intervals

Next, experiments were conducted using a two-electrode 5 V cell potential set-up but an inversion interval was now introduced; in separate experiments the inversion interval was varied from 4-0.5 min (Scheme 3.54, Table 3.1, entries 2-6). Decreasing the polarity inversion time, i.e. increasing the frequency at which the electrodes are switched from being anode to cathode and *vice versa*, should reduce passivation. Based on analysis of the ^1H NMR spectrum of the crude product, the yields for amine **3.116** were comparable with and without polarity inversion, but by using polarity inversion a higher current was maintained throughout the reaction. Crucially, this decreases the time required to pass 3.5 F mol^{-1} of charge (Figure 3.6, green line for 0.5 minute inversion) and also meant that the electrodes were easier to clean in-between reactions, increasing the overall electrode lifetime. Therefore, inversion improved the protocol. The 0.5 minute polarity inversion interval was used for the subsequent reactions.



Scheme 3.54 Effect of polarity inversion frequency on the yield of amine **3.116** in the electrochemical reduction of iminium ion **3.154**.

Table 3.1 The effect of polarity inversion on the outcome of the reduction of iminium ion **3.154** in the presence of acrylonitrile

Entry ^a	Polarity Inversion	Consumption of Iminium	Product 3.116 Yield
	Time / min	Ion 3.154 / % ^b	/ % ^b
1	-	98	58
2	4	98	60
3	3	98	62
4	2	97	60
5	1	99	58
6	0.5	98	62 (59% ^c)

^a 0.25 mmol of iminium salt **3.154** was dissolved in 9 mL of MeCN with 0.75 mmol acrylonitrile. ^b Determined by ¹H NMR spectroscopy using the aromatic region of triphenylphosphine/triphenylphosphine oxide as an internal standard. ^c Isolated yield.

Using the conditions in Table 3.1, entry 6, and the optimised silica plug purification, after column chromatography, the isolated yield of amine **3.116** was 59% yield as a 99:1 inseparable mixture of desired product and triphenylphosphine oxide. The isolated yield was in good agreement with the yield determined by ¹H NMR spectroscopy of the crude product.

The green and orange lines plotted in Figure 3.6 are the reductive/cathodic current recorded. As shown in Figure 3.7, this is slightly different to what is recorded by the ElectraSyn 2.0. When using a three-electrode set-up that included a reference electrode, a negative current was recorded by the ElectraSyn 2.0 (Figure 3.7, blue line) as the rate of electron flow

between the working and the counter electrode. However, when in a two-electrode configuration with a constant cell potential being applied, the current measured by the ElectroSyn 2.0 is the rate of electron flow from the anode to the cathode, i.e. it is a positive value (Figure 3.7, orange line). Conversely, when using polarity inversion, the ElectroSyn 2.0 outputs current values that oscillate either side of zero (Figure 3.7, green line). Therefore, in order to compare reductive current flow in all cases, the negative absolute current value recorded in all experiments has been plotted, referred to as “Cathodic Current” (Figure 3.6).

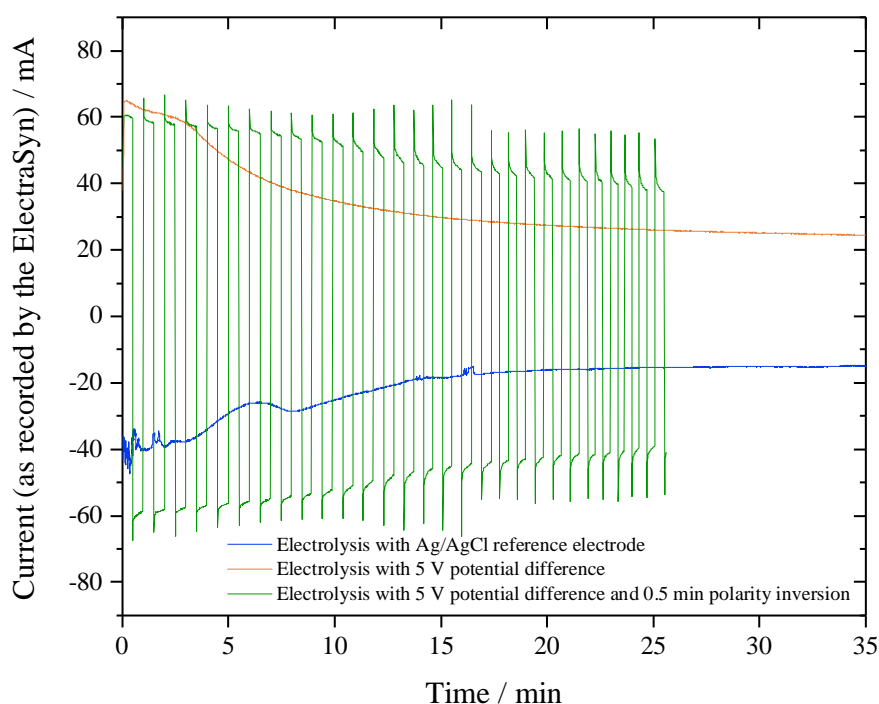


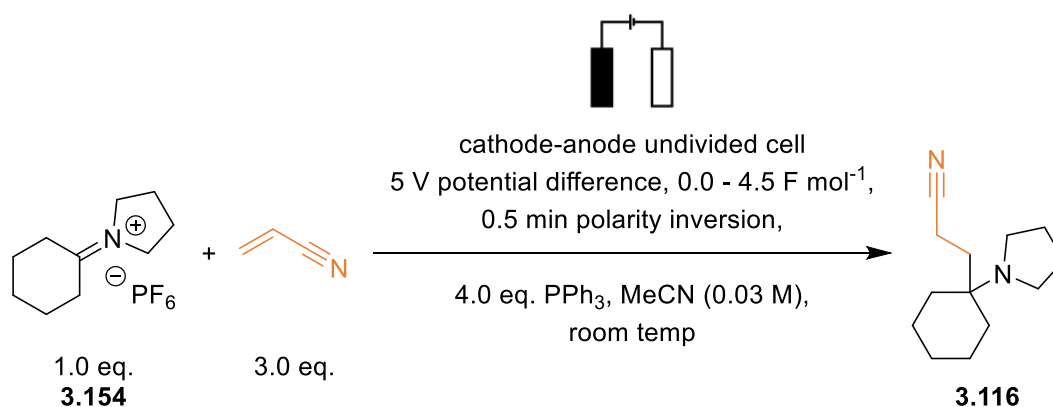
Figure 3.7 A graph showing the actual current output for the ElectroSyn vs time, for the first 35 minutes, for a series of electrochemical reductions of iminium ion **3.154** with and without a reference electrode and at 0.5 min polarity inversion intervals

3.2.5.3 Optimisation of Electrode Material and Electrochemical Parameters

Having optimised the electrochemical methodology, next the impact of the electrode material and reaction time were investigated (Scheme 3.55). Reticulated vitreous carbon (RVC), a carbon foam electrode with a large surface area, was tested as a replacement for graphite at both the anode and cathode since an increased electrode surface area may improve the yield. However, when RVC was used in a suitably modified set-up (see Experimental Section 5.3.4), the yield for amine **3.116** dropped to 36% by quantitative ^1H NMR

spectroscopy (Table 3.2 entry 2). It was theorised that the lower yield was due to increased radical adsorption due to the increased electrode surface area since very little starting material remained at the end of the reaction (96% conversion based on the consumption of starting material). Aluminium was also tried as the working electrode with a graphite counter electrode (no polarity inversion). As aluminium is a smoother electrode surface it may not passivate as readily as graphite.²²⁰ Unfortunately, only a 16% yield for amine **3.116** was determined by quantitative ¹H NMR spectroscopy (Table 3.2 entry 3). Therefore, graphite was kept as the electrode material for both the anode and cathode.

The reaction time, in F mol⁻¹ relative to the amount of iminium ion, was investigated as theoretically only 2 equivalents of electrons are needed (2.0 F mol⁻¹) to perform the two one-electron reductions. When 2.5 F mol⁻¹ were applied, a 50% yield of **3.116** was observed by quantitative ¹H NMR spectroscopy with an 89% conversion of starting material. The remaining 11% starting material meant that the reaction had not gone to completion and that there are potentially competing reduction reactions at the cathode which reduce the Faradaic efficiency of the reaction (Table 3.2 entry 4). When 4.5 F mol⁻¹ were used, the yield of **3.116** did not significantly change (Table 3.2 entry 5), implying amine **3.116** is stable under the electrolysis conditions and does not react further, such as through an oxidative pathway (see Section 3.2.6.2 for a further discussion of this). Finally, in the absence of an applied potential difference, the reaction did not proceed (Table 3.2 entry 6), proving that electricity is required to reduce the iminium ions. Following these screening experiments, 3.5 F mol⁻¹ of electrons were kept as the optimal amount of charge to pass.



Scheme 3.55 Effect of anode and cathode material and amount of charge passed on the yield of amine **3.116** in the electrochemical reduction of iminium ion **3.154**.

Table 3.2 The effect of changing electrode material and equivalents of charge on the outcome of the reduction of iminium ion **3.154** in the presence of acrylonitrile

Entry ^a	Cathode	Anode	Equivalents of Charge / F mol ⁻¹	Consumption of Iminium Ion 3.154 / % ^b	Product 3.116 Yield / % ^b
1	Graphite	Graphite	3.5	98	62
2 ^c	RVC	RVC	3.5	96	36
3 ^d	Aluminium	Graphite	3.5	85	16
4	Graphite	Graphite	2.5	89	50
5	Graphite	Graphite	4.5	99	58
6	Graphite	Graphite	0.0	0	0

^a 0.25 mmol of iminium salt **3.154** was dissolved in 9 mL of MeCN with 0.75 mmol acrylonitrile. ^b Determined by ¹H NMR spectroscopy using the aromatic region of triphenylphosphine/triphenylphosphine oxide as an internal standard. ^c Using modified set-up.³⁹ ^d No polarity inversion was performed as an aluminium anode would oxidise at the set potential.

3.2.5.4 Optimisation of Reaction Stoichiometry and Solvent

With the optimal electrochemical parameters determined, next, the reaction stoichiometry and solvent were probed (Scheme 3.56). Dimethylformamide (DMF) was successfully used as an alternative solvent, resulting in a comparable yield to acetonitrile (Table 3.3, entry 1). However, as acetonitrile has a wider potential window than DMF, meaning it has excellent electrochemical stability in both highly oxidising and highly reducing conditions, it was chosen as the preferred solvent.^{218,219}

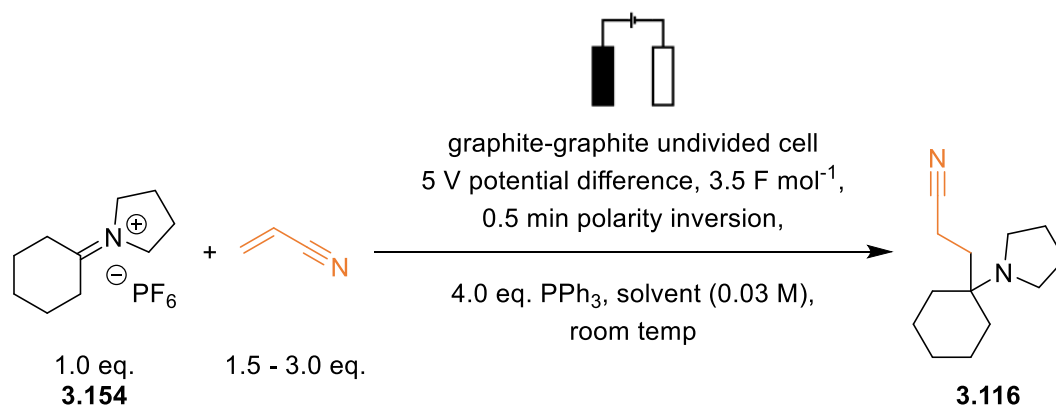
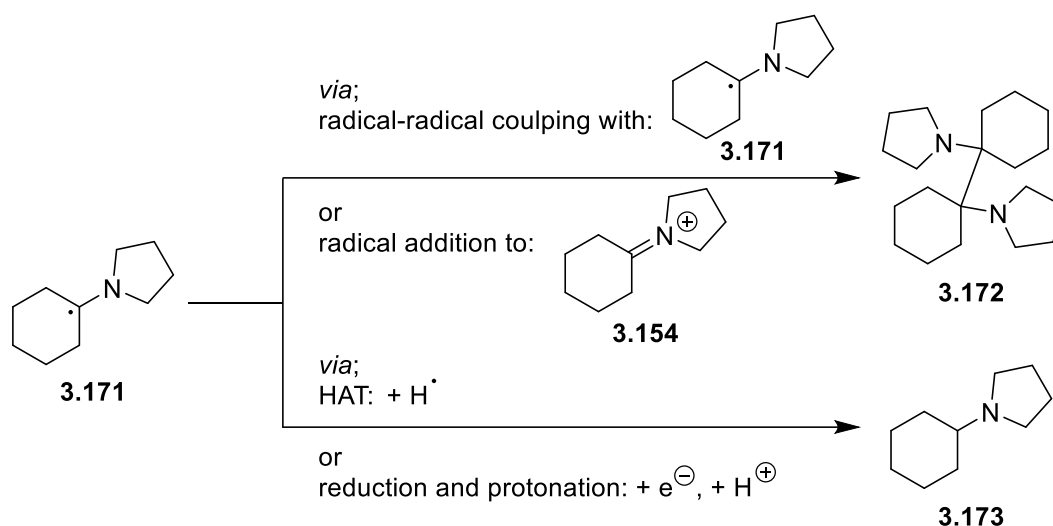
Scheme 3.56 Effect of solvent on the yield of amine **3.116** in the electrochemical reduction of iminium ion **3.154**.

Table 3.3 The effect of solvent and equivalents of alkene on the outcome of the reduction of iminium ion **3.154** in the presence of acrylonitrile

Entry ^a	Solvent	Eq. Acrylonitrile	Consumption of Iminium Ion 3.154 / % ^b	Product 3.116 Yield / % ^b
1	DMF	3.0	100	60
2	MeCN	3.0	98	62
3	MeCN	2.0	98	54
4	MeCN	1.5	98	52

^a 0.25 mmol of iminium salt **3.154** was dissolved in 9 mL of MeCN with 0.75 mmol acrylonitrile. ^b Determined by ¹H NMR spectroscopy using the aromatic region of triphenylphosphine/triphenylphosphine oxide as an internal standard.

A lower alkene concentration would improve the atom economy for the reaction and may lead to increased yields if the alkene participates in unwanted side reactions such as electrode passivation or radical oligomerisation.¹⁴⁵ When the amount of alkene was lowered from 3.0 eq. to 1.5 eq., the yield by quantitative ¹H NMR spectroscopy for amine **3.116** decreased (Table 3.3, entries 2-4). As the conversion remained the same, it is likely that at low alkene concentrations, the α -amino radical formed partook in competing side reactions. Potential side-products include diamine **3.172** and tertiary amine **3.173** (Scheme 3.57). Diamine **3.172** could be formed from either radical-radical coupling of two equivalents of α -amino radical **3.171**, or radical addition of **3.171** into an equivalent of iminium ion **3.154**. The radical coupling pathway is potentially less likely as the radicals are reasonably sterically hindered. Alternatively, tertiary amine side-product **3.173** could form from radical **3.171** either undergoing a direct HAT or undergoing a second electron reduction and then protonation (see Scheme 3.20). However, there was no evidence in the crude ¹H NMR spectrum that supported the formation of either product **3.172** or **3.173**.

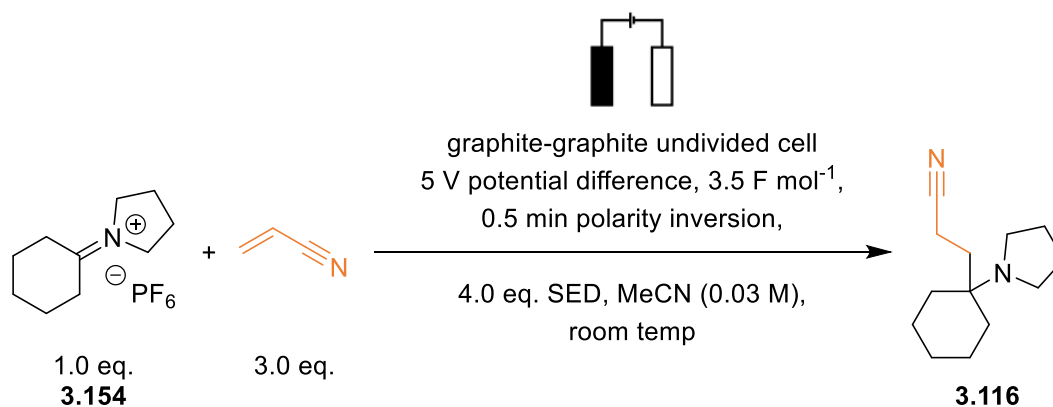
Scheme 3.57 Potential side reactions for α -amino radical **3.171**.

3.2.5.5 Optimisation of Sacrificial Electron Donor

Whilst good yields for amine **3.116** were achieved with triphenylphosphine as the sacrificial electron donor, the large molecular weight of triphenylphosphine ($262.29 \text{ g mol}^{-1}$) meant that the overall reaction had a large amount of waste and a poor E -factor (the mass of waste divided by the mass of the product).²²³ Triphenylphosphine oxide also co-eluted with amine **3.116** during column chromatography making isolation of pure product difficult. Other, smaller, SEDs were therefore investigated to try and improve the E -factor for the reaction and make isolation of the amine easier (Scheme 3.58). SEDs were chosen to be readily oxidisable and inert in non-electrochemical reactions.


As another phosphine SED, tributylphosphine was screened in the reaction since it should oxidise in a similar manner to triphenylphosphine, based on the oxidation maxima, E_{ox} , at +1.43 V vs Ag/AgCl compared to +1.88 V vs Ag/AgCl for triphenylphosphine (E_{ox} determined by cyclic voltammetry, see Section 3.2.6). Tributylphosphine has a slightly lower molecular weight, and the change from aryl to alkyl substituents was expected to aid product separation. However, no evidence of product **3.116** was observed in the ^1H NMR spectrum or the corresponding mass spectrum of the crude product (Table 3.4, entry 2). Additionally, there was no evidence of iminium ion **3.154** in the ^1H NMR spectrum of the crude product, suggesting that the iminium ion was reduced but then may have reacted with a derivative of tributylphosphine (see Section 3.2.6.1 for a further discussion of this).

Tetrahydrothiophene was also tested as an alternative to trisubstituted phosphine SEDs. Dialkylsulfides should be readily oxidised to the corresponding sulfoxide. The oxidation maxima, E_{ox} , was found to be +2.41 V vs Ag/AgCl (E_{ox} determined by cyclic voltammetry, see Section 3.2.6). Tetrahydrothiophene has a molecular weight (88.17 g mol⁻¹) significantly lower than either triphenyl- or tributylphosphine and the corresponding sulfoxide should be easier to separate from the amine product by chromatography. At the end of the reaction, an aliquot of the crude reaction mixture was taken and analysed by ¹H NMR spectroscopy and dibromomethane was added to the sample as an external standard to quantify the products. Whilst the yield by quantitative ¹H NMR spectroscopy was higher than when triphenylphosphine was used, the isolated yield was comparable (Table 3.4, entry 3). Importantly, the isolation of amine **3.116** from the crude mixture containing tetrahydrothiophene and the corresponding sulfoxide was much easier than the reaction with triphenylphosphine. Therefore, tetrahydrothiophene was chosen as the SED going forward.



Scheme 3.58 Effect of sacrificial electron donor on the yield of amine **3.116** in the electrochemical reduction of iminium ion **3.154**.

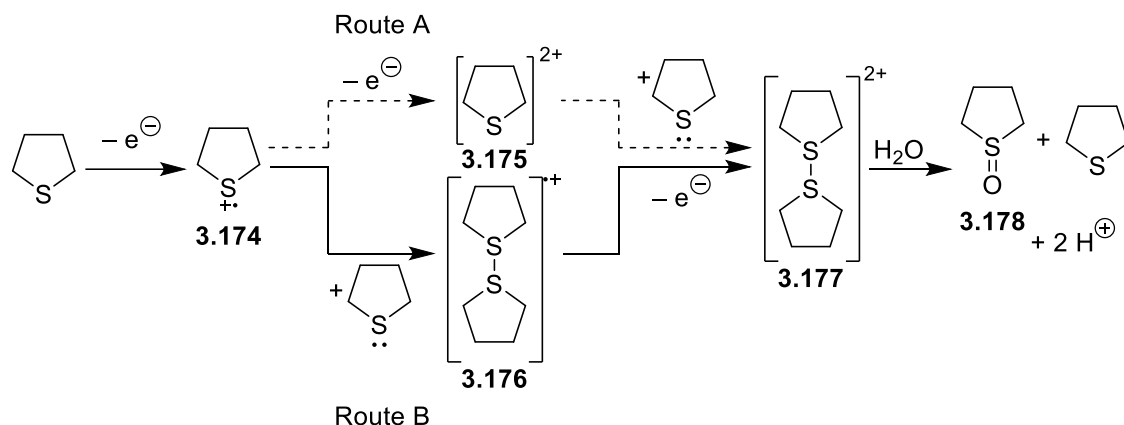
Table 3.4 The effect of sacrificial electron donor on the outcome of the reduction of iminium ion **3.154** in the presence of acrylonitrile

Entry ^a	SED	$E_{\text{ox}} / \text{V vs Ag/AgCl}$	Consumption of Iminium Ion 3.154 / % ^b	Product 3.116 Yield / % ^b	Isolated Yield 3.116 / %
1	PPh ₃	+ 1.88	98	62 ^b	59
2	PBu ₃	+ 1.43	100 ^d	-	-
3 ^c		+ 2.41	94 ^d	70 ^d	56

^a 0.25 mmol of iminium salt **3.154** was dissolved in 9 mL of MeCN with 0.75 mmol acrylonitrile. ^b Determined by ¹H NMR spectroscopy using the aromatic region of triphenylphosphine/triphenylphosphine oxide as an internal standard. ^c 0.50 mmol of iminium salt **3.154** was dissolved in 18 mL of MeCN with 1.50 mmol acrylonitrile. ^d Determined by ¹H NMR spectroscopy using dibromomethane as an external standard.

It was also found that the amount of SED could be successfully lowered. With 2.0 eq. of tetrahydrothiophene, amine **3.116** was isolated by column chromatography in a 57% yield.

Mechanistically, the anodic oxidation of tetrahydrothiophene could proceed *via* an analogous mechanism for the oxidation of amines (Scheme 3.4 Pathway A, see Section 3.1.2). Alternatively, Yanagihara and co-workers proposed two potential pathways for the oxidation of tetrahydrothiophene to sulfoxide **3.178** in acetonitrile and in the presence of copper (Scheme 3.59). It was suggested that, initially, tetrahydrothiophene was oxidised to radical cation **3.174**. In Route A, a second electron oxidation delivered dication **3.175** which reacted with a second equivalents of tetrahydrothiophene to give dimeric tetrahydrothiophene dication **3.177**. Radical cation **3.174** could also react with tetrahydrothiophene (Route B) giving radical cation **3.176** which would be oxidised a second time to dication **3.177**. Dicationic species containing intermolecular S-S bonds are known to be highly stable. Finally, hydrolysis would deliver sulfoxide **3.178**, reforming tetrahydrothiophene and two protons.²²⁴ Radical cation **3.176** has been detected by ESR, generated with hydroxy radicals, and radical cation **3.174** was shown to react rapidly with tetrahydrothiophene therefore the oxidation is likely to proceed *via* Route B.²²⁵



Scheme 3.59 Proposed mechanism for oxidation of tetrahydrothiophene to sulfoxide **3.177**.²²⁴

It is likely that the electrolysis of tetrahydrothiophene will proceed by a similar mechanism. Once dication **3.177** has formed, it should be sufficiently stable before hydrolysis in the work-up steps leads to sulfoxide **3.178**. The sulfoxide formed was then separated from the product by column chromatograph.

The yield of amine **3.116** was significantly higher than that achieved by Kunai and co-workers (37%, Scheme 3.32) where the perchlorate iminium ion was used with a mercury pool cathode and in a divided cell.¹⁹⁵ The use of graphite and an undivided cell, along with the higher yield makes this approach significantly more synthetically appealing.

3.2.6 Iminium Ion Reduction and Reaction with Acrylonitrile: Study the Mechanism with Cyclic Voltammetry

With optimised conditions determined for iminium ion reduction and subsequent addition to acrylonitrile to generate a good yield of amine **3.116**, the different electrochemical steps in the overall reaction were further studied by cyclic voltammetry. To be consistent with the reaction set-up, the cyclic voltammograms (CVs) were recorded using the ElectroSyn 2.0 CV package. The package contains a glassy carbon working electrode and Ag/AgCl reference electrode. An ElectroSyn graphite electrode was used as the counter electrode. Using this set-up, CVs could be recorded at a fixed electrode spacing, which is important for reproducible, reliable data. The electrodes were connected to a modified lid (see Experimental Section 5.3.2), and the CVs were performed with an EmStat potentiostat. CVs were also recorded using a supporting electrolyte (0.1 M tetrabutylammonium

hexafluorophosphate in acetonitrile) as there was no iminium ion present in some of the measurements.

3.2.6.1 Investigation of Oxidation of Sacrificial Electron Donors by Cyclic Voltammetry

The cyclic voltammograms used to determine the oxidation potential for each of the sacrificial electron donors are presented in Figure 3.8. All CVs were recorded at a SED concentration of 0.07 M, and the results show that, whilst thermodynamically the oxidation potentials were similar, the high current for tetrahydrothiophene meant that the rate of oxidation was faster. The increased current could be attributed to the smaller molecular weight for tetrahydrothiophene, meaning that diffusion at the electrode surface was faster.

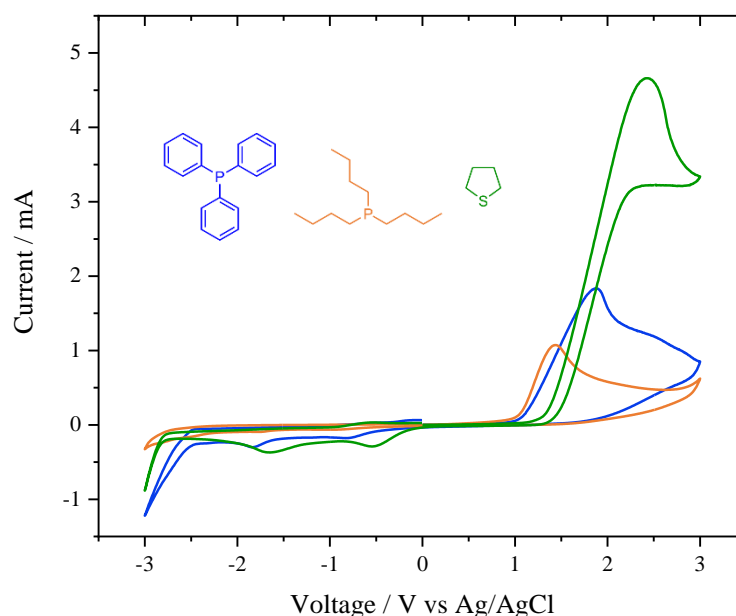


Figure 3.8 Cyclic voltammograms of the different sacrificial electron donors at 0.07 M, recorded at 500 mV s^{-1} .

Experimentally, the reaction with tributylphosphine did not yield the desired amine **3.116** whilst both triphenylphosphine and tetrahydrothiophene gave similar yields (Table 3.4). All reactions passed a reasonably significant reductive current (Figure 3.9) and it is therefore likely that the reduction of the iminium ion and oxidation of the SED were occurring. On comparing the current trace for the reactions, triphenylphosphine showed the highest current during electrolysis, then tetrahydrothiophene, then tributylphosphine, which is not consistent with the CV data, which showed that oxidation of tetrahydrothiophene has the highest

current. The current for the reaction is related to the flow of electrons at the electrode surface and the rate of reaction. As the current was reported, not current density (the current normalised to the electrode surface area), the high current for triphenylphosphine could have been because newer electrodes were used. New electrodes would have a larger surface area than electrodes that have been cleaned multiple times (as for the ones used with tetrahydrothiophene), and therefore the rate of reduction will be higher, resulting in a higher current.

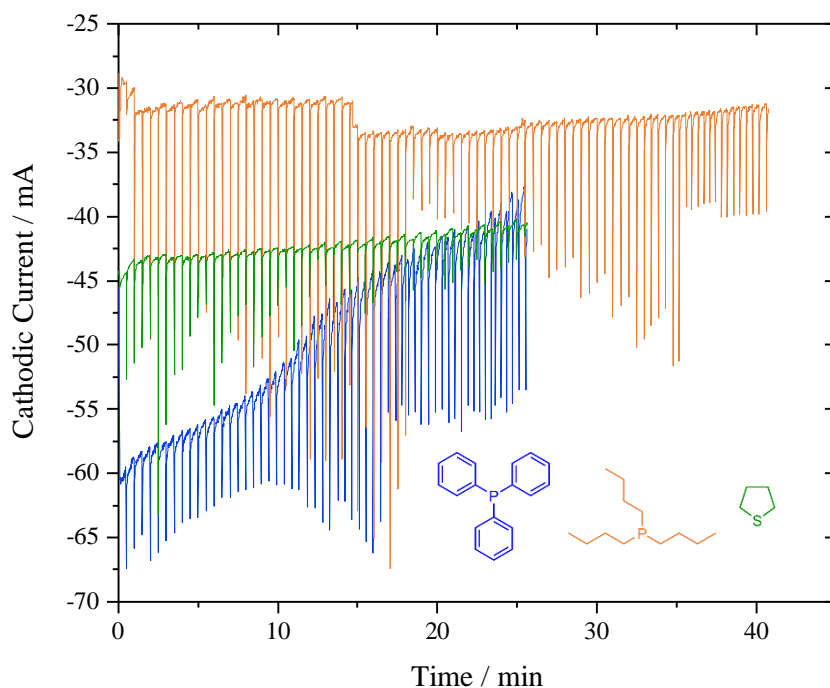


Figure 3.9 Overlaid current traces showing negative absolute current vs time for the different sacrificial electron donors.

One possible reason for consumption of iminium ion **3.154** without formation of amine **3.116** in the electrolysis with tributylphosphine could be due to a radical intermediate of tributylphosphine which reacts with the α -amino radical formed during electrolysis and therefore the desired **3.154** would not form. In order for this reaction to occur, the intermediate from tributylphosphine must be sufficiently stable, to travel from the anode to the cathode and react with the α -amino radical. By running the CVs at lower concentrations and slower scan rates, the two one-electron oxidations proposed for the SEDs should be visible as two separate peaks. CVs of the sacrificial electron donors were recorded at lower concentrations (0.03 M) and slower scan rates (100 mV s^{-1}) and are overlaid in Figure 3.10.

The CVs of tetrahydrothiophene and triphenylphosphine showed two peaks for the two separate oxidations (+1.79 V and +2.26 V vs Ag/AgCl for tetrahydrothiophene and +1.30 V and +2.01 V vs Ag/AgCl for triphenylphosphine), whilst only one peak was visible for tributylphosphine at E_{ox} +1.18 V vs Ag/AgCl (zoom region in Appendix C.5). Due to the absence of the second oxidation peak, it was speculated that the tributylphosphine intermediate was sufficiently long lived that it could theoretically react with the α -amino radical formed at the cathode, accounting for consumption of iminium ion **3.154** but with no evidence of the product **3.116** during the electrolysis reactions. However, as the radical is likely unstable with three alkyl groups, it is therefore unlikely to be long lived enough to travel between the anode and the cathode. An alternative reason for the absence of the second oxidative peak in the cyclic voltammogram is a rapid reaction with superoxide which is generated during cyclic voltammetry (see Section 3.2.6.3).

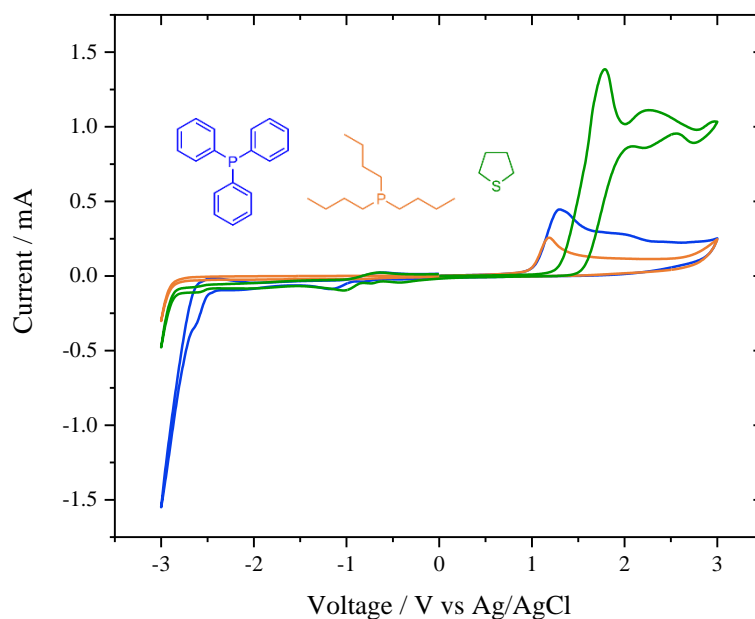


Figure 3.10 Cyclic voltammograms of the different sacrificial electron donors at 0.03 M, recorded at 100 $mV s^{-1}$.

3.2.6.2 Investigation of the Oxidation of Amine Product by Cyclic Voltammetry

In the electrolysis reaction, iminium ion **3.154** is reduced, and the resulting radical adds to acrylonitrile forming tertiary amine **3.116**. This amine should be relatively easy to oxidise, based on the information in Section 3.1.2. However, the results in Table 3.2 showed that the product was not consumed on passing more equivalents of electrons, which implies that the product is electrochemically stable in the applied potential window. A CV of amine **3.116** at 0.07 M revealed two oxidation peaks: an initial oxidation at E_{ox} +1.46 V vs Ag/AgCl, with

a smaller peak for a second oxidation at $E_{\text{ox}} + 1.92$ V vs Ag/AgCl (see Appendix C.3). These two peaks were associated with the oxidation of the amine to the radical cation and likely the radical cation to an iminium ion (as shown in Scheme 3.4).

To understand the relative oxidation of amine product **3.116** versus SED, CVs were recorded at various concentrations of amine **3.116** and with and without the sacrificial electron donor tetrahydrothiophene. The peak height for the first oxidation of amine **3.116** was compared (the overlay is presented in the Appendix C.4). Figure 3.11 shows overlaid CVs of amine **3.116** (0.012 M) with and without tetrahydrothiophene (0.049 M). These concentrations mimic the experimental stoichiometry of forming amine **3.116** in a *ca.* 50% yield. The oxidation of amine **3.116** was observed in both cases at *ca.* +1.0 V vs Ag/AgCl. However, the peak height for the oxidation of tetrahydrothiophene is almost 9 times higher than for the oxidation of amine **3.116**. This means that the oxidation of tetrahydrothiophene would happen quicker, therefore explaining why in the reaction the SED is preferentially oxidised over amine **3.116**. The local concentration of SED at the anode will also disfavour the oxidation of the amine formed at the cathode, which will have to travel from near the cathode where the α -amino radical is generated. Furthermore, the higher equivalents of SED will statistically favour the oxidation of the SED over the amine (e.g. **3.116**) formed.

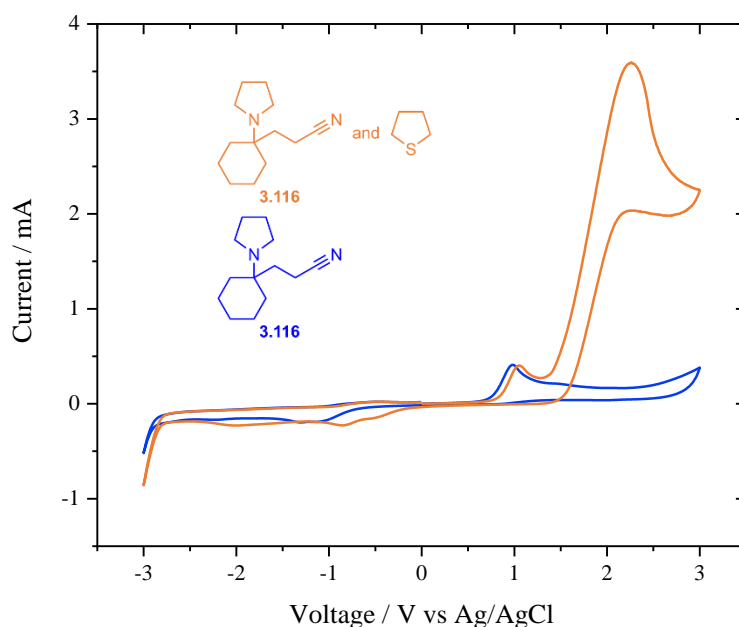


Figure 3.11 Cyclic voltammograms of amine **3.116** (0.012 M) with and without tetrahydrothiophene (0.049 M), recorded at 500 mV s^{-1} .

The rates of SED oxidation, relative to the rate of product **3.116** oxidation, may also explain difference in yields when exploring different SEDs. As the rate of oxidation of the tributylphosphine was lower than for the other SEDs, as observed both in the current trace (Figure 3.9) and overlaid CVs (Figure 3.10), amine **3.116** may have formed during electrolysis, and then preferentially oxidised over tributylphosphine. This would explain the high consumption of iminium ion **3.154**, yet no yield of amine **3.116** observed (Table 3.4, entry 2).

3.2.6.3 Investigation of the Reduction of Iminium Ion by Cyclic Voltammetry

In Figure 3.5, a literature-comparable CV of iminium ion **3.154** was presented, measured at a platinum working electrode. In order to collect data that is comparable to the electrosynthesis conditions, a CV of iminium ion **3.154** was also recorded using the modified ElectraSyn set-up and glassy carbon working electrode (Figure 3.12). At 0.026 M, a reduction maximum, E_{red} , was observed at -2.25 V vs Ag/AgCl that was attributed to the reduction of the iminium ion to the α -amino radical. The fact that this E_{red} value is more negative than that recorded at a platinum working electrode illustrates the important role that the working electrode material can play in determining the overpotential of a reaction. The E_{red} value of -2.25 V vs Ag/AgCl is still consistent with previously reported “all-alkyl” iminium ions (Figure 3.3).^{177,178}

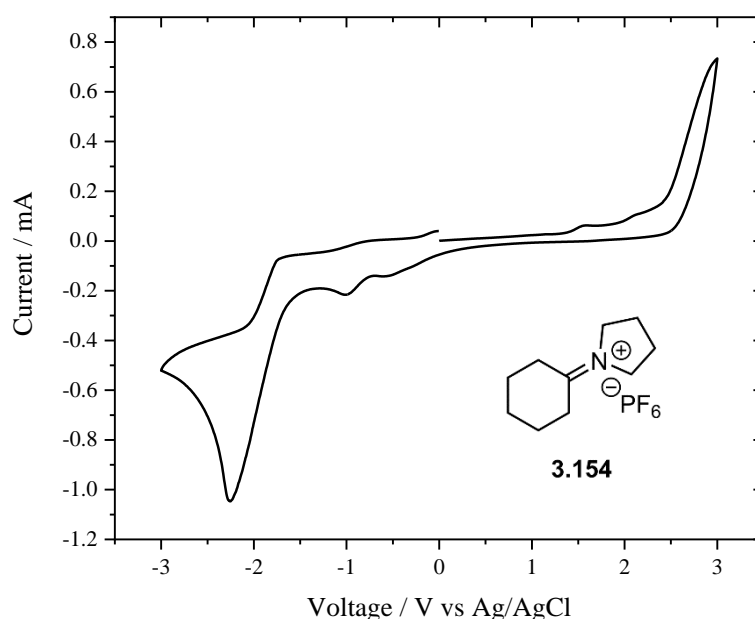


Figure 3.12 Cyclic voltammogram of iminium ion **3.154** recorded using the modified ElectraSyn set-up, at 0.026 M, 500 mV s^{-1} .

To further show that the peak at -2.25 V vs Ag/AgCl is the reduction of the iminium ion to the radical, acrylonitrile was titrated into CV experiments. If the peak at -1.02 V vs Ag/AgCl was the first electron reduction, then the peak at -2.25 V vs Ag/AgCl should disappear as the radical formed would add to the alkene. Figure 3.13 shows an overlay of the CVs recorded with up to 30 μL , (4.2 eq.) of acrylonitrile. On adding acrylonitrile, the peak at -2.25 V vs Ag/AgCl did not change and so it could be concluded that this was the peak for the reduction of iminium ion **3.154**. The peak which appeared at potentials more negative than -2.50 V vs Ag/AgCl was the electrochemical reduction of acrylonitrile (see Appendix C.1 for CV of acrylonitrile). A likely justification for the peak at -1.02 V vs Ag/AgCl is the reduction of oxygen to superoxide, which has previously been observed at *ca.* -1.0 V vs SCE (*ca.* 0.96 V vs Ag/AgCl) using a glassy carbon working electrode in 0.1 M tetraethylammonium tetrafluoroborate in acetonitrile, as the solvents weren't degassed before electrochemistry.²²⁶

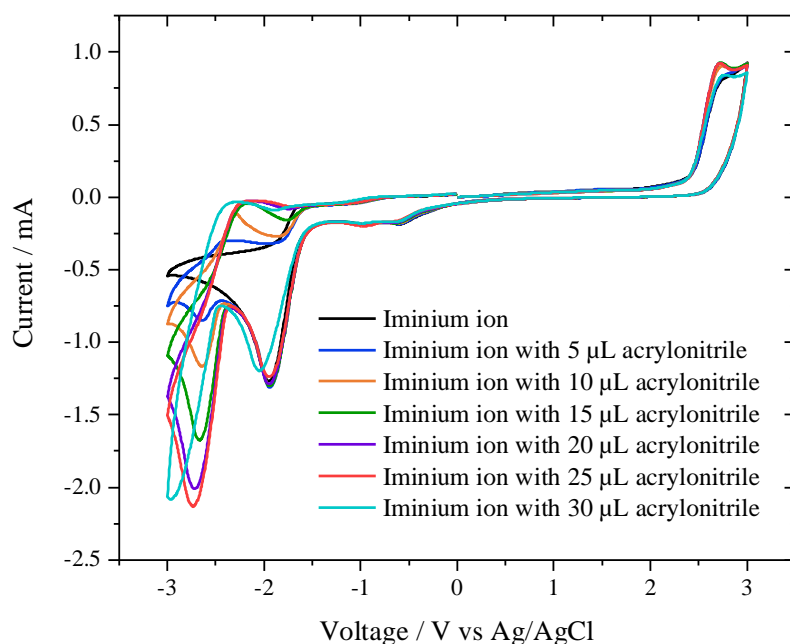


Figure 3.13 Overlaid cyclic voltammograms of iminium ion **3.154** (0.026 M) and increased amounts of acrylonitrile, recorded at 500 mV s^{-1} .

3.2.6.4 Investigation of the Electrolysis Reaction Mixture by Cyclic Voltammetry

A CV of the reaction mixture was also recorded (Figure 3.14) using iminium ion **3.154** (0.021 M), acrylonitrile (0.062 M) and tetrahydrothiophene (0.042 M) to validate the large voltage window, measured at greater than 4 V. The oxidation maxima for tetrahydrothiophene occurs at $+2.31$ V vs Ag/AgCl, whilst the reduction maxima for

iminium ion **3.154** occurs at -1.93 V vs Ag/AgCl, which means that the minimum voltage window needed to do both the desired oxidation and reduction is 4.24 V (Figure 3.14, orange line). The 5 V window that was applied experimentally meant that both the oxidation and reduction could thermodynamically occur, whilst this window is also narrow enough to ensure that the reduction of acrylonitrile will not readily compete.

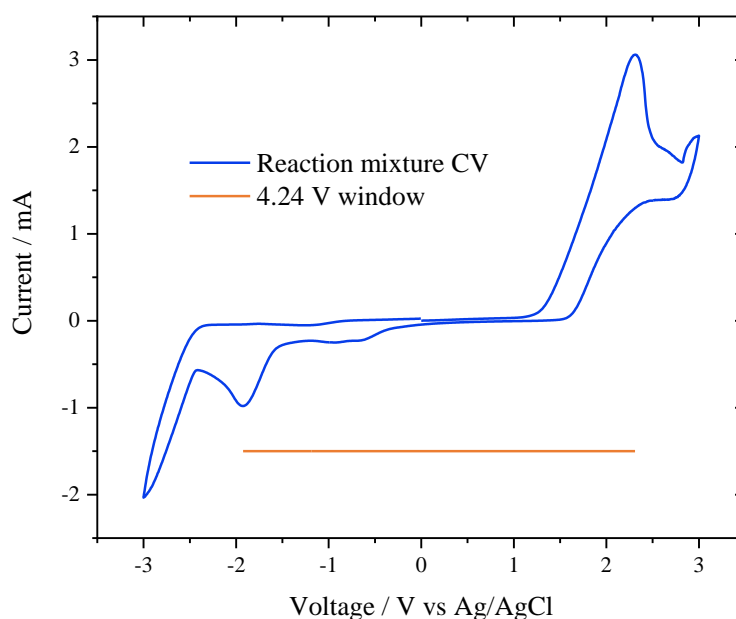


Figure 3.14 Cyclic voltammogram of iminium ion **3.154** (0.021 M), acrylonitrile (0.062 M) and tetrahydrothiophene (0.042 M), recorded at 500 mV s^{-1} .

3.2.7 Investigation of *In-Situ* Iminium Ion Formation with 4 \AA Molecular Sieves and Reaction with Acrylonitrile Under Electrolysis Conditions

With optimised reaction conditions for electrolysis determined, iminium ion formation was explored in conjunction with electrochemistry as a method of directly accessing the tertiary amine products (analogous to the photochemical transformations in Scheme 3.10). It was hypothesised that because the electrochemistry would consume the iminium ion, this would result in a shift in favour of the iminium ion in the equilibrium of the iminium ion forming reaction, resulting in higher yields for the intermediate and streamlining the process.

In an attempt to access tertiary amine **3.116** directly, cyclohexanone, pyrrolidine, and ammonium hexafluorophosphate were mixed in dry acetonitrile and activated 4 \AA molecular sieves were added to remove water (Scheme 3.60). The 4 \AA molecular sieves were added

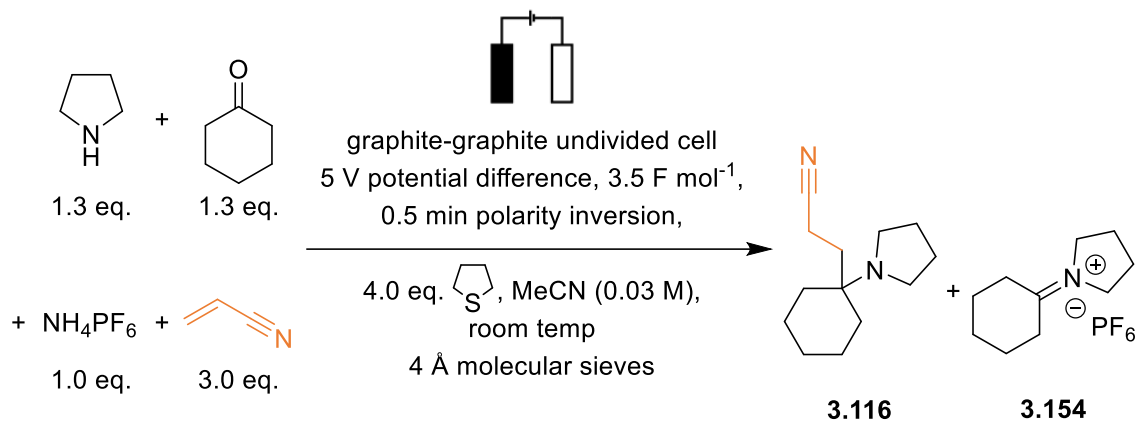
both during and prior to electrolysis. A 5 V potential difference was applied across the two electrodes and, after a total charge of 3.5 F (mol of ammonium hexafluorophosphate)⁻¹ was passed, the resulting solution was analysed by quantitative ¹H NMR spectroscopy using dibromomethane as an external standard. Reactions were performed under a nitrogen atmosphere to limit the ingress of water.

Initially, all the reagents were mixed in acetonitrile over activated 4 Å molecular sieves and the 5 V potential difference was applied immediately (Table 3.5, entry 1). Gratifyingly, a 21% yield of amine **3.116** was observed in the ¹H NMR spectrum of the crude product along with 12% unreacted iminium ion **3.154**. It was believed that the equilibrium between starting materials and iminium ion was established quickly, and subsequent water removal was slow. This had previously been observed in the ¹H NMR spectroscopy studies with 4 Å molecular sieves (Section 3.2.2). Therefore, the low yield of amine **3.116** was likely due to lack of iminium ion due to insufficient removal of water by the 4 Å molecular sieves in the timeframe of the reaction as little unreacted iminium ion **3.154** remained in the resulting crude mixture.

To further increase the amount of iminium ion **3.154**, and therefore the yield of amine **3.116**, increased reaction times were considered. Pyrrolidine, cyclohexanone, and ammonium hexafluorophosphate were mixed in an ElectraSyn vial with dry acetonitrile and activated 4 Å molecular sieves. The mixture was stirred for 1 hour to pre-form some of iminium ion **3.154** prior to electrolysis. After 1 hour, acrylonitrile and tetrahydrothiophene were added and the mixture was electrolysed. However, according to the ¹H NMR spectrum of the crude product, only a 15% yield of product **3.116** was achieved along with 6% of iminium ion **3.154** remaining (Table 3.5, entry 2). This indicates that, overall, less iminium ion had formed under these reaction conditions.

The presence of the 4 Å molecular sieves in the ElectraSyn 2.0 vial impeded the stirring, and it was hypothesised that this may have contributed to the poor yields of amine **3.116**. Therefore, pyrrolidine, cyclohexanone, and ammonium hexafluorophosphate were mixed in 19 mL of dry acetonitrile and pre-stirred in a Schlenk tube containing activated 4 Å molecular sieves for 2 hours prior to electrolysis. 18 mL of this mixture was then transferred into a dried ElectraSyn vial before acrylonitrile and tetrahydrothiophene were added and the mixture was electrolysed. Analysis of the resulting ¹H NMR spectrum of the crude product showed a 17% yield of both amine **3.116** and iminium ion **3.154** (Table 3.5, entry 3). The

results were comparable to 4 Å molecular sieves and immediate electrolysis (Table 3.5, entry 1). However, the yield of amine **3.116** was still low compared to using pre-formed iminium ion. It was therefore decided not to pursue this molecular sieve approach any further.



Scheme 3.60 In-situ formation of iminium ion **3.154** with 4 Å molecular sieves and electrochemical reduction to give **3.116**.

Table 3.5 The outcome of in-situ formation of iminium ion **3.154** and subsequent electrolysis to form amine **3.116**.

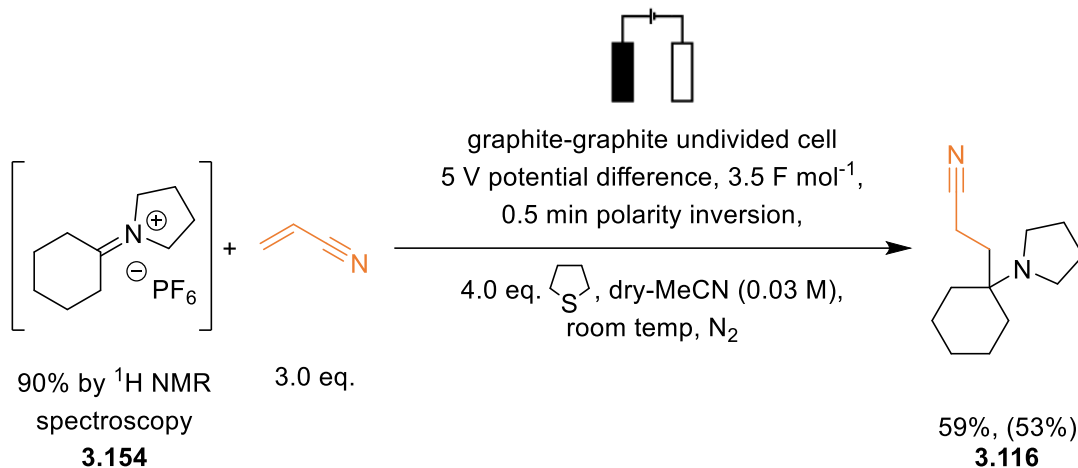
Entry	Conditions	Product 3.116	Iminium Ion
		Yield / % ^a	3.154 Yield / % ^a
1	All reagents with 4 Å molecular sieves and immediate electrolysis	21	12
2	Pyrrolidine, cyclohexanone, ammonium hexafluorophosphate and 4 Å molecular sieves pre-stirred for 1 h in ElectraSyn vial before acrylonitrile and tetrahydrothiophene added, then electrolysis	15	6
3	19 mL of reaction mixture pre-stirred for 2 h in Schlenk tube with 4 Å molecular sieves, then transferred to ElectraSyn vial with acrylonitrile and tetrahydrothiophene before electrolysis	17	17

^a Determined by ¹H NMR spectroscopy using dibromomethane as an external standard

3.2.8 Use of Unpurified Iminium Ions and Reaction with Acrylonitrile Under Electrolysis Conditions

As an *in-situ* approach to iminium ion generation using 4 Å molecular sieves and subsequent electrolysis did not prove effective, the feasibility of directly electrolyzing the unpurified iminium ions formed from azeotropic distillation route was tested. A solution of unpurified iminium ion **3.154** (90% yield by quantitative ^1H NMR spectroscopy, as prepared in Section 3.2.3) in dry acetonitrile was transferred into a flame-dried ElectraSyn vial. To the solution of iminium ion, acrylonitrile and tetrahydrothiophene were added and the solution was electrolysed for 3.5 F mol $^{-1}$ (assuming 100% purity of the iminium ion).

Amine **3.116** was isolated by column chromatography in a 53% yield for the two steps of iminium ion formation and electrolysis, based on the amount of ammonium hexafluorophosphate (the limiting reagent) used to make the iminium ion. The yield for just the electrolysis step could be determined at 59% (Scheme 3.61), based on the amount of iminium ion formed (90%). This yield is comparable to the electrolysis yield with purified, isolated iminium ion, suggesting that the presence of a small amount of unreacted amine, ketone or ammonium salt did not hinder the electrolysis.



Scheme 3.61 Synthesis of tertiary amine **3.116** by electrolysis of an unpurified mixture of iminium ion **3.154**. Isolated yield of amine product for electrolysis step reported, the yield over two steps accounting for iminium ion formation reported in brackets.

The yield for this reaction is comparable to the yield achieved by the Gaunt group for the photochemical reduction of enamines and addition to alkenes.¹⁷³ Moreover, this

electrochemical approach avoided the isolation of the intermediate iminium ions and more costly iridium photocatalysts.

3.2.8.1 Iminium Ion Scope: Changing the Ketone Component

Having established a method of accessing a range of iminium ions and optimum conditions for electrolysis, attention turned to exploring the scope of the electrochemical reaction (iminium ion reduction and reaction with acrylonitrile). As there are three components that make up the final tertiary amine, one component was varied at a time to observe the effect on the outcome of the reaction. Initially, the scope with respect to the ketone and amine components were explored using the unpurified iminium ions formed from the azeotropic distillation route for their preparation. For the reaction scope of the iminium ions, two yields are reported: the first, the yield for the electrolysis step, calculated as the proportion of iminium ion that has been converted into tertiary amine product (iminium ion quantity determined by quantitative ^1H NMR spectroscopy). Secondly, the yield quoted in brackets is the overall two-step yield, accounting for the iminium ion formation and electrolysis steps (based on the amount of ammonium hexafluorophosphate used to make the iminium ion).

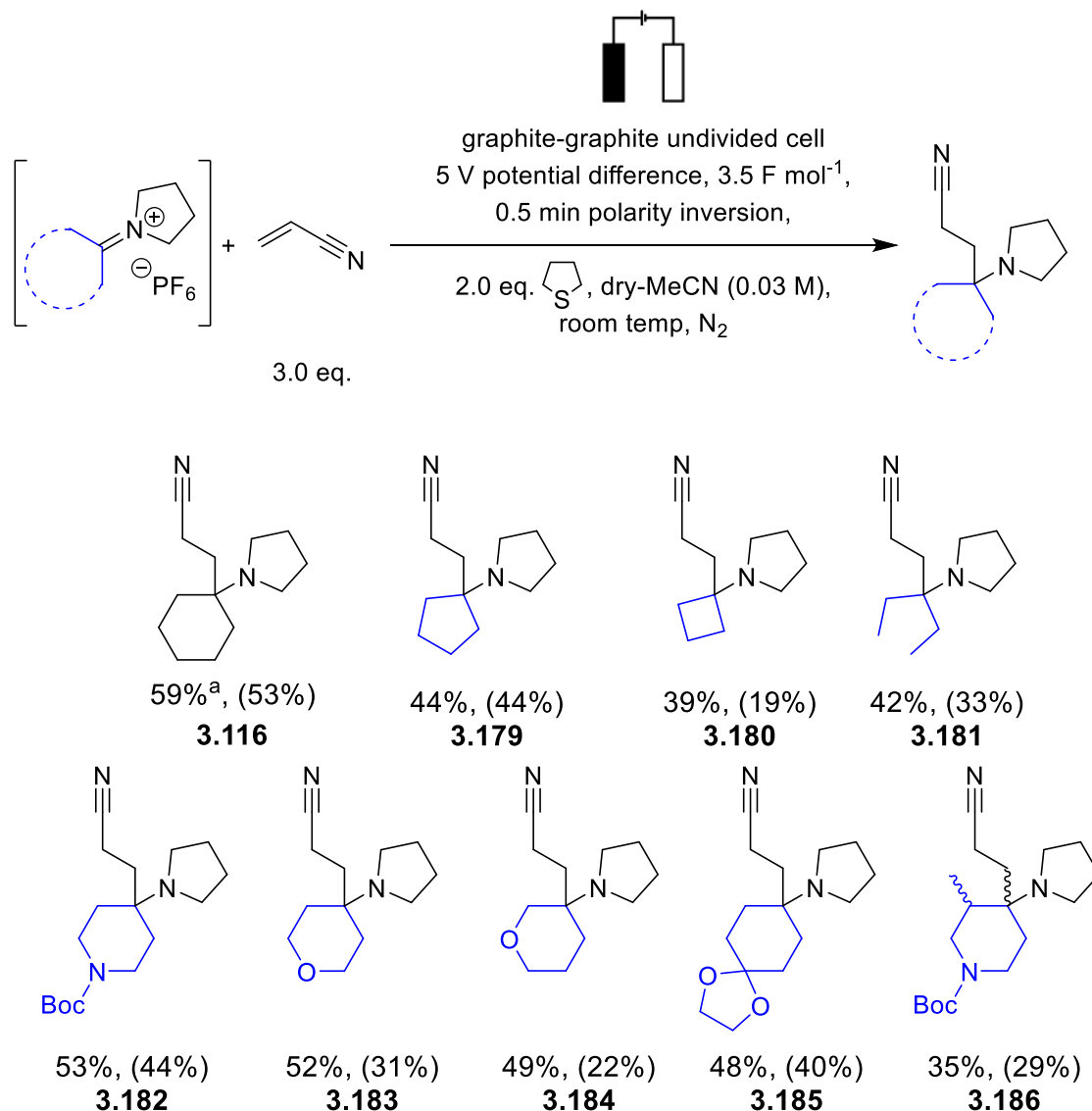
Some electrolyses were performed with 4.0 eq. of tetrahydrothiophene, as opposed to the optimised 2.0 eq., as these reactions were conducted during the optimisation process. As it was shown that the amount of SED (4.0 eq. or 2.0 eq.) did not affect the outcome of electrolysis, these reactions were not repeated at 2.0 eq. tetrahydrothiophene.

Iminium ions derived from pyrrolidine and a range of ketones were electrolysed first (Scheme 3.62). Initially, iminium ions bearing different sized alkyl rings were tested. Amine **3.179**, derived from cyclopentanone was isolated in a 44% yield and amine **3.180**, derived from cyclobutanone, was isolated in a 39% yield for the electrolysis step. It was found that decreasing the size of the ketone component resulted in reduced yields of tertiary amines. As the iminium ion was reasonably strained, radical formation at the electrode surface may be more difficult, resulting in poorer yields of tertiary amines. With iminium ions derived from acyclic ketones, the increased flexibility of the alkyl groups also resulted in lower yields due to increased steric hindrance. The acyclic ketone derived iminium ion with two ethyl groups resulted in **3.181**, isolated in a 42% yield for the electrolysis step which is comparable to the strained cyclic analogue. However, as the iminium ion derived from

cyclopentanone was formed in a near quantitative yield, the yield over two steps to amine **3.179** was higher than amine **3.181** derived from 3-pentanone, 44% and 33% respectively.

Amines derived from *N*-Boc-4-piperidineone **3.182** and tetrahydro-4*H*-pyran-4-one **3.183** were isolated in 53% and 52% yields for the electrolysis step respectively. This shows that the introduction of mildly electron withdrawing groups did not significantly reduce the nucleophilicity of the α -amino radical, which readily underwent addition with acrylonitrile in comparable yields to amine **3.116** derived from cyclohexanone. On moving the heteroatom closer to the α -amino radical, a slightly reduced yield for amine **3.184**, 49% for electrolysis, was observed. As the electron-withdrawing group was in closer proximity to the radical, the α -amino radical may have been slightly less nucleophilic and therefore led to a reduction in yield. Iminium ion **3.163**, was also successfully used as a starting material, resulting in amine **3.185** in a 48% yield for electrolysis. As the ketal group remained intact, this amine could undergo further diversification *via* the ketone after deprotection.

A decrease in yield was observed on introducing methyl substituents onto the ketone component as it made the α -amino radical more sterically congested, which hindered addition to the alkene. *N*-Boc protected piperidine analogue was electrolysed and amine **3.186** was subsequently isolated in a 35% yield for the electrolysis step, although it was not possible to determine the ratio of diastereoisomers or indeed if a mixture of diastereoisomers was in fact produced.



^a 4.0 eq of tetrahydrothiophene used

Scheme 3.62 Synthesis of tertiary amines by electrolysis of unpurified mixtures of iminium ions derived from various ketones. Isolated yields of amine products for electrolysis step reported, the yield over two steps accounting for iminium ion formation reported in brackets.

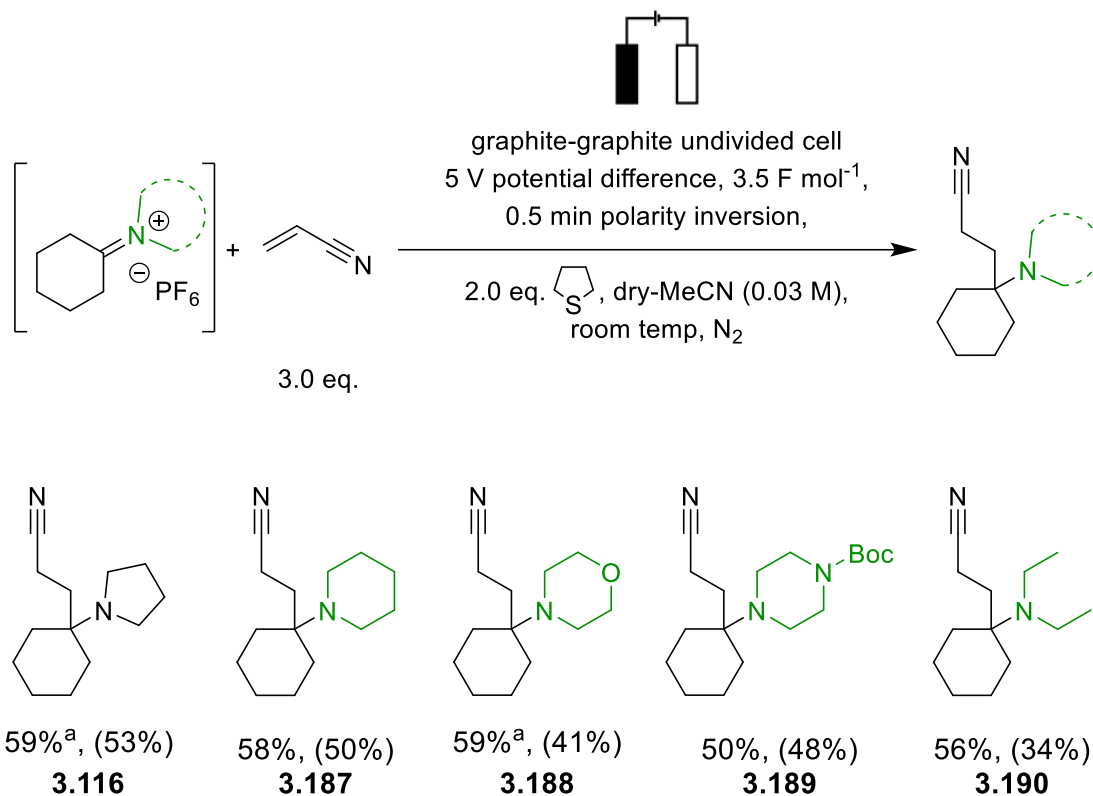
Generally, as expected based on screening reactions of iminium ion formation (Section 3.2.3) on changing the ketone component, the steric effect of smaller rings or more flexible alkyl groups resulted in reduced yields compared to reactions using iminium ions derived from cyclohexanone. Additionally, the introduction of methyl groups resulted in poorer yields due to increased steric hindrance which impeded the radical addition. Finally, mildly electron withdrawing substituents were compatible in the 4-position of the ketone and had

little effect on the yield of the reaction. Moving electron-withdrawing groups closer to the α -amino radical resulted in poorer yields as the resulting radical was less nucleophilic.

3.2.8.2 Iminium Ion Scope: Changing the Amine Component

Next, iminium ions synthesised from cyclohexanone with different cyclic and acyclic secondary amines were electrolysed in the presence of acrylonitrile (Scheme 3.63). Piperidine was successfully incorporated, and amine **3.187** was isolated by column chromatography in a 58% yield for the electrolysis step. The yield over two steps was 50% yield relative to the amount of ammonium hexafluorophosphate, which is comparable to the yield over two steps for the iminium ion derived from pyrrolidine. With iminium ions derived from morpholine and piperazine, the resulting amines were achieved in similar yields for electrolysis, 59% and 50% for **3.188** and **3.189** respectively. This shows that electron-withdrawing heteroatoms in the 4-position of the amine component are likely far enough away from the α -amino radical that they do not significantly change the nucleophilicity of the radical, and the addition to alkenes is unaffected.

Amine **3.190** was prepared in a 56% yield for the electrolysis step from an iminium ion derived from diethylamine. Unlike with the ketone component, flexible ethyl groups did not hinder radical addition as the yield for electrolysis is comparable to iminium ions derived from cyclic amines.



^a 4.0 eq of tetrahydrothiophene used

Scheme 3.63 Synthesis of tertiary amines by electrolysis of unpurified mixtures of iminium ions derived from various amines. Isolated yields of amine products for electrolysis step reported, the yield over two steps accounting for iminium ion formation reported in brackets.

Overall, it was therefore found that changing the amine component in the electrolysis of unpurified iminium ions only had a small effect on the outcome of the reaction. The electrolysis yields with larger ring sizes, acyclic amines and on introducing electron-withdrawing heteroatoms were comparable and ranged from between 50% to 59%.

3.2.9 Use of Pure Iminium Ions and Reaction with Different Alkenes Under Electrolysis Conditions

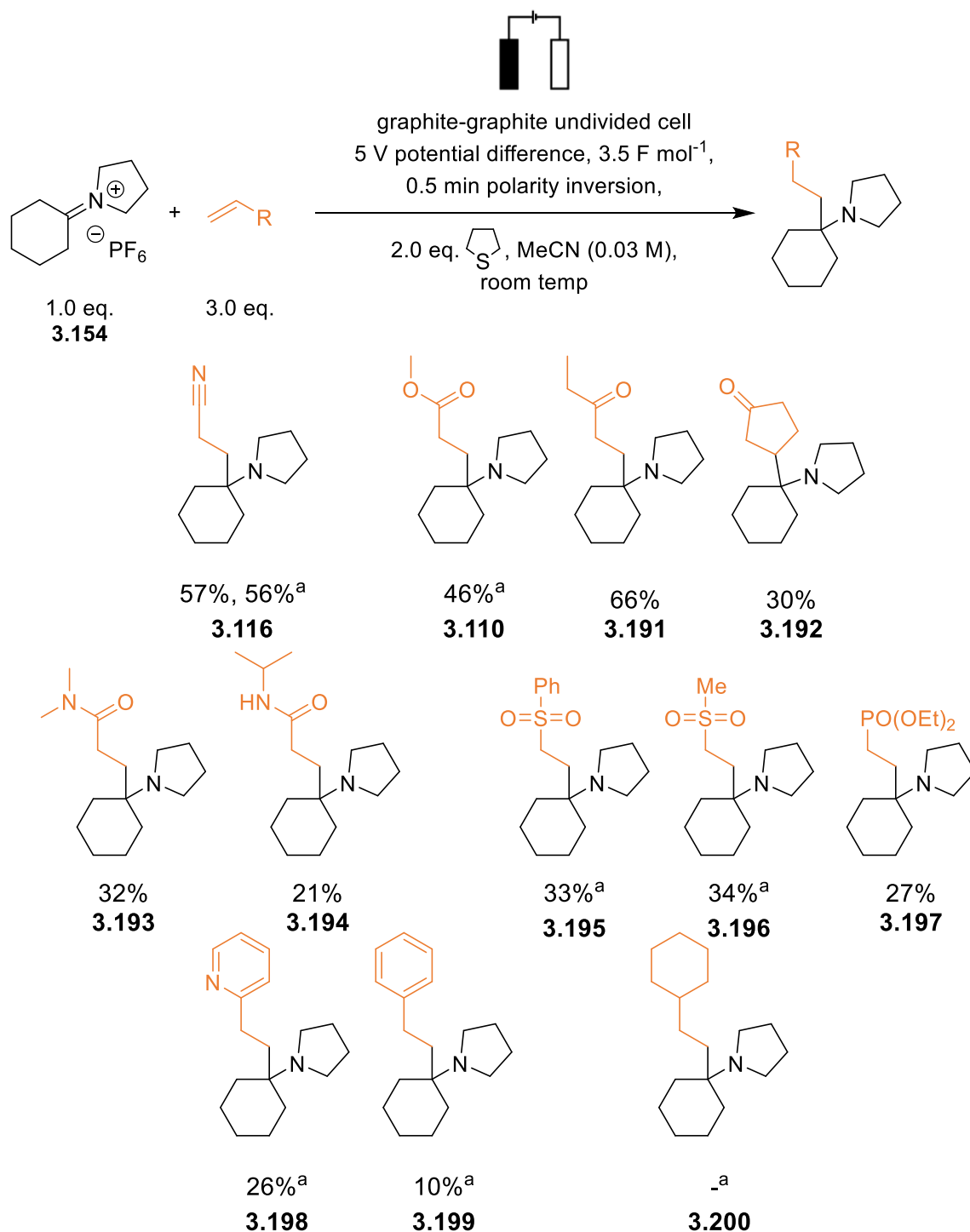
It was shown that the overall yield of tertiary amines over the two steps was limited in some cases by the amount of iminium ion formed in the first step. Therefore, on exploring the scope with respect to the alkene, purified preformed iminium ion **3.154** was used. As the same iminium ion was to be used in all the alkene scope studies, it was decided to use a pure iminium ion. The two factors that control the rate of radical addition to alkenes are the sterics and electronics of the alkene.¹⁵ Alkenes with both strongly and weakly electron-withdrawing

groups were studied which delivered tertiary amines with a broad range of α -substituents (Scheme 3.64).

Amine **3.116** was successfully prepared in a 57% yield using acrylonitrile. Other strongly electron-withdrawing groups such as esters and ketones gave tertiary amines in moderate to high yields of 46% and 66% for **3.110** and **3.191** respectively. Cyclopentenone was used as a bulkier, cyclic alkene and this gave amine **3.192** in only 30% yield, presumably due to the increased steric hindrance. A reduction in yield for a similar radical addition has previously been observed.²²⁷

Amides are less withdrawing than ketones and esters therefore the SOMO-LUMO energy gap will be larger. As a result, poorer yields were observed with both tertiary and secondary acrylamides. Amine **3.193** was isolated in a 32% yield whilst amine **3.194** was only achieved in a 21% yield. The difference in yield between the secondary and tertiary amide could be due to a difference in the electronic effects: tertiary amides withdraw electron density more strongly than secondary amides. Alternatively, secondary amides may undergo side reactions more readily than tertiary amides.

The reaction was somewhat compatible with alkenes containing other carbonyl-derived electron-withdrawing groups incorporating different heteroatoms. Sulfones are strong electron withdrawing groups but low yields were achieved. Initially, it was hypothesised that the low 33% yield for amine **3.195** was due to a side reaction between the phenyl group of the alkene acceptor and the graphite electrode. This is because there could be a strong affinity between the aromatic rings and the carbon electrode. However, when the methyl variant was tried, a comparable 34% yield for amine **3.196** was achieved, therefore disproving the theory. Another potential side reaction would be electrochemical reduction of the sulfone. However, the ¹H NMR spectrum of the crude product appeared relatively clean with the major peaks corresponding to the tertiary amine product and excess unreacted vinyl sulfone. Therefore, the poor yield for addition to vinyl sulfones remains unexplained. With diethyl vinyl phosphonate, only a 27% yield was achieved for amine **3.197**. Whilst phosphonates are also very strong withdrawing groups, it is not uncommon to observe lower yields for addition to vinyl phosphonates compared to nitriles although the reason why this occurs is unclear.^{173,181}



^a 4.0 eq of tetrahydrothiophene used

Scheme 3.64 Synthesis of amines by electrolysis of iminium ion 3.154 and various electron-deficient alkenes. Isolated yields of amine products for electrolysis step reported.

Alkenes bearing aromatic substituents were also tested. Pyridine is weakly electron withdrawing and only a 26% yield for amine **3.198** was achieved. Additionally, a rapid drop

in the reductive current was observed in the first 20 minutes of the reaction (Figure 3.15), implying rapid passivation of the electrode surface. This level of passivation was not observed for any other alkenes and could thus account for the low yield in this reaction. Styrene has a poor electron withdrawing group and only a 10% yield for amine **3.199** was isolated. Furthermore, the reduction potential for the second electron reduction, of the styryl radical to the anion, is more negative than for the electron deficient alkenes, *ca.* -1.6 V vs Ag/AgCl.^{228,229} This means the alkyl (styryl) radical formed after radical addition may not undergo second reduction to an anion in the applied potential window. The alkyl radical formed could then participate in side reactions, such as oligomerisation, leading to a poor yield of amine **3.199**. Unlike reaction with vinyl pyridine, the current was maintained throughout the reaction which suggests little to no passivation. Finally, as expected, coupling to electron rich alkenes proved unsuccessful (**3.200**).

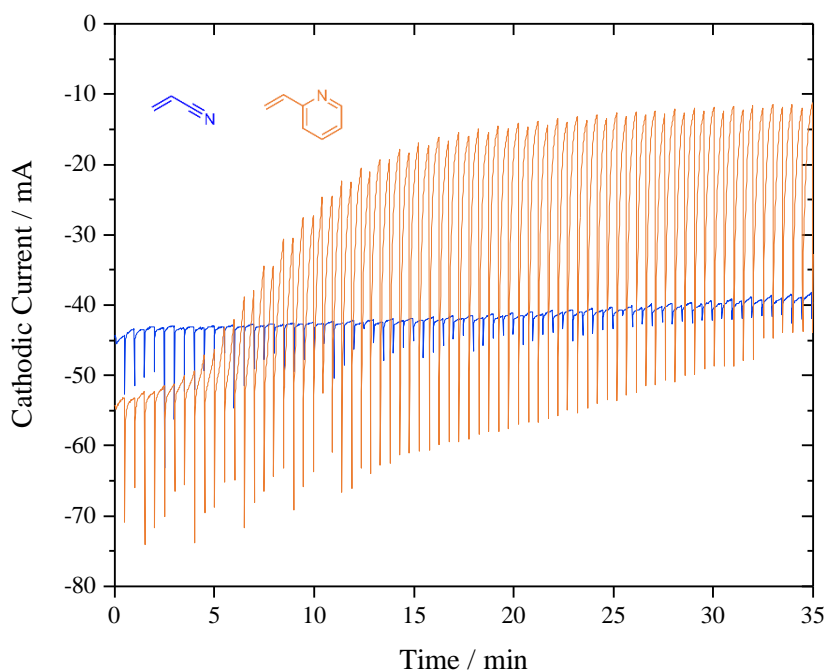


Figure 3.15 A graph showing current vs time, for the first 35 minutes, for electrolysis with vinyl pyridine and acrylonitrile.

3.3 Conclusions and Future Work

In conclusion, an electrochemical approach to the synthesis of sterically hindered tertiary amines has been developed. Iminium ions, either purified or used in crude form, have successfully been electrochemically reduced and the α -amino radicals formed have undergone addition to a range of electron-deficient alkenes.

Iminium ions were prepared *via* condensation reactions of commercially available, typically cyclic, amines and ketones. Whilst molecular sieves were used in the analogous photoredox approach, they were found to be less effective at forming iminium ions in an *in-situ* electrochemical approach. This was because, relatively, the photochemical reductions were performed over longer periods of time to allow for slow iminium ion formation. Therefore, iminium ions were preformed *via* azeotropic distillations and often used unpurified in the electrolysis experiments. The iminium ion formation step is effective using different sized ketone and amine rings, acyclic examples, and the introduction of electron-withdrawing heteroatoms. The iminium ion forming reaction was incompatible with very strongly electron-withdrawing groups and examples where the withdrawing group was close to the iminium ion C=N group as it resulted in an unstabilised iminium ion. The formation of iminium ions was more sensitive to changes to the ketone component than the amine.

The electrochemical reduction of iminium ions and subsequent addition to alkenes used mild reaction conditions and electrons as reagents, which avoided the need for costly transition metal catalysts, or stoichiometric amounts of toxic reducing agents. The nature of the amine component had a very little effect on the yield of the amine from the electrolysis step, whilst the introduction of electron-withdrawing groups on the ketone component resulted in less nucleophilic radicals and a slight reduction in yield. A-Methyl groups on the ketone also hindered addition to alkenes and thus resulted in low yields of the amine after electrolysis. Low yields over two steps were often observed for examples where the iminium ion was formed in low yields.

Compared to other electrochemical approaches to amine synthesis *via* iminium ions, this method was high yielding, and generated a complex α -tertiary carbon centre.^{195,196} It utilised a range of readily available alkenes, making it analogous to the recent photochemical variants of the reaction.¹⁷³ The reaction was tolerant of a range of electron-withdrawing functional groups on the alkene component with more electron withdrawing groups resulting in improved yields of the desired amine.

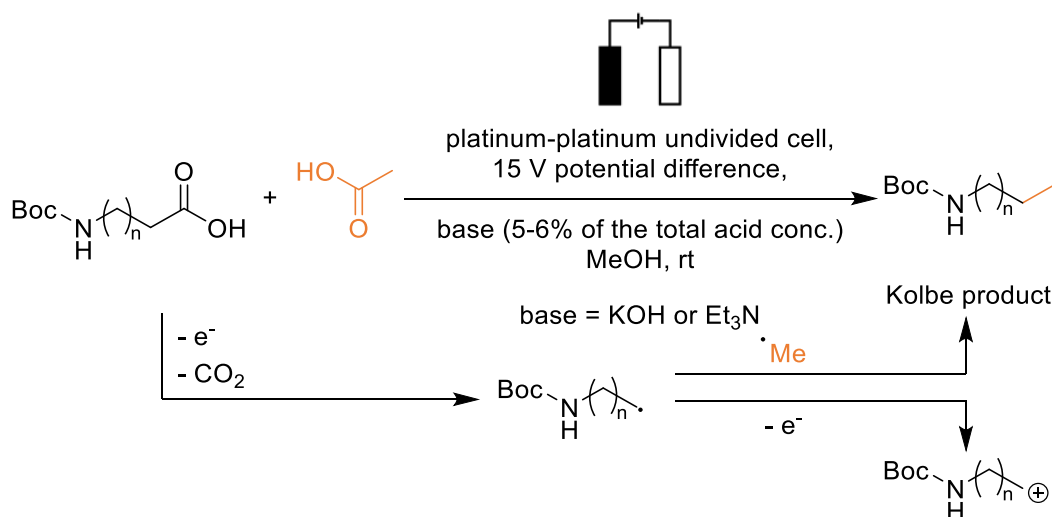
Overall, 23 different sterically hindered tertiary amines have been prepared by this method with yields ranging from 10% to 66%. Lower yields were typically observed by increasing the steric bulk around the α -amino radical or alkene or with less electron-deficient alkenes, such as styrene. Moderate to good yields were observed with addition to very electron deficient alkene such as acrylonitrile or ethyl vinyl ketone.

Future developments of this electrolysis reaction could include expanding the scope of all three components. For example, acyclic, asymmetrical amines and ketones as well as iminium ions derived from aldehydes could be tested. The alkene component could also be varied to include more sterically hindered alkenes such as cyclopent-1-enecarbonitrile or more functionalised alkenes like methyl-2-(di(tert-butoxycarbonyl)amino)but-2-enoate **3.66** used by the Dixon group to create protected novel amino acids.¹⁷⁵ Finally, the scale of electrolysis was limited by the concentration and current in the ElectraSyn 2.0, therefore developing a method to scale up the reaction (to gram scale) would allow larger quantities of tertiary amines to be synthesised efficiently.

Chapter 4: Overall Conclusions and Future Work

Electrochemistry has been shown to be a valuable tool in developing new radical methodologies for synthetic applications. Alkyl radicals have been generated by both oxidation and reduction which were subsequently used for the construction of carbon-carbon bonds.

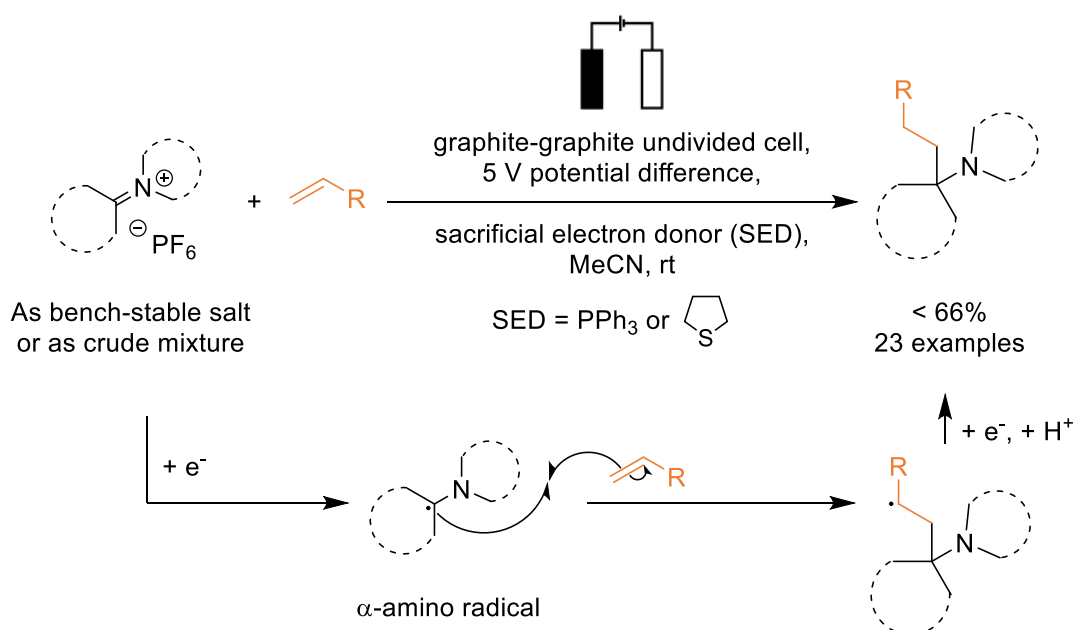
In Chapter 2, Kolbe electrolysis was used for the coupling of two anodically generated alkyl radicals. One radical was a methyl radical, derived from acetic acid and the other was an alkyl radical from a protected linear amino acid (Scheme 4.1). The electrolysis conditions were varied, however, overall the Kolbe reaction was found to be highly substrate dependent where the alkyl radicals formed from the protected amino acid were in competition with a second electron oxidation and the formation of carbocation derived non-Kolbe products. Alkyl radicals with low ionization potentials, such as α -amino radicals, readily formed carbocations and gave high yields of non-Kolbe products whilst δ -amino radicals gave high Kolbe:non-Kolbe product ratios. This presents a large limitation for the applicability of Kolbe electrolysis and potentially for oxidative generation of alkyl radicals, which may also be in competition with carbocation formation. The development of electroactive redox esters that can undergo reductive pathways may offer an alternative route to decarboxylative alkyl radical generation.⁴⁹



Scheme 4.1 General mechanism for Kolbe electrolysis of Boc-protected amino acids, showing one and two electron pathways.

In Chapter 3, cathodically generated alkyl radicals underwent facile addition to electron-deficient alkenes to create a range of sterically hindered tertiary amines (Scheme 4.2). Based on recent photochemical transformation, α -amino alkyl radicals were generated from the reduction of iminium ions that were pre-formed and either purified or used as crude mixtures.¹⁷³ The reaction was effective at generating complex α -tertiary carbon centres and was compatible with a range of electron withdrawing substituents of the alkene. One of the limitations of the electrolysis reaction was the requirement that iminium ions had to be pre-formed as this limited the scope of the reaction with respect to the ketone and amine components. The development of an alternative route to iminium ions would allow the scope of the reaction to be further expanded to create more complex tertiary amines.

Compared to previously reported electrochemical variants of this reaction, the scope with respect to the iminium ion components and alkene has been greatly improved, and for analogous substrates this procedure gave higher yields of sterically hindered tertiary amines.^{195,196} The photochemical variants were often higher yielding than this approach for the construction of tertiary amines, however, the scope of these reactions mainly focused on acyclic or conjugated systems.^{173–176} More closely related examples from photochemistry, with congested α -tertiary centres, had similar yields (Scheme 3.14, 32–83%) meaning this electrochemical approach would be a viable alternative which avoids costly transition metal photocatalysts.¹⁷³



Scheme 4.2 General mechanism for the electrochemical reduction of iminium hexafluorophosphates and radical addition to alkenes.

Overall, synthetic electrochemistry has effectively been employed for the generation of alkyl radicals for synthetic applications. One of the major problems faced in both reactions was the fouling or passivation of the electrode surfaces. Whilst polarity inversion was successfully used to maintain a constant current during electrolysis and minimise the effect of passivation, electrodes required thorough cleaning between reactions. In the case of graphite, cleaning by abrasion meant eventually the electrodes had to be replaced. Alternative methods to avoid passivation, such as mediators, could be investigated to improve the longevity of the electrodes. Mediators could also be used to try and prevent over-oxidation in Kolbe electrolysis.

One of the key advantages of electrochemistry over other methods of radical generation is the ability to scale up reactions more easily. Therefore, developing or adapting the set-ups to increase the scale of both electrochemical reactions, particularly the reduction of iminium ions, would make the approaches more attractive.

Finally, with the knowledge acquired on both reductive and oxidative electrosynthetic reactions, efforts to further develop complimentary electrochemical approaches for existing photochemical reactions could provide alternative routes to medicinally and agrochemically relevant compounds.

Chapter 5: Experimental

5.1 General

5.1.1 General Methods

Anhydrous solvents were obtained from an Innovative Technology Inc. PureSolv® solvent purification system. Flash column chromatography was carried out using 220-400 mesh silica gel (Sigma-Aldrich). For thin layer chromatography, Merck Kieselgel 60 F₂₅₄ silica coated TLC plates were used and visualised using UV light (254 nm) and/or by using a ninhydrin stain or oxidation with aqueous potassium permanganate solution. NMR spectra were recorded on a Jeol ECX-400 operating at 400 MHz (¹H) and 100.5 MHz (¹³C{¹H}). Chemical shifts, reported in parts per million (ppm), were referenced to residual solvent signals of the stated solvent. Coupling constants (*J*) were reported in Hertz. ¹³C{¹H} NMR spectra were recorded and assigned using DEPT experiments. Infrared spectra were recorded on a Perkin Elmer Spectrum 2 InfraRed instrument with an ATR (UATR – single reflection diamond) attachment. Melting points were recorded on Gallenkamp melting point apparatus. Mass spectra were recorded on a Bruker micrOTOF MS-Agilent series 1260LC spectrometer.

5.1.2 General Procedure for Calculating the End Point of Electrochemical Reactions

The anode and cathode voltages and current were recorded every 15 seconds using LabJack® (U12). From the current (Amps = C s⁻¹) and the time (s) the charge (C) could be determined, (Equation 5.1).

$$\text{Charge (C)} = \text{Current (C s}^{-1}\text{)} \times \text{Time (s)} \quad \text{Equation 5.1}$$

The moles of electrons passed could be calculated using Faraday's Constant, (Equation 5.2).

$$\frac{\text{Charge (C)}}{\text{Faraday Constant (96485.33 C mol}^{-1}\text{)}} = \text{Moles of electrons passed (mol)} \quad \text{Equation 5.2}$$

The equivalents could then be determined from the moles of acid in the reaction, (Equation 5.3).

$$\frac{\text{Moles of electrons passed (mol)}}{\text{Moles of acid (mol)}} = \text{Equivalents passed} \quad \text{Equation 5.3}$$

5.2 Experimental for Chapter 2

5.2.1 General Methods for Chapter 2

Platinised titanium mesh was supplied by CM Scientific Ltd. 0.2 mm Fisherbrand platinum wire was supplied by Fisher Scientific Ltd. 0.25 mm gold wire, annealed, Premion™, 99.999% (metals basis) and 0.25 mm palladium wire, 99.97% (metals basis) were supplied by Alfa Aesar. A DC power supply (Two HQ-Power, PS1503SB) was used at a fixed voltage to achieve the desired current flow. A LabJack® (U12) was used to record the anode and cathode voltages and current every 15 s. Polarity inversion was performed every 5 min to avoid electrode passivation. Temperature was recorded on a Traceable® Total-Range Thermometer (FB50281) supplied by Fisher Scientific. Gas chromatography was performed on a Thermo Trace 1300 instrument fitted with an AI1310 autosampler. 1 µL of sample was injected (splitless injection at 280 °C) into a DB-5MS column (30 m × 0.35 mm × 0.25 µm). Samples were heated from 50 °C to 90 °C at a ramp rate of 50 °C min⁻¹ then from 90 °C to 300 °C at a ramp rate of 15 °C min⁻¹. A flame ionization detector (FID) was used set at 330 °C. Carrier gas was hydrogen at a flow rate of 1.5 mL min⁻¹. Products were quantified based on calibration curves of pure products.

5.2.2 Platinised Titanium Electrodes and 9 mL Electrochemical Cell

A home-made undivided cell was used. The cell was designed as a test tube shaped glass container with a rubber seal at the top. The electrodes were two platinised titanium meshes with a separation of 2.0 mm and a surface of 3.3 cm² each. Teflon was used as an electrode mount and platinum wire was used to electrochemically connect the mesh to the circuit. The electrodes were inserted into the rubber seal along with the thermocouple and needles for the reagent/gas inlet/outlet. There was also a glass joint at the side of the cell that could fit a water condenser if needed.

5.2.3 Platinum Wire Electrodes and 2 mL Electrochemical Cell

A Wheaton sample vial (2 mL) was used as an undivided cell. Platinum wire (0.20 mm diameter) was wrapped around a glass slide (25.6 mm by 0.96 mm) with two grooves cut 1.0 mm apart. The wire was wrapped around three times and twisted together to allow connection to the crocodile clips. Each electrode had a surface area of 0.84 cm². The electrodes were suspended by the wires into the reaction mixture by crocodile clips. Small crocodile clips were glued to a plastic mount to take the weight off the wire on the electrodes.

5.2.4 Variations of the Platinum Wire Electrodes and 2 mL Electrochemical Cell

Electrodes for Anode Material Study (Gold and Palladium)

A Wheaton sample vial (2 mL) was used as an undivided cell. In the same way as the platinum wire cell was made, the anode metal and platinum cathode were wrapped around a glass slide with grooves cut. The cathode was platinum (0.2 mm diameter wire) and had a surface area of 0.91 cm². The gold anode (0.25 mm diameter wire) had a surface area of 1.14 cm² and the palladium anode (0.25 mm diameter wire) had a surface area of 1.17 cm². No polarity inversion was performed with this cell.

Smaller Surface Area Platinum Electrodes

A Wheaton sample vial (2 mL) was used as an undivided cell. In the same way as the platinum wire cell was made, platinum was wrapped around a glass slide with grooves cut. Both the anode and cathode wires were wrapped round once as opposed to three times to reduce the surface area. Each electrode had a surface area of 0.29 cm².

Smaller Surface Area Platinum Anode, Larger Surface Area Platinum Cathode Electrodes

A Wheaton sample vial (2 mL) was used as an undivided cell. In the same way as the platinum wire cell was made, platinum was wrapped around a glass slide with grooves cut. The anode wire was wrapped round once whilst the cathode wire was wrapped round three times. The anode surface area was 0.28 cm² whilst the cathode surface area was 0.84 cm². No polarity inversion was performed with this cell.

5.2.5 General Procedures for Chapter 2

General Procedure 2A: Electrolysis Using KOH as the Base, Based on Schäfer and Co-Workers¹⁰⁸

General Procedure 2A.1 Electrolysis with the Platinised Titanium Electrodes and 9 mL Cell Using KOH as the Base

N-Boc amino acid (1.17 mmol, 1.0 eq.) was dissolved in MeOH (8 mL) and stirred in the bespoke 9 mL electrochemical cell. 0.29 M KOH in MeOH (1.0 mL, 0.29 mmol KOH, 0.25 eq. KOH) was added along with the co-acid, acetic acid (0.27 mL, 4.7 mmol, 4.0 eq.). The

platinised titanium electrodes were inserted into the undivided cell. The electrodes were connected to the circuit *via* crocodile clips. Electrosynthesis was carried out at the desired voltage (typically 15 V) in air and at room temperature. After 1.6 F mol⁻¹ of charge was passed, the resulting solution was combined with brine (10 mL) and washed with DCM (3 × 25 mL). The organic layers were collected, dried over MgSO₄ and carefully evaporated *in vacuo* to give the crude mixture, a white solid. Products were isolated by column chromatography.

General Procedure 2A.2: Electrolysis with the Platinum Wire Electrodes and 2 mL Cell Using KOH as the Base and ¹H NMR Spectroscopy for Analysis

N-Boc amino acid (0.26 mmol, 1.0 eq.) was dissolved in MeOH-*d*₄ (1.75 mL) and stirred in a 2 mL vial. 0.29 M KOH in MeOH-*d*₄ (0.25 mL, 0.073 mmol KOH, 0.25 eq. KOH) was added along with the co-acid, acetic acid (0.060 mL, 1.0 mmol, 4.0 eq.). The platinum wire electrodes were inserted into the undivided cell. The electrodes were connected to the circuit *via* crocodile clips. Electrosynthesis was carried out at the desired voltage (typically 15 V) in air and at room temperature. After 1.6 F mol⁻¹ of charge was passed the reaction was stopped. From the resulting solution, an aliquot (250 μL) was taken and combined in an NMR tube with a 0.14 M mesitylene in MeOH-*d*₄ stock solution (50 μL) and a 0.57 M benzoic acid in MeOH-*d*₄ stock (50 μL) and MeOH-*d*₄ (0.3 mL). The NMR tube lid was secured, and the NMR tube was shaken before being sent for ¹H NMR analysis.

General Procedure 2B: Electrolysis Using Et₃N as the Base, Based on Seebach and Co-Workers⁹⁷

General Procedure 2B.1: Electrolysis with the Platinised Titanium Electrodes and 9 mL Cell Using Et₃N as the Base

N-Boc amino acid (0.86 mmol, 1.0 eq.) was dissolved in MeOH (9 mL) and stirred in the bespoke 9 mL electrochemical cell. Et₃N (0.047 mL, 0.34 mmol, 0.39 eq.) was added along with the co-acid, acetic acid (0.29 mL, 5.1 mmol, 6.0 eq.). The platinised titanium electrodes were inserted into the undivided cell. The electrodes were connected to the circuit *via* crocodile clips. Electrosynthesis was carried out at the desired voltage (typically 15 V) under N₂ and at room temperature. After 1.5 F mol⁻¹ of charge was passed, the crude mixture was quantified by gas chromatography before work-up or resulting solution was combined with brine (10 mL) and washed with DCM (3 × 25 mL). The organic layers were collected, dried

over MgSO₄ and carefully evaporated *in vacuo* to give the crude mixture, a white solid. Products were isolated by column chromatography..

General Procedure 2B.2: Electrolysis with the Platinum Wire Electrodes and 2 mL Cell Using Et₃N as the Base and ¹H NMR Spectroscopy for Analysis

N-Boc amino acid (0.19 mmol, 1.0 eq.) was dissolved in MeOH-*d*₄ (1 mL) and stirred in a 2 mL vial. 0.07 M Et₃N in MeOH-*d*₄ (typically 1 mL, 0.07 mmol Et₃N, 0.39 eq. Et₃N) was added along with the co-acid, acetic acid (0.065 mL, 1.1 mmol, 6.0 eq.). The electrodes were inserted into the undivided cell. The platinum wire electrodes were connected to the circuit *via* crocodile clips. Electrosynthesis was carried out at the desired voltage (typically 15 V) in air and at room temperature. After 1.5 F mol⁻¹ of charge was passed the reaction was stopped. From the resulting solution, an aliquot (250 μL) was taken and combined in an NMR tube with a 0.14 M mesitylene in MeOH-*d*₄ stock solution (50 μL) and a 0.57 M benzoic acid in MeOH-*d*₄ stock (50 μL) and MeOH-*d*₄ (0.3 mL). The NMR tube lid was secured, and the NMR tube was shaken before being sent for ¹H NMR analysis.

General Procedure 2B.3: Electrolysis with the Platinum Wire Electrodes and 2 mL Cell Using Et₃N as the Base and Gas Chromatography for Analysis

N-Boc amino acid (0.19 mmol, 1.0 eq.) was dissolved in MeOH (1 mL) and stirred in a 2 mL vial. 0.07 M Et₃N in MeOH (typically 1 mL, 0.07 mmol Et₃N, 0.39 eq. Et₃N) was added along with the co-acid, acetic acid (0.065 mL, 1.1 mmol, 6.0 eq.). The platinum wire electrodes were inserted into the undivided cell. The electrodes were connected to the circuit *via* crocodile clips. Electrosynthesis was carried out at the desired voltage (typically 15 V) in air and at room temperature. After 1.5 F mol⁻¹ of charge was passed the reaction was stopped. From the resulting solution, aliquots (3 × 50 μL) were taken and diluted in a 2 mL volumetric flask. The resulting solution was filtered through a 0.22 μm nylon syringe filter into a GC vial and analysed by gas chromatography. The yields of Kolbe product **2.90**, non-Kolbe side product **2.91** and remaining starting material **2.89** were calculated based on calibration curves of authentic samples. Figure 5.1-Figure 5.3 for calibration curves, See Appendix D for example GC trace of crude reaction mixture and for retention times and peaks areas for example trace.

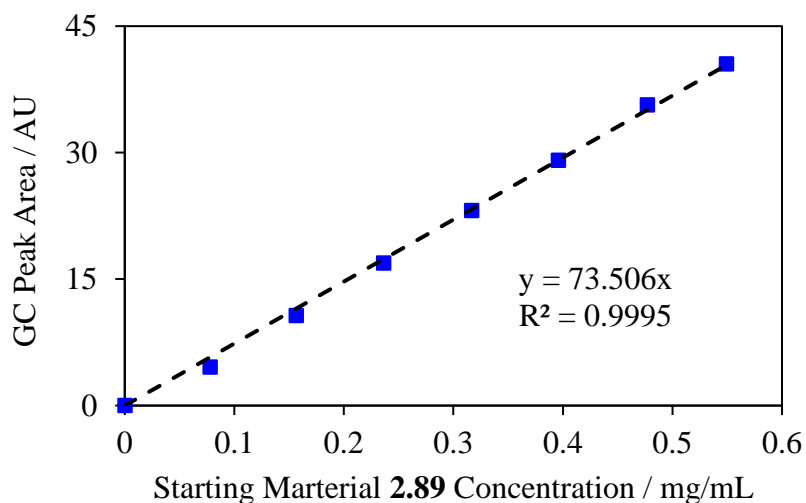


Figure 5.1 Calibration curve for quantification of *N*-Boc β -alanine **2.89**

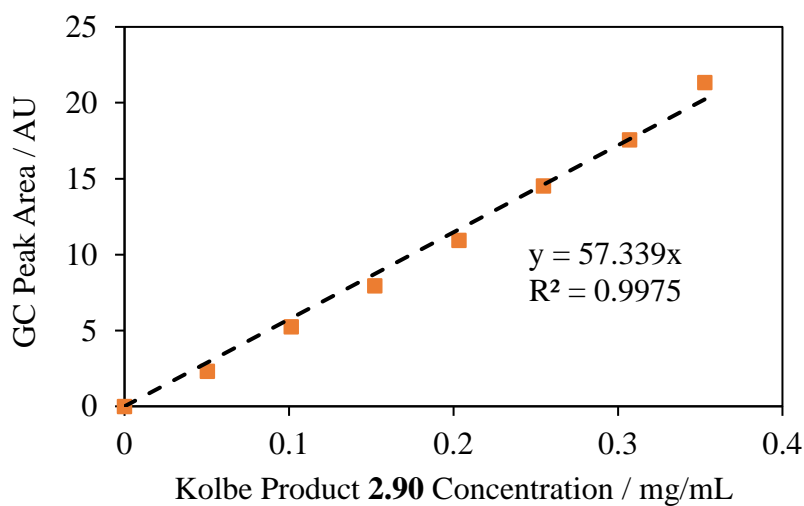


Figure 5.2 Calibration curve for quantification of Kolbe product **2.90**

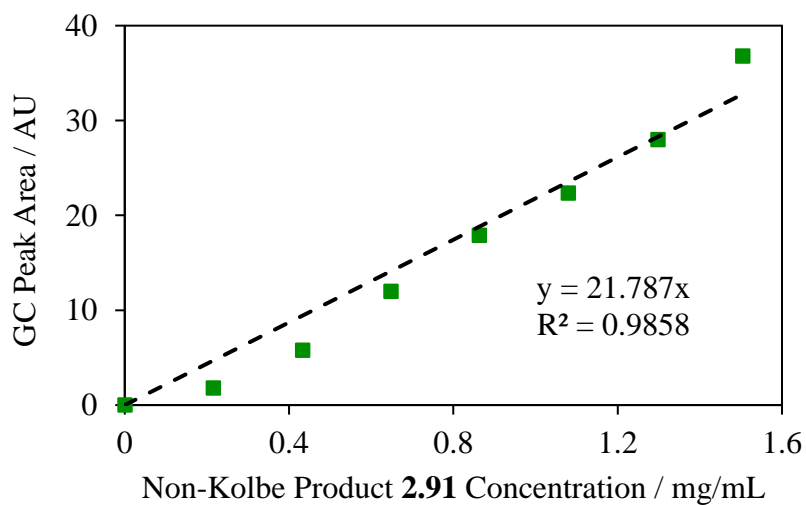


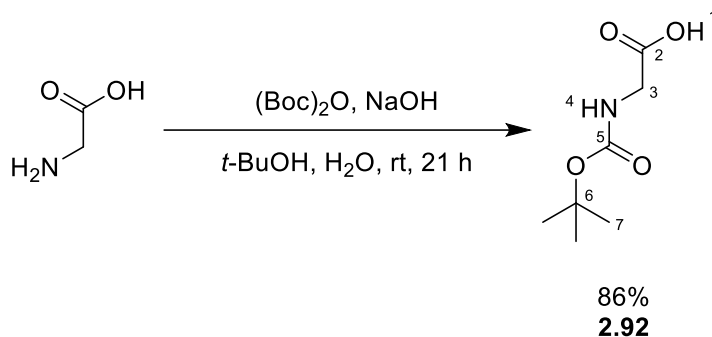
Figure 5.3 Calibration curve for quantification of non-Kolbe product **2.91**

General Procedure 2C: Electrolysis Monitoring with ^1H NMR Spectroscopy

Kolbe electrolysis was performed according to either General Procedure 2A.1 or 2B.1, but methanol was replaced with deuterated methanol (9 mL). The power packs were turned off periodically and aliquots of the reaction mixture (50 μL) were taken and added to NMR tubes filled with a 0.14 M mesitylene solution in $\text{MeOH-}d_4$ (50 μL). Deuterated methanol (500 μL) was then added followed by an aliquot of 0.57 M benzoic acid in $\text{MeOH-}d_4$ (50 μL). The accuracy of small volume addition was checked and corrected by weight resulting in more reliable data. 10 aliquots (including initial reaction mixture) were taken at regular time intervals (either 5 or 10 minutes). The data is shown in Chapter 2, Section 2.2.3.

5.2.6 Experimental Procedures and Characterisation Data for Chapter 2

Boc Protection of Amino Acids

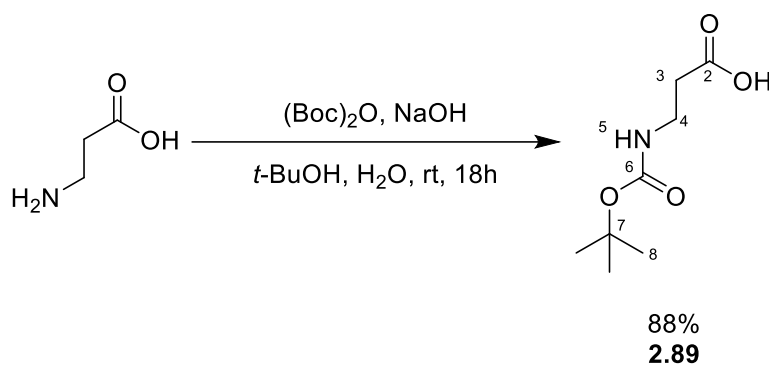
Synthesis of (*tert*-butoxycarbonyl)glycine (2.92)

To a stirring solution of NaOH (1.99 g, 49.9 mmol) in *tert*-butanol (30 mL) and water (45 mL), glycine (3.00 g, 40.0 mmol) was added. Next, di-*tert*-butyldicarbonate (8.78 g, 40.2 mmol) was added before the solution was vigorously stirred for 21 hours. The resulting colourless solution was acidified using potassium hydrogen sulfate to pH 3. The organic layer was separated and washed with EtOAc (3 × 25 mL). The organic layers were collected, dried over MgSO₄ and evaporated *in vacuo* to give a crude product (a colourless oil). The crude was recrystallised from hot hexane, and the product was washed with ice cold hexane and dried to give the white crystalline product. Yield 6.00 g (86%).

Mp 85 – 86 °C (Lit.,²³⁰ 86 – 88 °C), R_F (petroleum ether:EtOAc, 55:45 *v/v*) 0.30; IR (ATR) 3407, 3342 (N-H), 2978 (O-H), 2940, 1739 (C=O), 1668 (C=O), 1530 (N-H), 1408, 1366, 1156, 856, 580 cm⁻¹; ¹H NMR (400 MHz, Chloroform-*d*) (3:2 mixture of rotamers) δ 10.48 (br s, 1H, H¹), 6.69 (br s, 0.4H, H⁴), 5.30 (br s, 0.6H, H⁴), 3.92 – 3.84 (m, 2H, H³), 1.41 (s, 9H, H⁷); ¹³C NMR (101 MHz, Chloroform-*d*) (3:2 mixture of rotamers) δ 174.4 (C² – major), 173.9 (C² – minor), 157.3 (C⁵ – minor), 156.1 (C⁵ – major), 81.8 (C⁶ – minor), 80.3 (C⁶ – major), 43.3 (C³ – minor), 42.1 (C³ – major), 28.2 (C⁷ – major), 28.1 (C⁷ – minor); HRMS (ESI⁺) m/z calcd for C₇H₁₃NNaO₄ [M + Na]⁺: 198.0737, found: 198.0738 (–0.8 ppm error).

Based on procedure by Voskuhl *et al.* and spectroscopic data are consistent with those reported in the literature.²³¹

Lab Book Reference: JCC-1-1

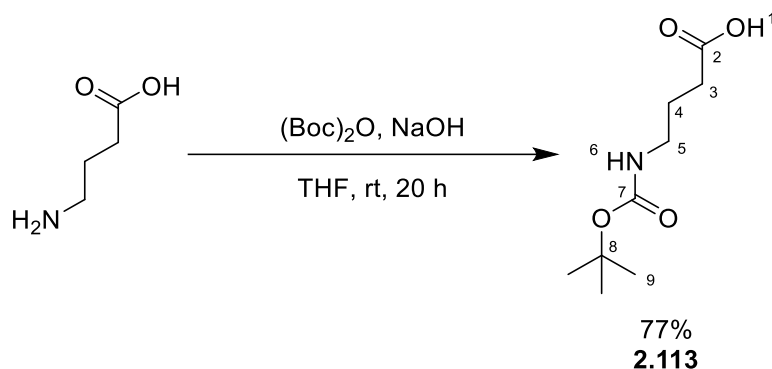
Synthesis of 3-((*tert*-butoxycarbonyl)amino)propanoic acid (2.89)

To a stirring solution of NaOH (1.93 g, 48.2 mmol) in *tert*-butanol (43 mL) and water (19 mL), β -alanine (3.93 g, 44.1 mmol) was added. Next, di-*tert*-butyldicarbonate (10.5 g, 48.1 mmol) was added before the solution was vigorously stirred for 18 hours. The resulting white solution was diluted with H₂O (32 mL) and washed with hexane (3 \times 40 mL). The aqueous layer was cooled to 5 °C in an ice bath and acidified with 1 M aq. citric acid to pH 4 and washed with EtOAc (4 \times 50 mL). The organic layers were collected, dried over MgSO₄ and evaporated *in vacuo* to a colourless oil before the product was obtained by recrystallisation from hot hexane. The recrystallised product was washed with ice cold hexane and dried to give the white crystalline product. Yield 7.32 g (88%).

Mp 78 – 80 °C (Lit.,²³² 78 – 79 °C), R_F (petroleum ether:EtOAc, 55:45 v/v) 0.30; IR (ATR) 3495, 3440 (N-H), 2966 (O-H), 1753 (C=O), 1700 (C=O), 1512 (N-H), 1236, 1168, 979, 781, 550 cm⁻¹; ¹H NMR (400 MHz, Chloroform-*d*) (70:30 mixture of rotamers) δ 9.05 (br s, 1H, H¹), 6.30 (br s, 0.3H, H⁵), 5.12 (br s, 0.7H, H⁵), 3.41 – 3.34 (m, 2H, H⁴), 2.58 – 2.51 (m, 2H, H³), 1.42 (s, 9H, H⁸); ¹³C NMR (101 MHz, Chloroform-*d*) (rotamers) δ 177.5 (C² – major), 176.3 (C² – minor), 157.5 (C⁶ – minor), 155.9 (C⁶ – major), 81.1 (C⁷ – minor), 79.7 (C⁷ – major), 37.1 (C⁴ – minor), 35.8 (C⁴ – major), 34.4 (C³), 28.3 (C⁸); HRMS (ESI⁺) m/z calcd for C₈H₁₅NNaO₄ [M + Na]⁺: 212.0893, found: 212.0892 (0.4 ppm error).

Based on procedure by Stover *et al.*²³³ spectroscopic data are consistent with those reported in the literature.²³⁴

Lab Book Reference: JCC-1-3

Synthesis of 4-((*tert*-butoxycarbonyl)amino)butanoic acid (2.113)

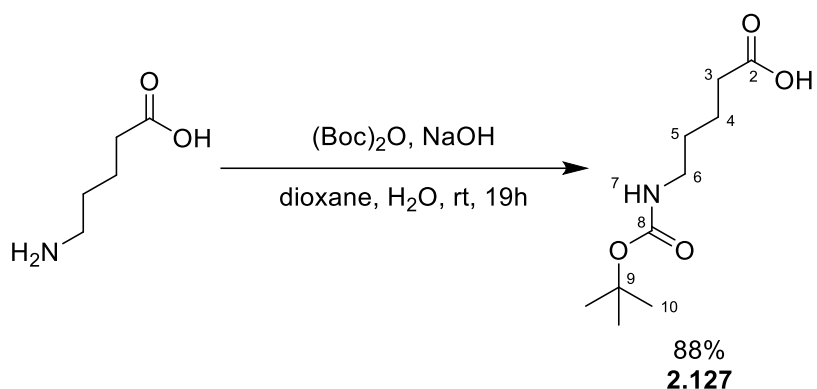
To a stirring solution of 1 M NaOH_(aq) (29.4 mL) in THF (45 mL) at 0 °C, γ -aminobutyric acid (3.01 g, 29.2 mmol) was added. Next, di-*tert*-butyldicarbonate (8.03 g, 36.8 mmol) was added before the solution was warmed to room temperature and vigorously stirred for 20 hours. The resulting solution was evaporated *in vacuo* before being dissolved in H₂O (18 mL) and washed with Et₂O (12 mL). The resulting aqueous layer was acidified with 1 M HCl_(aq) to pH 2 and washed with Et₂O (3 \times 12 mL). The organic layers were collected, dried over MgSO₄ and evaporated *in vacuo* to a colourless oil before the product was obtained by recrystallisation from hot hexane. The recrystallised product was washed with ice cold hexane and dried to give the white crystalline product. Yield 4.55 g (77%).

Mp 50 – 52 °C (Lit.,²³⁵ 49 – 52 °C), R_F (petroleum ether:EtOAc, 55:45 v/v) 0.30; IR (ATR) 3369 (N-H), 2968 (O-H), 2940, 1706 (C=O), 1684 (C=O), 1516 (N-H), 1366, 1158, 938, 782, 604 cm⁻¹; ¹H NMR (400 MHz, Chloroform-*d*) (2:1 mixture of rotamers) δ 10.43 (br s, 1H, H¹), 6.19 (br s, 0.33H, H⁶), 4.89 (br s, 0.67H, H⁶), 3.13 – 3.08 (m, 2H, H⁵), 2.33 (t, J = 7.5 Hz, 2H, H³), 1.76 (apparent quin, J = 7.0 Hz, 2H, H⁴), 1.39 (s, 9H, H⁹); ¹³C NMR (101 MHz, Chloroform-*d*) (2:1 mixture of rotamers) δ 178.1 (C²), 157.8 (C⁷ – minor), 156.2 (C⁷ – major), 80.7 (C⁸ – minor), 79.3 (C⁸ – major), 40.7 (C⁵ – minor), 39.6 (C⁵ – major), 31.2 (C³ – major), 31.1 (C³ – minor), 28.2 (C⁹), 24.9 (C⁴); HRMS (ESI⁺) m/z calcd for C₉H₁₈NO₄ [M + H]⁺: 204.1230, found: 204.1232 (-0.9 ppm error), calcd for C₉H₁₇NNaO₄ [M + Na]⁺: 226.1050, found: 226.1050 (-0.3 ppm error).

Based on procedure by Buchini *et al.* and spectroscopic data are consistent with those reported in the literature.²³⁶

Lab Book Reference: JCC-1-2

Synthesis of 5-((*tert*-butoxycarbonyl)amino)pentanoic acid (**2.127**)

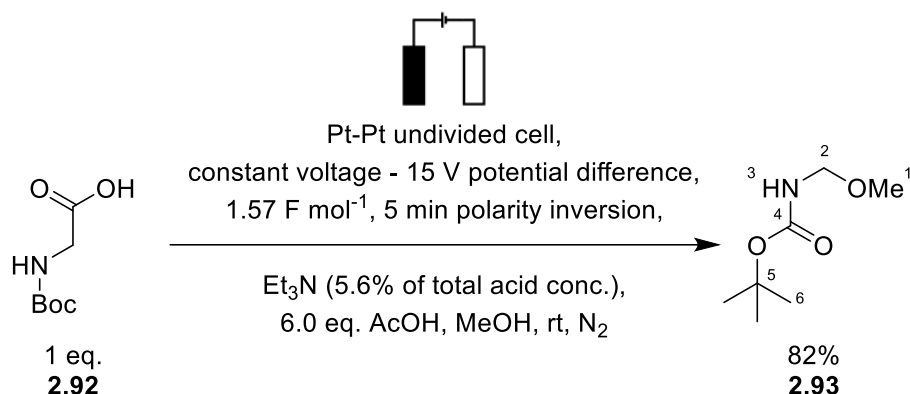


To a stirring solution of NaOH (0.68 g, 17 mmol) in dioxane (40 mL) and water (20 mL), 5-aminopentanoic acid (2.00 g, 17.1 mmol) was added. Next, di-*tert*-butyldicarbonate (4.10 g, 18.8 mmol) was added before the solution was vigorously stirred for 19 hours. The resulting white solution was concentrated *in vacuo* before the resulting residue was re-dissolved in H_2O (100 mL) and washed with ethyl acetate (3×60 mL). The aqueous layer was acidified with 1 M aq. HCl to pH 1-2 and washed with EtOAc (3×100 mL). The organic layers were collected, dried over MgSO_4 and evaporated *in vacuo* to a colourless oil before the product was obtained by recrystallisation from hot hexane. The recrystallised product was washed with ice cold hexane and dried to give the white crystalline product. Yield 3.26 g (88%).

Mp 50 – 52 °C (Lit.,²³⁷ 49 – 52 °C), R_F (petroleum ether:EtOAc, 55:45 v/v) 0.24; IR (ATR) 3371 (N-H), 2984 (O-H), 2952, 2878, 1707 (C=O), 1684 (C=O), 1520 (N-H), 1363, 1277, 1165, 993, 931, 870, 595 cm^{-1} ; ^1H NMR (400 MHz, Chloroform-*d*) (25:75 mixture of rotamers) δ 10.19 (br s, 1H, H^1), 5.72 (br s, 0.25H, H^7), 4.58 (br s, 0.75H, H^7), 3.15 – 3.10 (m, 2H, H^6), 2.36 (t, $J = 7.5$, 2H, H^5), 1.68 – 1.61 (m, 2H, H^4), 1.56 – 1.48 (m, 2H, H^3), 1.42 (s, 9H, H^{10}); ^{13}C NMR (101 MHz, Chloroform-*d*) δ 178.5 (C^2), 156.0 (C^8), 79.3 (C^9), 40.1 (C^6), 33.4 (C^3), 29.4 (C^5), 28.4 (C^{10}), 21.8 (C^4); HRMS (ESI⁺) m/z calcd for $\text{C}_{10}\text{H}_{19}\text{NNaO}_4$ [$\text{M} + \text{Na}$]⁺: 240.1206, found: 240.1203 (1.4 ppm error).

Based on procedure by Gavande *et al.* and spectroscopic data are consistent with those reported in the literature.²³⁸

Lab Book Reference: JCC-1-4

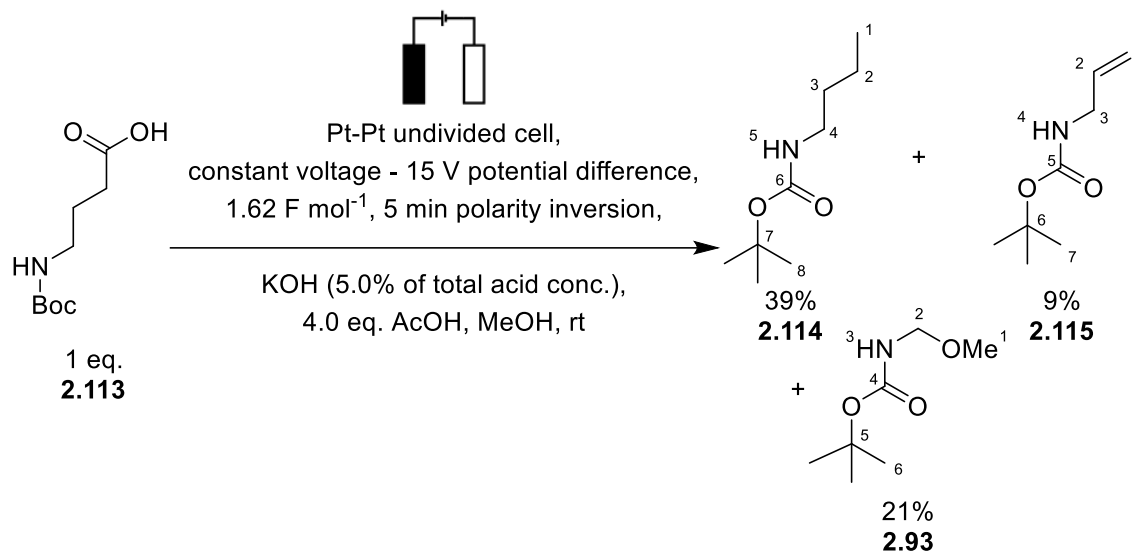
Electrolysis of *N*-Boc Protected Amino Acids with Acetic AcidElectrolysis of *N*-Boc Glycine

Using General Procedure 2B.1, *N*-Boc glycine **2.92** (0.150 g, 0.856 mmol, 1.0 eq.), acetic acid (0.29 mL, 5.1 mmol, 6.0 eq.) and Et₃N (0.047 mL, 0.34 mmol, 0.40 eq.) in MeOH (9 mL) were used. After 1.57 F mol⁻¹ of charge (914 C of charge for 79 minutes) was passed (average current density of 58.5 mA cm⁻²). Purification by flash column chromatography on silica (petroleum ether:EtOAc, 55:45 v/v) gave *tert*-butyl (methoxymethyl)carbamate (**2.93**), as a colourless oil. Yield 0.12 g (82%).

R_F (petroleum ether:EtOAc, 80:20 v/v) 0.18; IR (ATR) 3344 (N-H), 2979, 2934, 1700 (C=O), 1517, 1367, 1249, 1165, 1126, 1065, 953, 907, 862, 586 cm⁻¹; ¹H NMR (400 MHz, Chloroform-*d*) 5.38 (br s, 1H, H³), 4.55 (d, $J = 7.0$ Hz, 2H, H²), 3.30 (s, 3H, H¹), 1.44 (s, 9H, H⁶); ¹³C NMR (101 MHz, Chloroform-*d*) δ 155.7 (C⁴), 80.0 (C⁵), 73.2 (C²), 55.4 (C¹), 28.2 (C⁶); HRMS (ESI⁺) m/z calcd for C₇H₁₅NNaO₃ [M + Na]⁺: 184.0944, found: 184.0947 (-1.6 ppm error).

Based on procedure by Seebach *et al.*⁹⁷

Lab-book reference JCC-E-1-42

Electrolysis of *N*-Boc γ -Aminobutyric Acid

Using General Procedure 2A.1, *N*-Boc γ -aminobutyric acid **2.113** (0.238 g, 1.17 mmol, 1.0 eq.), acetic acid (0.27 mL, 4.6 mmol, 4.0 eq.) and KOH (0.016 g, 0.5 mL from a 0.30 M stock solution in methanol, 0.29 mmol, 0.25 eq.) in MeOH (9 mL) were used. After 1.62 F mol⁻¹ of charge (913 C of charge for 108 minutes) was passed (average current density of 42.7 mA cm⁻²). Purification by flash column chromatography on silica (gradient eluent petroleum ether:Et₂O, 90:10 *v/v* to petroleum ether:Et₂O, 60:40 *v/v*) gave *tert*-butyl butylcarbamate (**2.114**), *tert*-butyl allylcarbamate (**2.115**) and *tert*-butyl (methoxymethyl)carbamate (**2.93**).

tert-Butyl butylcarbamate (**2.114**), as a colourless oil. Yield 0.03 g (13%, overall 39%), *R_F* (petroleum ether:EtOAc, 80:20 *v/v*) 0.38; IR (ATR) 3350 (N-H), 2960, 2930, 2874, 1690 (C=O), 1520, 1365, 1249, 1171, 1048, 1010, 781 cm⁻¹; ¹H NMR (400 MHz, Chloroform-*d*) 4.50 (br s, 1H, H⁵), 3.13 – 3.08 (m, 2H, H⁴), 1.50 – 1.45 (m, 2H, H³), 1.44 (s, 9H, H⁸), 1.38 – 1.28 (m, 2H, H²), 0.91 (t, *J* = 7.5 Hz, 2H, H¹); ¹³C NMR (101 MHz, Chloroform-*d*) δ 156.0 (C⁶), 79.0 (C⁷), 40.3 (C⁴), 32.1 (C³), 28.4 (C⁸), 19.9 (C²), 13.7 (C¹); HRMS (ESI⁺) *m/z* calcd for C₉H₁₉NNaO₂ [M + Na]⁺: 196.1308, found: 196.1308 (0.1 ppm error). Spectroscopic data are consistent with those reported in the literature.²³⁹

0.07 g mixture of *tert*-butyl allylcarbamate (**2.115**) with *tert*-butyl butylcarbamate (**2.114**) as a colourless oil which equated to 0.02 g and 0.05 g of **2.115** and **2.114** respectively.

tert-Butyl allylcarbamate (**2.115**), 9% yield, *R_F* (petroleum ether:EtOAc, 80:20 *v/v*) 0.32; IR (ATR) 3345 (N-H), 2958, 2930, 2873, 1689 (C=O), 1515, 1365, 1249, 1173, 1048, 1009,

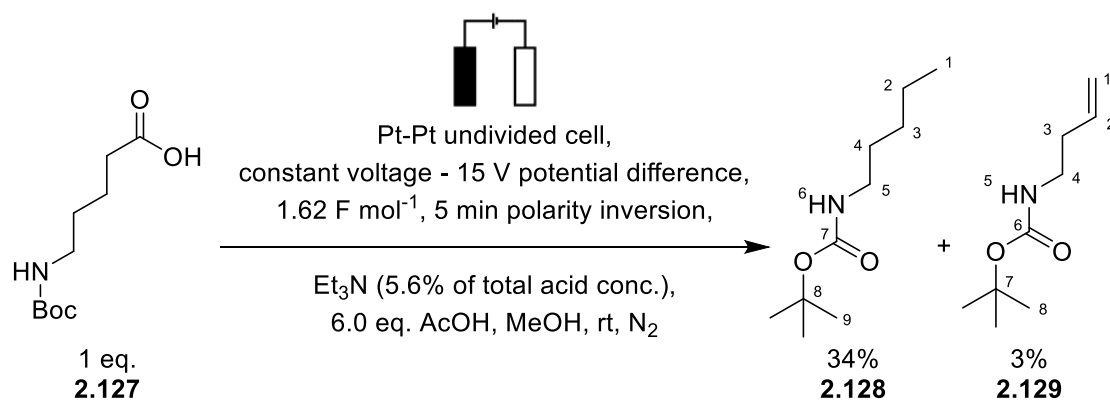
872 cm^{-1} ; ^1H NMR (400 MHz, Chloroform-*d*) 5.83 (ddt, $J = 16.0, 10.5, 5.5$, 1H, H^2), 5.19 – 5.07 (m, 2H, H^1), 4.59 (br s, 1H, H^4), 3.74 – 3.72 (m, 2H, H^3), 1.44 (s, 9H, H^7), ^{13}C NMR (101 MHz, Chloroform-*d*) δ 156.0 (C^5), 134.9 (C^2), 115.7 (C^1) 79.0 (C^6), 40.3 (C^3), 28.2 (C^7); HRMS (ESI $^+$) m/z calcd for $\text{C}_8\text{H}_{15}\text{NNaO}_2$ [$\text{M} + \text{Na}$] $^+$: 180.0995, found: 180.0995 (–0.2 ppm error). Spectroscopic data are consistent with those reported in the literature.²⁴⁰

tert-Butyl (methoxymethyl)carbamate (**2.93**), as a colourless oil. Yield 0.04 g (21%), R_F (petroleum ether:EtOAc, 80:20 v/v) 0.18, ^1H NMR (400 MHz, Chloroform-*d*) δ 5.28 (s, 1H, H^3), 4.56 (d, $J = 7.0$ Hz, 2H, H^2), 3.32 (s, 3H, H^1), 1.46 (s, 9H, H^6); HRMS (ESI $^+$) m/z calcd for $\text{C}_7\text{H}_{15}\text{NNaO}_3$ [$\text{M} + \text{Na}$] $^+$: 184.0944, found: 184.0935 (4.7 ppm error). Data consistent with previously reported for **2.93**.

Based on procedure by Huhtasaari *et al.*¹⁰⁸

Lab-book reference JCC-E-1-59

Electrolysis of *N*-Boc 5-Aminopentanoic Acid



Using General Procedure 2B.1, *N*-Boc 5-aminopentanoic acid **2.127** (0.186 g, 0.856 mmol, 1.0 eq.), acetic acid (0.29 mL, 5.1 mmol, 6.0 eq.) and Et $_3$ N (0.047 mL, 0.34 mmol, 0.40 eq.) in MeOH (9 mL) were used. After 1.62 F mol $^{-1}$ of charge (935 C of charge for 78 minutes) was passed (average current density of 60.9 mA cm $^{-2}$). Purification by flash column chromatography on silica (gradient eluent petroleum ether:Et $_2$ O, 85:15 v/v to petroleum ether:Et $_2$ O, 50:50 v/v) gave *tert*-butyl pentylcarbamate (**2.128**) and *tert*-butyl but-3-enylcarbamate (**2.129**).

tert-Butyl pentylcarbamate (**2.128**), as a colourless oil. Yield 0.05 g (34%), R_F (petroleum ether:Et $_2$ O, 85:15 v/v) 0.27; IR (ATR) 3347 (N-H), 2959, 2930, 2862, 1688 (C=O), 1518, 1365, 1251, 1171, 1020, 868, 780 cm^{-1} ; ^1H NMR (400 MHz, Chloroform-*d*) δ 4.49 (br s, 1H,

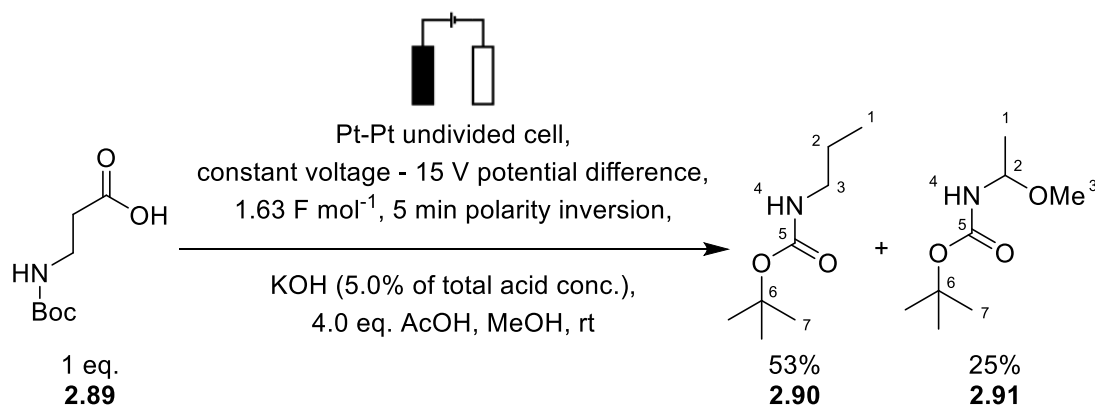
H⁶), 3.10 (apparent quin, $J = 7.0$ Hz, 2H, H⁵), 1.51 – 1.40 (m, 11H, H⁴ and H⁹), 1.38 – 1.17 (m, 4H, H² and H³), 0.89 (t, $J = 7.0$ Hz, 3H, H¹); ¹³C NMR (101 MHz, Chloroform-d) δ 156.0 (C⁷), 79.0 (C⁸), 40.6 (C⁵), 29.8 (C⁴), 29.0 (C³), 28.4 (C⁹), 22.3 (C³), 14.0 (C¹); HRMS (ESI⁺) m/z calcd for C₁₀H₂₁NNaO₂ [M + Na]⁺: 210.1464, found: 210.1464 (0.1 ppm error). Spectroscopic data are consistent with those reported in the literature.²⁴¹

tert-Butyl but-3-en-1-ylcarbamate (**2.129**) as a colourless oil. Yield 0.004 g (3%), R_F (petroleum ether:Et₂O, 85:15 v/v) 0.20, IR (ATR) 3356 (N-H), 2978, 2932, 2864, 1690 (C=O), 1514, 1365, 1250, 1170, 917, 734 cm⁻¹; ¹H NMR (400 MHz, Chloroform-*d*) δ 5.75 (ddt, $J = 17.0, 10.0, 7.0$ Hz, 1H, H²), 5.21 – 5.00 (m, 2H, H¹), 4.55 (br s, 1H, H⁵), 3.19 (apparent quin, $J = 6.5$ Hz, 2H, H⁴), 2.40 – 2.07 (m, 2H, H³), 1.44 (s, 9H, H⁸). ¹³C NMR (101 MHz, Chloroform-*d*) δ 155.9 (C⁶), 135.3 (C²), 117.0 (C¹), 79.1 (C⁷), 39.6 (C⁴), 34.1 (C³), 28.4 (C⁸); HRMS (ESI⁺) m/z calcd for C₈H₁₅NnaO₂ [M + Na]⁺: 194.1157, found: 194.1151 (1.0 ppm error). Spectroscopic data are consistent with those reported in the literature.²⁴²

Based on procedure by Seebach *et al.*⁹⁷

Lab-book reference JCC-E-2-159

Electrolysis of *N*-Boc β -Alanine



Using General Procedure 2A.1, *N*-Boc β -alanine **2.89** (0.222 g, 1.17 mmol, 1.0 eq.), acetic acid (0.27 mL, 4.6 mmol, 4.0 eq.) and KOH (0.016 g, 0.5 mL from a 0.30 M stock solution in methanol, 0.29 mmol, 0.25 eq.) in MeOH (9 mL) were used. After 1.63 F mol⁻¹ of charge (915 C of charge for 98 minutes) was passed (average current density of 47.1 mA cm⁻²). Purification by flash column chromatography on silica (eluent petroleum ether:Et₂O, 90:10

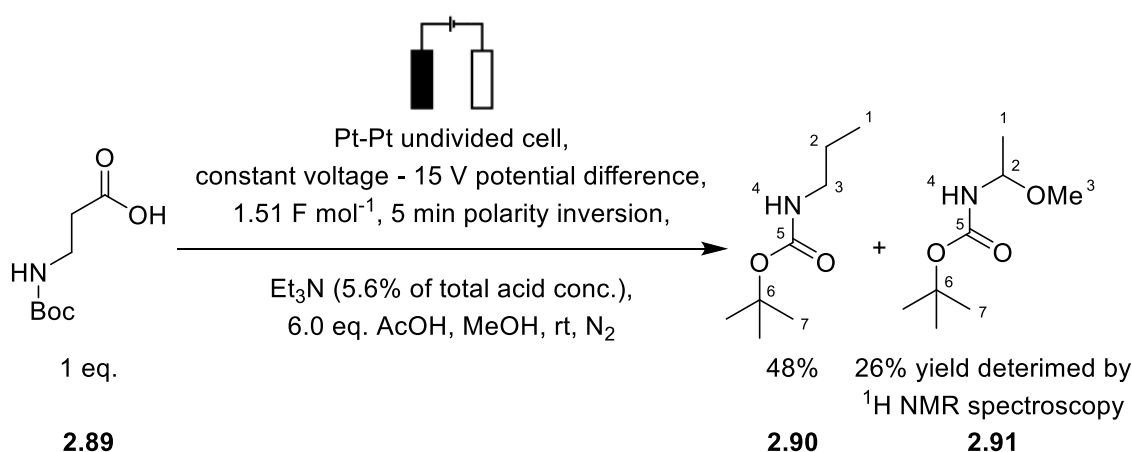
v/v) gave *tert*-butyl propylcarbamate (**2.90**) and *tert*-butyl (1-methoxyethyl)carbamate (**2.91**).

tert-Butyl propylcarbamate (**2.90**), as a colourless oil. Yield 0.10 g (53%), R_F (petroleum ether:EtOAc, 80:20 *v/v*) 0.35., IR (ATR) 3349 (N-H), 2965, 2927, 2876, 1690 (C=O), 1520, 1365, 1245, 1171, 1043 cm^{-1} ; ^1H NMR (400 MHz, Chloroform-*d*) 4.56 (br s, 1H, H⁴), 3.09 – 3.04 (m, 2H, H³), 1.53 – 1.47 (m, 2H, H¹), 1.43 (s, 9H, H⁷) 0.90 (t, $J = 7.5$ Hz, 3H, H¹); ^{13}C NMR (101 MHz, Chloroform-*d*) δ 156.0 (C⁵), 79.0 (C⁶), 42.3 (C³), 28.4 (C⁷), 23.2 (C²), 11.2 (C¹); HRMS (ESI⁺) m/z calcd for C₈H₁₇NNaO₂ [M + Na]⁺: 182.1151, found: 182.1151 (0.5 ppm error). Spectroscopic data are consistent with those reported in the literature.²⁴³

tert-Butyl (1-methoxyethyl)carbamate (**2.91**), as a white solid. Yield 0.05 g (25%), mp 73 – 75 °C, R_F (petroleum ether:EtOAc, 80:20 *v/v*) 0.24; IR (ATR) 3323 (N-H), 2980, 2926, 2854, 1686 (C=O), 1527, 1457, 1364, 1251, 1152, 1134, 920, 869, 667 cm^{-1} ; ^1H NMR (400 MHz, Chloroform-*d*) δ 5.08 – 4.92 (m, 1H, H²), 4.79 (s, 1H, H⁴), 3.33 (s, 3H, H³), 1.46 (s, 9H, H⁷), 1.32 (d, $J = 6.0$ Hz, 3H, H¹); ^{13}C NMR (101 MHz, Chloroform-*d*) δ 155.3 (C⁵), 80.0 (C⁶), 79.4 (C²), 55.1 (C³), 28.3 (C⁷), 21.7 (C¹); HRMS (ESI⁺) m/z calcd for C₈H₁₇NNaO₃ [M + Na]⁺: 198.1101, found: 198.1103 (–1.0 ppm error). Spectroscopic data are consistent with those reported in the literature.²⁴⁴

Based on procedure by Huhtasaari *et al.*¹⁰⁸

Lab-book reference JCC-E-1-57



Using General Procedure 2B.1, *N*-Boc β -alanine **2.89** (0.162 g, 0.856 mmol, 1.0 eq.), acetic acid (0.29 mL, 5.1 mmol, 6.0 eq.) and Et₃N (0.047 mL, 0.34 mmol, 0.40 eq.) in MeOH (9 mL) were used. After 1.51 F mol⁻¹ of charge (877 C of charge for 78 minutes) was passed

(average current density of 56.8 mA cm⁻²). Purification by flash column chromatography on silica (gradient eluent petroleum ether:EtOAc, 93:7 v/v to petroleum ether:EtOAc, 80:20 v/v) gave *tert*-butyl propylcarbamate (**2.90**) and *tert*-butyl (1-methoxyethyl)carbamate (**2.91**).

tert-Butyl propylcarbamate (**2.90**), as a colourless oil. Yield 0.07 g (48%), data consistent with previously reported for **2.90**.

tert-Butyl (1-methoxyethyl)carbamate (**2.91**) was observed in the crude ¹H NMR spectrum in a 26% yield based on δ 1.31 ppm (d, *J* = 6.0 Hz, 3H, H¹), however, it was not isolated.

Based on procedure by Seebach *et al.*⁹⁷

Lab-book reference JCC-E-1-13

5.2.7 Overview of Changes and Yields for Section 2.2

Table 5.1 Summary of electrochemical changes for optimising Kolbe electrolysis of *N*-Boc β -alanine and acetic acid, including amount of charge passed, average current density, average voltage, and yields of the Kolbe product **2.90** and non-Kolbe product **2.91**

Entry	Deviation from Standard Conditions ^a	Eq. of Charge / F mol ⁻¹	Base conc. / % total acid	Time / minutes	Average current density / mA cm ⁻²	Average voltage / V	Kolbe Product		Non-Kolbe Product		Lab book ref.
							(2.90) yield / %	(2.91) yield / %			
1	None	1.52	5.6	53	73	15.1	58	27		JCC-E-2-91	
2	DMF ^b	1.24	5.6	214	17	30.5	49	-		JCC-E-3-209	
3	MeCN	1.43	5.6	249	17	30.7	42	-		JCC-E-3-214	
4	Methanol-H ₂ O (2.5%)	1.50	5.6	143	27	15.3	21	-		JCC-E-2-125	
5	Dry methanol	1.51	5.6	74	52	15.1	55	27		JCC-E-2-113	
6	Au anode ^c	1.50	5.6	57	67	15.1	54	19		JCC-E-2-127	
7	Pd anode ^c	1.51	5.6	62	45	15.3	41	51		JCC-E-1-47	
8	1 eq. electrolyte (0.67 M)	1.53	5.6	47	59	15.1	19	29		JCC-E-2-111	
9	2 eq. electrolyte (1.33 M)	1.68	5.6	11	379	15.4	0	24		JCC-E-2-130	
10	Small surface area Pt anode and cathode ^d	1.65	5.6	12	343	15.4	0	22	Trace (0.1%)	JCC-E-2-129	
11	30 V potential difference	1.51	5.6	83	134	15.1	57	22		JCC-E-2-106	
12	Small surface area Pt anode and cathode ^d , 30 V potential difference	1.65	5.6	25	171	30.1	46	29		JCC-E-2-104	
13	Small surface area Pt anode and large surface area cathode ^e , 30 V potential difference ^f	1.55	5.6	35	331	30.1	50	21		JCC-E-2-116	
14	11 % neutralisation	1.54	5.6	37	321	30.2	44	24		JCC-E-2-146	
15	Small surface area Pt anode and cathode ^d , 30 V potential difference, 11 % neutralisation ^f	1.61	5.6	51	243	30.1	38	20		JCC-E-2-147	
		1.57	11.2	32	124	15.0	48	23		JCC-E-2-120	
		1.54	11.2	35	326	30.1	50	18		JCC-E-2-140	
		1.55	11.2	26	450	30.1	37	21		JCC-E-2-141	
		1.61	11.2	26	452	30.1	43	20		JCC-E-2-142	

^a Electrolysis of *N*-Boc β -alanine with acetic acid performed in MeOH (2 mL), Et₃N (5.6% of the total acid concentration), platinum wire anode and cathode (0.84 cm²), 2 mL cell, 15 V potential difference, ^b 9 mL cell, average values taken over two reactions, ^c reaction quantified with ¹H NMR spectroscopy, ^d 0.29 cm² anode and cathode, ^e 0.28 cm² anode and 0.84 cm² cathode, ^f average value taken over multiple reactions

5.3 Experimental for Chapter 3

5.3.1 General Methods for Chapter 3

The ElectraSyn 2.0 and accessories were supplied by IKA and the reticulated vitreous carbon (RVC) electrodes were supplied by Goodfellow (product code: VC00-FA-000125).

5.3.2 Electrolysis Set-Up – ElectraSyn 2.0

Preparative electrolysis was performed using an IKA ElectraSyn 2.0 with ElectraSyn 2.0 lid (Figure 5.4, 1) and SK-50 graphite working and counter electrodes (Figure 5.4, 4), spaced 5.0 mm apart, in either a 10 mL vial (for optimisation) or 20 mL vial (for scope Figure 5.4, 2) and IKA ElectraSyn stirrer bar (Figure 5.4, 6) set at 700 rpm. For reactions performed under N₂, an O ring (internal diameter 27.0 mm, thickness 2.7 mm, Figure 5.4, 3) was fitted under ElectraSyn vial lid to form a better seal and a 17 suba-seal septum (Figure 5.4, 5) was fitted into the ElectraSyn lid (Figure 5.4, 7). See Appendix E for how to set up a reaction on the ElectraSyn 2.0.

The cyclic voltammograms were acquired using a 5 mL electrochemical cell vial containing a glassy carbon disk working electrode, graphite counter electrode and Ag/AgCl reference electrode, all from the IKA ElectraSyn range. The cell lid was modified in-house (Figure 5.4, 8 and 9) to permit connection to an EmStat potentiostat (PalmSens) and the data was collected using the complementary PStTrace software.



Figure 5.4: 1. ElectraSyn vial lid, 2. 20 mL ElectraSyn Vial, 3. 27 mm internal diameter O ring, 4. ElectraSyn SK-50 graphite electrodes, 5. 17 suba seal, 6. ElectraSyn stirrer bar, 7. Suba seal fitted in ElectraSyn vial lid, 8. Modified ElectraSyn vial lid (top view), 9. Modified ElectraSyn vial lid (side view).

5.3.3 Cleaning ElectraSyn 2.0 Graphite Electrodes

Between reactions, both graphite electrodes were cleaned by abrasion using 1800 grit emery paper. Excess graphite on the surface of the electrodes was removed by sonication in acetonitrile (3×10 min, replacing the solvent each time). Graphite electrodes were typically used for 10 reactions before becoming too thin to clean (*ca.* 0.6 mm, original thickness 1.9 mm). Figure 5.5 shows graphite electrodes after 10 reactions worth of cleaning and new electrodes.

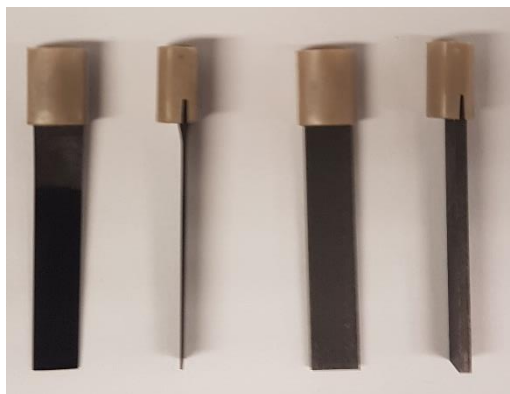


Figure 5.5: Left. Graphite electrodes after 10 reactions showing visible electrode fouling and reduction in thickness due to abrasive cleaning. Right. New graphite electrodes

5.3.4 Modified ElectraSyn 2.0 Set-Up to Accommodate Reticulated Vitreous Carbon (RVC) Electrodes

RVC (3000 C foam, bulk density 0.05 g cm^{-3} , porosity 96.5%, 24 pores cm^{-1}) was cut into rectangular electrodes ($48.0 \text{ mm} \times 5.5 \text{ mm} \times 6.5 \text{ mm}$), sections of cut syringe were used to prevent the electrodes touching. Tinned copper wire was then screwed into the RVC foam, and the wires were then inserted through a subbaseal (using needles to create the holes) and connected to the modified ElectraSyn lid with crocodile clips. The electricity was then supplied by the ElectraSyn 2.0. A 20 mL boiling tube was used as the reaction vessel and a stirrer bar was added (controlled by a second stirrer plate). Figure 5.6 shows the modified set-up (with added reference electrode).

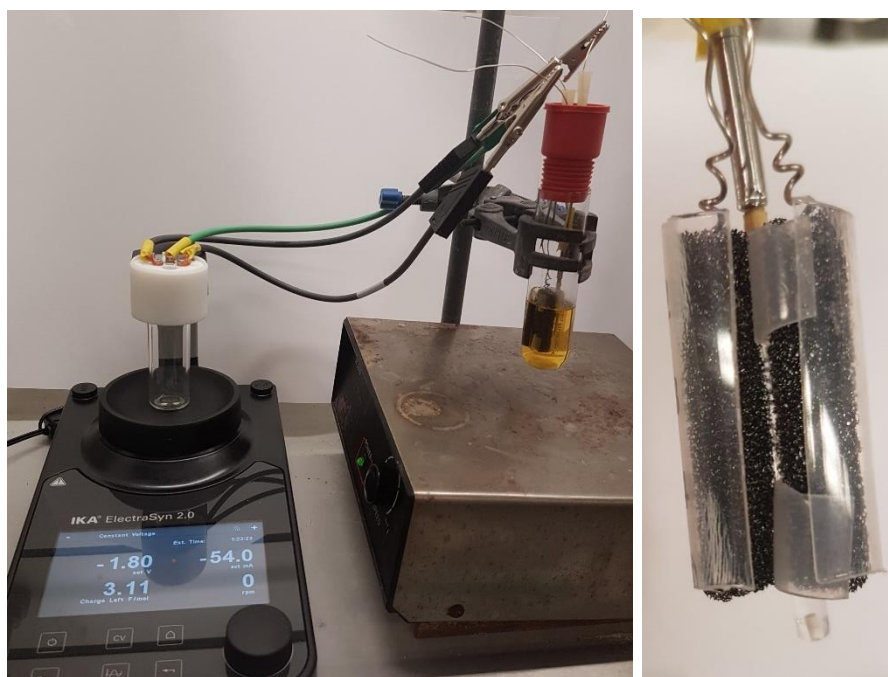
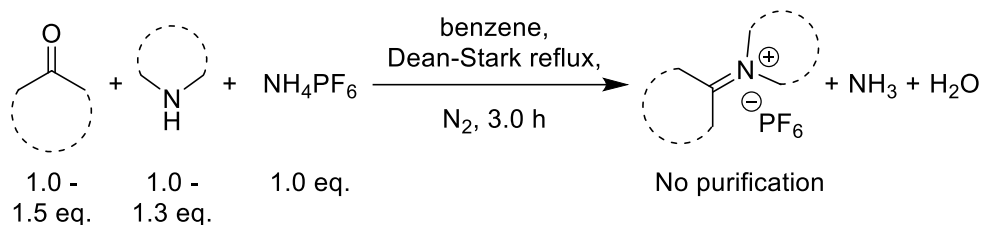


Figure 5.6 Modified ElectroSyn 2.0 set-up to allow the reaction to be performed with RVC electrodes

The method of attaching the RVC foam was adapted from a procedure by Kawamate *et al.*²⁴⁵

5.3.5 General Procedures for Chapter 3

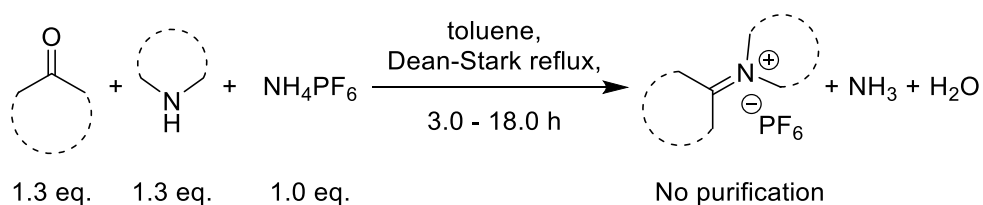
General Procedure 3A: Synthesis and Quantification of Iminium Hexafluorophosphate to Use Crude in Electrolysis with Benzene



To a round bottom flask equipped with a magnetic stirrer bar, ammonium hexafluorophosphate (0.408 g, 2.50 mmol, 1.0 eq.) was added followed by benzene (5 mL). Amine (1.0 – 1.3 eq.) and ketone (1.0 – 1.5 eq.) were added before the reaction mixture was sparged with N₂ for 20 min. The flask was fitted with a Dean-Stark apparatus and a condenser and purged with N₂ for 20 min. The mixture was stirred and heated at reflux with the constant removal of water in the Dean-Stark trap. After 3 h, the condenser was removed and the flask was cooled under N₂ on a Schlenk line. The remaining solvent was removed *in vacuo* before the dried crude mixture was dissolved in dry acetonitrile (20 mL) to give a stock solution of iminium hexafluorophosphate (maximum concentration 0.125 M). From this solution of iminium hexafluorophosphate in acetonitrile, an aliquot (0.25 mL) was transferred to a dried Young's tap NMR tube and the acetonitrile was removed *in vacuo* before a 0.14 M dibromomethane in acetonitrile-*d*₃ stock solution (0.6 mL) was added. The NMR tube lid was secured under N₂ and the NMR tube was shaken before ¹H NMR analysis to quantify the amount of intermediate iminium hexafluorophosphate.

Based on procedure by Saba *et al.*²¹⁰

General Procedure 3B: Synthesis and Quantification of Iminium Hexafluorophosphate to Use Crude in Electrolysis with Toluene

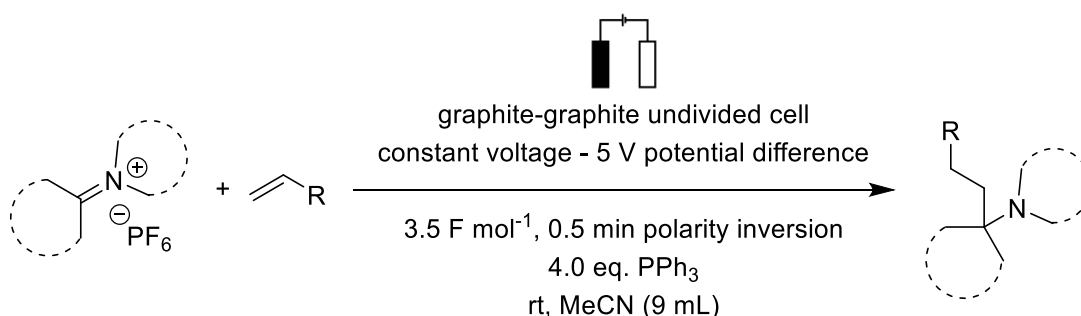


To a round bottom flask equipped with a magnetic stirrer bar, ammonium hexafluorophosphate (0.50 – 2.50 mmol) was added followed by toluene (5 mL). Amine (1.3 eq.) and ketone (1.3 eq.) were added the flask was fitted with a Dean-Stark apparatus. The

mixture was stirred and heated at reflux with the constant removal of water in the Dean-Stark trap. After 3 – 18 h, the condenser was removed and the flask was cooled under N₂ on a Schlenk line. The remaining solvent was removed *in vacuo* before the dried crude mixture was dissolved in dry acetonitrile (20 mL) to give a stock solution of iminium hexafluorophosphate (maximum concentration 0.125 M). From this solution of iminium hexafluorophosphate in acetonitrile, an aliquot (0.25 mL) was transferred to a dried Young's tap NMR tube and the acetonitrile was removed *in vacuo* before a 0.14 M dibromomethane in acetonitrile-*d*₃ stock solution (0.6 mL) was added. The NMR tube lid was secured under N₂ and the NMR tube was shaken before ¹H NMR analysis to quantify the amount of intermediate iminium hexafluorophosphate.

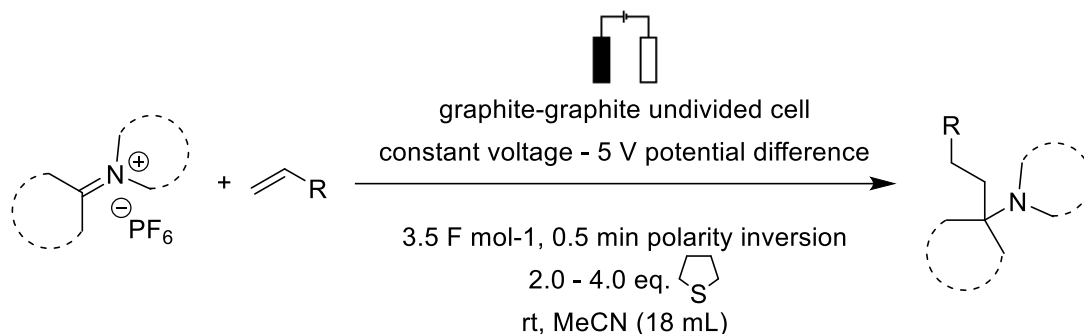
Based on procedure by Saba *et al.*²¹⁰

General Procedure 3C: Electrolysis of Preformed Iminium Hexafluorophosphate with Triphenylphosphine



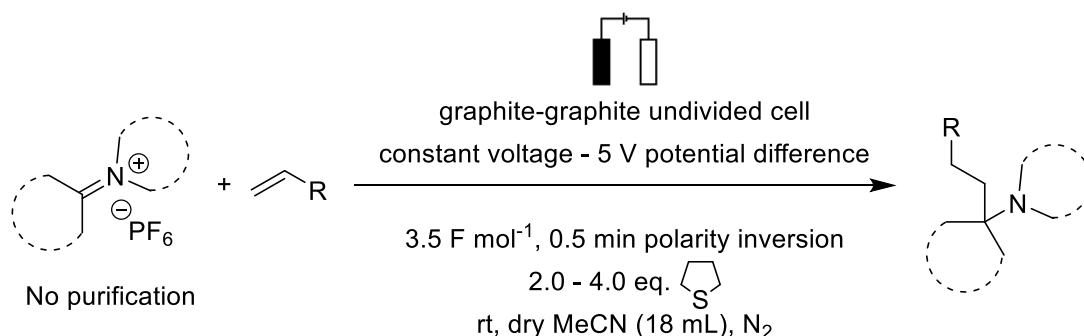
A 10 mL ElectraSyn 2.0 vial was charged with a stirrer bar, iminium salt (0.25 mmol) and triphenylphosphine (0.262 g, 1.00 mmol, 4.0 eq.) followed by MeCN (9 mL). Alkene (0.75 mmol, 3.0 eq.) was added, and the vial was sealed with the ElectraSyn 2.0 vial lid equipped with two graphite electrodes and connected to the ElectraSyn 2.0 apparatus. The ElectraSyn 2.0 was set to run constant voltage at 5 V with no reference electrode, with 0.5 min polarity inversion for 3.5 F mol⁻¹ of charge based on 0.5 mmol of iminium hexafluorophosphate. After completion, the solution was concentrated *in vacuo*. The crude mixture was acidified by stirring with 2 M HCl_(aq) (0.2 mL) in Et₂O:DCM (10 mL, 1:1 v/v) and concentrated *in vacuo* prior to purification by flash column chromatography (General Procedure 3G).

General Procedure 3D: Electrolysis of Preformed Iminium Hexafluorophosphate with Tetrahydrothiophene



A 20 mL ElectraSyn 2.0 vial was charged with a stirrer bar and iminium salt (0.5 mmol) followed by MeCN (18 mL). Alkene (1.5 mmol, 3.0 eq.) and tetrahydrothiophene (0.088 – 0.176 mL, 1.0 – 2.0 mmol, 2.0 – 4.0 eq.) were added and the vial was sealed with the ElectraSyn 2.0 vial lid equipped with two graphite electrodes and connected to the ElectraSyn 2.0 apparatus. The ElectraSyn 2.0 was set to run constant voltage at 5 V with no reference electrode, with 0.5 min polarity inversion for 3.5 F mol⁻¹ of charge based on 0.5 mmol of iminium hexafluorophosphate. After completion, the solution was concentrated *in vacuo* and purified by flash column chromatography.

General Procedure 3E: Electrolysis of Crude Iminium Hexafluorophosphate with Tetrahydrothiophene



A 20 mL ElectraSyn 2.0 vial was charged with a stirrer bar and the vial was sealed with the ElectraSyn 2.0 vial lid equipped with two graphite electrodes and O ring under the ElectraSyn vial lid (Figure 5.4). A suba-seal was fitted into the lid and the vial was flame dried under a flow of N₂. Once cooled, the iminium hexafluorophosphate in acetonitrile stock solution was added (4 mL, maximum concentration 0.125 M) followed by dry acetonitrile (14 mL), alkene (1.5 mmol, 3.0 eq.) and tetrahydrothiophene (0.088 – 0.176 mL, 1.0 – 2.0

mmol, 2.0–4.0 eq.). The vial was connected to the ElectraSyn 2.0. The ElectraSyn 2.0 was set to run constant voltage at 5 V with no reference electrode, with 0.5 min polarity inversion for 3.5 F mol^{-1} of charge based on 0.5 mmol of iminium hexafluorophosphate. After completion, the solution was concentrated *in vacuo* and purified by flash column chromatography.

General Procedure 3F: Quantifying Crude Reaction Mixtures with ^1H NMR Spectroscopy

In cases where triphenylphosphine was the sacrificial electron donor, spectra were quantified by ^1H NMR spectroscopy using the aromatic peaks of $\text{PPh}_3/\text{Ph}_3\text{PO}$ and alpha to nitrile CH_2 peaks of the product (see Appendix F1). When the sacrificial electron donor was not triphenylphosphine, reactions were quantified by ^1H NMR spectroscopy using dibromomethane as an external standard and the alpha to nitrile CH_2 peaks of the product (see Appendix F2).

General Procedure 3G: Purification of Tertiary Amines with a Silica Plug

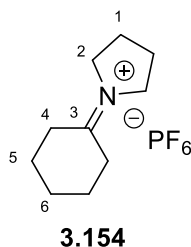
In cases where the crude ^1H NMR spectrum after electrolysis showed large amounts of non-amine contaminants (e.g. non-volatile starting materials), which had a similar R_F value to the product by TLC, products were isolated *via* a silica plug. The crude mixture was dissolved in $\text{Et}_2\text{O}:\text{DCM}$ (20 mL, 1:1 v/v), stirred with 2 M $\text{HCl}_{(\text{aq})}$ (1 mL) and concentrated *in vacuo* prior to loading onto and purification by flash column chromatography. This converted the amine product into an ammonium salt which would not move on silica. EtOAc in petroleum ether was used as the first eluent to remove the contaminants, then the eluent was changed to EtOAc in petroleum ether with 2% base (either triethylamine or *N,N*-dimethylethylamine) to reform and elute the amine as a free base.

General Procedure 3H: Recording NMR Spectra of Tertiary Amines

In some cases, the ^1H NMR spectra of purified products appeared broad as the amine became partially protonated in chloroform which resulted in broadening due to proton exchange. Samples thus required basifying to achieve reasonable spectra. To basify, samples were dissolved in acetonitrile and stirred with K_2CO_3 for 2 h. The K_2CO_3 was filtered out and the acetonitrile removed *in vacuo* before the samples were dissolved in CDCl_3 prior to submitting the NMR samples. Some samples were basified with K_2CO_3 directly in CDCl_3 however, this resulted in the formation of new peaks at δ_{H} 8.07 and 4.66 and 1.24 ppm likely due to the formation of dichlorocarbene adducts.

Synthesis and Characterisation of Unpurified Iminium Ions

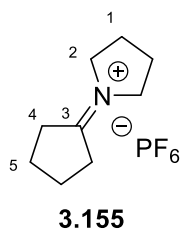
The following iminium hexafluorophosphates that were used unpurified in electrolysis were quantified and characterised by ^1H NMR spectroscopy only.

***N*-Cyclohexylidenepyrrrolidinium hexafluorophosphate (3.154)**

Synthesised using General Procedure 3B, using cyclohexanone (84 μL , 0.81 mmol, 1.3 eq.), pyrrolidine (68 μL , 0.81 mmol, 1.3 eq.), ammonium hexafluorophosphate (0.103 g, 0.632 mmol, 1.0 eq.) and toluene (5 mL). Heated at reflux for 18 h. 90% yield was calculated for the iminium hexafluorophosphate from the crude ^1H NMR spectrum by integrating H^2 relative to Br_2CH_2 . As a mixture with cyclohexanone (38%) and pyrrolidine (42%).

^1H NMR (400 MHz, Acetonitrile- d_3) δ 3.91 – 3.80 (m, 4H, H^2), 2.67 (t, $J = 6.5$ Hz, 4H, H^4), 2.11 – 2.05 (m, 4H, H^1), 1.90 – 1.78 (m, 4H, H^5 – signals overlap with residual cyclohexanone), 1.73 – 1.62 (m, 2H, H^6 – signals overlap with residual cyclohexanone).

Lab book reference JCC-2-61

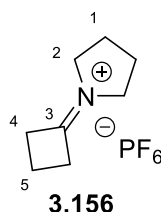
***N*-Cyclopentylidenepyrrrolidinium hexafluorophosphate (3.155)**

Synthesised using General Procedure 3A, using cyclopentanone (0.33 mL, 3.8 mmol, 1.5 eq.), pyrrolidine (0.21 mL, 2.5 mmol, 1.0 eq.), ammonium hexafluorophosphate (0.408 g, 2.50 mmol, 1.0 eq.) and benzene (5 mL). Heated at reflux for 3 h. 99% yield was calculated for the iminium hexafluorophosphate from the crude ^1H NMR spectrum by integrating H^2 relative to Br_2CH_2 . As a mixture with pyrrolidine (1%).

^1H NMR (500 MHz, Acetonitrile- d_3) δ 3.81 – 3.72 (m, 4H, H²), 2.76 – 2.66 (m, 4H, H⁴), 2.16 – 2.07 (m, 4H, H¹), 2.01 – 1.96 (m, 4H, H⁵).

Lab book reference JCC-2-90

***N*-Cyclobutylidenepyrrrolidinium hexafluorophosphate (3.156)**

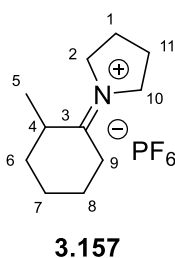


Synthesised using General Procedure 3A, using cyclobutanone (0.28 mL, 3.8 mmol, 1.5 eq.), pyrrolidine (0.21 mL, 2.5 mmol, 1.0 eq.), ammonium hexafluorophosphate (0.408 g, 2.50 mmol, 1.0 eq.) and benzene (5 mL). Heated at reflux for 3 h. 49% yield was calculated for the iminium hexafluorophosphate from the crude ^1H NMR spectrum by integrating H² relative to Br₂CH₂. As a mixture with pyrrolidine (43%).

^1H NMR (400 MHz, Acetonitrile- d_3) δ 3.81 – 3.65 (m, 4H, H²), 3.24 – 3.15 (m, 4H, H⁴ – signals overlap with residual pyrrolidine), 2.24 (quin, $J = 8.0$ Hz, 2H, H⁵), 2.14 – 2.05 (m, 4H, H¹).

Lab book reference JCC-2-96

***N*-(2-Methylcyclohexylidene)pyrrrolidinium hexafluorophosphate (3.157)**

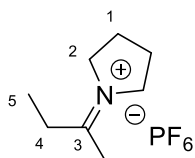


Synthesised using General Procedure 3A, using 2-methylcyclohexanone (0.30 mL, 2.5 mmol, 1.0 eq.), pyrrolidine (0.21 mL, 2.5 mmol, 1.0 eq.), ammonium hexafluorophosphate (0.408 g, 2.50 mmol, 1.0 eq.) and benzene (5 mL). Heated at reflux for 3 h. 91% yield was calculated for the iminium hexafluorophosphate from the crude ^1H NMR spectrum by integrating H² and H¹⁰ relative to Br₂CH₂. As a mixture with 2-methylcyclohexanone (3%) and pyrrolidine (28%).

^1H NMR (400 MHz, Acetonitrile- d_3) δ 4.01 – 3.85 (m, 2H, $\text{H}^{2/10}$), 3.85 – 3.67 (m, 2H, $\text{H}^{2/10}$), 3.16 – 2.99 (m, 1H, $\text{H}^{4/9}$), 2.82 – 2.69 (m, 1H, $\text{H}^{4/9}$), 2.66 – 2.50 (m, 1H, $\text{H}^{4/9}$), 2.13 – 1.96 (m, 4H, H^1 and H^{11} – signals overlap with residual pyrrolidine), 1.87 – 1.50 (m, 6H, H^{6-8}), 1.24 (d, $J = 7.0$ Hz, 3H, H^5).

Lab book reference JCC-2-83

***N*-(Pentan-3-ylidene)pyrrolidinium hexafluorophosphate (3.158)**



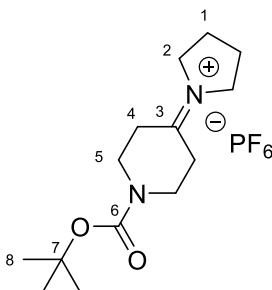
3.158

Synthesised using General Procedure 3A, using 3-pentanone (0.40 mL, 3.8 mmol, 1.5 eq.), pyrrolidine (0.21 mL, 2.5 mmol, 1.0 eq.), ammonium hexafluorophosphate (0.408 g, 2.50 mmol, 1.0 eq.) and benzene (5 mL). Heated at reflux for 3 h. 80% yield was calculated for the iminium hexafluorophosphate from the crude ^1H NMR spectrum by integrating H^2 relative to Br_2CH_2 . As a mixture with pyrrolidine (29%).

^1H NMR (400 MHz, Acetonitrile- d_3) δ 3.91 – 3.84 (m, 4H, H^2), 2.66 (q, $J = 7.5$ Hz, 4H, H^4), 2.16 – 2.05 (m, 4H, H^1 – signals overlap with residual pyrrolidine), 1.21 (t, $J = 7.5$ Hz, 6H, H^5).

Lab book reference JCC-2-93

***N*-(1-(*tert*-Butoxycarbonyl)piperidin-4-ylidene)pyrrolidinium hexafluorophosphate (3.159)**



3.159

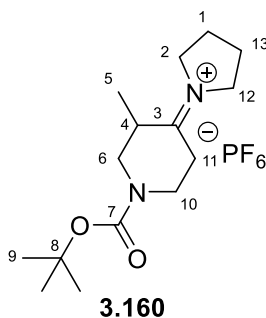
Synthesised using General Procedure 3A, using *N*-(*tert*-butoxycarbonyl)-4-piperidone (0.648 g, 3.25 mmol, 1.3 eq.), pyrrolidine (0.27 mL, 3.3 mmol, 1.3 eq.), ammonium

hexafluorophosphate (0.408 g, 2.50 mmol, 1.0 eq.) and benzene (5 mL). Heated at reflux for 3.0 h. 83% yield was calculated for the iminium hexafluorophosphate from the crude ^1H NMR spectrum by integrating H^2 relative to Br_2CH_2 . As a mixture with *N*-(*tert*-butoxycarbonyl)-4-piperidone (17%) and pyrrolidine (17%).

^1H NMR (400 MHz, Acetonitrile- d_3) δ 3.84 (br. s, 4H, H^2), 3.73 – 3.56 (m, 4H, H^5 – signals overlap with residual *N*-(*tert*-butoxycarbonyl)-4-piperidone), 2.79 (br. s, 4H, H^4), 2.10 (br. s, 4H, H^1), 1.45 (br. s, 9H, H^8 – signals overlap with residual *N*-(*tert*-butoxycarbonyl)-4-piperidone).

Lab book reference JCC-2-75

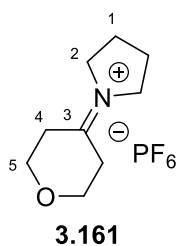
***N*-(1-(*tert*-Butoxycarbonyl)-2-methylpiperidin-4-ylidene)pyrrolidinium hexafluorophosphate (3.160)**



Synthesised using General Procedure 3A, using *tert*-butyl-3-methyl-4-oxopiperidine-1-carboxylate (0.870 g, 3.75 mmol, 1.5 eq.), pyrrolidine (0.21 mL, 2.5 mmol, 1.3 eq.), ammonium hexafluorophosphate (0.408 g, 2.50 mmol, 1.0 eq.) and benzene (5 mL). Heated at reflux for 2.5 h. 83% yield was calculated for the iminium hexafluorophosphate from the crude ^1H NMR spectrum by integrating H^5 relative to Br_2CH_2 . As a mixture with *tert*-butyl-3-methyl-4-oxopiperidine-1-carboxylate (51%) and pyrrolidine (15%).

^1H NMR (400 MHz, Acetonitrile- d_3) δ 4.03 – 3.71 (m, 6H, H^2 , H^{12} , H^{6a} and H^{10a} – overlaps with *tert*-butyl-3-methyl-4-oxopiperidine-1-carboxylate), 3.06 (br s, 2H, H^{6b} and H^{10b}), 2.84 – 2.70 (m, 3H, H^4 and H^{11}), 2.11 – 2.03 (m, 4H, H^1 and H^{13}), 1.43 (s, 9H, H^9 – overlaps with *tert*-butyl-3-methyl-4-oxopiperidine-1-carboxylate), 1.21 (d, $J = 7.0$ Hz, 3H, H^5).

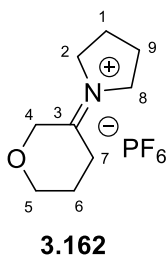
Lab book reference JCC-2-87

***N*-(Tetrahydro-4H-pyran-4-ylidene)pyrrolidinium hexafluorophosphate (3.161)**

Synthesised using General Procedure 3A, using tetrahydro-4*H*-pyran-4-one (0.23 mL, 2.5 mmol, 1.0 eq.), pyrrolidine (0.21 mL, 2.5 mmol, 1.0 eq.), ammonium hexafluorophosphate (0.408 g, 2.50 mmol, 1.0 eq.) and benzene (5 mL). Heated at reflux for 3 h. 60% yield was calculated for the iminium hexafluorophosphate from the crude ¹H NMR spectrum by integrating H¹ relative to Br₂CH₂. As a mixture with pyrrolidine (4%).

¹H NMR (400 MHz, Acetonitrile-*d*₃) δ 3.93 – 3.83 (m, 8H, H² and H⁵), 2.81 – 2.75 (m, 4H, H⁴), 2.13 – 2.07 (m, 4H, H¹).

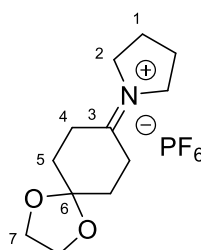
Lab book reference JCC-2-81

***N*-(Dihydro-2H-pyran-3(4H)-ylidene)pyrrolidinium hexafluorophosphate (3.162)**

Synthesised using General Procedure 3A, using tetrahydropyran-3-one (0.376 g, 3.75 mmol, 1.5 eq.), pyrrolidine (0.21 mL, 2.5 mmol, 1.0 eq.), ammonium hexafluorophosphate (0.408 g, 2.50 mmol, 1.0 eq.) and benzene (5 mL). Heated at reflux for 3 h. 47% yield was calculated for the iminium hexafluorophosphate from the crude ¹H NMR spectrum by integrating H⁷ relative to Br₂CH₂. As a mixture with pyrrolidine (63%).

¹H NMR (400 MHz, Acetonitrile-*d*₃) δ 4.53 – 4.47 (m, 2H, H⁴), 3.86 – 3.66 (m, 6H, H², H⁵ and H⁸), 2.91 – 2.81 (m, 2H, H⁷), 2.14 – 2.04 (m, 4H, H¹ and H⁹). H⁶ not observed as obscured by either remain starting material or residual solvent peak.

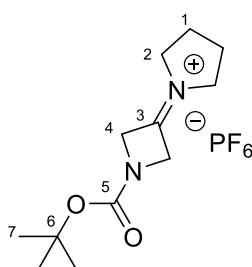
Lab book reference JCC-2-89

***N*-(1,4-Dioxaspiro[4.5]decan-8-ylidene)pyrrolidinium hexafluorophosphate (3.163)****3.163**

Synthesised using General Procedure 3A, using 1,4-cyclohexanedione monoethylene acetate (0.390 g, 2.50 mmol, 1.0 eq.), pyrrolidine (0.21 mL, 2.5 mmol, 1.0 eq.), ammonium hexafluorophosphate (0.408 g, 2.50 mmol, 1.0 eq.) and benzene (5 mL). Heated at reflux for 3 h. 83% yield was calculated for the iminium hexafluorophosphate from the crude ^1H NMR spectrum by integrating H^2 relative to Br_2CH_2 . As a mixture with 1,4-cyclohexanedione monoethylene acetate (6%) and pyrrolidine (12%).

^1H NMR (400 MHz, Acetonitrile- d_3) δ 3.97 (s, 4H, H^7), 3.88 – 3.81 (m, 4H, H^2), 2.86 – 2.77 (m, 4H, H^4), 2.13 – 2.06 (m, 4H, H^1), 1.97 – 1.95 (m, 4H, H^5 – signal overlaps with residual acetonitrile).

Lab book reference JCC-2-84

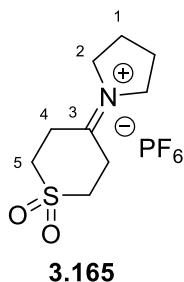
***N*-(1-(*tert*-Butoxycarbonyl)azetidin-3-ylidene)pyrrolidinium hexafluorophosphate (3.164)****3.164**

Synthesised using General Procedure 3A, using *tert*-butyl-3-oxoazetidine-1-carboxylate (0.644 g, 3.75 mmol, 1.5 eq.), pyrrolidine (0.21 mL, 2.5 mmol, 1.0 eq.), ammonium hexafluorophosphate (0.408 g, 2.50 mmol, 1.0 eq.) and benzene (5 mL). Heated at reflux for 3 h. 5% yield was calculated for the iminium hexafluorophosphate from the crude ^1H NMR spectrum by integrating H^2 relative to Br_2CH_2 . As a mixture with *tert*-butyl-3-oxoazetidine-1-carboxylate (4%) and pyrrolidine (39%).

^1H NMR (400 MHz, Acetonitrile- d_3) δ 4.66 (br s, 4H, H^4), 4.49 (br s, 4H, H^2), other peaks overlapped with residual solvent or starting materials and therefore could not be reliably assigned.

Lab book reference JCC-2-86

***N*-(1,1-Dioxidotetrahydro-4H-thiopyran-4-ylidene)pyrrolidinium hexafluorophosphate (3.165)**

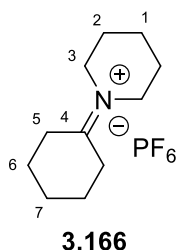


Synthesised using General Procedure 3A, using tetrahydrothiopyran-4-one 1,1-dioxide (0.556 g, 3.75 mmol, 1.5 eq.), pyrrolidine (0.21 mL, 2.5 mmol, 1.0 eq.), ammonium hexafluorophosphate (0.408 g, 2.50 mmol, 1.0 eq.) and benzene (5 mL). Heated at reflux for 3 h. 6% yield was calculated for the iminium hexafluorophosphate from the crude ^1H NMR spectrum by integrating H^2 relative to Br_2CH_2 . As a mixture with tetrahydrothiopyran-4-one 1,1-dioxide (36%) and pyrrolidine (94%).

^1H NMR (400 MHz, Acetonitrile- d_3) δ 3.90 (br s, 4H, H^2), other peaks overlapped with residual solvent or starting materials and therefore could not be reliably assigned.

Lab book reference JCC-2-85

***N*-Cyclohexylidenepiperidinium hexafluorophosphate (3.166)**



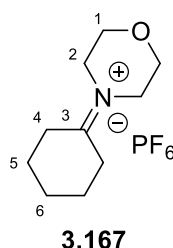
Synthesised using General Procedure 3A, using cyclohexanone (0.26 mL, 2.5 mmol, 1.0 eq.), piperidine (0.25 mL, 2.5 mmol, 1.0 eq.), ammonium hexafluorophosphate (0.408 g, 2.50 mmol, 1.0 eq.) and benzene (5 mL). Heated at reflux for 3 h. 86% yield was calculated

for the iminium hexafluorophosphate from the crude ^1H NMR spectrum by integrating H^3 relative to Br_2CH_2 . As a mixture with cyclohexanone (8%) and piperidine (17%).

^1H NMR (400 MHz, Acetonitrile- d_3) δ 4.00 – 3.91 (m, 4H, H^3), 2.78 (t, $J = 6.5$ Hz, 4H, H^5), 1.92 – 1.58 (m, 12H, H^{1-2} and H^{6-7} – signals overlap with residual cyclohexanone and piperidine).

Lab book reference JCC-2-80

N-Cyclohexylidenemorpholinium hexafluorophosphate (3.167)

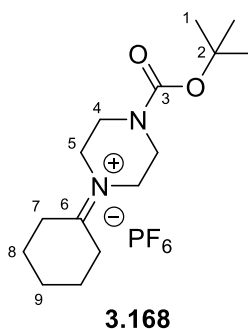


Synthesised using General Procedure 3B, using cyclohexanone (0.34 mL, 3.3 mmol, 1.3 eq.), morpholine (0.28 mL, 3.3 mmol, 1.3 eq.), ammonium hexafluorophosphate (0.408 g, 2.50 mmol, 1.0 eq.) and toluene (5 mL). Heated at reflux for 3 h. 70% yield was calculated for the iminium hexafluorophosphate from the crude ^1H NMR spectrum by integrating H^2 relative to Br_2CH_2 . As a mixture with cyclohexanone (16%) and morpholine (9%).

^1H NMR (400 MHz, Acetonitrile- d_3) δ 4.04 – 3.99 (m, 4H, H^1), 3.93 – 3.85 (m, 4H, H^2), 2.79 (t, $J = 6.5$ Hz, 4H, H^4), 1.92 – 1.87 (m, 4H, H^5 – signal overlaps with residual acetonitrile), 1.74 – 1.66 (m, 2H, H^6).

Lab book reference JCC-2-63

N-(*tert*-Butoxycarbonyl)-*N*-cyclohexylidenepiperazinium hexafluorophosphate (3.168)

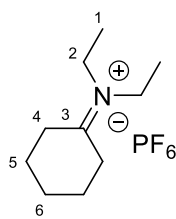


Synthesised using General Procedure 3A, using cyclohexanone (0.38 mL, 3.8 mmol, 1.5 eq.), *tert*-butyl piperazine-1-carboxylate (0.466 g, 2.50 mmol, 1.0 eq.), ammonium hexafluorophosphate (0.408 g, 2.50 mmol, 1.0 eq.) and benzene (5 mL). Heated at reflux for 3 h. 96% yield was calculated for the iminium hexafluorophosphate from the crude ^1H NMR spectrum by integrating H^5 relative to Br_2CH_2 . As a mixture with cyclohexanone (9%) and *tert*-butyl piperazine-1-carboxylate (11%).

^1H NMR (400 MHz, Acetonitrile- d_3) (60:40 mixture of rotamers) δ 4.05 – 3.94 (m, 2.4H, H^5), 3.72 – 3.61 (m, 2.4H, H^4), 3.57 – 3.50 (m, 1.6H, H^5), 3.06 – 3.00 (m, 1.6H, H^4), 2.78 (t, $J = 6.5$ Hz, 2.4H, H^7), 1.99 – 1.84 (m, 5.6H, H^7 and H^8 – signals overlap with residual acetonitrile), 1.75 – 1.62 (m, 2H, H^9), 1.46 (s, 5.4H, H^1), 1.43 (s, 3.6H, H^1).

Lab book reference JCC-2-88

***N*-Cyclohexylideneethylethanaminium hexafluorophosphate (3.169)**

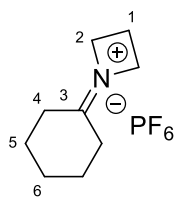


3.169

Synthesised using General Procedure 3A, using cyclohexanone (0.38 mL, 3.8 mmol, 1.5 eq.), diethylamine (0.26 mL, 2.5 mmol, 1.0 eq.), ammonium hexafluorophosphate (0.408 g, 2.50 mmol, 1.0 eq.) and benzene (5 mL). Heated at reflux for 3 h. 61% yield was calculated for the iminium hexafluorophosphate from the crude ^1H NMR spectrum by integrating H^2 relative to Br_2CH_2 . As a mixture with cyclohexanone (4%) and diethylamine (23%).

^1H NMR (400 MHz, Acetonitrile- d_3) δ 3.83 (q, $J = 7.5$ Hz, 4H, H^2), 2.73 (t, $J = 6.5$ Hz, 4H, H^4), 1.93 – 1.87 (m, 4H, H^5 – signal overlaps with residual acetonitrile), 1.73 – 1.65 (m, 2H, H^6), 1.31 (t, $J = 7.5$ Hz, 6H, H^1).

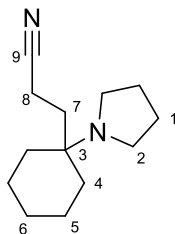
Lab book reference JCC-2-94

***N*-Cyclohexylideneazetidinium hexafluorophosphate (3.170)****3.170**

Azetidine hydrochloride (1.75 g, 18.7 mmol) was dissolved in water (5 mL) and added to a separating funnel along with benzene (2 mL). Sat. K_2CO_3 was then added until the pH became basic. The organic layer was removed, and the aqueous layer was washed with benzene (2 mL). The organic layers were combined to make a stock solution of azetidine in benzene (5 mL, theoretical concentration of 3.7 M). Then the iminium hexafluorophosphate was synthesised using General Procedure 3A, using cyclohexanone (0.38 mL, 3.8 mmol, 1.5 eq.), azetidine hydrochloride (7.5 mmol, 3.0 eq., added as 2 mL of the stock solution of azetidine in benzene), ammonium hexafluorophosphate (0.408 g, 2.50 mmol, 1.0 eq.) and benzene (3 mL). Heated at reflux for 3 h. 24% yield was calculated for the iminium hexafluorophosphate from the crude ^1H NMR spectrum by integrating H^2 relative to Br_2CH_2 . As a mixture with cyclohexanone (6%).

^1H NMR (400 MHz, Acetonitrile- d_3) δ 4.53 (tt, $J = 8.0, 1.5$ Hz, 4H, H^2), 2.46 (apparent quin., $J = 8.0$ Hz, 2H, H^1), 2.39 (t, $J = 6.5$ Hz, 4H, H^4), 1.84 – 1.73 (m, 4H, H^5 – signals overlap with residual cyclohexanone), 1.70 – 1.57 (m, 2H, H^6 – signals overlap with residual cyclohexanone).

Lab book reference JCC-2-97

Synthesis and Characterisation of Tertiary Amines – Using *N*-Cyclohexylidenepyrrrolidinium hexafluorophosphate (3.154)**3-(1-(Pyrrolidin-1-yl)cyclohexyl)propanenitrile (3.116)****3.116**

Synthesised using General Procedure 3C, using iminium hexafluorophosphate **3.154** (74 mg, 0.25 mmol, 1.0 eq.), acrylonitrile (49 μL , 0.75 mmol, 3.0 eq.), triphenylphosphine (262 mg, 1.00 mmol, 4.0 eq.) and acetonitrile (9 mL). Electrolysed for 3.5 F mol⁻¹ of charge. Crude mixture was acidified with 2 M HCl_(aq) (0.2 mL) in Et₂O:DCM (10 mL, 1:1 v/v) prior to purification by flash column chromatography (EtOAc then DCM:Et₂O:NH₄OH_(aq), 70:30:2 v/v/v). The product (**3.116**) was isolated as a colourless oil (31.1 mg, 59%).

Lab book reference JCC-E-5-297

Synthesised using General Procedure 3D, using iminium hexafluorophosphate **3.154** (148 mg, 0.50 mmol, 1.0 eq.), acrylonitrile (98 μL , 1.5 mmol, 3.0 eq.), tetrahydrothiophene (176 μL , 2.0 mmol, 4.0 eq.) and acetonitrile (18 mL). Electrolysed for 3.5 F mol⁻¹ of charge. Purification by flash column chromatography (petroleum ether:EtOAc:Et₃N, 50:50:1 v/v/v). The product (**3.116**) was isolated as a colourless oil (57.2 mg, 56%).

Lab book reference JCC-E-6-354

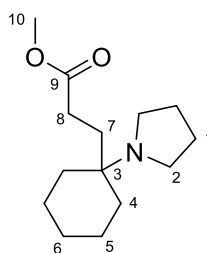
Synthesised using General Procedure 3D, using iminium hexafluorophosphate **3.154** (148 mg, 0.50 mmol, 1.0 eq.), acrylonitrile (98 μL , 1.5 mmol, 3.0 eq.), tetrahydrothiophene (88 μL , 1.0 mmol, 2.0 eq.) and acetonitrile (18 mL). Electrolysed for 3.5 F mol⁻¹ of charge. Purification by flash column chromatography (petroleum ether:EtOAc:EtNMe₂, 90:10:1 v/v/v). The product (**3.116**) was isolated as a colourless oil (58.8 mg, 57%).

R_F (petroleum ether:EtOAc:EtNMe₂, 80:20:1 v/v/v) 0.29; IR (ATR) 2931, 2854, 2245 (C≡N), 1627, 1445, 914, 732 cm⁻¹; ¹H NMR (400 MHz, Chloroform-*d*) δ 2.59 – 2.55 (m, 4H, H²), 2.36 – 2.29 (m, 2H, H⁸), 1.90 – 1.84 (m, 2H, H⁷), 1.71 – 1.66 (m, 4H, H¹), 1.65 – 1.18 (m, 10H, H⁴⁻⁶); ¹³C NMR (101 MHz, Chloroform-*d*) δ 121.3 (C⁹), 55.4 (C³), 43.8 (C²),

28.9 (C⁷), 24.0 (C¹), 30.6 (C⁴), 26.1 (C⁶), 22.0 (C⁵), 11.2 (C⁸); HRMS (ESI⁺) m/z calcd for C₁₃H₂₃N₂ [M + H]⁺: 207.1856, found: 207.1853 (1.3 ppm error). Spectroscopic data are consistent with those reported in the literature.¹⁹⁵

Lab book reference JCC-E-7-412

Methyl 3-(1-(pyrrolidin-1-yl)cyclohexyl)propanoate (3.110)



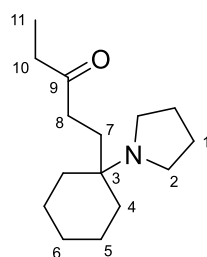
3.110

Synthesised using General Procedure 3D, using iminium hexafluorophosphate **3.154** (148 mg, 0.50 mmol, 1.0 eq.), methyl acrylate (135 μ L, 1.5 mmol, 3.0 eq.), tetrahydrothiophene (176 μ L, 2.0 mmol, 4.0 eq.) and acetonitrile (18 mL). Electrolysed for 3.5 F mol⁻¹ of charge. Purification by flash column chromatography (petroleum ether:EtOAc:Et₃N, 50:50:1 v/v/v). The product (**3.110**) was isolated as a colourless oil (55.2 mg, 46%).

R_F (petroleum ether:EtOAc:Et₃N, 50:50:1 v/v/v) 0.23; IR (ATR) 2935, 2863, 1734 (C=O), 1655, 1438, 1199, 1174, 627 cm⁻¹; ¹H NMR (400 MHz, Chloroform-*d*) δ 3.65 (s, 3H, H¹⁰), 2.65 – 2.57 (m, 4H, H²), 2.35 – 2.26 (m, 2H, H⁸), 1.83 – 1.77 (m, 2H, H⁷), 1.70 – 1.65 (m, 4H, H¹), 1.65 – 1.22 (m, 10H, H⁴⁻⁶); ¹³C NMR (101 MHz, Chloroform-*d*) δ 175.3 (C⁹), 55.6 (C³), 51.5 (C¹⁰), 43.9 (C²), 28.7, 27.7 (C⁷⁻⁸) 24.1 (C¹), 31.4, 26.2, 22.0 (C⁴⁻⁶); HRMS (ESI⁺) m/z calcd for C₁₄H₂₆NO₂ [M + H]⁺: 240.1958, found: 240.1960 (-0.7 ppm error). Spectroscopic data are consistent with those reported in the literature.¹⁹⁵

Lab book reference JCC-E-6-357

1-(1-(Pyrrolidin-1-yl)cyclohexyl)pentan-3-one (3.191)



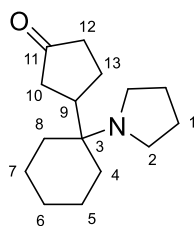
3.191

Synthesised using General Procedure 3D, using iminium hexafluorophosphate **3.154** (148 mg, 0.50 mmol, 1.0 eq.), ethyl vinyl ketone (149 μL , 1.5 mmol, 3.0 eq.), tetrahydrothiophene (88 μL , 1.0 mmol, 2.0 eq.) and acetonitrile (18 mL). Electrolysed for 3.5 F mol⁻¹ of charge. Purification by flash column chromatography (petroleum ether:EtOAc:EtNMe₂, 80:20:1 v/v/v). The product (**3.191**) was isolated as a colourless oil (78.4 mg, 66%).

R_F (petroleum ether:EtOAc: EtNMe₂, 80:20:1 v/v/v) 0.21; IR (ATR) 2931, 2854, 2803, 1712 (C=O), 1447, 1411, 1356, 1267, 1163, 1112, 1019, 983, 850, 730 cm⁻¹; ¹H NMR (400 MHz, Chloroform-*d*) δ 2.61 – 2.55 (m, 4H, H²), 2.46 – 2.36 (m, 4H, H⁸ and H¹⁰), 1.76 – 1.71 (m, 2H, H⁷), 1.68 – 1.63 (m, 4H, H¹), 1.60 – 1.21 (m, 10H, H⁴⁻⁶), 1.03 (t, $J = 7.5$ Hz, 3H, H¹¹); ¹³C NMR (101 MHz, Chloroform-*d*) δ 212.7 (C⁹), 55.5 (C³), 43.9 (C²), 36.7, 36.1 (C⁸ and C¹⁰), 24.1 (C¹), 31.3, 26.4, 26.2, 22.1 (C⁴⁻⁷), 7.9 (C¹¹); HRMS (ESI⁺) m/z calcd for C₁₅H₂₈NO [M + H]⁺: 238.2165, found: 238.2161 (2.1 ppm error).

Lab book reference JCC-E-7-394

3-(1-(Pyrrolidin-1-yl)cyclohexyl)cyclopentan-1-one (**3.192**)



3.192

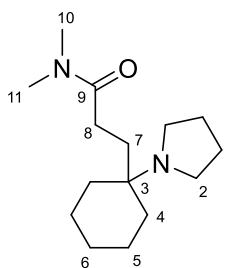
Synthesised using General Procedure 3D, using iminium hexafluorophosphate **3.154** (148 mg, 0.50 mmol, 1.0 eq.), 2-cyclopenten-1-one (126 μL , 1.5 mmol, 3.0 eq.), tetrahydrothiophene (88 μL , 1.0 mmol, 2.0 eq.) and acetonitrile (18 mL). Electrolysed for 3.5 F mol⁻¹ of charge. Purification by flash column chromatography (petroleum ether:EtOAc:EtNMe₂, 70:30:1 v/v/v). The product (**3.192**) was isolated as a colourless oil (78.4 mg, 66%).

R_F (petroleum ether:EtOAc:EtNMe₂, 40:60:1 v/v/v) 0.60; IR (ATR) 2991, 2855, 1738 (C=O), 1446, 1402, 1353, 1174, 1078, 989, 915, 731, 646 cm⁻¹; ¹H NMR (400 MHz, Chloroform-*d*) δ 2.77 – 2.61 (m, 4H, H²), 2.56 – 1.89 (m, 7H, H⁹⁻¹⁰ and H¹²⁻¹³), 1.73 – 1.64 (m, 4H, H¹), 1.64 – 1.06 (m, 10H, H⁴⁻⁸); ¹³C NMR (101 MHz, Chloroform-*d*) δ 220.0 (C¹¹), 56.0 (C³), 44.3 (C²), 42.5 (C⁹), 41.5, 38.5 (C¹⁰ and C¹²), 24.5 (C¹), 32.1, 31.2, 26.4, 25.6, 21.6, 21.6 (C⁴⁻⁸ and C¹³); HRMS (ESI⁺) m/z calcd for C₁₅H₂₆NO [M + H]⁺: 236.2009, found:

236.2005 (1.7 ppm error), calcd for $C_{15}H_{25}NNaO$ $[M + Na]^+$: 258.1828, found: 258.1826 (0.7 ppm error).

Lab book reference JCC-E-7-425

***N,N*-Dimethyl-3-(1-(pyrrolidin-1-yl)cyclohexyl)propenamide (3.193)**

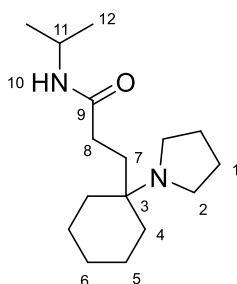


3.193

Synthesised using General Procedure 3D, using iminium hexafluorophosphate **3.154** (148 mg, 0.50 mmol, 1.0 eq.), *N,N*-dimethylacrylamide (155 μ L, 1.5 mmol, 3.0 eq.), tetrahydrothiophene (88 μ L, 1.0 mmol, 2.0 eq.) and acetonitrile (18 mL). Electrolysed for 3.5 F mol⁻¹ of charge. Purification by flash column chromatography using General Procedure 3G (initially using petroleum ether:EtOAc, 50:50 v/v followed by petroleum ether:EtOAc:EtNMe₂, 90:10:2 v/v/v). The product (**3.193**) was isolated as a colourless oil (40.4 mg, 32%).

R_F (petroleum ether:EtOAc:EtNMe₂, 60:40:2 v/v/v) 0.22; IR (ATR) 3407, 2934, 2863, 2239, 2198, 1719, 1634, 1496, 1447, 1401, 1361, 1263, 1136, 921, 909, 728, 645 cm⁻¹; ¹H NMR (400 MHz, Chloroform-*d*) δ 3.01 (s, 3H, H^{10/11}), 2.93 (s, 3H, H^{10/11}), 2.68 – 2.58 (m, 4H, H²), 2.33 – 2.26 (m, 2H, H⁸), 1.86 – 1.77 (m, 2H, H⁷), 1.71 – 1.63 (m, 4H, H¹), 1.60 – 1.36 (m, 10H, H⁴⁻⁶); ¹³C NMR (101 MHz, Chloroform-*d*) δ 174.1 (C⁹), 55.7 (C³), 44.0 (C²), 37.3, 35.4 (C¹⁰ and C¹¹), 24.1 (C¹), 27.9, 27.5 (C⁷⁻⁸), 31.4, 26.2, 22.0 (C⁴⁻⁶); HRMS (ESI⁺) m/z calcd for $C_{15}H_{29}N_2O$ $[M + H]^+$: 253.2274, found: 253.2275 (-0.2 ppm error).

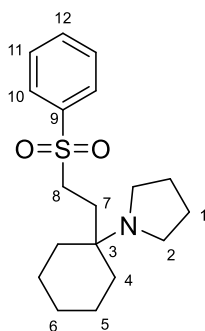
Lab book reference JCC-E-7-400

***N*-Isopropyl-3-(1-(pyrrolidin-1-yl)cyclohexyl)propenamide (3.194)****3.194**

Synthesised using General Procedure 3D, using iminium hexafluorophosphate **3.154** (148 mg, 0.50 mmol, 1.0 eq.), *N*-isopropylacrylamide (170 mg, 1.5 mmol, 3.0 eq.), tetrahydrothiophene (88 μ L, 1.0 mmol, 2.0 eq.) and acetonitrile (18 mL). Electrolysed for 3.5 F mol⁻¹ of charge. Purification by flash column chromatography using General Procedure 3G (initially using petroleum ether:EtOAc, 50:50 *v/v* followed by petroleum ether:EtOAc:EtNMe₂, 80:20:2 *v/v/v*). The product (**3.194**) was isolated as a colourless oil (28.3 mg, 21%).

R_F (petroleum ether:EtOAc:EtNMe₂, 80:20:2 *v/v/v*) 0.07; IR (ATR) 3266, 3063, 2961, 2934, 2867, 2236, 1639, 1546, 1456, 1385, 1366, 1261, 1173, 1130, 1084, 983, 922, 851, 729, 644 cm⁻¹; ¹H NMR (400 MHz, Chloroform-*d*) δ 5.98 (s, 1H, H¹⁰), 4.09 – 4.00 (m, 1H, H¹¹), 2.78 – 2.67 (m, 4H, H²), 2.26 – 2.18 (m, 2H, H⁸), 1.88 – 1.83 (m, 2H, H⁷), 1.77 – 1.72 (m, 4H, H¹), 1.65 – 1.21 (m, 10H, H⁴⁻⁶), 1.13 (d, $J = 6.5$ Hz, 6H, H¹²); ¹³C NMR (101 MHz, Chloroform-*d*) δ 172.7 (C⁹), 44.4 (C³), 41.2, 41.1 (C² and C¹¹), 24.2 (C¹), 31.1, 28.1, 26.0, 22.8, 22.7, 22.1 (C⁴⁻⁸ and C¹²); HRMS (ESI⁺) m/z calcd for C₁₆H₃₁N₂O [M + H]⁺: 267.2431, found: 267.2430 (0.5 ppm error).

Lab book reference JCC-E-7-404

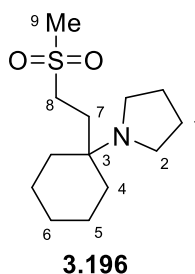
1-(1-(2-(Phenylsulfonyl)ethyl)cyclohexyl)pyrrolidine (3.195)**3.195**

Synthesised using General Procedure 3D, using iminium hexafluorophosphate **3.154** (148 mg, 0.50 mmol, 1.0 eq.), phenyl vinyl sulfone (252 mg, 1.5 mmol, 3.0 eq.), tetrahydrothiophene (176 μL , 2.0 mmol, 4.0 eq.) and acetonitrile (18 mL). Electrolysed for 3.5 F mol⁻¹ of charge. Purification by flash column chromatography using General Procedure 3G (initially using petroleum ether:EtOAc, 70:30 v/v followed by petroleum ether:EtOAc:EtNMe₂, 85:15:2 v/v/v). The product (**3.195**) was isolated as a colourless oil (52.7 mg, 33%).

R_F (petroleum ether:EtOAc:EtNMe₂, 80:20:2 v/v/v) 0.25; IR (ATR) 3055, 2931, 2858, 1727, 1650, 1447, 1407, 1302, 1146, 1087, 1024, 998, 906, 736, 689, 588, 566, 538 cm⁻¹; ¹H NMR (400 MHz, Chloroform-*d*) δ 7.94 – 7.89 (m, 2H, H¹⁰), 7.68 – 7.61 (m, 1H, H¹²), 7.60 – 7.54 (m, 2H, H¹¹), 3.16 – 3.07 (m, 2H, H⁸), 2.54 – 2.41 (m, 4H, H²), 1.94 – 1.87 (m, 2H, H⁷), 1.70 – 1.60 (m, 4H, H¹), 1.60 – 1.10 (m, 10H, H⁴⁻⁶); ¹³C NMR (101 MHz, Chloroform-*d*) δ 139.5 (C⁹), 133.5 (C¹²), 129.2 (C¹¹), 128.0 (C¹⁰), 55.7 (C³), 51.8 (C⁸), 43.8 (C²), 24.0 (C¹), 30.9, 26.0, 25.1, 22.0 (C⁴⁻⁶ and C⁷); HRMS (ESI⁺) m/z calcd for C₁₈H₂₈NO₂S [M + H]⁺: 322.1835, found: 322.1835 (0.0 ppm error)

Lab book reference JCC-E-6-370

1-(1-(2-(Methylsulfonyl)ethyl)cyclohexyl)pyrrolidine (**3.196**)



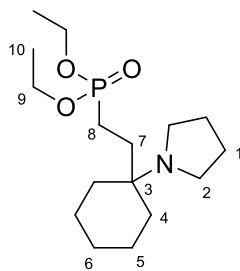
Synthesised using General Procedure 3D, using iminium hexafluorophosphate **3.154** (148 mg, 0.50 mmol, 1.0 eq.), methyl vinyl sulfone (128 μL , 1.5 mmol, 3.0 eq.), tetrahydrothiophene (176 μL , 2.0 mmol, 4.0 eq.) and acetonitrile (18 mL). Electrolysed for 3.5 F mol⁻¹ of charge. Purification by flash column chromatography using General Procedure 3G (initially using petroleum ether:EtOAc, 50:50 v/v followed by petroleum ether:EtOAc:EtNMe₂, 80:20:2 v/v/v). The product (**3.196**) was isolated as a colourless oil (43.5 mg, 34%).

R_F (petroleum ether:EtOAc:EtNMe₂, 80:20:2 v/v/v) 0.16; IR (ATR) 2983, 2932, 2869, 1638, 1449, 1293, 1128, 957, 774, 733 cm⁻¹; ¹H NMR (400 MHz, Chloroform-*d*) δ 3.08 – 3.02 (m,

2H, H⁸), 2.91 (s, 3H, H⁹), 2.66 – 2.58 (m, 4H, H²), 2.05 – 1.98 (m, 2H, H⁷), 1.73 – 1.67 (m, 4H, H¹), 1.66 – 1.36 (m, 10H, H⁴⁻⁶); ¹³C NMR (101 MHz, Chloroform-*d*) δ 56.0 (C³), 50.1 (C⁸), 44.5 (C²), 41.0 (C⁹), 24.2 (C¹), 30.8, 25.9, 22.1, 21.7 (C⁴⁻⁷); HRMS (ESI⁺) *m/z* calcd for C₁₃H₂₆NO₂S [M + H]⁺: 260.1679, found: 260.1679 (-0.1 ppm error)

Lab book reference JCC-E-6-377

Diethyl (2-(1-(pyrrolidin-1-yl)cyclohexyl)ethyl)phosphonate (**3.197**)

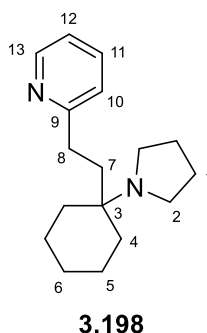


3.197

Synthesised using General Procedure 3D, using iminium hexafluorophosphate **3.154** (148 mg, 0.50 mmol, 1.0 eq.), diethyl vinylphosphonate (231 μL, 1.5 mmol, 3.0 eq.), tetrahydrothiophene (88 μL, 1.0 mmol, 2.0 eq.) and acetonitrile (18 mL). Electrolysed for 3.5 F mol⁻¹ of charge. Purification by flash column chromatography using General Procedure 3G (initially using petroleum ether:EtOAc, 20:80 *v/v* followed by petroleum ether:EtOAc:EtNMe₂, 20:80:2 *v/v/v*). The product (**3.197**) was isolated as a colourless oil (34 mg, 27%).

R_F (petroleum ether:EtOAc:EtNMe₂, 20:80:2 *v/v/v*) 0.25; IR (ATR) 2988, 2932, 2862, 1651, 1446, 1392, 1357, 1219, 1019, 963, 826, 788, 531, 494 cm⁻¹; ¹H NMR (400 MHz, Chloroform-*d*) δ 4.16 – 4.00 (m, 4H, H⁹), 2.86 – 2.44 (m, 4H, H²), 1.86 – 1.33 (m, 18H, H¹ and H⁴⁻⁸), 1.31 (t, *J* = 7.0 Hz, 6H, H¹⁰); ¹³C NMR (101 MHz, Chloroform-*d*) δ 61.4 (d, *J* = 6.5 Hz, C⁹), 55.6 (d, *J* = 16.0 Hz, C³), 43.8 (C²), 24.9 (d, *J* = 4.7 Hz, C⁷), 24.1 (C¹), 31.0, 26.2, 22.0 (C⁴⁻⁶), 19.7 (d, *J* = 140.0 Hz, C⁸), 16.5 (d, *J* = 6.0 Hz, C¹⁰); HRMS (ESI⁺) *m/z* calcd for C₁₆H₃₃NO₃P [M + H]⁺: 318.2193, found: 318.2191 (0.6 ppm error).

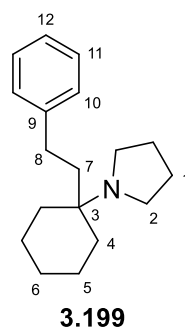
Lab book reference JCC-E-7-411

2-(2-(1-(Pyrrolidin-1-yl)cyclohexyl)ethyl)pyridine (3.198)

Synthesised using General Procedure 3D, using iminium hexafluorophosphate **3.154** (148 mg, 0.50 mmol, 1.0 eq.), 2-vinylpyridine (162 μL , 1.5 mmol, 3.0 eq.), tetrahydrothiophene (176 μL , 2.0 mmol, 4.0 eq.) and acetonitrile (18 mL). Electrolysed for 3.5 F mol⁻¹ of charge. Purification by flash column chromatography using General Procedure 3G (initially using EtOAc, followed by petroleum ether:EtOAc:Et₃N, 60:40:2 v/v/v). The product (**3.198**) was isolated as a colourless oil (33.0 mg, 26%).

R_F (petroleum ether:EtOAc:Et₃N, 60:40:2 v/v/v) 0.46; IR (ATR) 3384, 3052, 2931, 2861, 1631, 1592, 1569, 1474, 1435, 775, 732 cm⁻¹; ¹H NMR (400 MHz, Chloroform-*d*) δ 8.51 (dd, $J = 5.0, 2.0$ Hz, 1H, H¹³), 7.56 (apparent td, $J = 7.5, 2.0$ Hz, 1H, H¹¹), 7.13 (dd, $J = 12.5, 8.0$ Hz, 1H, H¹²), 7.07 (dd, $J = 7.5, 5.0$ Hz, 1H, H¹⁰), 2.85 – 2.62 (m, 6H, H² and H⁸), 1.89 – 1.82 (m, 2H, H⁷), 1.77 – 1.66 (m, 4H, H¹), 1.66 – 1.30 (m, 10H, H⁴⁻⁶); ¹³C NMR (101 MHz, Chloroform-*d*) δ 163.6 (C⁹), 149.2 (C¹³), 136.2 (C¹¹), 122.7 (C¹⁰), 120.7 (C¹²), 55.8 (C³), 43.9 (C²), 24.2 (C¹), 33.2, 33.0, 32.1, 26.3, 22.0 (C⁴⁻⁸).

Lab book reference JCC-E-6-360

1-(1-Phenethylcyclohexyl)pyrrolidine (3.199)

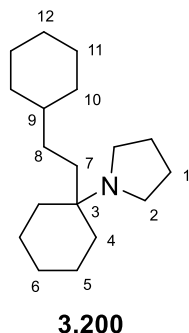
Synthesised using General Procedure 3D, using iminium hexafluorophosphate **3.154** (148 mg, 0.50 mmol, 1.0 eq.), styrene (172 μL , 1.5 mmol, 3.0 eq.), tetrahydrothiophene (176 μL ,

2.0 mmol, 4.0 eq.) and acetonitrile (18 mL). Electrolysed for 3.5 F mol⁻¹ of charge. Purification by flash column chromatography using General Procedure 3G (initially using petroleum ether:EtOAc 50:50 v/v, followed by petroleum ether:EtOAc:Et₃N, 70:30:2 v/v/v). The product (**3.199**) was isolated as a colourless oil (13.2 mg, 10%).

R_F (petroleum ether:EtOAc:Et₃N, 70:30:2 v/v/v) 0.22; IR (ATR) 3025, 2929, 2854, 1648, 1495, 1451, 1361, 1260, 1178, 1030, 909, 842, 732, 700 cm⁻¹; ¹H NMR (400 MHz, Chloroform-*d*) δ 7.34 – 7.26 (m, 2H, H^{10/11/12}), 7.22 – 7.14 (m, 3H, H^{10/11/12}), 2.75 – 2.65 (m, 4H, H²), 2.61 – 2.52 (m, 2H, H⁸), 1.79 – 1.68 (m, 6H, H¹ and H⁷), 1.66 – 1.36 (m, 10H, H⁴⁻⁶); ¹³C NMR (101 MHz, Chloroform-*d*) δ 128.3, 128.3, 125.6 (C¹⁰⁻¹²), 120.1 (C⁹), 44.2 (C²), 24.3 (C¹), 35.2, 31.9, 30.2, 26.2, 22.1 (C⁴⁻⁸), C³ quaternary carbon not visible due to insufficient amount of sample; HRMS (ESI⁺) *m/z* calcd for C₁₈H₂₈N [M + H]⁺: 258.2216, found: 258.2219 (-1.2 ppm error).

Lab book reference JCC-E-6-361

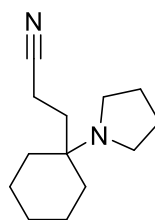
1-(1-(2-Cyclohexylethyl)cyclohexyl)pyrrolidine (**3.200**)



Synthesised using General Procedure 3D, using iminium hexafluorophosphate **3.154** (148 mg, 0.50 mmol, 1.0 eq.), vinylcyclohexane (680 μL, 5.0 mmol, 10.0 eq.), tetrahydrothiophene (176 μL, 2.0 mmol, 4.0 eq.) and acetonitrile (18 mL). Electrolysed for 3.5 F mol⁻¹ of charge. The product (**3.200**) was not observed by ¹H NMR spectroscopy or mass spectrometry.

Lab book reference JCC-E-5-327

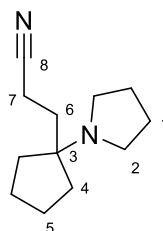
Synthesis and Characterisation of Tertiary Amines – Using Unpurified Iminium Ions

3-(1-(Pyrrolidin-1-yl)cyclohexyl)propanenitrile (3.116)**3.116**

Synthesised using General Procedure 3E, using iminium hexafluorophosphate **3.154** (0.44 mmol as 4 mL of stock solution of crude iminium hexafluorophosphate in acetonitrile), acrylonitrile (98 μL , 1.5 mmol), tetrahydrothiophene (176 μL , 2.0 mmol) and acetonitrile (14 mL). Electrolysed for 3.5 F mol⁻¹ of charge. Purification by flash column chromatography (hexane:EtOAc:Et₃N, 70:30:2 v/v/v). The product (**3.116**) was isolated as a colourless oil (54.4 mg, 59% for the electrolysis step).

R_F (hexane:EtOAc:Et₃N, 70:30:2 v/v/v) 0.21. Data consistent with previously reported for **3.116**

Lab book reference JCC-6-352

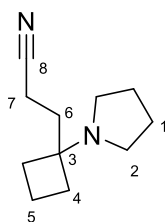
3-(1-(Pyrrolidin-1-yl)cyclopentyl)propanenitrile (3.179)**3.179**

Synthesised using General Procedure 3E, using iminium hexafluorophosphate **3.155** (0.50 mmol as 4 mL of stock solution of crude iminium hexafluorophosphate in acetonitrile), acrylonitrile (98 μL , 1.5 mmol), tetrahydrothiophene (88 μL , 1.0 mmol) and acetonitrile (14 mL). Electrolysed for 3.5 F mol⁻¹ of charge. Purification by flash column chromatography using General Procedure 3G (initially using EtOAc, followed by petroleum ether:EtOAc:EtNMe₂, 85:15:2 v/v/v). The product (**3.179**) was isolated as a colourless oil (43.6 mg, 44% for the electrolysis step).

R_F (petroleum ether:EtOAc:EtNMe₂, 85:15:2 v/v/v) 0.25; IR (ATR) 2989, 2950, 2873, 2244 (C≡N), 1652, 1447, 1333, 1220, 1140, 1035, 914, 731, 598 cm⁻¹; ¹H NMR (400 MHz, Chloroform-*d*) δ 2.57 – 2.48 (m, 4H, H²), 2.48 – 2.39 (m, 2H, H⁷), 1.92 – 1.83 (m, 2H, H⁶), 1.74 – 1.68 (m, 4H, H¹), 1.67 – 1.52 (m, 4H, H⁴), 1.37 – 1.27 (m, 4H, H⁵); ¹³C NMR (101 MHz, Chloroform-*d*) δ 121.2 (C⁸), 66.4 (C³), 46.3 (C²), 23.7 (C¹) 36.2, 32.4, 25.3, (C⁴⁻⁶), 12.0 (C⁷); HRMS (ESI⁺) m/z calcd for C₁₂H₂₁N₂ [M + H]⁺: 193.1699, found: 193.1703 (-1.8 ppm error).

Lab book reference JCC-E-7-420

3-(1-(Pyrrolidin-1-yl)cyclobutyl)propanenitrile (**3.180**)

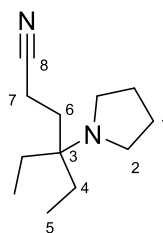


3.180

Synthesised using General Procedure 3E, using iminium hexafluorophosphate **3.156** (0.25 mmol as 4 mL of stock solution of crude iminium hexafluorophosphate in acetonitrile), acrylonitrile (98 μL, 1.5 mmol), tetrahydrothiophene (88 μL, 1.0 mmol) and acetonitrile (14 mL). Electrolysed for 3.5 F mol⁻¹ of charge. Purification by flash column chromatography (petroleum ether:EtOAc:EtNMe₂, 80:20:1 v/v/v). The product (**3.180**) was isolated as a colourless oil (17.3 mg, 39% for the electrolysis step).

R_F (petroleum ether:EtOAc:EtNMe₂, 80:20:1 v/v/v) 0.17; IR (ATR) 2937, 2242 (C≡N), 1661, 1452, 1272 cm⁻¹; ¹H NMR (400 MHz, Chloroform-*d*) δ 2.59 – 2.50 (m, 4H, H²), 2.41 – 2.32 (m, 2H, H⁷), 2.31 – 2.20 (m, 2H, H⁵), 2.04 – 1.95 (m, 2H, H⁶), 1.79 – 1.49 (m, 8H, H¹ and H⁴); ¹³C NMR (101 MHz, Chloroform-*d*) δ 121.2 (C⁸), 61.1 (C³), 46.1 (C²), 34.3 (C⁶), 26.7 (C⁵), 23.9 (C¹), 13.1 (C⁴), 11.4 (C⁷); HRMS (ESI⁺) m/z calcd for C₁₁H₁₉N₂ [M + H]⁺: 179.1543, found: 179.1538 (2.8 ppm error).

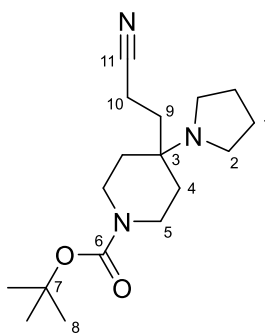
Lab book reference JCC-E-7-426

4-Ethyl-4-(pyrrolidin-1-yl)hexanenitrile (3.181)**3.181**

Synthesised using General Procedure 3E, using iminium hexafluorophosphate **3.158** (0.40 mmol as 4 mL of stock solution of crude iminium hexafluorophosphate in acetonitrile), acrylonitrile (98 μL , 1.5 mmol), tetrahydrothiophene (88 μL , 1.0 mmol) and acetonitrile (14 mL). Electrolysed for 3.5 F mol⁻¹ of charge. Purification by flash column chromatography using General Procedure 3G (initially using EtOAc, followed by petroleum ether:EtOAc:EtNMe₂, 85:15:2 v/v/v). The product (**3.181**) was isolated as a colourless oil (32.4 mg, 42% for the electrolysis step).

R_F (petroleum ether:EtOAc:EtNMe₂, 85:15:2 v/v/v) 0.43; IR (ATR) 2970, 2946, 2885, 2248 (C \equiv N), 1685, 1646, 1460, 1382, 1238, 1154, 917, 732, 644 cm⁻¹; ¹H NMR (400 MHz, Chloroform-*d*) δ 2.78 – 2.67 (m, 4H, H²), 2.37 – 2.29 (m, 2H, H⁷), 1.80 – 1.72 (m, 2H, H⁶), 1.72 – 1.66 (m, 4H, H¹), 1.66 – 1.54 (m, 4H, H⁴), 0.85 (t, $J = 7.5$ Hz, 6H, H⁵); ¹³C NMR (101 MHz, Chloroform-*d*) δ 121.3 (C⁸), 57.7 (C³), 45.2 (C²), 31.4, 26.3, (C⁴ and C⁶), 24.1 (C¹), 11.6 (C⁷), 9.0 (C⁵); HRMS (ESI⁺) m/z calcd for C₁₂H₂₃N₂ [M + H]⁺: 195.1856, found: 195.1852 (1.8 ppm error).

Lab book reference JCC-E-7-424

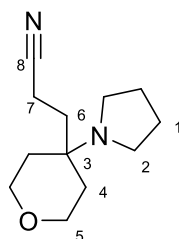
***tert*-Butyl-4-(2-cyanoethyl)-4-(pyrrolidin-1-yl)piperidine-1-carboxylate (3.182)****3.182**

Synthesised using General Procedure 3E, using iminium hexafluorophosphate **3.159** (0.42 mmol as 4 mL of stock solution of crude iminium hexafluorophosphate in acetonitrile), acrylonitrile (98 μL , 1.5 mmol.), tetrahydrothiophene (88 μL , 1.0 mmol) and acetonitrile (14 mL). Electrolysed for 3.5 F mol⁻¹ of charge. Purification by flash column chromatography (petroleum ether:EtOAc:EtNMe₂, 90:20:1 v/v/v). The product (**3.182**) was isolated as a colourless oil (67.0 mg, 53% for the electrolysis step).

R_F (petroleum ether:EtOAc:EtNMe₂, 60:40:1 v/v/v) 0.39; IR (ATR) 2974, 2933, 2872, 2248 (C \equiv N), 1682 (C=O), 1425, 1366, 1248, 1159, 914, 732, 646 cm⁻¹; ¹H NMR (400 MHz, Chloroform-*d*) δ 3.50 (ddd, $J = 13.0, 7.5, 4.0$ Hz, 2H, H^{5a}), 3.32 (ddd, $J = 13.0, 7.5, 4.0$ Hz, 2H, H^{5b}), 2.59 – 2.54 (m, 4H, H²), 2.36 – 2.28 (m, 2H, H¹⁰), 1.91 – 1.85 (m, 2H, H⁹), 1.73 – 1.68 (m, 4H, H¹), 1.64 (ddd, $J = 12.0, 7.0, 3.5$ Hz, 2H, H^{4a}), 1.44 – 1.35 (m, 11H, H^{4b} and H⁸); ¹³C NMR (101 MHz, Chloroform-*d*) δ 154.9 (C⁶), 120.5 (C¹¹), 79.4 (C⁷), 54.1 (C³), 51.2 (C⁵), 44.0 (C²), 28.4 (C⁸), 28.2 (C⁹), 24.1 (C¹), 23.2 (C⁴), 11.6 (C¹⁰); HRMS (ESI⁺) m/z calcd for C₁₇H₃₀N₃O₂ [M + H]⁺: 308.2333, found: 308.2334 (-0.4 ppm error).

Lab book reference JCC-E-7-399

3-(4-(Pyrrolidin-1-yl)tetrahydro-2H-pyran-4-yl)propanenitrile (**3.183**)



3.183

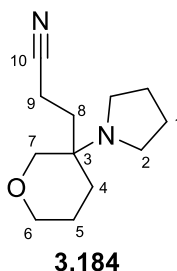
Synthesised using General Procedure 3E, using iminium hexafluorophosphate **3.161** (0.30 mmol as 4 mL of stock solution of crude iminium hexafluorophosphate in acetonitrile), acrylonitrile (98 μL , 1.5 mmol), tetrahydrothiophene (88 μL , 1.0 mmol) and acetonitrile (14 mL). Electrolysed for 3.5 F mol⁻¹ of charge. Purification by flash column chromatography (petroleum ether:EtOAc:EtNMe₂, 85:15:1 v/v/v). The product (**3.183**) was isolated as a colourless oil (32.7 mg, 52% for the electrolysis step).

R_F (petroleum ether:EtOAc:EtNMe₂, 60:40:1 v/v/v) 0.29; IR (ATR) 2948, 2862, 2245 (C \equiv N), 1651, 1450, 1359, 1302, 1237, 1148, 1102, 1014, 843, 740, 548 cm⁻¹; ¹H NMR (400 MHz, Chloroform-*d*) δ 3.82 (ddd, $J = 11.5, 6.0, 4.0$ Hz, 2H, H^{5a}), 3.56 (ddd, $J = 11.5, 8.5, 3.0$ Hz, 2H, H^{5b}), 2.63 – 2.55 (m, 4H, H²), 2.39 – 2.29 (m, 2H, H⁷), 1.99 – 1.91 (m, 2H, H⁶),

1.80 – 1.68 (m, 6H, H¹ and H^{4a}), 1.42 (dddd, $J = 13.5, 6.0, 3.0, 1.0$ Hz, 2H, H^{4b}); ¹³C NMR (101 MHz, Chloroform-*d*) δ 120.7 (C⁸), 63.8 (C⁵), 53.7 (C³), 44.1 (C²), 31.4 (C⁴), 28.7 (C⁶), 24.1 (C¹), 11.4 (C⁷); HRMS (ESI⁺) m/z calcd for C₁₂H₂₁N₂O [M + H]⁺: 209.1648, found: 209.1650 (-0.9 ppm error)

Lab book reference JCC-E-7-407

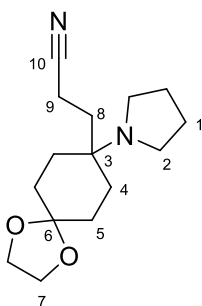
3-(3-(Pyrrolidin-1-yl)tetrahydro-2H-pyran-3-yl)propanenitrile (**3.184**)



Synthesised using General Procedure 3E, using iminium hexafluorophosphate **3.162** (0.24 mmol as 4 mL of stock solution of crude iminium hexafluorophosphate in acetonitrile), acrylonitrile (98 μ L, 1.5 mmol), tetrahydrothiophene (88 μ L, 1.0 mmol) and acetonitrile (14 mL). Electrolysed for 3.5 F mol⁻¹ of charge. Purification by flash column chromatography (petroleum ether:EtOAc:EtNMe₂, 85:15:1 v/v/v). The product (**3.184**) was isolated as a colourless oil (23.1 mg, 49% for electrolysis).

R_F (petroleum ether:EtOAc:EtNMe₂, 60:40:1 v/v/v) 0.29; IR (ATR) 2951, 2860, 2247 (C \equiv N), 1649, 1449, 1271, 1198, 1148, 1092, 1041, 922, 866, 731 cm⁻¹; ¹H NMR (400 MHz, Chloroform-*d*) δ 3.91 – 3.84 (m, 1H, H^{6a}), 3.54 (dd, $J = 11.5, 2.5$ Hz, 1H, H^{7a}), 3.40 (dd, $J = 11.5, 1.0$ Hz, 1H, H^{7b}), 3.41 – 3.25 (m, 1H, H^{6b}), 2.68 – 2.55 (m, 4H, H²), 2.50 – 2.27 (m, 2H, H⁹), 2.21 (ddd, $J = 14.0, 10.5, 5.5$ Hz, 1H, H^{8a}), 1.89 (dddd, $J = 14.0, 10.5, 5.5, 1.0$ Hz, 1H, H^{8b}), 1.80 – 1.64 (m, 6H, H¹ and H^{4/5}), 1.63 – 1.54 (m, 2H, H^{4/5}); ¹³C NMR (101 MHz, Chloroform-*d*) δ 121.0 (C¹⁰), 71.1 (C⁷), 68.7 (C⁶), 54.2 (C³), 44.3 (C²), 28.6 (C⁸), 23.7 (C¹), 26.8, 22.8 (C⁴⁻⁵), 11.0 (C⁹); HRMS (ESI⁺) m/z calcd for C₁₂H₂₁N₂O [M + H]⁺: 209.1648, found: 209.1649 (-0.2 ppm error).

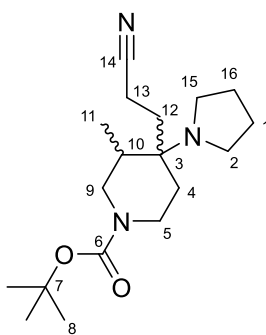
Lab book reference JCC-E-7-417

3-(8-(Pyrrolidin-1-yl)-1,4-dioxaspiro[4.5]decan-8-yl)propanenitrile (3.185)**3.185**

Synthesised using General Procedure 3E, using iminium hexafluorophosphate **3.163** (0.42 mmol as 4 mL of stock solution of crude iminium hexafluorophosphate in acetonitrile), acrylonitrile (98 μL , 1.5 mmol), tetrahydrothiophene (88 μL , 1.0 mmol) and acetonitrile (14 mL). Electrolysed for 3.5 F mol⁻¹ of charge. Purification by flash column chromatography (petroleum ether:EtOAc:EtNMe₂, 80:20:1 v/v/v). The product (**3.185**) was isolated as a colourless oil (52.2 mg, 48% for the electrolysis step).

R_F (petroleum ether:EtOAc:EtNMe₂, 50:50:1 v/v/v) 0.46; IR (ATR) 3054, 2955, 2882, 2246 (C \equiv N), 1682, 1447, 1374, 1267, 1110, 1035, 945, 914, 738, 702 cm⁻¹; ¹H NMR (400 MHz, Chloroform-*d*) δ 3.92 (t, $J = 2.0$ Hz, 4H, H⁷), 2.66 – 2.54 (m, 4H, H²), 2.35 – 2.26 (m, 2H, H⁹), 1.93 – 1.64 (m, 10H, H¹, H⁸ and H^{4/5}), 1.57 – 1.43 (m, 4H, H^{4/5}); ¹³C NMR (101 MHz, Chloroform-*d*) δ 120.7 (C¹⁰), 108.5 (C⁶), 64.2 (C⁷), 54.9 (C³), 44.2 (C²), 33.8, 30.5 (C⁴ and C⁵), 27.9 (C⁸), 24.2 (C¹), 12.0 (C⁹); HRMS (ESI⁺) m/z calcd for C₁₅H₂₅N₂O₂ [M + H]⁺: 265.1911, found: 265.1913 (-0.9 ppm error)

Lab book reference JCC-E-7-410

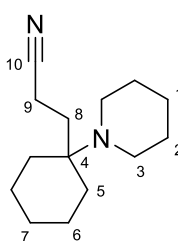
tert-Butyl 4-(2-cyanoethyl)-3-methyl-4-(pyrrolidin-1-yl)piperidine-1-carboxylate (3.186)**3.186**

Synthesised using General Procedure 3E, using iminium hexafluorophosphate **3.160** (0.42 mmol as 4 mL of stock solution of crude iminium hexafluorophosphate in acetonitrile), acrylonitrile (98 μL , 1.5 mmol), tetrahydrothiophene (88 μL , 1.0 mmol) and acetonitrile (14 mL). Electrolysed for 3.5 F mol⁻¹ of charge. Purification by flash column chromatography (petroleum ether:EtOAc:EtNMe₂, 80:20:1 v/v/v). The product (**3.186**) was isolated as a colourless oil (47.4 mg, 35% for the electrolysis step).

R_F (petroleum ether:EtOAc:EtNMe₂, 60:40:1 v/v/v) 0.41; IR (ATR) 2972, 2936, 2878, 2246 (C≡N), 1683 (C=O), 1427, 1365, 1247, 1146, 1093, 982, 919, 874, 732, 646 cm⁻¹; ¹H NMR (400 MHz, Chloroform-*d*) δ 4.04 – 3.71 (m, 1H, H^{5/9}), 3.61 (ddd, $J = 13.5, 4.0, 1.5$ Hz, 1H, H^{5/9}), 3.09 (dd, $J = 14.0, 3.0$ Hz, 1H, H^{5/9}), 2.97 – 2.83 (m, 1H, H^{5/9}), 2.78 – 2.70 (m, 4H, H² and H¹⁵), 2.41 – 2.29 (m, 1H, H^{4/10}), 2.27 – 2.12 (m, 2H, H¹³), 1.97 – 1.73 (m, 3H, H¹² and H^{4/10}), 1.72 – 1.63 (m, 4H, H¹ and H¹⁶), 1.45 – 1.38 (m, 10H, H⁸ and H^{4/10}), 0.94 (d, $J = 7.0$ Hz, 3H, H¹¹); ¹³C NMR (101 MHz, Chloroform-*d*) (mixture of diastereoisomers and or rotamers) δ 155.2 (C⁶), 120.7 (C¹⁴), 79.4 (C⁷), 56.2 (C³), 47.2, 46.3, 45.9, 44.9 (C², C⁵, C⁹ and C¹⁵), 29.6 (C¹²), 29.1 (C¹²), 28.3 (C⁸), 28.3, 28.2, 20.8 (C⁴ and C¹⁰) 24.4, 23.8 (C¹ and C¹⁶), 14.6 (C¹¹), 14.2 (C¹¹), 11.7 (C¹³); HRMS (ESI⁺) m/z calcd for C₁₈H₃₂N₃O₂ [M + H]⁺: 322.2489, found: 322.2488 (0.4 ppm error), m/z calcd for C₁₈H₃₁N₃NaO₂ [M + Na]⁺: 344.2308, found: 344.2309 (-0.2 ppm error)

Lab book reference JCC-E-7-414

3-(1-(Piperidin-1-yl)cyclohexyl)propanenitrile (**3.187**)



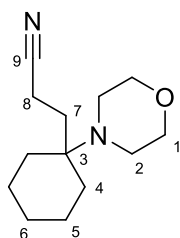
3.187

Synthesised using General Procedure 3E, using iminium hexafluorophosphate **3.166** (0.43 mmol as 4 mL of stock solution of crude iminium hexafluorophosphate in acetonitrile), acrylonitrile (98 μL , 1.5 mmol), tetrahydrothiophene (88 μL , 1.0 mmol) and acetonitrile (14 mL). Electrolysed for 3.5 F mol⁻¹ of charge. Purification by flash column chromatography (petroleum ether:EtOAc:EtNMe₂, 90:10:1 v/v/v). The product (**3.187**) was isolated as a colourless oil (55 mg, 58% for the electrolysis step).

R_F (petroleum ether:EtOAc:EtNMe₂, 90:10:1 v/v/v) 0.29; IR (ATR) 2928, 2852, 2792, 2246 (C≡N), 1650, 1453, 1442, 1277, 1257, 1111, 963, 732, 648 cm⁻¹; ¹H NMR (400 MHz, Chloroform-*d*) δ 2.54 – 2.39 (m, 4H, H³), 2.34 – 2.26 (m, 2H, H⁹), 1.85 – 1.77 (m, 2H, H⁸), 1.68 – 1.56 (m, 4H, H²), 1.55 – 1.13 (m, 12H, H¹ and H⁵⁻⁷); ¹³C NMR (101 MHz, Chloroform-*d*) δ 121.1 (C¹⁰), 57.1 (C⁴), 45.6 (C³), 31.2 (C⁵), 28.8, 27.2, 26.0, 25.1, 21.7 (C¹⁻² and C⁶⁻⁸), 11.7 (C⁹); HRMS (ESI⁺) m/z calcd for C₁₄H₂₅N₂ [M + H]⁺: 221.2012, found: 221.2010 (0.9 ppm error).

Lab book reference JCC-E-7-405

3-(1-Morpholinocyclohexyl)propanenitrile (**3.188**)



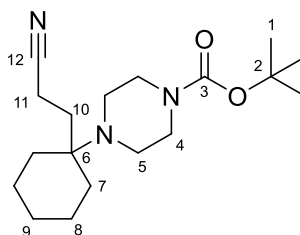
3.188

Synthesised using General Procedure 3E, using iminium hexafluorophosphate **3.167** (0.35 mmol as 4 mL of stock solution of crude iminium hexafluorophosphate in acetonitrile), acrylonitrile (98 μL, 1.5 mmol), tetrahydrothiophene (176 μL, 2.0 mmol) and acetonitrile (14 mL). Electrolysed for 3.5 F mol⁻¹ of charge. Purification by flash column chromatography (petroleum ether:EtOAc:Et₃N, 70:30:1 v/v/v). The product (**3.188**) was isolated as a colourless oil (46.1 mg, 59% for the electrolysis step).

R_F (petroleum ether:EtOAc:Et₃N, 70:30:1 v/v/v) 0.36; IR (ATR) 2929, 2851, 2813, 2244 (C≡N), 1708, 1454, 1293, 1265, 1118, 976, 869, 854 cm⁻¹; ¹H NMR (400 MHz, Chloroform-*d*) δ 3.69 – 3.62 (m, 4H, H¹), 2.55 – 2.50 (m, 4H, H²), 2.35 – 2.28 (m, 2H, H⁸), 1.88 – 1.81 (m, 2H, H⁷), 1.77 – 1.17 (m, 10H, H⁴⁻⁶); ¹³C NMR (101 MHz, Chloroform-*d*) δ 120.8 (C⁹), 67.9 (C¹), 56.7 (C³), 44.9 (C²), 30.6 (C⁴), 28.1 (C⁷), 25.9, 21.6 (C⁵⁻⁶), 11.4 (C⁸); HRMS (ESI⁺) m/z calcd for C₁₃H₂₃N₂O [M + H]⁺: 223.1805, found: 223.1806 (-0.7 ppm error), m/z calcd for C₁₃H₂₂N₂NaO [M + Na]⁺: 245.1624, found: 245.1627 (-1.2 ppm error).

Lab book reference JCC-E-6-363

tert-Butyl-4-(1-(2-cyanoethyl)cyclohexyl)piperazine-1-carboxylate (**3.189**)

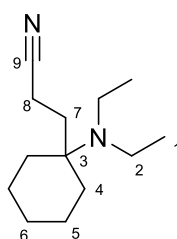
**3.189**

Synthesised using General Procedure 3E, using iminium hexafluorophosphate **3.168** (0.48 mmol as 4 mL of stock solution of crude iminium hexafluorophosphate in acetonitrile), acrylonitrile (98 μL , 1.5 mmol), tetrahydrothiophene (88 μL , 1.0 mmol) and acetonitrile (14 mL). Electrolysed for 3.5 F mol⁻¹ of charge. Purification by flash column chromatography (petroleum ether:EtOAc:EtNMe₂, 90:10:1 v/v/v). The product (**3.189**) was isolated as a colourless oil (77.4 mg, 50% for the electrolysis step).

R_F (petroleum ether:EtOAc:EtNMe₂, 60:40:1 v/v/v) 0.52; IR (ATR) 2979, 2937, 2859, 2820, 2251 (C \equiv N), 1682 (C=O), 1456, 1428, 1367, 1251, 1170, 1128, 909, 734, 648 cm⁻¹; ¹H NMR (400 MHz, Chloroform-*d*) δ 3.36 (t, $J = 5.0$ Hz, 4H, H⁴), 2.49 (t, $J = 5.0$ Hz, 4H, H⁵), 2.33 – 2.27 (m, 2H, H¹¹), 1.87 – 1.80 (m, 2H, H¹⁰), 1.69 – 1.52 (m, 4H, H⁷), 1.45 (s, 9H, H¹), 1.41 – 1.23 (m, 6H, H⁸⁻⁹); ¹³C NMR (101 MHz, Chloroform-*d*) δ 154.7 (C³), 120.8 (C¹²), 79.5 (C²), 56.9 (C⁶), 44.4, 31.1 (C⁴⁻⁵), 28.6 (C¹⁰), 28.4 (C¹), 25.9, 23.8, 21.6 (C⁷⁻⁹), 11.60 (C¹¹); HRMS (ESI⁺) m/z calcd for C₁₈H₃₂N₃O₂ [M + H]⁺: 322.2489, found: 322.2491 (-0.5 ppm error), m/z calcd for C₁₈H₃₁N₃NaO₂ [M + Na]⁺: 344.2308, found: 344.2311 (-0.6 ppm error).

Lab book reference JCC-E-7-415

3-(1-(Diethylamino)cyclohexyl)propanenitrile (**3.190**)

**3.190**

Synthesised using General Procedure 3E, using iminium hexafluorophosphate **3.169** (0.31 mmol as 4 mL of stock solution of crude iminium hexafluorophosphate in acetonitrile), acrylonitrile (98 μL , 1.5 mmol), tetrahydrothiophene (88 μL , 1.0 mmol) and acetonitrile (14 mL). Electrolysed for 3.5 F mol⁻¹ of charge. Purification by flash column chromatography

(petroleum ether:EtOAc:EtNMe₂, 95:5:1 v/v/v). The product (**3.190**) was isolated as a pale-yellow oil (35.4 mg, 50% for the electrolysis step).

R_F (petroleum ether:EtOAc:EtNMe₂, 95:5:1 v/v/v) 0.21; IR (ATR) 2930, 2866, 2813, 2245 (C≡N), 1447, 1381, 1265, 1064, 1027, 909, 736, 705, 650 cm⁻¹; ¹H NMR (400 MHz, Chloroform-*d*) δ 2.51 (q, $J = 7.0$ Hz, 4H, H²), 2.36 – 2.28 (m, 2H, H⁸), 1.89 – 1.83 (m, 2H, H⁷), 1.70 – 1.09 (m, 10H, H⁴⁻⁶), 0.98 (t, $J = 7.0$ Hz, 6H, H¹); ¹³C NMR (101 MHz, Chloroform-*d*) δ 121.4 (C⁹), 58.4 (C³), 41.4 (C²), 31.7, 29.3, 26.0, 22.4 (C⁴⁻⁷), 16.8 (C¹), 11.2 (C⁸); HRMS (ESI⁺) m/z calcd for C₁₃H₂₅N₂ [M + H]⁺: 209.2012, found: 209.2016 (-1.6 ppm error).

Lab book reference JCC-E-7-423

Appendix

Appendix A. Overlay of Current Density vs. Time Traces for Kolbe Electrolysis Reproducibility

Current density versus time plots for Kolbe electrolysis of *N*-Boc β -alanine and acetic acid with and without polarity inversion using both General Procedure 2A (Figure A.1) and General Procedure 2B (Figure A.2), corresponding to the results in Table 2.10. The black line in both graphs shows that without polarity inversion, a lower current density was achieved (prior to consumption of starting material).

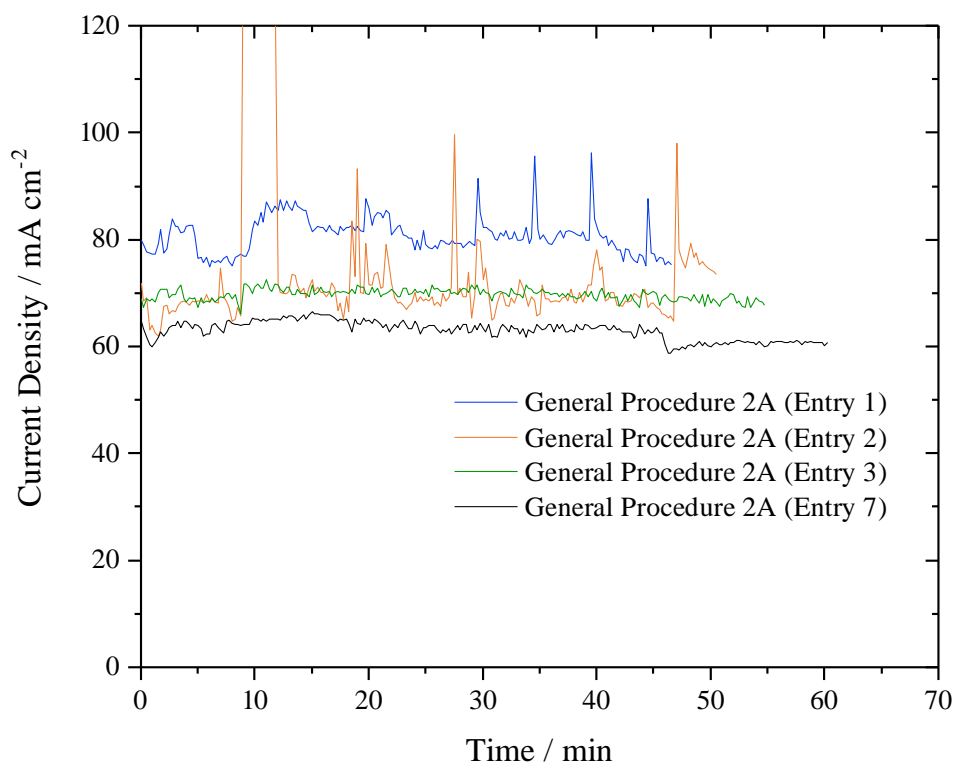


Figure A.1 Overlay of current density vs time plot for General Procedure 2A with and without polarity inversion

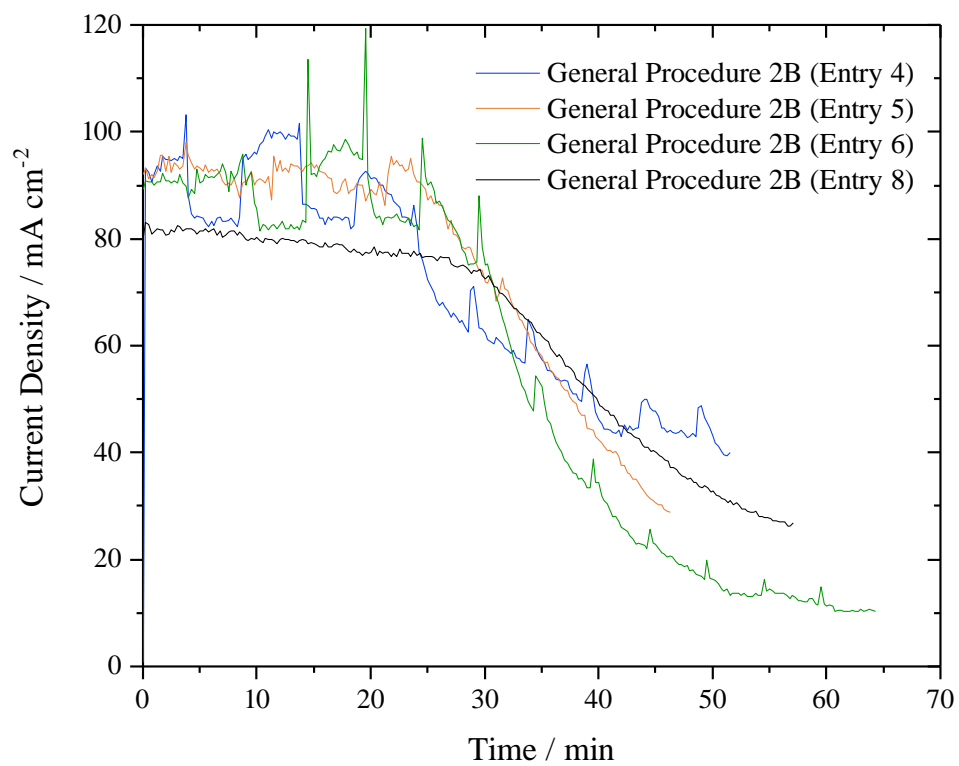


Figure A.2 Overlay of current density vs time plot for General Procedure 2B with and without polarity inversion

Appendix B. ^1H NMR Spectrum of Tertiary Amine 3.116 with Different Sacrificial Electron Donors and Purification Methods

1. Triphenylphosphine and Column Chromatography

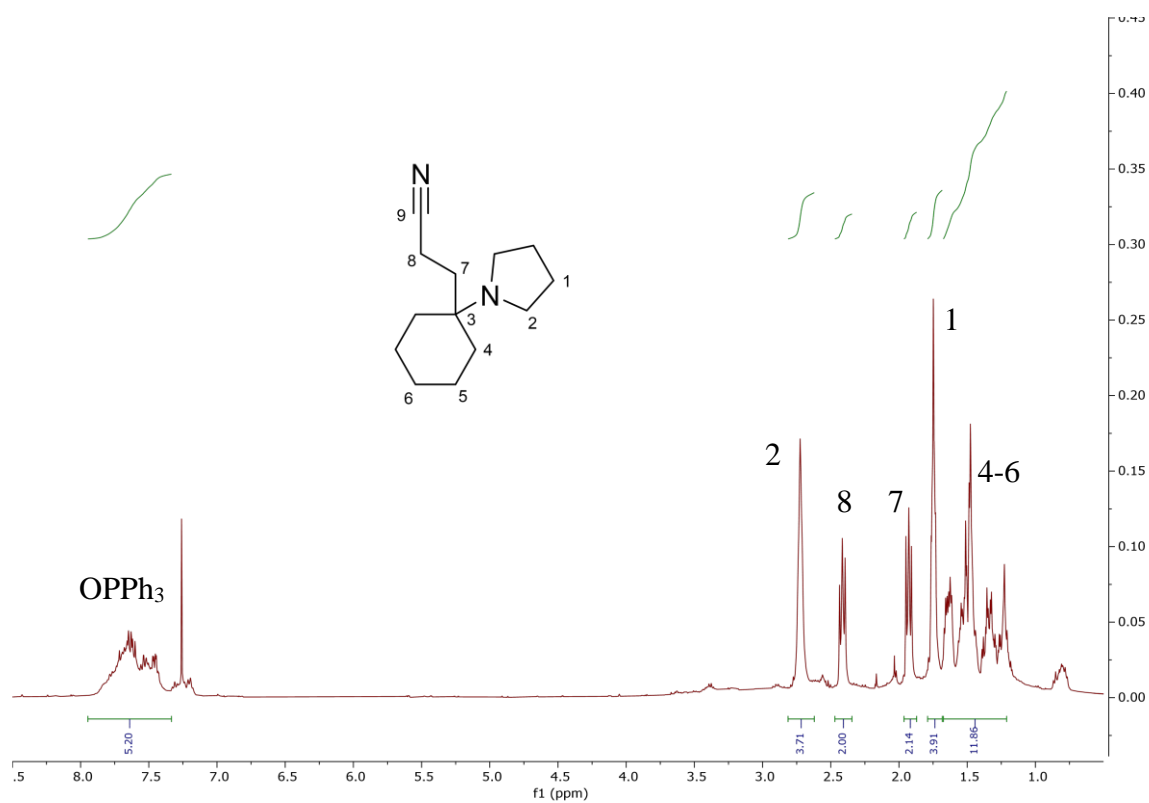


Figure A.3 ^1H NMR spectrum of tertiary amine 3.116 after isolation by column chromatography showing 77:23 mixture of tertiary amine 3.116 to triphenylphosphine

2. Triphenylphosphine and Silica Plug

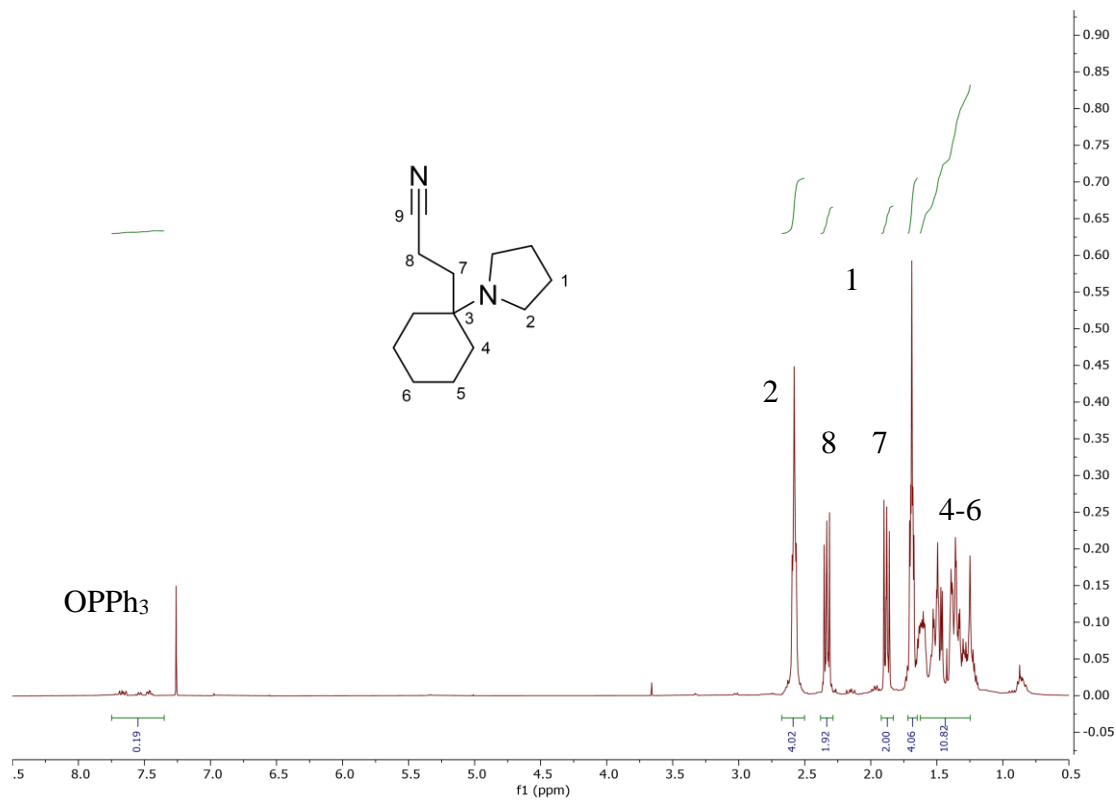


Figure A.4 ^1H NMR spectrum of tertiary amine **3.116** after isolation by silica plug showing 93:7 mixture of tertiary amine **3.116** to triphenylphosphine

3. Tetrahydrothiophene and Column Chromatography

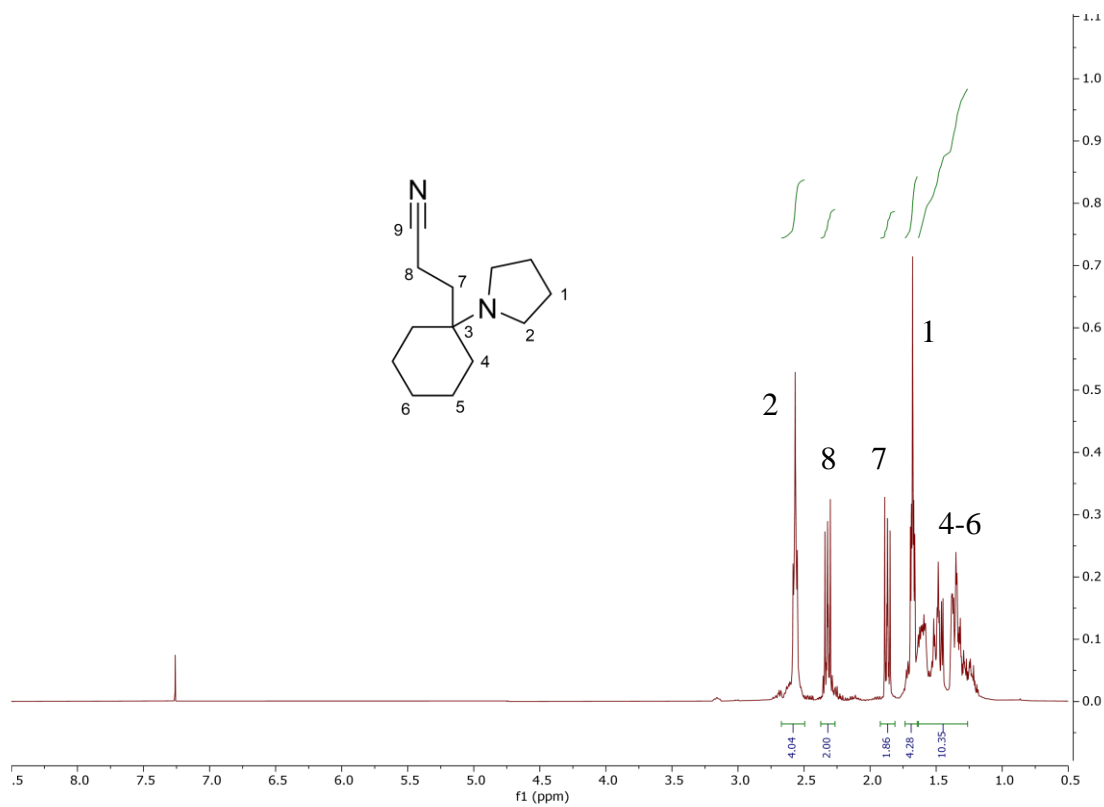


Figure A.5 ^1H NMR spectrum of tertiary amine **3.116** after isolation by column chromatography when tetrahydrothiophene was used as the SED

Appendix C. Supporting Cyclic Voltammograms

1. Cyclic Voltammograms of Starting Materials

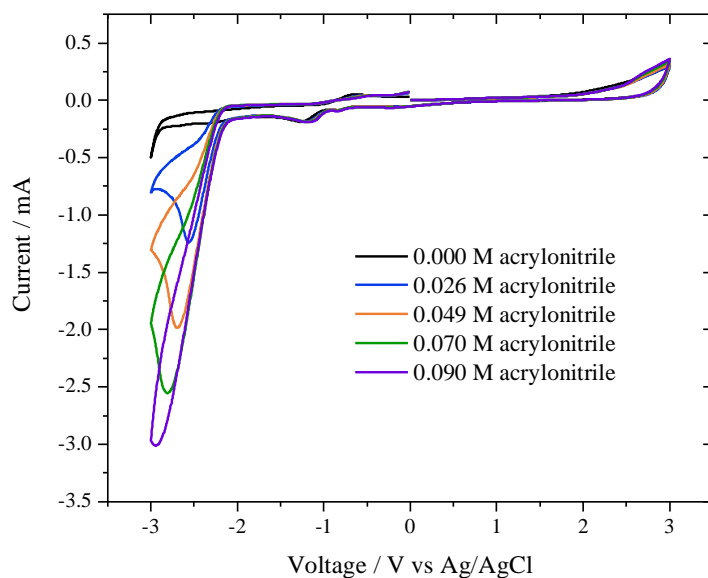


Figure A.6 Cyclic voltammogram of acrylonitrile at various concentrations. Recorded using the ElectroSyn glassy carbon working electrode, graphite counter electrode and an Ag/AgCl reference electrode. The CV was performed with an EmStat potentiostat with 0.1 M Bu_4NPF_6 in acetonitrile as the solvent, scan rate 500 mV s^{-1}

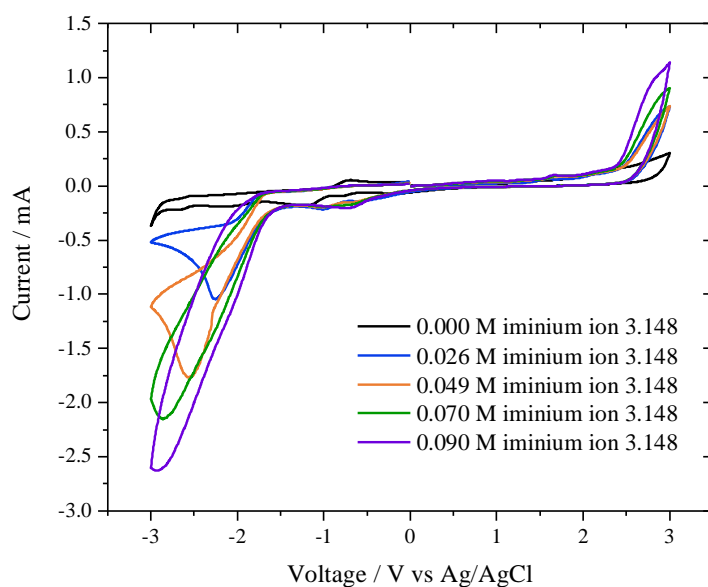


Figure A.7 Cyclic voltammogram of iminium ion 3.154 at various concentrations. Recorded using the ElectroSyn glassy carbon working electrode, graphite counter electrode and an Ag/AgCl reference electrode. The CV was performed with an EmStat potentiostat with 0.1 M Bu_4NPF_6 in acetonitrile as the solvent, scan rate 500 mV s^{-1}

2. Cyclic Voltammograms of Sacrificial Electron Donors

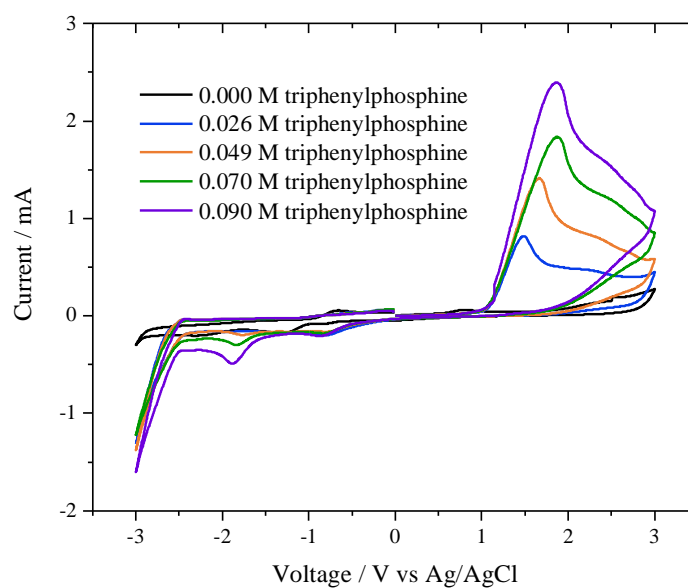


Figure A.8 Cyclic voltammogram of triphenylphosphine at various concentrations. Recorded using the ElectroSyn glassy carbon working electrode, graphite counter electrode and an Ag/AgCl reference electrode. The CV was performed with an EmStat potentiostat with 0.1 M Bu_4NPF_6 in acetonitrile as the solvent, scan rate 500 mV s^{-1}

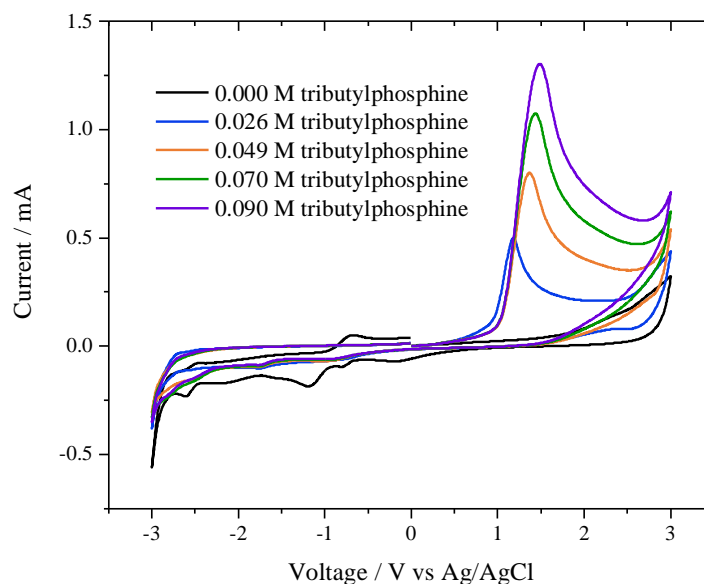


Figure A.9 Cyclic voltammogram of tributylphosphine at various concentrations. Recorded using the ElectroSyn glassy carbon working electrode, graphite counter electrode and an Ag/AgCl reference electrode. The CV was performed with an EmStat potentiostat with 0.1 M Bu_4NPF_6 in acetonitrile as the solvent, scan rate 500 mV s^{-1}

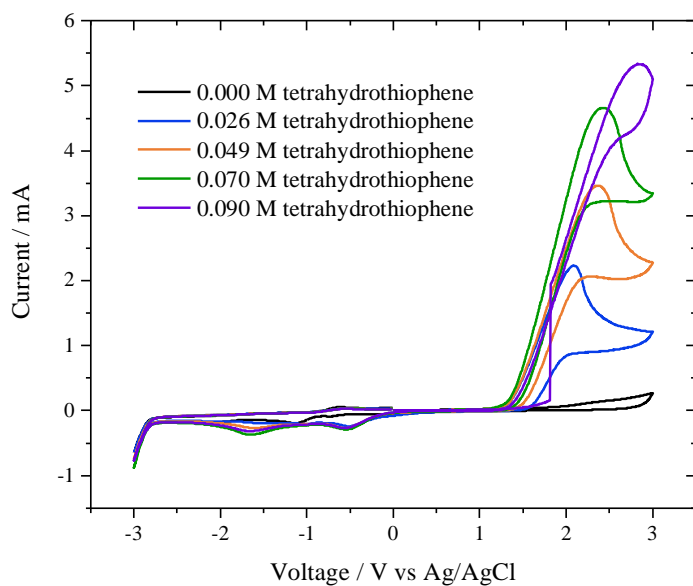


Figure A.10 Cyclic voltammogram of tetrahydrothiophene at various concentrations. Recorded using the ElectroSyn glassy carbon working electrode, graphite counter electrode and an Ag/AgCl reference electrode. The CV was performed with an EmStat potentiostat with 0.1 M Bu_4NPF_6 in acetonitrile as the solvent, scan rate 500 mV s^{-1}

3. Cyclic Voltammograms of Tertiary Amine Product 3.116

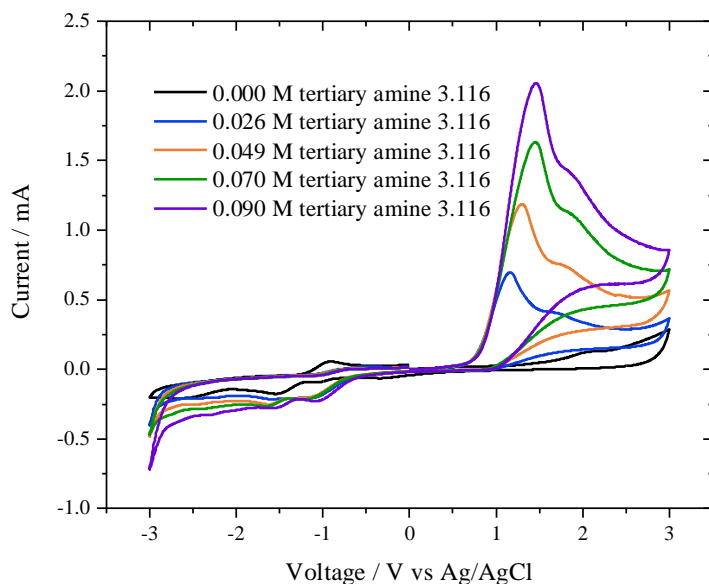


Figure A.11 Cyclic voltammogram of tertiary amine 3.116 at various concentrations. Recorded using the ElectroSyn glassy carbon working electrode, graphite counter electrode and an Ag/AgCl reference electrode. The CV was performed with an EmStat potentiostat with 0.1 M Bu_4NPF_6 in acetonitrile as the solvent, scan rate 500 mV s^{-1}

4. Cyclic Voltammograms of Tertiary Amine Product and Tetrahydrothiophene

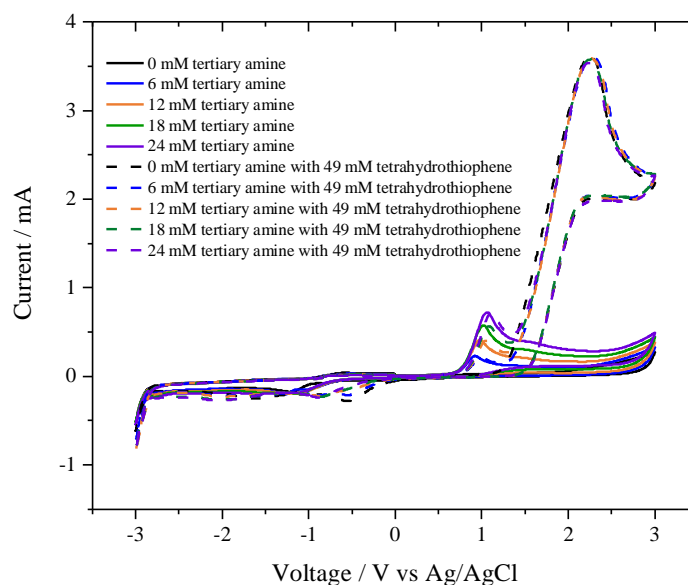


Figure A.12 Cyclic voltammogram of tertiary amine **3.116** with and without tetrahydrothiophene at various concentrations. Recorded using the ElectroSyn glassy carbon working electrode, graphite counter electrode and an Ag/AgCl reference electrode. The CV was performed with an EmStat potentiostat with 0.1 M Bu_4NPF_6 in acetonitrile as the solvent, scan rate 500 mV s^{-1}

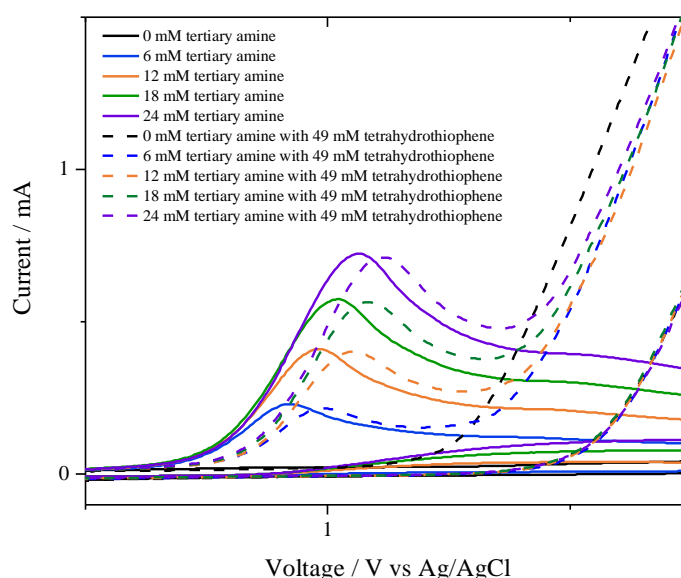


Figure A.13 Cyclic voltammogram of tertiary amine **3.116** with and without tetrahydrothiophene at various concentrations. Recorded using the ElectroSyn glassy carbon working electrode, graphite counter electrode and an Ag/AgCl reference electrode. The CV was performed with an EmStat potentiostat with 0.1 M Bu_4NPF_6 in acetonitrile as the solvent, scan rate 500 mV s^{-1} , zoom region between +0.5 and +1.75 V vs Ag/AgCl

5. Zoom Cyclic Voltammograms Sacrificial Electron Donors

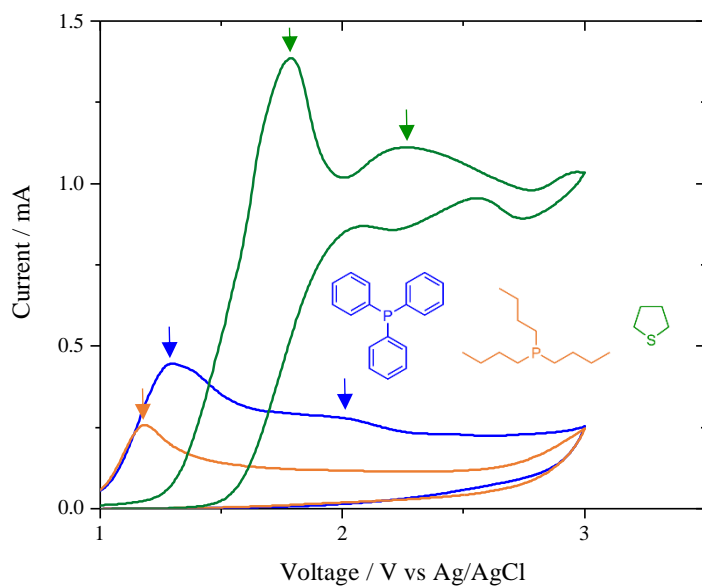


Figure A.14 Zoom region of cyclic voltammogram of triphenylphosphine, tributylphosphine and tetrahydrothiophene (0.03 M). Recorded using the ElectroSyn glassy carbon working electrode, graphite counter electrode and an Ag/AgCl reference electrode. The CV was performed with an EmStat potentiostat with 0.1 M Bu_4NPF_6 in acetonitrile as the solvent, scan rate 100 mV s^{-1} , zoom region between +1.0 and +3.5 V vs Ag/AgCl. The arrows indicate E_{ox} .

Appendix D. Example Gas Chromatogram for Crude Kolbe Electrolysis Mixture

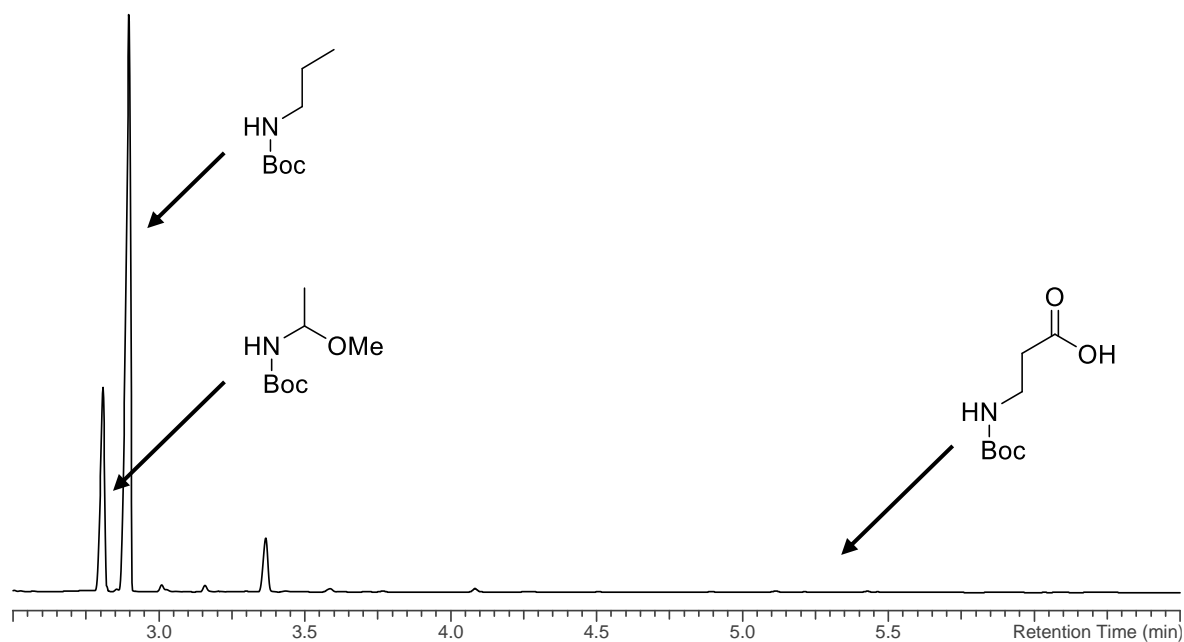
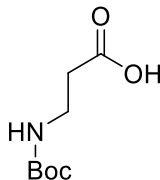
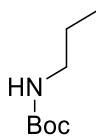
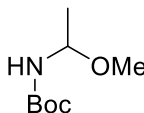


Figure A.15 Example representative gas chromatograph for Kolbe electrolysis of *N*-Boc β -alanine and acetic acid between 2.5 and 8.5 minutes, lab book reference JCC-E-2-172

Table A.1 Retention times of *N*-Boc β -alanine, Kolbe product **2.90** and non-Kolbe product **2.91** and peak areas in Figure A.15

Starting Material/Product	Retention Time / min	Peak Area / AU
	5.33	-
	2.91	15.88
	2.82	5.00

Appendix E. Setting Up an Electrochemical Method on The ElectraSyn

2.0

To set up a new reaction on the ElectraSyn 2.0 (Figure A.16):

1. Select “New Experiment”.
2. Select “Constant Voltage”.
3. Select “5V”.
4. Select “No” (for the use of a reference electrode).
5. Select “Total Charge”.
6. Set “0.5 mmol” of substrate and “3.5 Fmol⁻¹” for the equiv. of electrons.
7. Select “Yes” (for alternate the polarity).
8. Set “0.5 min” for polarity inversion time.
9. Select “Yes” (for save experiment) – optional.
10. Insert name for reaction conditions – optional
11. Select “Start”. (Once experiment started turning the stirring rate up to 700 rpm.)

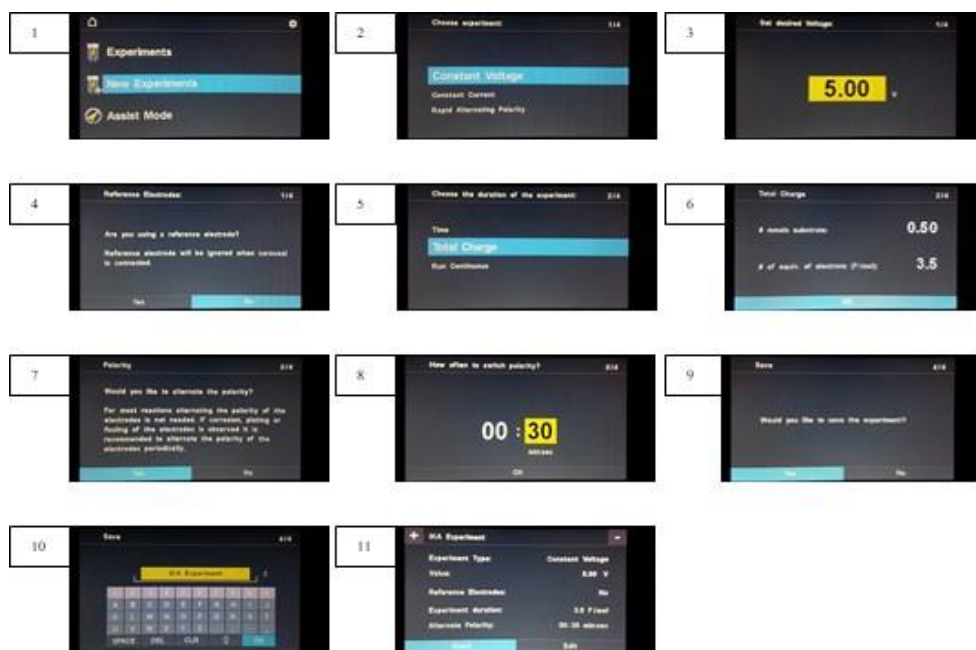


Figure A.16 Setting up a new method on the ElectraSyn 2.0

To open the reaction condition of a saved reaction (Figure A.17):

1. Select “Experiment”.
2. Select “Saved Experiment”.
3. Select the saved experiment to open.
4. Select “Start”. (Once experiment started turning the stirring rate up to 700 rpm.)



Figure A.17 Choosing an existing method on the ElectraSyn 2.0

Appendix F. Quantification of Crude Reaction Mixtures in the Electrolysis of Iminium Ions

1. Using Triphenylphosphine/Triphenylphosphine Oxide as an Internal Standard

When triphenylphosphine was used as the sacrificial electron donor, no additional external standard was added. To determine the yield of the desired product from the crude ^1H NMR spectrum. After the reaction, an aliquot (1 mL) was taken and dried *in vacuo* and dissolved in chloroform- d_3 (0.6 mL). It was assumed that the aromatic protons in the ^1H NMR spectrum could only arise from triphenylphosphine or triphenylphosphine oxide both with 15 protons and so the moles of this region were known (1.00 mmol). This was integrated relative to the 2H multiplet of the product (α to the nitrile group) located at δ_{H} 2.4 and 1.8 ppm (appearing at δ_{H} 2.6 and 2.2 ppm in the crude spectrum). The yield of the product could then be determined from the crude ^1H NMR spectrum. For the example below (Figure A.18);

$$\text{Aromatic region} = 15 \text{ protons of either } \text{PPh}_3 \text{ or } \text{Ph}_3\text{PO} = \text{Integration } 15$$

$$\text{Integration } 15 = 1.00 \text{ mmol of either } \text{PPh}_3 \text{ or } \text{Ph}_3\text{PO}$$

$$\text{Product multiplet at } 2.4 \text{ ppm} = 2 \text{ protons}$$

$$= \text{Integration } 0.31 \text{ (relative to } \text{PPh}_3 \text{ or } \text{Ph}_3\text{PO)}$$

$$\frac{0.31 \text{ integration}}{2 \text{ protons}} = 0.155$$

$$\frac{15 \text{ integration}}{15 \text{ protons}} = 1 \quad \frac{1 \text{ mmol}}{1} = 1 \text{ mmol}$$

$$1 \text{ mmol} \times 0.155 = 0.155 \text{ mmol}$$

1 mmol of PPh_3 was used in the reaction (4.0 eq.), therefore limiting reagent moles (starting material, 1.0 eq.) is 0.25 mmol.

$$\frac{0.155 \text{ mmol}}{0.25 \text{ mmol (theoretical yield)}} \times 100 = 62 \%$$

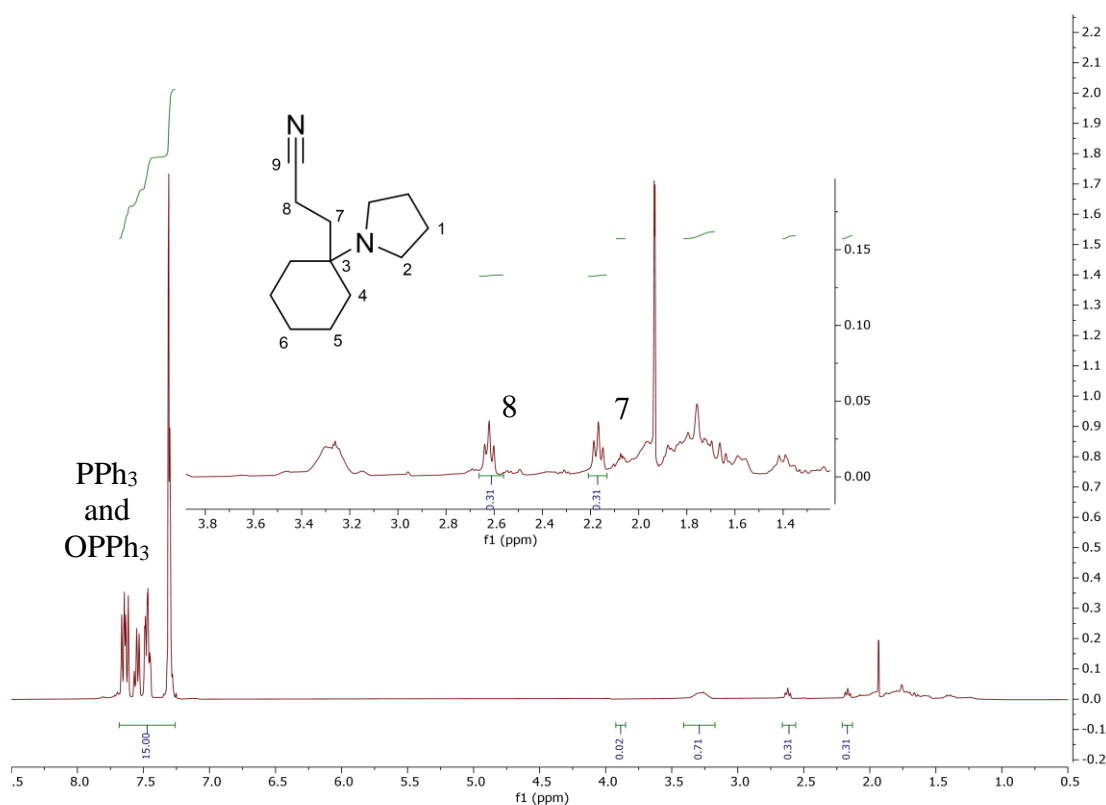


Figure A.18 Crude ^1H NMR spectrum of the reduction of iminium salt **3.154** using PPh_3 as the sacrificial electron donor, lab book reference JCC-E-5-297

2. Using Dibromomethane as an External Standard

To determine the yield of the desired product from the crude ^1H NMR spectrum. After the reaction, an aliquot (1 mL) was taken and dried *in vacuo*. A measured amount of dibromomethane was added and the sample was dissolved in acetonitrile- d_3 (0.6 mL). Dibromomethane was integrated relative to the 2H multiplet of the product (α to the nitrile group) located at δ_{H} 2.4 and 1.8 ppm (appearing at δ_{H} 2.50 and 2.13 ppm in the crude spectrum). The yield of the product could then be determined based on the moles of dibromomethane added. For the example below (Figure A.19) where 2.2 mg of dibromomethane was added;

$$\text{Dibromomethane} = 2 \text{ protons} = \text{Integration 1}$$

$$\text{Integration 1} = 0.013 \text{ mmol of dibromomethane}$$

$$\text{Product multiplet at 2.5 ppm} = 2 \text{ protons}$$

$$= \text{Integration 1.53 (relative to dibromomethane)}$$

$0.013 \text{ mmol} \times 1.53 = 0.019 \text{ mmol product in 1 mL aliquot}$

$$\frac{0.019 \text{ mmol} \times 18 \text{ (dilution factor)}}{0.50 \text{ mmol (theoretical yield)}} \times 100 = 70\%$$

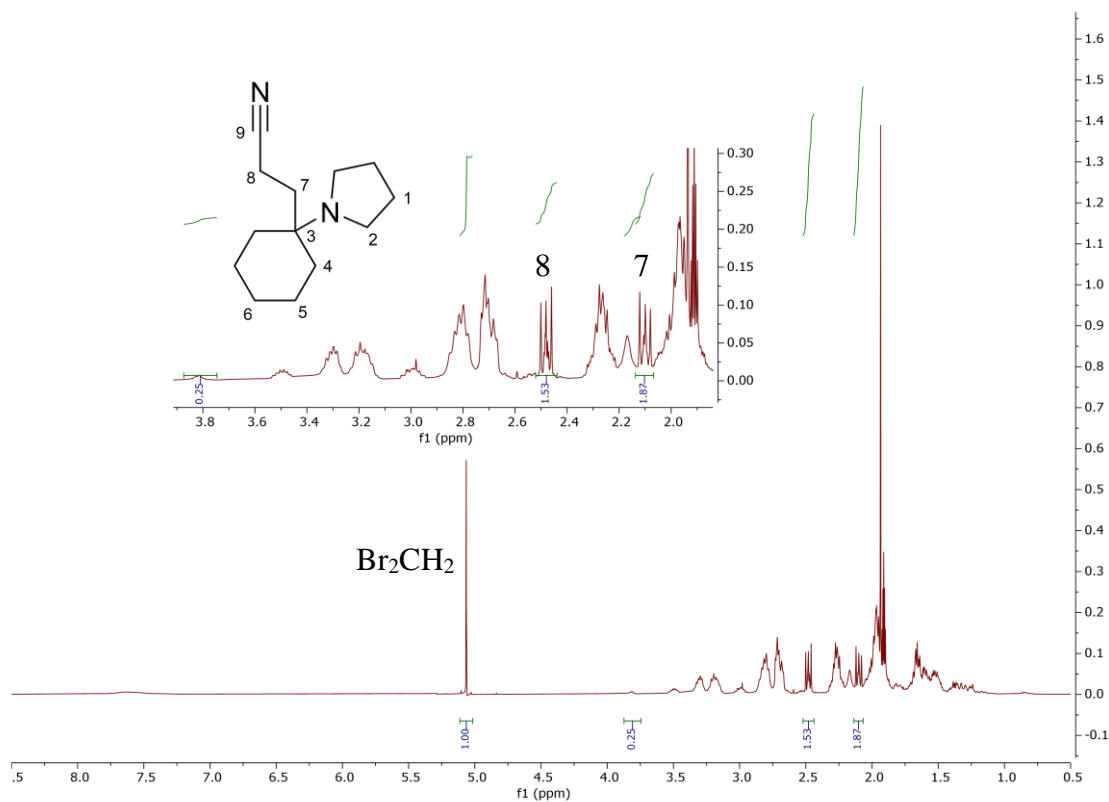


Figure A.19 Crude ^1H NMR spectrum of the reduction of iminium salt **3.154** using tetrahydrothiophene as the sacrificial electron donor and dibromomethane as an external standard, lab book reference JCC-E-6-354

References

- 1 E. J. Horn, B. R. Rosen and P. S. Baran, *ACS Cent. Sci.*, 2016, **2**, 302–308.
- 2 D. A. DiRocco, K. Dykstra, S. Krska, P. Vachal, D. V. Conway and M. Tudge, *Angew. Chem. Int. Ed.*, 2014, **53**, 4802–4806.
- 3 A. Wiebe, T. Gieshoff, S. Möhle, E. Rodrigo, M. Zirbes and S. R. Waldvogel, *Angew. Chem. Int. Ed.*, 2018, **57**, 5594–5619.
- 4 K. Lam, A. Dobbs, M. C. Leech, A. Petti and A. D. Garcia, *React. Chem. Eng.*, 2020, **5**, 977–990.
- 5 D. J. Hart, *Science.*, 1984, **223**, 883–887.
- 6 M. Gomberg, *J. Am. Chem. Soc.*, 1900, **22**, 757–771.
- 7 E. G. Rozantsev and D. V. Loshadkin, *Des. Monomers Polym.*, 2001, **4**, 281–300.
- 8 K. U. Ingold, *Pure Appl. Chem.*, 1997, **69**, 241–244.
- 9 C. Walling, *Tetrahedron*, 1985, **41**, 3887–3900.
- 10 S. Z. Zard, *Org. Lett.*, 2017, **19**, 1257–1269.
- 11 M. Yan, J. C. Lo, J. T. Edwards and P. S. Baran, *J. Am. Chem. Soc.*, 2016, **138**, 12692–12714.
- 12 K. J. Romero, M. S. Galliher, D. A. Pratt and C. R. J. Stephenson, *Chem. Soc. Rev.*, 2018, **47**, 7851–7866.
- 13 C. R. J. Stephenson, A. Studer and D. P. Curran, *Beilstein J. Org. Chem.*, 2013, **9**, 2778–2780.
- 14 C. P. Jasperse, D. P. Curran and T. L. Fevig, *Chem. Rev.*, 1991, **91**, 1237–1286.
- 15 B. Giese, *Angew. Chem. Int. Ed.*, 1983, **22**, 753–764.
- 16 N. Kvasovs and V. Gevorgyan, *Chem. Soc. Rev.*, 2021, **50**, 2244–2259.
- 17 S. Crespi and M. Fagnoni, *Chem. Rev.*, 2020, **120**, 9790–9833.
- 18 A. F. Parsons, *An Introduction to Free Radical Chemistry*, Blackwell Science Ltd,

- Oxford, 1st edn., 2000.
- 19 H. G. Kuivila and L. W. Menapace, *J. Org. Chem.*, 1963, **28**, 2165–2167.
- 20 D. H. R. Barton and S. W. McCombie, *J. Chem. Soc. Perkin Trans. 1*, 1975, 1574–1585.
- 21 S. W. McCombie, B. Quiclet-Sire and S. Z. Zard, *Tetrahedron*, 2018, **74**, 4969–4979.
- 22 C. K. Prier, D. A. Rankic and D. W. C. MacMillan, *Chem. Rev.*, 2013, **113**, 5322–5363.
- 23 M. H. Shaw, J. Twilton and D. W. C. MacMillan, *J. Org. Chem.*, 2016, **81**, 6898–6926.
- 24 N. A. Romero and D. A. Nicewicz, *Chem. Rev.*, 2016, **116**, 10075–10166.
- 25 M. A. Ischay, M. E. Anzovino, J. Du and T. P. Yoon, *J. Am. Chem. Soc.*, 2008, **130**, 12886–12887.
- 26 D. A. Nicewicz and D. W. C. MacMillan, *Science.*, 2008, **322**, 77–80.
- 27 J. M. R. Narayanam, J. W. Tucker and C. R. J. Stephenson, *J. Am. Chem. Soc.*, 2009, **131**, 8756–8757.
- 28 M. Yan, Y. Kawamata and P. S. Baran, *Angew. Chem. Int. Ed.*, 2017, **57**, 4149–4155.
- 29 N. E. S. Tay, D. Lehnherr and T. Rovis, *Chem. Rev.*, 2021, **122**, 2487–2649.
- 30 M. Yan, Y. Kawamata and P. S. Baran, *Chem. Rev.*, 2017, **117**, 13230–13319.
- 31 C. Schotten, T. P. Nicholls, R. A. Bourne, N. Kapur, B. N. Nguyen and C. E. Willans, *Green Chem.*, 2020, **22**, 3358–3375.
- 32 J. B. Sperry and D. L. Wright, *Chem. Soc. Rev.*, 2006, **35**, 605.
- 33 K. Lam and I. E. Markó, *Org. Lett.*, 2009, **11**, 2752–2755.
- 34 S. B. Beil, D. Pollok and S. R. Waldvogel, *Angew. Chem. Int. Ed.*, 2021, **60**, 14750–14759.
- 35 B. A. Frontana-Uribe, R. D. Little, J. G. Ibanez, A. Palma and R. Vasquez-Medrano, *Green Chem.*, 2010, **12**, 2099–2119.
- 36 S. R. Waldvogel and B. Janza, *Angew. Chem. Int. Ed.*, 2014, **53**, 7122–7123.

-
- 37 R. Francke and R. D. Little, *Chem. Soc. Rev.*, 2014, **43**, 2492–2521.
- 38 S. R. Waldvogel, S. Möhle, M. Zirbes, E. Rodrigo, T. Gieshoff and A. Wiebe, *Angew. Chem. Int. Ed.*, 2018, **57**, 6018–6041.
- 39 C. Li, Y. Kawamata, H. Nakamura, J. C. Vantourout, Z. Liu, Q. Hou, D. Bao, J. T. Starr, J. Chen, M. Yan and P. S. Baran, *Angew. Chem. Int. Ed.*, 2017, **56**, 13088–13093.
- 40 Z. W. Hou, Z. Y. Mao, Y. Y. Melcamu, X. Lu and H.-C. Xu, *Angew. Chem. Int. Ed.*, 2018, **57**, 1636–1639.
- 41 F. Xu, L. Zhu, S. Zhu, X. Yan and H.-C. Xu, *Chem. Eur. J.*, 2014, **20**, 12740–12744.
- 42 A. Wiebe, S. Lips, D. Schollmeyer, R. Franke and S. R. Waldvogel, *Angew. Chem. Int. Ed.*, 2017, **56**, 14727–14731.
- 43 E. Rodrigo and S. R. Waldvogel, *Chem. Sci.*, 2019, **10**, 2044–2047.
- 44 H. J. Zhang, L. Chen, M. S. Oderinde, J. T. Edwards, Y. Kawamata and P. S. Baran, *Angew. Chem. Int. Ed.*, 2021, **60**, 20700–20705.
- 45 A. Petti, P. Natho, K. Lam and P. J. Parsons, *European J. Org. Chem.*, 2021, **2021**, 854–858.
- 46 B. R. Rosen, E. W. Werner, A. G. O'Brien and P. S. Baran, *J. Am. Chem. Soc.*, 2014, **136**, 5571–5574.
- 47 D. Li, T. K. Ma, R. J. Scott and J. D. Wilden, *Chem. Sci.*, 2020, **11**, 5333–5338.
- 48 P. Hu, B. K. Peters, C. A. Malapit, J. C. Vantourout, P. Wang, J. Li, L. Mele, P. G. Echeverria, S. D. Minter and P. S. Baran, *J. Am. Chem. Soc.*, 2020, **142**, 20979–20986.
- 49 X. Chen, X. Luo, X. Peng, J. Guo, J. Zai and P. Wang, *Chem. Eur. J.*, 2020, **26**, 3226–3230.
- 50 X. Luo, X. Ma, F. Lebreux, I. E. Markó and K. Lam, *Chem. Commun.*, 2018, **54**, 9969–9972.
- 51 M. C. Leech and K. Lam, *Acc. Chem. Res.*, 2020, **53**, 121–134.
- 52 H. Li, C. P. Breen, H. Seo, T. F. Jamison, Y. Q. Fang and M. M. Bio, *Org. Lett.*, 2018,
-

- 20, 1338–1341.
- 53 M. Quertenmont, I. Goodall, K. Lam, I. Markó and O. Riant, *Org. Lett.*, 2020, **22**, 1771–1775.
- 54 The 10 Green Chemicals for UK economic growth - UKBioChem10, <http://ukbiochem10.co.uk/>, (accessed 3 June 2020).
- 55 H. J. Schäfer, in *Comprehensive Organic Synthesis*, eds. B. M. Trost and I. Fleming, Pergamon, Oxford, 1991, vol. 3, pp. 633–658.
- 56 A. K. Vijh and B. E. Conway, *Chem. Rev.*, 1967, **67**, 623–664.
- 57 H. Kolbe, *Liebigs Ann.*, 1849, **69**, 257–294.
- 58 H. J. Schäfer, in *Topics in Current Chemistry*, ed. E. Steckhan, Springer-Verlag, Berlin, Heidelberg, 1990, vol. 152, pp. 91–151.
- 59 L. Ebersson and K. Nyberg, *Tetrahedron*, 1976, **32**, 2185–2206.
- 60 G. E. Svadkovskaya and S. A. Voitkevich, *Russ. Chem. Rev.*, 1960, **29**, 161–180.
- 61 O. J. Walker and G. L. E. Wild, *J. Chem. Soc.*, 1935, 207–210.
- 62 S. Glasstone and A. Hickling, *Chem. Rev.*, 1939, **25**, 407–441.
- 63 S. Glasstone and A. Hickling, *J. Chem. Soc.*, 1934, 1878–1888.
- 64 F. J. Holzhäuser, J. B. Mensah and R. Palkovits, *Green Chem.*, 2020, **22**, 286–301.
- 65 L. Ebersson, *Electrochim. Acta*, 1967, **12**, 1473–1478.
- 66 T. Dickinson and W. F. K. Wynne-Jones, *Trans. Faraday. Soc.*, 1961, **58**, 382–387.
- 67 T. Dickinson and W. F. K. Wynne-Jones, *Trans. Faraday. Soc.*, 1961, **58**, 388–399.
- 68 T. Dickinson and W. F. K. Wynne-Jones, *Trans. Faraday. Soc.*, 1961, **58**, 400–404.
- 69 H. J. Schäfer, in *Organic Electrochemistry*, eds. O. Hammerich and B. Speiser, CRC Press, Boca Raton, 5th edn., 2016, pp. 705–773.
- 70 H. Dahms and M. Green, *J. Electrochem. Soc.*, 1963, **110**, 1075.
- 71 A. G. Dubinin, L. A. Mirkind, V. E. Kazarinov and M. Y. Fiochin, *Sov. Electrochem.*, 1979, **15**, 1156–1159.

-
- 72 B. E. Conway and T. C. Liu, *J. Electroanal. Chem.*, 1988, **242**, 317–322.
- 73 B. Kraeutler, C. D. Jaeger and A. J. Bard, *J. Am. Chem. Soc.*, 1978, **100**, 4903–4905.
- 74 Y. Abe, S. Y. Seno, K. Sakakibara and M. Hirota, *J. Chem. Soc. Perkin Trans. 2*, 1991, 897–903.
- 75 L. Ebersson and G. Ryde-Petterson, *Acta Chem. Scand.*, 1973, **27**, 1159–1161.
- 76 L. Ebersson, K. Nyberg and R. Servin, *Acta Chem. Scand.*, 1976, **30B**, 906–907.
- 77 H. Tanaka, M. Kuroboshi and S. Torii, in *Organic Electrochemistry*, eds. O. Hammerich and B. Speiser, CRC Press, Boca Raton, 5th edn., 2016, pp. 1267–1307.
- 78 S. Gilman, *Electrochim. Acta*, 1964, **9**, 1025–1046.
- 79 B. E. Conway and A. K. Vijh, *Electrochim. Acta*, 1967, **12**, 102–104.
- 80 S. Gilman, *Trans. Faraday. Soc.*, 1965, **61**, 2546–2560.
- 81 S. Gilman, *Trans. Faraday. Soc.*, 1965, **61**, 2561–2568.
- 82 M. Fleischmann, J. R. Mansfield and W. F. K. Wynne-Jones, *J. Electroanal. Chem.*, 1965, **10**, 511–521.
- 83 M. Fleischmann, J. R. Mansfield and W. F. K. Wynne-Jones, *J. Electroanal. Chem.*, 1965, **10**, 522–537.
- 84 E. Klocke, A. Matzeit, M. Gockeln and H. J. Schäfer, *Chem. Ber.*, 1993, **126**, 1623–1630.
- 85 B. C. L. Linstead, R. P. Shepard, B. R. Weedon, *J. Chem. Soc.*, 1951, 2854–2858.
- 86 L. Ebersson, *Acta Chem. Scand.*, 1963, **17**, 2004–2018.
- 87 D. L. Muck and E. R. Wilson, *J. Electrochem. Soc.*, 1970, **117**, 1358–1362.
- 88 I. Sekine and H. Ohkawa, *Electrochim. Acta*, 1980, **25**, 1647–1653.
- 89 M. Finkelstein and S. D. Ross, *J. Org. Chem.*, 1969, **34**, 2923–2927.
- 90 W. J. Koehl, *J. Am. Chem. Soc.*, 1964, **86**, 4686–4690.
- 91 H. J. Schäfer, *Eur. J. Lipid Sci. Technol.*, 2012, **114**, 2–9.
- 92 J. Knolle and H. J. Schäfer, *Electrochim. Acta*, 1978, **23**, 5–8.
-

- 93 Q. N. Porter and J. H. P. Utley, *J. Chem. Soc. Chem. Commun.*, 1978, 255–256.
- 94 A. G. Wills, D. L. Poole, C. M. Alder and M. Reid, *ChemElectroChem*, 2020, **7**, 2771–2776.
- 95 M. R. Rifi and F. H. Covitz, *Introduction to Organic Electrochemistry*, Marcel Dekker Inc., New York, 1974.
- 96 G. E. Hawkes, J. H. P. Utley and G. B. Yates, *J. Chem. Soc. Perkin Trans. 2*, 1976, 1709–1716.
- 97 D. Seebach and P. Renaud, *Helv. Chim. Acta*, 1985, **68**, 2342–2349.
- 98 J. P. Coleman, R. Lines, J. H. P. Utley and B. C. L. Weedon, *J. Chem. Soc. Perkin Trans. 2*, 1974, 1064–1069.
- 99 J. P. Coleman, Naser-ud-din, H. G. Gilde, J. H. P. Utley, B. C. L. Weedon and L. Ebersson, *J. Chem. Soc. Perkin Trans. 2*, 1973, 1903–1908.
- 100 R. G. Woolford, *Can. J. Chem.*, 1962, **40**, 1846–1850.
- 101 Y. Okada, K. Kamimura and K. Chiba, *Tetrahedron*, 2012, **68**, 5857–5862.
- 102 M. Harenbrock, A. Matzeit and H. J. Schäfer, *Liebigs Ann.*, 1996, **1996**, 55–62.
- 103 F. Lebreux, F. Buzzo and I. E. Markó, *Synlett*, 2008, **2008**, 2815–2820.
- 104 A. Weiper-Idelmann, M. Aus Dem Kahmen, H. J. Schäfer and M. Gockeln, *Acta Chem. Scand.*, 1998, **52**, 672–682.
- 105 A. V. Shtelman and J. Y. Becker, *J. Org. Chem.*, 2011, **76**, 4710–4714.
- 106 J. W. Wilt, M. Peeran, J. Luszyk and K. U. Ingold, *J. Am. Chem. Soc.*, 1988, **110**, 281–287.
- 107 I. T. Davidson, T. J. Barton, K. J. Hughes, S. Ijadi-Maghsoodi, A. Revis and G. C. Paul, *Organometallics*, 1987, **6**, 644–646.
- 108 M. Huhtasaari, H. J. Schäfer and L. Becking, *Angew. Chem. Int. Ed.*, 1984, **23**, 980–981.
- 109 L. Becking and H. J. Schäfer, *Tetrahedron Lett.*, 1988, **29**, 2797–2800.
- 110 L. Brakha and J. Y. Becker, *Electrochim. Acta*, 2012, **77**, 143–149.

-
- 111 T. Tajima, H. Kurihara and T. Fuchigami, *J. Am. Chem. Soc.*, 2007, **129**, 6680–6681.
- 112 S. Lateef, S. R. K. Mohan and S. R. J. Reddy, *Tetrahedron Lett.*, 2007, **48**, 77–80.
- 113 G. Mohammadi Ziarani, F. Soltani Hasankiadeh and F. Mohajer, *ChemistrySelect*, 2020, **5**, 14349–14379.
- 114 D. S. Corrigan, E. K. Krauskopf, L. M. Rice, A. Wieckowski and M. J. Weaver, *J. Phys. Chem.*, 1988, **92**, 1596–1601.
- 115 W. Pritzkow, G. Thomas and L. Willecke, *J. für Prakt. Chemie*, 1985, **327**, 847–851.
- 116 P. Q. Huang and Z. Y. Li, *Tetrahedron Asymmetry*, 2005, **16**, 3367–3370.
- 117 T. Suenaga, C. Schutz and T. Nakata, *Tetrahedron Lett.*, 2003, **44**, 5799–5801.
- 118 S. Berrell, PhD Thesis, University of York, 2020.
- 119 K. Neubert, M. Schmidt and F. Harnisch, *ChemSusChem*, 2021, **14**, 3097–3109.
- 120 H. G. Roth, N. A. Romero and D. A. Nicewicz, *Synlett*, 2016, **27**, 714–723.
- 121 J. Ghilane, P. Martin, H. Randriamahazaka and J. C. Lacroix, *Electrochem. commun.*, 2010, **12**, 246–249.
- 122 C. Agami and F. Couty, *Tetrahedron*, 2002, **58**, 2701–2724.
- 123 F. Wang, M. Rafiee and S. S. Stahl, *Angew. Chem. Int. Ed.*, 2018, **57**, 1–6.
- 124 A. M. Jones and C. E. Banks, *Beilstein J. Org. Chem.*, 2014, **10**, 3056–3072.
- 125 D. Griller and F. P. Lossing, *J. Am. Chem. Soc.*, 1981, **103**, 1586–1587.
- 126 T. J. Burkey, A. L. Castelhana, D. Griller and F. P. Lossing, *J. Am. Chem. Soc.*, 1983, **105**, 4701–4703.
- 127 M. Sablier and T. Fujii, *Chem. Rev.*, 2002, **102**, 2855–2924.
- 128 J. M. Dyke, A. R. Ellis, N. Jonathan, N. Keddar and A. Morris, *Chem. Phys. Lett.*, 1984, **111**, 207–210.
- 129 B. Ruscic and J. Berkowitz, *J. Chem. Phys.*, 1994, **101**, 10936–10946.
- 130 F. P. Lossing and G. P. Semeluk, *Can. J. Chem.*, 1970, **48**, 955–965.
- 131 D. V. Dearden and J. L. Beauchamp, *J. Phys. Chem.*, 1985, **89**, 5359–5365.
-

- 132 T. W. Baughman, J. C. Sworen and K. B. Wagener, *Tetrahedron*, 2004, **60**, 10943–10948.
- 133 S. W. Wu, J. L. Liu and F. Liu, *Org. Lett.*, 2016, **18**, 1–3.
- 134 K. Xu, Z. Wang, J. Zhang, L. Yu and J. Tan, *Org. Lett.*, 2015, **17**, 4476–4478.
- 135 C. A. Grob and P. W. Schiess, *Angew. Chem. Int. Ed.*, 1967, **6**, 1–15.
- 136 C. A. Grob, *Angew. Chem. Int. Ed.*, 1969, **8**, 535–546.
- 137 I. V. Vrček, V. Vrček and H. U. Siehl, *J. Phys. Chem. A*, 2002, **106**, 1604–1611.
- 138 L. Rand and A. F. Mohar, *J. Org. Chem.*, 1965, **30**, 3156–3157.
- 139 M. Finkelstein and R. Petersen, *J. Org. Chem.*, 1960, **25**, 136–137.
- 140 K. Sarmini and E. Kenndler, *J. Biochem. Biophys. Methods*, 1999, **38**, 123–137.
- 141 E. Rossini, A. D. Bochevarov and E. W. Knapp, *ACS Omega*, 2018, **3**, 1653–1662.
- 142 A. Jouyban and S. Soltanpour, *J. Chem. Eng. Data*, 2010, **55**, 2951–2963.
- 143 C. D. Russell and F. C. Anson, *Anal. Chem.*, 1961, **33**, 1282–1284.
- 144 G. Åkerlöf, *J. Am. Chem. Soc.*, 1932, **54**, 4125–4139.
- 145 D. M. Heard and A. J. J. Lennox, *Angew. Chem.*, 2020, **132**, 19026–19044.
- 146 B. E. Conway and M. Dzieciuch, *Can. J. Chem.*, 1963, **41**, 55–67.
- 147 N. Sato, T. Sekine and K. Sugino, *J. Electrochem. Soc.*, 1968, **115**, 242–246.
- 148 J. Liu, J. Ye, C. Xu, S. P. Jiang and Y. Tong, *J. Power Sources*, 2008, **177**, 67–70.
- 149 J. A. Leitch, T. Rossolini, T. Rogova, J. A. P. Maitland and D. J. Dixon, *ACS Catal.*, 2020, **10**, 2009–2025.
- 150 A. Trowbridge, S. M. Walton and M. J. Gaunt, *Chem. Rev.*, 2020, **120**, 2613–2692.
- 151 A. Hager, N. Vrieling, D. Hager, J. Lefranc and D. Trauner, *Nat. Prod. Rep.*, 2016, **33**, 491–522.
- 152 E. Vitaku, D. T. Smith and J. T. Njardarson, *J. Med. Chem.*, 2014, **57**, 10257–10274.
- 153 S. D. Roughley and A. M. Jordan, *J. Med. Chem.*, 2011, **54**, 3451–3479.

-
- 154 O. I. Afanasyev, E. Kuchuk, D. L. Usanov and D. Chusov, *Chem. Rev.*, 2019, **119**, 11857–11911.
- 155 A. F. Abdel-Magid, K. G. Carson, B. D. Harris, C. A. Maryanoff and R. D. Shah, *J. Org. Chem.*, 1996, **61**, 3849–3862.
- 156 Q. Yang, Y. Zhao and D. Ma, *Org. Process Res. Dev.*, 2022, **26**, 1690–1750.
- 157 P. Ruiz-castillo and S. L. Buchwald, *Chem. Rev.*, 2016, **116**, 12564–12649.
- 158 R. Dorel, C. P. Grugel and A. M. Haydl, *Angew. Chem. Int. Ed.*, 2019, **58**, 17118–17129.
- 159 Y. Pellegrin and F. Odobel, *Comptes Rendus Chim.*, 2017, **20**, 283–295.
- 160 J. W. Beatty and C. R. J. Stephenson, *Acc. Chem. Res.*, 2015, **48**, 1474–1484.
- 161 D. D. M. Wayner, J. J. Dannenberg and D. Griller, *Chem. Phys. Lett.*, 1986, **131**, 189–191.
- 162 Y. Wang, X. Hu, C. A. Morales-Rivera, G. X. Li, X. Huang, G. He, P. Liu and G. Chen, *J. Am. Chem. Soc.*, 2018, **140**, 9678–9684.
- 163 A. S. H. Ryder, W. B. Cunningham, G. Ballantyne, T. Mules, A. G. Kinsella, J. Turner-Dore, C. M. Alder, L. J. Edwards, B. S. J. McKay, M. N. Grayson and A. J. Cresswell, *Angew. Chem. Int. Ed.*, 2020, **59**, 14986–14991.
- 164 D. Reich, A. Trowbridge and M. J. Gaunt, *Angew. Chem. Int. Ed.*, 2020, **59**, 2256–2261.
- 165 J. B. McManus, N. P. R. Onuska and D. A. Nicewicz, *J. Am. Chem. Soc.*, 2018, **140**, 9056–9060.
- 166 J. B. McManus, N. P. R. Onuska, M. S. Jeffreys, N. C. Goodwin and D. A. Nicewicz, *Org. Lett.*, 2020, **22**, 679–683.
- 167 A. McNally, C. K. Prier and D. W. C. MacMillan, *Science.*, 2011, **334**, 1114–1117.
- 168 C. K. Prier and D. W. C. MacMillan, *Chem. Sci.*, 2014, **5**, 4173–4178.
- 169 Y. Ma, X. Yao, L. Zhang, P. Ni, R. Cheng and J. Ye, *Angew. Chem. Int. Ed.*, 2019, **58**, 16548–16552.
-

- 170 D. T. Ahneman and A. G. Doyle, *Chem. Sci.*, 2016, **7**, 7002–7006.
- 171 B. G. Stevenson, E. H. Spielvogel, E. A. Loiaconi, V. M. Wambua, R. V. Nakhamiyayev and J. R. Swierk, *J. Am. Chem. Soc.*, 2021, **143**, 8878–8885.
- 172 Y. Mo, Z. Lu, G. Rughoobur, P. Patil, N. Gershenfeld, A. I. Akinwande, S. L. Buchwald and K. F. Jensen, *Science.*, 2020, **368**, 1352–1357.
- 173 A. Trowbridge, D. Reich and M. J. Gaunt, *Nature*, 2018, **561**, 522–527.
- 174 N. J. Flodén, A. Trowbridge, D. Willcox, S. M. Walton, Y. Kim and M. J. Gaunt, *J. Am. Chem. Soc.*, 2019, **141**, 8426–8430.
- 175 T. Rossolini, J. A. Leitch, R. Grainger and D. J. Dixon, *Org. Lett.*, 2018, **20**, 6794–6798.
- 176 M. C. Nicastri, D. Lehnherr, Y. H. Lam, D. A. Dirocco and T. Rovis, *J. Am. Chem. Soc.*, 2020, **142**, 987–998.
- 177 J. R. Ames, S. Brandänge, B. Rodriguez, N. Castagnoli, M. D. Ryan and P. Kovacic, *Bioorg. Chem.*, 1986, **14**, 228–241.
- 178 C. P. Andrieux and J. M. Savéant, *J. Electroanal. Chem.*, 1970, **26**, 223–235.
- 179 D. Hager and D. W. C. MacMillan, *J. Am. Chem. Soc.*, 2014, **136**, 16986–16989.
- 180 X. Guo and O. S. Wenger, *Angew. Chem. Int. Ed.*, 2018, **57**, 2469–2473.
- 181 C. C. Nawrat, C. R. Jamison, Y. Slutskyy, D. W. C. MacMillan and L. E. Overman, *J. Am. Chem. Soc.*, 2015, **137**, 11270–11273.
- 182 P. H. McCabe, N. J. Milne and G. A. Sim, *J. Chem. Soc. Perkin Trans 2.*, 1989, 1459–1462.
- 183 D. Leifert and A. Studer, *Angew. Chem. Int. Ed.*, 2020, **59**, 74–108.
- 184 L. Sun, K. Sahloul and M. Mellah, *ACS Catal.*, 2013, **3**, 2568–2573.
- 185 M. Szostak, N. J. Fazakerley, D. Parmar and D. J. Procter, *Chem. Rev.*, 2014, **114**, 5959–6039.
- 186 M. Shabangi, M. L. Kuhlman and R. A. Flowers, *Org. Lett.*, 1999, **1**, 2133–2135.
- 187 M. Szostak, M. Spain and D. J. Procter, *J. Org. Chem.*, 2014, **79**, 2522–2537.

-
- 188 A. Dahlén and G. Hilmersson, *Chem. Eur. J.*, 2003, **9**, 1123–1128.
- 189 H. M. Peltier, J. P. McMahon, A. W. Patterson and J. A. Ellman, *J. Am. Chem. Soc.*, 2006, **128**, 16018–16019.
- 190 R. Annunziata, M. Benaglia, M. Caporale and L. Raimondi, *Tetrahedron Asymmetry*, 2002, **13**, 2727–2734.
- 191 R. Annunziata, M. Benaglia, M. Cinquini, F. Cozzi and L. Raimondi, *Tetrahedron Lett.*, 1998, **39**, 3333–3336.
- 192 M. Kim, B. W. Knettle, A. Dahlén, G. Hilmersson and R. A. Flowers, *Tetrahedron*, 2003, **59**, 10397–10402.
- 193 S. F. Martin, C. P. Yang, W. L. Laswell and H. Rüeger, *Tetrahedron Lett.*, 1988, **29**, 6685–6687.
- 194 J. B. Kerr, P. E. Iversen, B. Nilsson, C. R. Enzell and T. Matsuno, *Acta Chem. Scand.*, 1978, **32b**, 405–412.
- 195 A. Kunai, J. Harada, M. Nishihara, Y. Yanagi and K. Sasaki, *Bull. Chem. Soc. Jpn.*, 1983, **56**, 2442–2446.
- 196 S. Suga, S. Suzuki and J. Yoshida, *J. Am. Chem. Soc.*, 2002, **124**, 30–31.
- 197 D. Lehnerr, Y. H. Lam, M. C. Nicastrì, J. Liu, J. A. Newman, E. L. Regalado, D. A. Dirocco and T. Rovis, *J. Am. Chem. Soc.*, 2020, **142**, 468–478.
- 198 S. Suga, M. Okajima, K. Fujiwara and J. I. Yoshida, *J. Am. Chem. Soc.*, 2001, **123**, 7941–7942.
- 199 J. Yoshida and S. Suga, *Chem. Eur. J.*, 2002, **8**, 2650–2658.
- 200 A. J. Y. Lan, R. O. Heuckeroth and P. S. Mariano, *J. Am. Chem. Soc.*, 1987, **109**, 2738–2745.
- 201 H. G. Reiber and T. D. Stewart, *J. Am. Chem. Soc.*, 1940, **62**, 3026–3030.
- 202 N. J. Leonard and J. V. Paukstelis, *J. Org. Chem.*, 1963, **28**, 3021–3024.
- 203 E. H. Cordes and W. P. Jencks, *J. Am. Chem. Soc.*, 1962, **84**, 832–837.
- 204 G. J. S. Evans, K. White, J. A. Platts and N. C. O. Tomkinson, *Org. Biomol. Chem.*,
-

- 2006, **4**, 2616–2627.
- 205 P. Y. Sollenberger and R. B. Martin, *J. Am. Chem. Soc.*, 1970, **92**, 4261–4270.
- 206 J. H. Atherton, J. Blacker, M. R. Crampton and C. Grosjean, *Org. Biomol. Chem.*, 2004, **2**, 2567–2571.
- 207 K. Taguchi and F. H. Westheimer, *J. Org. Chem.*, 1971, **36**, 1570–1572.
- 208 W. W. Schoeller, J. Niemann and P. Rademacher, *J. Chem. Soc. Perkin Trans. 2*, 1988, 369–373.
- 209 G. Stork, A. Brizzolara, H. Landesman, J. Szmuszkovicz and R. Terrell, *J. Am. Chem. Soc.*, 1963, **85**, 207–222.
- 210 S. Saba, D. Vrkic, C. Cascella, I. DaSilva, K. Carta and A. Kojtari, *J. Chem. Res.*, 2008, **2008**, 301–304.
- 211 D. R. Lide and H. P. R. Frederikse, *CRC Handbook of Chemistry and Physics*, CRC, 77th edn., 1995.
- 212 A. Kolleth, A. Lumbroso, G. Tanriver, S. Catak, S. Sulzer-Mossé and A. De Mesmaeker, *Tetrahedron Lett.*, 2016, **57**, 2697–2702.
- 213 M. Pizzonero, S. Dupont, M. Babel, S. Beaumont, N. Bienvenu, R. Blanqué, L. Cherel, T. Christophe, B. Crescenzi, E. De Lemos, P. Delerive, P. Deprez, S. De Vos, F. Djata, S. Fletcher, S. Kopiejewski, C. Lebraly, J. M. Lefrançois, S. Lavazais, M. Manioc, L. Nelles, L. Oste, D. Polancec, V. Quénéhen, F. Soulas, N. Triballeau, E. M. Van Der Aar, N. Vandeghinste, E. Wakselman, R. Brys and L. Saniere, *J. Med. Chem.*, 2014, **57**, 10044–10057.
- 214 H. Mughal and M. Szostak, *Org. Biomol. Chem.*, 2021, **19**, 3274–3286.
- 215 J. Nagasawa, S. Govek, M. Kahraman, A. Lai, C. Bonnefous, K. Douglas, J. Sensintaffar, N. Lu, K. Lee, A. Aparicio, J. Kaufman, J. Qian, G. Shao, R. Prudente, J. D. Joseph, B. Darimont, D. Brigham, K. Maheu, R. Heyman, P. J. Rix, J. H. Hager and N. D. Smith, *J. Med. Chem.*, 2018, **61**, 7917–7928.
- 216 G. Schiavon, S. Zecchin, G. Cogoni and G. Bontempelli, *J. Electroanal. Chem.*, 1973, **48**, 425–431.
- 217 D. C. Batesky, M. J. Goldfogel and D. J. Weix, *J. Org. Chem.*, 2017, **82**, 9931–9936.

- 218 M. Mertens, C. Calberg, L. Martinot and R. Jérôme, *Macromolecules*, 1996, **29**, 4910–4918.
- 219 H. J. Schäfer, *Chem. Phys. Lipids*, 1979, **24**, 321–333.
- 220 M. Mechelhoff, G. H. Kelsall and N. J. D. Graham, *Chem. Eng. Sci.*, 2013, **95**, 301–312.
- 221 N. Elgrishi, K. J. Rountree, B. D. McCarthy, E. S. Rountree, T. T. Eisenhart and J. L. Dempsey, *J. Chem. Educ.*, 2018, **95**, 197–206.
- 222 C. G. Zoski, *Handbook of Electrochemistry*, Elsevier, Amsterdam, 1st edn., 2007.
- 223 R. A. Sheldon, *Green Chem.*, 2017, **19**, 18–43.
- 224 N. Yanagihara, S. Tanikawa, N. Suzuki, M. Rivera and T. Ogura, *Main Group Chem.*, 1997, **2**, 161–163.
- 225 B. C. Gilbert, D. K. C. Hodgeman and R. O. C. Norman, *J. Chem. Soc. Perkin Trans. 2*, 1973, 1748–1752.
- 226 A. A. Folgueiras-amador, A. E. Teuten, M. Salam-perez, J. E. Pearce, G. Denuault, D. Pletcher, P. J. Parsons, D. C. Harrowven and R. C. D. Brown, *Angew. Chem. Int. Ed.*, 2022, **61**, 1-7 e202203694.
- 227 T. Constantin, M. Zanini, A. Regni, N. S. Sheikh, F. Juliá and D. Leonori, *Science.*, 2020, **367**, 1021–1026.
- 228 Q. Zhu and D. G. Nocera, *J. Am. Chem. Soc.*, 2020, **142**, 17913–17918.
- 229 D. D. M. Wayner, D. J. McPhee and D. Griller, *J. Am. Chem. Soc.*, 1988, **110**, 132–137.
- 230 V. R. Dola, A. Soni, P. Agarwal, H. Ahmad, K. S. R. Raju, M. Rashid, M. Wahajuddin, K. Srivastava, W. Haq, A. K. Dwivedi, S. K. Puri and S. B. Katti, *Antimicrob. Agents Chemother.*, 2017, **61**, 1–26.
- 231 J. Voskuhl, M. Waller, S. Bandaru, B. A. Tkachenko, C. Fregonese, B. Wibbeling, P. R. Schreiner and B. J. Ravoo, *Org. Biomol. Chem.*, 2012, **10**, 4524–4530.
- 232 R. Ponsinet, G. Chassaing, J. Vaissermann and S. Lavielle, *European J. Org. Chem.*, 2000, **2000**, 83–90.

- 233 J. S. Stover, J. Shi, W. Jin, P. K. Vogt and D. L. Boger, *J. Am. Chem. Soc.*, 2009, **131**, 3342–3348.
- 234 G. R. Pettit, N. Melody and J. C. Chapuis, *J. Nat. Prod.*, 2020, **83**, 1571–1576.
- 235 Z. Ma, Z. Liu, T. Jiang, T. Zhang, H. Zhang, L. Du and M. Li, *ACS Med. Chem. Lett.*, 2016, **7**, 967–971.
- 236 S. Buchini, A. Buschiazzo and S. G. Withers, *Angew. Chem. Int. Ed.*, 2008, **47**, 2700–2703.
- 237 E. C. Jorgensen, G. C. Windridge and T. C. Lee, *J. Med. Chem.*, 1970, **13**, 352–356.
- 238 N. Gavande, H. L. Kim, M. R. Doddareddy, G. A. R. Johnston, M. Chebib and J. R. Hanrahan, *ACS Med. Chem. Lett.*, 2013, **4**, 402–407.
- 239 A. P. Ingale, D. Ukale, D. N. Garad and S. V. Shinde, *Synth. Commun.*, 2021, **51**, 1656–1668.
- 240 S. Engl and O. Reiser, *European J. Org. Chem.*, 2020, **2020**, 1523–1533.
- 241 S. Chowdhury and R. F. Standaert, *J. Org. Chem.*, 2016, **81**, 9957–9963.
- 242 K. Hyodo, G. Hasegawa, H. Maki and K. Uchida, *Org. Lett.*, 2019, **21**, 2818–2822.
- 243 P. Li, N. Ma, Z. Wang, Q. Dai and C. Hu, *J. Org. Chem.*, 2018, **83**, 8233–8240.
- 244 M. Terada, K. Machioka and K. Sorimachi, *Angew. Chem. Int. Ed.*, 2009, **48**, 2553–2556.
- 245 Y. Kawamata, M. Yan, Z. Liu, D. H. Bao, J. Chen, J. T. Starr and P. S. Baran, *J. Am. Chem. Soc.*, 2017, **139**, 7448–7451.